Phenomena affecting ink transfer in offset lithographic printing.

Vlachopoulos, Georgios

Swansea University
Prifysgol Abertawe

Phenomena Affecting Ink Transfer in Offset Lithographic Printing

Submitted to the University of Wales in fulfilment of the requirements for the Degree of Doctor of Philosophy
By

Georgios Vlachopoulos

Welsh Centre for Printing and Coating
School of Engineering
Swansea University

2010

Summary

The ink transfer mechanisms in the offset lithographic printing process is consisted by a complex inking roller train which a series of alternately rigid and deformable rollers, are used to precondition and deliver the printing fluid from the ink and fount reservoirs to the image carrier. The lithographic printing inks are complex formulated non-Newtonian fluids with high viscoelastic rheological profile and thixotropic behaviour. A set of ink dilutions was produced based on coldset lithographic printing ink diluted in concentration with Butyl-Diglycol.

The rheological profile of the produced inks was examined by detailed rheological characterisation with particular interest on viscosity on tack, thixotropy, viscoelasticity, surface tension, extension and shear viscosity. Further examination established the relationships between shear viscosity and tack focusing on a printing nip between a rigid and elastic roller. A decrease in tack was found to be associated with a decrease in shear and the apparent extension viscosity.

Developed imprinting and photographic techniques used to capture and characterise the fundamental phenomena of ribbing and misting associated with ink film splitting at the rollers nip in offset printing. Such techniques used to capture the dynamic profile of those mechanisms on a closed loop distribution system by using a tack meter. The detailed profile of those phenomena was characterised with particular interest on the relationship with the fluids rheological profile and the Capillary number. Extension rheometer was also used to analyse the mechanisms of ribbing and misting phenomena by experimental simulation of a printing nip.

A factorial experiment was undertaken based on L18 Orthogonal Array techniques. The parameters of rollers ratio, ink film thickness, temperature, distribution speed, distribution time and inks viscosity were found to have an influence on misting and ribbing phenomena. Results and analysis established responses and interactions between the process parameters but also between ribbing and misting as essential phenomena with the ink transfer mechanisms in lithographic printing process.

DECLARATION

This work has not been previously been accepted in substance for any degree and is not being concurrently submitted in candidature for any degree.

Signed .....(candidate)

Date ....6/12/2010.....

STATEMENT 1

This thesis is the result of my own investigations, except where otherwise stated. Other sources are acknowledged giving explicit references. A bibliography is appended.

Signed .....(candidate)

Date ....6/12/2010.....

STATEMENT 2

I hereby give my consent for my thesis, if accepted, to be available for photocopying and for inter-library loan, and for the title and summary to be made available to outside organisations

Signed .....(candidate)

Date ....6/12/2010.....

Acknowledgments

First, I thank my supervisor Professor Tim Claypole, for his continuous support through my Ph.D. program. I would like also to thank Professor David Gethin, because he was always there to listen and to give advice. I thank students and staff of Welsh Centre for Printing and Coating, Christine, Tatyana, Libby, Davide, John, Chris, Simon, Eifion, David, Glyn, Frank, Soo, Yusof, Martyn, Chris and Ruobo. They stand me more than a family all those years by supporting my work and proposed ideas for continuing my research. I also thank Alex Lubansky for his friendly help on extension rheology. Special thanks goes to Yiannis for his unlimited support and who has been a close friend and mentor all those years. Without his encouragement I could not have finished this dissertation. My truly thanks go to Jo, Gorka and Julia because they had always a good reason for a break. I would like to thanks my parents and my sister for been supportive all those years independently of my ideas. I also thank all my friends and co-workers Vassilis, Mitsos, Yiannis, Takis, Nikos, Sotiris, Christos, Margarita, Apostolis, Katerina, Elina, Manolis, Victoras, Yorgos, Zaxarias and many more that been always close even from miles away. I would like also to thank IKY (Greek State Scholarship Foundation) who gave me the opportunity in a first place and financial supported me to complete a part of my dreams. I wish to all to live their dreams in health and happiness.

Table of Contents

List of Figures

List of Tables

Nomenclature

Symbol	*Name*	*Units*
Ca	Capillary number	-
Dmid	Filament radius	mm
Dpr	Print density at film thickness h	-
Dsr	Saturation density	-
H	Hysterisis	w/cm^2
g	Gravity	N
G'	Elastic modulus	Pa
G"	Viscous modulus	Pa
h	Ink film thickness	$gr/meters^2$
K	Bulk modulus	Pas
M	Mass	kg
N	Length	mm
Pn	Number of ribbing Peaks	-
Pw	Peak Width	mm
Px	Ribbing Peak value	-
R	Roller radius	mm
r	Radius	mm
Rsr	Saturation reflectance	-
Sav	Moving Average	-
t	Time	sec
Tr	Trouton ratio	-
Y	Ribbing grey values	-
ε'	Strain rate	s^{-1}
η	Shear viscosity	Pa.s
λ	Extension viscosity	Pa
μ	Separation velocity	mm/sec
ρ	Density	kg/m^3
σ	Surface tension	$dynes/cm^3$
τ	Stress	Pa
ω	Angular velocity	rpm

1. Introduction

1.1 Introduction

Offset lithographic printing is one of the main volume printing processes used extensively for graphic printing, e.g. for the production of newspapers, books, magazines, packaging and tinplates. The estimate for the 2008 European print production value was about 140-145.000 Million Euros of which 70% was produced by offset printing. The 40% of this comes from Web Offset and 60% from Sheetfed Offset presses. In offset lithography the inking train, a series of alternately rigid and deformable rollers, are used to precondition and deliver the printing fluid (a combination of ink and fount solution) from the ink and fount reservoirs to the image carrier. At each roller, the printing fluid is forced through a nip after which it splits as the two rolling surfaces separate. The ink transfer mechanisms in the inking roller train are complex and not fully understood. The objective of the work reported in this thesis was to undertake a study of the phenomena associated with ink film splitting between rollers in offset printing, in particular *ribbing* and *misting*. Understanding these phenomena is also highly relevant to high speed roller coating, where similar film splitting occurs.

The ribbing is ink film thickness variation across the width of the rollers (i.e. orthogonal to the direction of rolling). This variation affects the ink transfer between the rollers. The misting is the detachment of small droplets and ligands of ink as the ink film splits in the rollers train. While both of these phenomena are generated by ink splitting mechanisms, not much research has been published on them and they are not taken into account when the transfer mechanism is simulated with mathematical models. This is despite uneven ink distribution resulting in poor print quality and ink misting being a major problem for high speed printing, such as used in newspapers and packaging.

The inking train of a litho press is designed under the concept of mass conservation. Ideally the amount of ink that is feed into the inking train is extracted from the system by printing. The ink is transferred onto the substrate while at the same rate

fresh ink is delivered from the metering roller. The roller train can act as a reservoir ink with both long and short term transients through a built up of ink on the rollers. Many parameters affect the flow of ink through the roller train, such as roller surface qualities, temperature, speed, and fountain solution. Ink transfer instabilities are usually related to the press inking unit configuration and length of the inking train.

This thesis focuses on how ribbing and misting phenomena affect the ink transfer mechanism and are responsible for ink transfer instabilities in the roller train distribution systems. It investigates how these phenomena are influenced by parameters such as ink film thickness, temperature, distribution speed, distribution time and viscosity. This is in essence the study of the ink splitting mechanism between two rolling surfaces after a printing nip. Printing nips are where the surfaces of two rollers covered with a film of printing fluid are forced into intimate contact and occur throughout the litho roller train.

There are practical difficulties in investigating the science of the ribbing and misting in printing presses such as the narrow roller gaps, the high printing speed, the thin ink film thickness and the process noise. This is coupled with the dynamics of the printing press caused by ink transients when the supply and removal of ink do not matched. Therefore, the work has focused on developing laboratory simulations to allow the phenomena to be investigated under controlled conditions.

The next section introduces the concept of offset lithography, while the final section contains the layout of the thesis described with respect to the objectives.

1.2 An overview of the Lithographic printing process

The term of lithography comes from the Greek words "Lithos" which means "stone" and the verb "Grafo" which means "write". The principles of lithography can be traced to 1798 when Alois Senefelder began to experiment with printing, as a cheap printing process to publish his own theatrical plays. The repellent character of the typographic oil-based ink with the water, led him to investigate the lithographic printing process. A detailed description of the process is given by Alois Senefelder in his book "The invention of lithography" that was translated by Muller in 1911. The

fine surface of a limestone is rubbed by sea-sand and water to remove any oleophilic (oil acceptance) surface elements and provide a most hydrophilic (water acceptance) surface. The image is created by an oleophilic crayon writing directly on the stone surface and as a result a hydrophobic (water repellent) image is generated on it. An emulsion of water, gum arabic and nitric acid is used to cover and to chemically corrode the surface around the image areas while the image areas remain slightly finer and higher than the non image areas with hydrophobic characteristics (Figure 1-1) The chemical process increases the roughness and the surface energy of the stone for the fountain solution (water with gum arabic). The image repels the water to the non-image areas. The ink is repelled by the water on the non-image areas and it is transferred to the image areas.

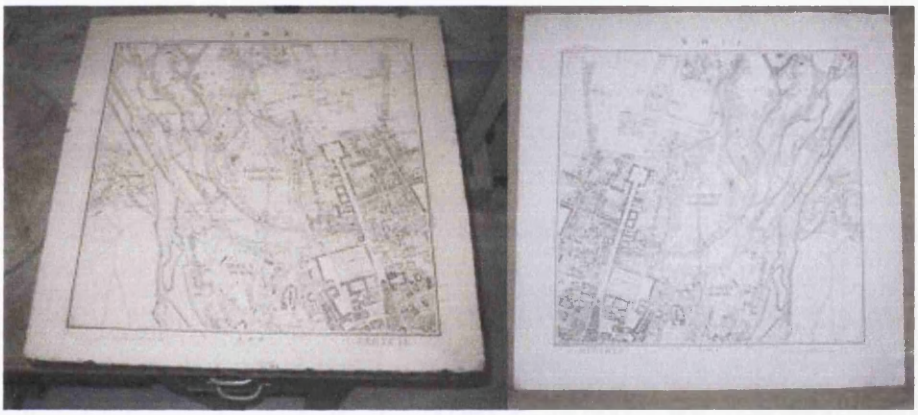

Figure 1-1 The limestone was the first material that was used for lithographic plate. The image areas repel the water to the non-image areas. The ink is repelled by the water on the non-image areas and it is transferred to the image areas.

Lithography was a monochrome printing process based on the layout of a flat-bed typographic printing press. The cheap production process and the reusable plates was one of the most important reasons that it became very popular and soon more colours (plates) were added and chromolithography was born. The offset process where an intermediate roller is used to transfer the image from the plate to the substrate was established around 1900 by a variety of engineers (Figure 1-2). The first offset application was probably located in England in a tin plate printing company. At similar time, Christopher Hermann in Germany and Ira Rubel in America had noticed the offset phenomenon of the litho-press rubber impression cylinder to print a ghost image on the back of the substrate. This was the inspiration for the rubber blanket application in an experimental offset press. The first offset litho press was

developed in America by Charles and Albert Harris of the Harris Automatic Press Company. This was the first single unit of an offset press. This eventually supported more colour units and finally replaced the chromolithography process (Meggs 1998).

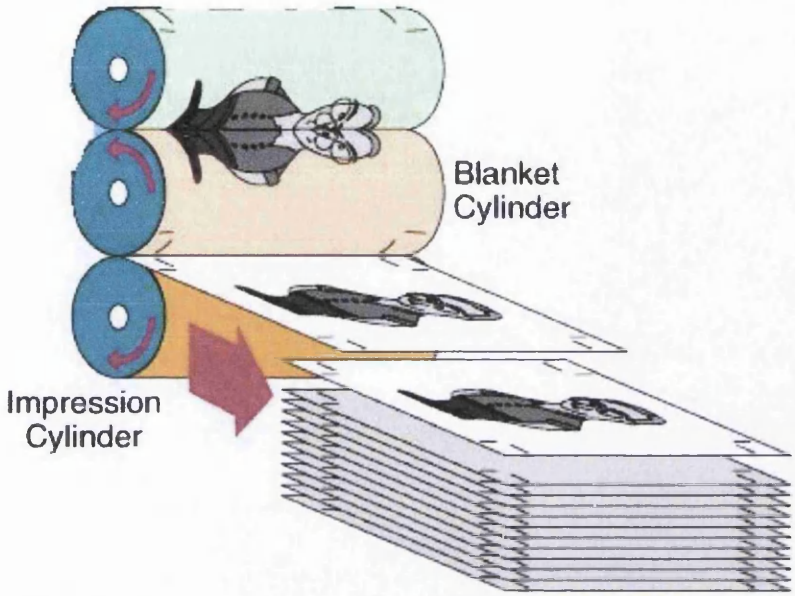

Figure 1-2 The offset lithographic process uses a blanket coated drum in order to transfer indirect the image to the substrate.

It is characterised as planographic (flat image) because the image is in the same layer as the none-image areas of the plate. It is also indirect because the inked image is transferred to the substrate by the blanket cylinder. The complexity is dependent on the ink formulation, the inking train and the inking process. Litho-inks are Non-Newtonian fluids with thixotropic behaviour and viscoelastic character. The design of the ink train of an offset-press varies according to the number of rollers, diameters, and surface qualities. Also, the need to deliver the water, known based fount solution to create a water-ink emulsion as part of the image inking process is a further complication to the inking train. Finally, there is the interaction of the image and non-image areas with the inking train which can create image ghosting.

A typical layout of an offset lithographic press is shown in Figure 1-3. The image is mounted around the whole cylinder (drum) and there is no space between the head and the footage of the plate that carries the image.

The ink feeding mechanism comprises the ink feed roller (meter roller, also referred to as ductor), which controls the flow of ink.

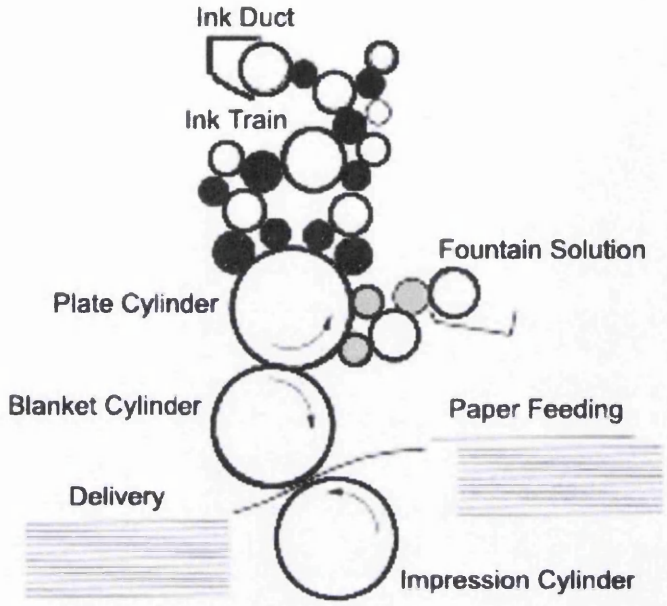

Figure 1-3 Schematic layout of a lithographic press.

The ink train comprises of rigid rollers coated with copper and deformable polymer coated rollers in nip contact. The number, dimensions and configuration of the rollers depends on the design of the press. Some of the rollers oscillate from side to side in order to achieve a uniform ink film thickness. The rollers rotate by friction between rigid and deformable roller to avoid damage due to differences in surface speed.

The dampening train delivers the fount solution and is of similar concept to the inking train, with rigid and deformable rollers, but is much shorter.

The image carrying plate is a thin anodised aluminium sheet which is mounted on a drum. The plates are usually between 20 to 30 μm thick. The plate is coated by photopolymer emulsion that is exposed photographically or by laser. The developing process removes the non-image areas and the image is generated by the oleophilic emulsion that remains on the plate surface. The non-image areas provide hydrophilic surface. The plate comes into contact with the dampening roller first and as a result fountain solution is transferred to the non-image areas while it is repelled by image

areas. The dampened non-image areas repel the ink while image areas attract it and as a result the ink is transferred only to the image (Figure 1-4).

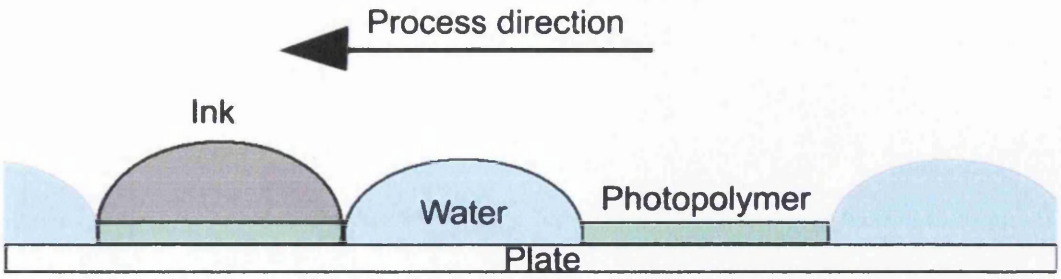

Figure 1-4 Schematic diagram of the offset plate.

The blanket is a multi-fabric layer substrate with rubber coating on the top (Figure 1-5). It is tightly mounted around the drum of the blanket cylinder. The multiple layers allow deformation of the plate at the nip region in order to except ink from the plate or to transfer the ink on the substrate. The blanket qualities vary by the number and make up of the layers, and the surface properties of the rubber.

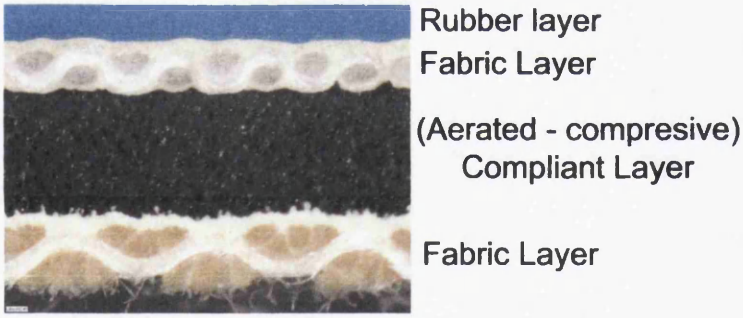

Figure 1-5 Cross section of a typical blanket.

The impression cylinder applies impression pressure between the offset image and the substrate. In web systems, the blanket cylinder of the image being printed on the reverse side of the substrate acts as the impression cylinder (blanket-to-blanket impression).

The substrate can be paper, polymer film, tin plate or aluminium foil.

The Lithographic inks are usually non Newtonian and highly viscous in character. The inks consist of the binder, the colorants and the additives. The binders are

usually resins, drying oils and vegetable esters. Colorants can be pigments or dyes, typically lithographic formulated inks use pigments. The ink contains also additives, such as antifoaming agents, to help improve its performance. The wide range of applications forces the ink industry to produce specific inks for different applications. The inks vary also by the drying mechanism, such as coldset, heatset, UV (ultra violet), IR (infrared radiation) and electron beam. Coldset inks dry by absorption of the printed substrate while heatset ones dry by oxidation of the solvent. UV, IR and e-beam inks dry by polymerisation that is carried out by instant exposure of the printed substrate.

The fountain solution or dampening solution contains a mix of water with gum arabic, anticorrosion additives and isopropyl alcohol. Usually the term of "water" is referred to the fountain solution of the press. Water quality is very important because it interacts both with the plate and the ink. In order to protect the non-image areas of the plate from corrosion pH stabilisers are used in the fountain solution.

The distribution of ink across the roller train is not uniform as it has to supply the amount of ink corresponding to the image in the direction of printing. To achieve this the metering roller has a blade which controls the flow of ink into the roller train. The blade is separated by inking zones, the gap for each of which is controlled by a screw, know as a *key*. The actual ink key setting on ink duct is a result of the average grey density of the image at the specific zone in regard with the following inking zones (Figure 1-6). The ink setting can be changed during the printing process. The ink setting response time depends on the press configuration and also on the abilities and experience of the operator.

Critical to the understanding of the flow of ink through the inking train is the mechanisms which occur in the rolling nips between rollers. This process can be separated in three regions (Figure 1-7):

The entrance region where the ink on the roller surfaces come together prior to the nip region;

The nip region where the ink is compressed and can be the subject of shear between the rolling surfaces or is immobilised on the roller surface;

The nip exit region where after the nip, the ink is forced to follow one of the two curved regions, extends and finally splits.

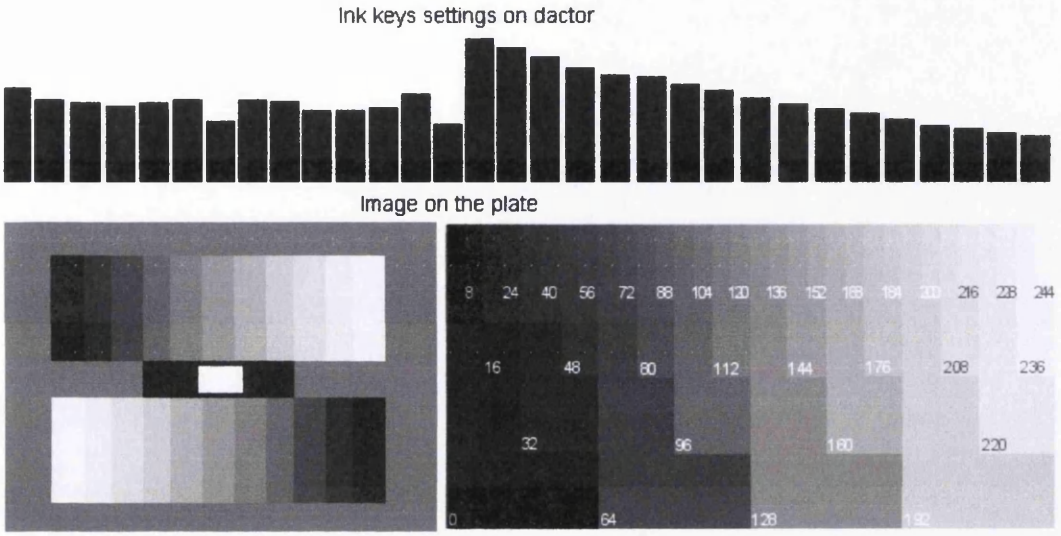

Figure 1-6 The ink key setting on the ductor depends on the grey levels of the image on the plate.

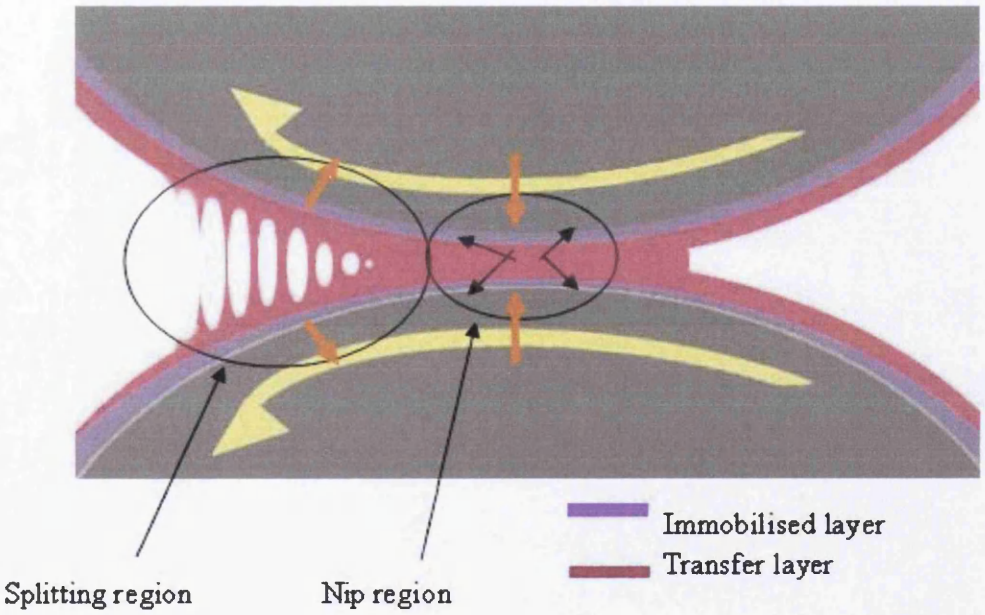

Figure 1-7 The ink passes through the nip region of the roller and splits at the nip exit region due to rollers rotation by friction.

1.3 Closure and thesis layout

This chapter has introduced the offset printing process and the objectives of the thesis. Previous published work on the splitting mechanism and the instabilities are reviewed in Chapter 2.

Chapter 3 sets out the instrumentation and methodologies that have been used through the development of experimental methodology and analysis of ribbing and misting phenomena in offset lithographic printing.

Chapter 4 describes the rheological characterisation of the fluids used in this study. It focuses on establishing the relationship between rheology and printing characteristics such as tack value and printing density.

Chapter 5 describes the development of extension rheometry methodologies. It comprises techniques and analysis for extensional rheometry with particular reference to viscoelastic fluids such lithographic inks. It discusses solutions effects under tensile stress and compares extension with shear viscosities.

Chapter 6 investigates ribbing phenomena on distribution systems. The detailed methodology is described with particular interest to the ribbing profile along the rollers. It includes developing techniques for accurate and repeatable studies on ribbing phenomena with thin films of lithographic inks. The onset of ribbing through elongation is analysed with interest on thin film mechanisms.

Chapter 7 deals with the misting phenomena on distribution systems. It describes the developing techniques of the experimental work for characterisation of the misting profile. It analyses the effect of the parameters and relations with the rheological properties.

Chapter 8 presents the systematic study with a subset of a full factorial experiment based on orthogonal arrays. It draws together rheology and interactions between misting and ribbing phenomena. It investigates the effects of the factors on such phenomena and relations with the ink transfer mechanism. The experiment explores the relations and the differences between misting and ribbing generation.

Chapter 9 discusses the results in the context of the ink distribution systems and in lithographic offset printing process.

Finally, Chapter 10 draws conclusions of the thesis and proposes recommendation for further work.

2. Literature review on ink transfer

2.1 Introduction

Ink splitting occurs throughout the ink roller train at the nip exit to the nip between two rollers. This chapter reviews the theory and the background research on phenomena related to the ink splitting mechanism in the lithographic offset printing process. Section 2.2 reviews studies and methodologies on ink splitting ratio which is primarily discussed by the studies that are involved with the ink splitting mechanism. Section 2.3 covers previous work on mathematical models for the ink transfer, and highlights the importance of the phenomena that are related to the transfer instabilities. Section 2.4 deals with immobilisation phenomena that can influence the ink distribution mechanisms. Section 2.5 provides a description and a review on ribbing phenomena. Section 2.6 characterises and reviews studies and methodologies on misting phenomena. Section 2.7 deals with the rheological properties that make up the rheological profile of the lithographic printing inks. Finally, Section 2.8 reviews studies on the effects of the fountain solution that emulsifies with the ink on lithographic printing press and affects inks rheology and transfer mechanisms.

2.2 The ink splitting ratio

The ink splitting mechanism between two rollers has been extensively examined since 1950. Banks and Mill (1954) established the location of the ink splitting using rigid forward rollers configuration. Splitting was characterised by negative pressures (10^5Pa) at the nip exit where tensile forces create cavities. These cavities expand and filaments were formed between the two surfaces. Finally the filaments extended and split. Miller and Meyers (1958) examined filament formation with printing inks using rotation cone roller on a flat disk configuration to simulate the splitting mechanism on the rollers. They concluded in a four-step mechanism of nip pass, generation of cavities, filaments elongation, and rupture, which leads to filament split and formation of droplets. Thompson and Young (1975) used high speed image capturing. They found the ink filaments were elongated and after splitting they pulled-back to the nip exit and fell over.

The main arguments were whether the ink splitting is symmetric or asymmetric, and the parameters that affect the ink volume that follows the roller surfaces. Various methodologies have been established to accurately calculate the split ratio. Bradford (1954) used radiotracers to establish the split ratio between two rollers. He concluded on the asymmetric splitting with the 0.42 split ratio which becomes symmetric as the ink film thickness decreases. Smith (1956) used photographic techniques to analyse the ink splitting. He found that the ink filament pattern becomes finer as the speed increases and reaches a symmetric splitting. Banks and Mill (1954 and 1968) used experimental techniques with castor oil and ink. Polythene and aluminium strips were weighed and placed on the rotation cylinders. After the ink distribution process the strips were removed and weighted again. Their results supported the theory of symmetric splitting with results close to 0.5 split ratio. Wirz (1964) developed an ink train and used a glass drum at the position of the form rollers in order to calculate the built-up ink thickness. A light source was set in the glass drum and a light detector analysed the light while the ink built-up on the drum surface through distribution. He concluded that split ratio was close to 0.4 between the form roller and plate and that more form rollers supply thinner film thickness. De Grâce (1988) also printed and weighed samples to calculate the split ratio. He found the split ratio was reduced by thinner ink film layers and higher speed. It also decreased as the printing area increased. Most of the experimental techniques were based on narrow areas of the nip or in some cases only on the rollers nip profile side. The majority of the studies found a trend towards symmetric splitting.

2.3 Mathematical ink transfer model

Mathematical models were tested to investigate the ink train behaviour and improve press configuration. Wood (1918) and Adams (1954) studied a simple mathematical model without any complicated parameters. The model used the 50/50 split ratio with continues ink feeding mechanism and a continuous solid printed image. It was actually a rotary sink system with a continuous input and output ink volume. The symmetrical splitting theory was accepted and was also used in further studies of the printing mechanism. Hull (1968) calculated the steady-state of ink film thickness through the ink train using similar modelling techniques. Guerrette (1985) studied the effect of inking train configurations and the effect of different split ratios in order

to determine ghosting effects. MacPhee (1995) confirmed this with good agreement on steady state with the mathematical model. He also argued that the actual time constants that described system response to decreases in ink feed-rate were much greater that those calculated using the model. Chou et al (1996, 1998) used similar mathematical models to study the ink transfer effects on image coverage by the mechanisms of ink feeding. Such mathematical model divides all the inking rollers, plate and blanket into very small cells of the same size. The number of the cells between two rollers has to be carried out to nearest number across the length and the width of the rollers as shown in Figure 2-1 (Chou 1997). As a result, each roller is represented by a different number of cells with the same dimensions. This provides a constant mechanism, eliminating the effects generated through the distribution process such as squeeze of the flow at the nip, roller slippage, ink loss and emulsification or water ink interaction. Chou (1997) also studied the effects of vibrator oscillation on image layout and the ghosting effects of the form rollers configuration. Their results agreed with the previous studies and confirmed that vibration oscillation has negligible effects on the ink flow ratios of form rollers configuration. Equal size of form roller and plate produce more uniform ink film thickness. Paikos (2003) used a similar concept to study transient effects of printing press configuration through start-up time. He found very good agreement with previous authors on press responses and image coverage but found that the mathematical model overestimates the initial ink build-up on the paper. Patzelt and Ruder developed a mathematical model (INKTEAM) in order to simulate the printing press. The model took into account the parameters of inking unit geometry, continuous or interrupted ink feeding, rotation and oscillation, dampening solution, influence of temperature and ghosting. The results did not show a good agreement with the press and a number of parameters modified in order to provide a success model (Kipphan 2000). Finally, the results showed similar response between model and press at printing steady state but higher volumes (Figure 2-2). However, the model overestimates the ink volume but shows similar trends at steady state conditions.

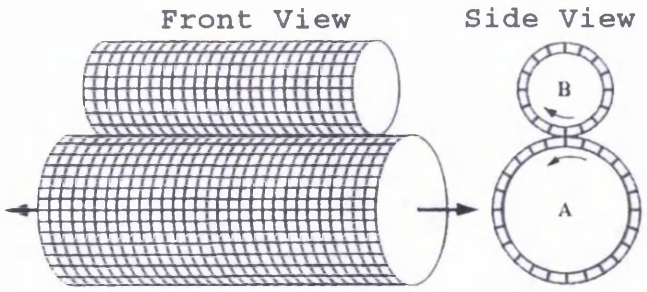

Figure 2-1 Division of the rollers into equal size cells across the length and the perimeter (Chou 1997).

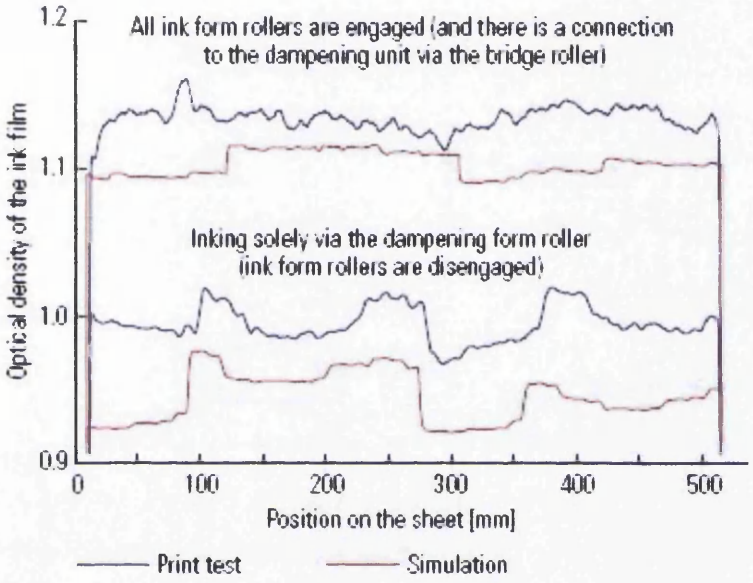

Figure 2-2 Results of the INKTEAM model press. The model takes into account the parameters of inking unit geometry, continuous or interrupted ink feeding, rotation and oscillation, dampening solution, influence of temperature and ghosting.

Many of the mathematical models on the offset printing do not agree with the responses from a full scale printing press. The mathematical models do not include the effects of misting, ribbing, ink viscosity, system temperature, distribution speed, distribution time and immobilisation. Chou (1997) claimed that the onset of ribbing generates negligible effects on transfer mechanism through his experimental results. However, he did not explain how ribbing was formed or how the ink film thickness affects that phenomenon. Even if ribbing has not much influence on the ink transfer mechanism, some parameters will affect those instabilities between theoretical and experimental results. The accuracy of a mathematical model depends on at which point in the splitting mechanism the model begins and which starting point is relevant.

2.4 Ink immobilisation

Ink immobilisation occurs within ink splitting, and is divided in two types; *ink to substrate immobilisation* and *ink to rollers immobilisation.*

Ink to substrate immobilisation (Figure 2-3) is the stabilisation of the ink due to penetration into the porous surface of the substrate. The ink rheological characteristics within the nip can affect its penetration level. The immobilisation level can vary with the printing copies because of ghosting that produces randomly image ink effects which dominate also across the units (multi colour process) due to decreased porosity of the ink trapping (ink on ink) effects. This can affect also the amount of ink that circulates in the ink train.

The ink to paper immobilisation was established by Walker and Fetsko (1955 and 1958). During splitting, the ink is immobilised within the paper surface and the ink splits asymmetrically. The splitting asymmetry decreases close to 0.5 as the printing speed or the amount of the parameter b (immobilised ink) increases. Their theory describes three stages during splitting:

a) contact and adhesion between the ink and paper surface,

b) immobilisation of a portion of the ink into the paper pores

c) splitting of the remaining portion of the free ink

$$Y = b + F(X - b) \qquad (1)$$

Where:

Y = Ink transfer to the paper

b = amount of ink immobilized in the microstructure of the paper

X = Ink film thickness at the nip inlet

F = split factor

Lepoutre (1979) claimed that the amount of ink immobilized in the microstructure of the paper, b, is also affected by the surface microstructure of the substrate because it affects the print contact area. Coco and Cockerline (1988) stated that ink immobilisation is also affected by ink formulation components such as vehicles and solvents.

However, this is not the main interest on ink distribution systems because ink transfer to the substrate is related to the outgoing ink of the inking unit. It is more relevant when other parameters are studied such as absorption or porosity of the substrates qualities. This thesis focuses on the behaviour of the ink that remains on the rollers distribution system. The Walker and Fetsko equation was also used by others (Melia 1974) in further studies to describe immobilisation on roller surface of the ink train.

$$y = A + fy\,(x_o + y_o - bx - by) \qquad (2)$$

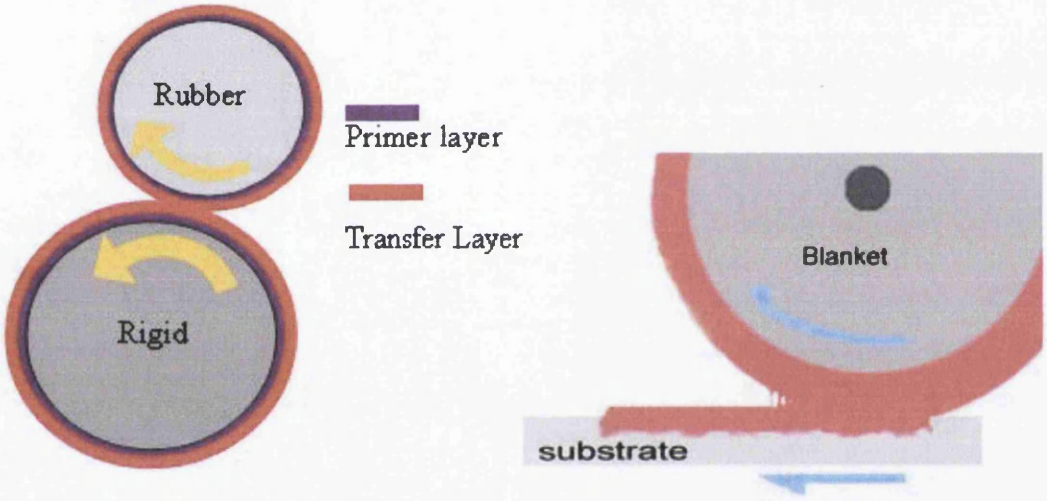

Figure 2-3 The ink immobilisation on rollers creates a thin film that is not transferred through distribution (left). The immobilised ink is absorbed by the surface of the substrate (right).

Ink to rollers immobilisation (Figure 2-3) occurs to train surface qualities with an effect of ink vehicle due to its internal structure (Chou et al 1990). The ink to ink train immobilisation was first discussed and examined by Melia (1974). In her thesis, the immobilised ink is characterised by the stabilised ink film thickness on rollers surface that could not be transferred or printed. She used a printability tester to print samples without re-inking of the printing disc. The effect of not ink transfer (negligible print density) calculated the amount of ink that was stabilised into the blanket surface. She also found that an amount of ink is immobilised both to the blanket and to the photopolymer layer that constitutes the image on the plate. She

applied the Walker and Fetsko equation to calculate the amount of immobilised ink on those surfaces.

However, her results showed that the splitting factor was close to 0.5 but was dependent on the squeeze pressure at the nip contact.

The concept of the ink stabilised on the roller surface was also discussed by MacPhee (1998). He suggested an amount of ink was absorbed or stabilised to the roller surface and this is responsible for the 0.67 split ratio at the first contact when a roller receives ink for the first time. He characterised as a "receptor" the roller that inserts to the nip with the lower ink film thickness and tends to receive ink from the roller with the higher ink film thickness (Figure 2-4). However, he did not identify accurately what amount of ink was stabilised on rollers and which one was active during distribution.

The ink to roller train immobilisation is important when the ink distribution system is studied and especially on press responses as described in 2.3. It has not been investigated to what extent the immobilised ink and variations of the parameter are due to ink film thickness, distribution time and distribution speed, temperature, viscosity and rollers surface qualities.

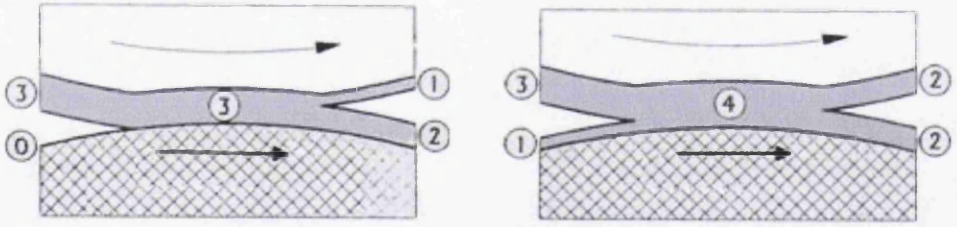

Figure 2-4 The first contact with the roller generates 0.67 ink split ratio (left). After that the splitting is 0.5 and the roller with the thinner ink film thickness is characterised as "receptor" (right) (MacPhee 1998).

2.5 Ribbing phenomena at the nip exit

Ribbing is characterised by fluid thickness variation on the rotating surfaces. MacPhee (1998) refers to ribbing as the onset of a type of hydraulic instability

(Figure 2-5) according to the work of Pitts and Greiller in 1961. Banks and Mill (1954) had previously investigated the ribbing pattern created by fluid during rotation and found that ribbing was a function of the ratio of the gap to the roller radius. They suggested that cavities patterns were affected by ribbing phenomena and those patterns were randomised by the oscillator roller mechanisms. Savage (1977) and Coyle (1984) studied the perturbation of the ink splitting mechanism using two-dimensional approximations of the Navier-Stokes equation to analyse ribbing phenomena of Newtonian fluids between rigid rollers. However, their theoretical results were not in good agreement with the experimental instabilities. Carvalho et al (1994) described ribbing as three-dimensional periodic flow variation in forward roll coating film splitting. They used the capillary number to predict the onset of ribbing due to deformation of the soft rubber roller at the nip. A forward roller coating system was used to generate ribbing with an adapted ruler on the top side of the roller. The ribbing pattern was captured by a camera in such angle in order to capture the ruler axis in parallel with the ribbing wavelength. When both rollers are rigid, the flow was stable at values of capillary number up to about 0.1, but it was unstable at higher values. However, they concluded in higher capillary numbers for the onset of ribbing than Savage (1992) and Coyle (1992). On the other hand their capturing technique focused on a narrow scale across the rollers length while they used high coating film thickness.

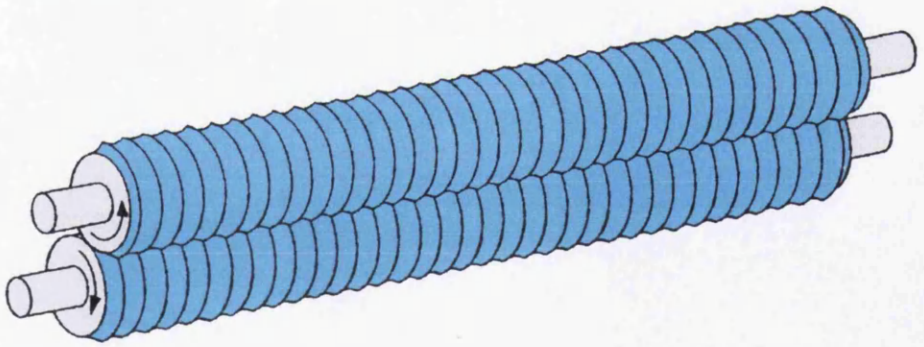

Figure 2-5 The onset of hydraulic instability (ribbing) due to rollers rotation (MacPhee 1998). This is described as the period increase of ink film thickness along the rollers length.

Lopez et al (2002) used a convective Maxwell model to keep track of deformation along the nip. They used also a Runge-Kutta boundary value algorithm to solve the ribbing profile. Pressure was found to increase everywhere along the nip, especially at higher shear zones. However, their calculation did not follow the Newtonian case

and with viscoelastic properties the ribbing threshold was reduced. They also found that the periodic steady variation of ink film thickness became unsteady when speed was increased.

Many authors (Savage 1984, Coyle et al 1990, Carvalho 1996, MacPhee 1998, Lopez et al 2002, Owens 2005) have concluded that ribbing instability strictly depends on the capillary number

$$Ca = \mu V / \sigma \qquad (3)$$

The capillary number was used to explain the onset of the meniscus at the free surface of the nip exit. Newtonian liquids produced unstable flow in higher Capillary numbers than with Non-Newtonian fluids. Zevallos et al (2004) used two-dimensional flow of viscoelastic liquids in a forward roll coating gap, analysed by solving the continuity and momentum equations coupled with two differential constitutive equations, the Oldroyd-B and FENE-P models. They found that the stress field changed with rising liquid elasticity. They concluded that a critical Weissenberg number makes the fluid meniscus unstable. The elastic forces change the flow characteristics near the free surface. At a fixed capillary number, the stresses at the free surface were raised because of the strong extensional character of the flow at the nip exit region.

However, these studies used Newtonian liquids and did not focus on thin film thicknesses on distribution systems. They also studied the formation of the meniscus at the nip exit and not directly the ribbing effects or its variations. Theoretical models gave values away of the experimental results. The perturbation theory tends to average the phenomenon and denigrate the effect on transfer mechanism which is also related to the misting phenomena on the distribution systems.

2.6 Misting phenomena

Misting phenomena are related to the ink splitting mechanisms. It occurs during the ink splitting when ink filaments are ruptured in multiple points and particles flow away of the press (Figure 2-6). Sjobal (1949) used photographic techniques to

observe misting is generated due to filament break-up. Voet (1952 and 1956) focused on the study of misting phenomena of rotary news letterpress. He found misting was affected by rotation speed, ink additives and fluid properties, film thickness and the presence of moisture in the system. The decrease of ink viscosity increased misting in his study and it also increased with the ink film thickness. The increase of pigment size and concentration decreases misting. Water in ink also decreased misting effects. However, Voet based his study on letterpress system and inks. Bisset et al (1979) argued that smaller roller diameter and higher ink film thickness tends to increase misting on distribution systems. These results were confirmed by others such as Cristiansen (1995), and McKay (1994). Furthermore, others found that misting also increases with temperature (Evans 1995 and Traber et al 1992). Temperature affects viscosity as was reported by Fuchs et al (1991). Blayo et al (1998) used a tack-o-scope tester to study misting phenomena. They used aluminium foil to cover the tester in order to trap the misting ink. The weighted the samples to carry out the amount of ink that been lost from the distribution rollers. They concluded that misting was increased by decrease of tack and viscosity (Blayo et al 2003). Their work carried out the average amount of ink that been lost from the system and they did not calculated distribution system transits or variations of the droplets profile with the changes into viscosity or tack.

MacPhee (1998) used the Maxwell viscoelastic model to determine the inks elongation mechanisms. His theory based on the elongation responses of a spring and a dashpot that constitutes the Maxwell model. The spring mechanism responds immediately to the elongation rate while the dashpot behaves like a solid. He concluded that misting is also affected by the ink elasticity. Zevallos et al (2005) concluded that Maxwell and Kelvin viscoelastic models (Figure 2-7) were not suitable for very thin viscoelastic fluid films.

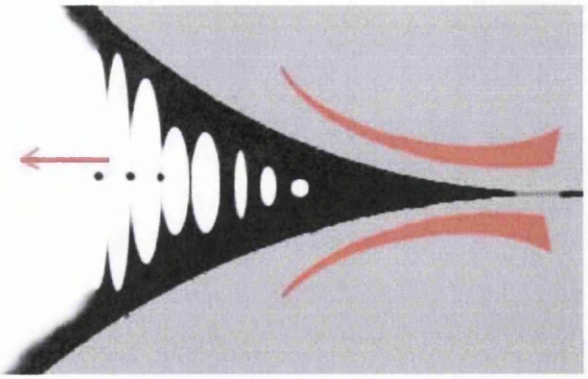

Figure 2-6 The misting ink is generated during the splitting of the ink at the nip exit, when filaments are ruptured in multiple areas.

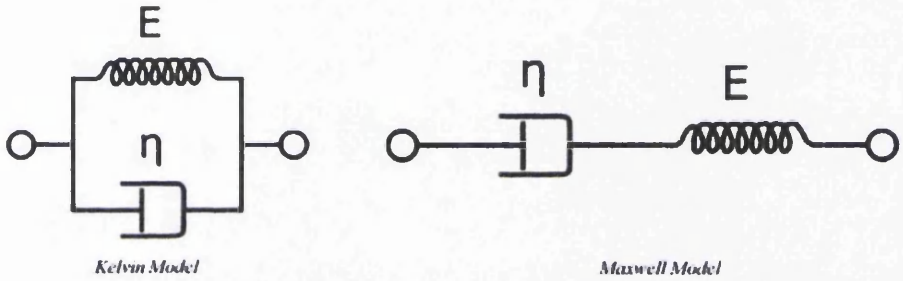

Figure 2-7 The viscoelastic models of Kelvin and Maxwell are consisted by a spring and a dashpot mechanisms but vary on the geometry (MacPhee 1997).

Owens (2005) studied misting mechanisms of Newtonian and polymer solutions. He used an Aerosizer DSP^{TM} system to calculate the droplets size and count the amount of droplets that were generated at the nip exit. He also extended his study by studying droplet formation using an extension rheometer. His experimental methodology had extremely good results but the experimental analysis focused on an extremely narrow area (1.25mm inner diameter tube) along the rollers nip. He concluded that misting can decrease with low surface tension and more elasticity of the coating fluids, larger rollers with reverse roll. He stated that polymers form larger droplets than Newtonian fluids through capillary thinning experiments. His results also show that dilute linearly polymer solutions had longer relaxation times and a greater steady-state stress than dilute-branched polymer solution of equal molecular weight and at equal deformation rate. His simple misting model is described by $V= \omega R$, where: ω is the angular velocity and R is the roller radius. He developed the the dimensionless Misting number,

$$\eta V/\sigma \qquad (4)$$

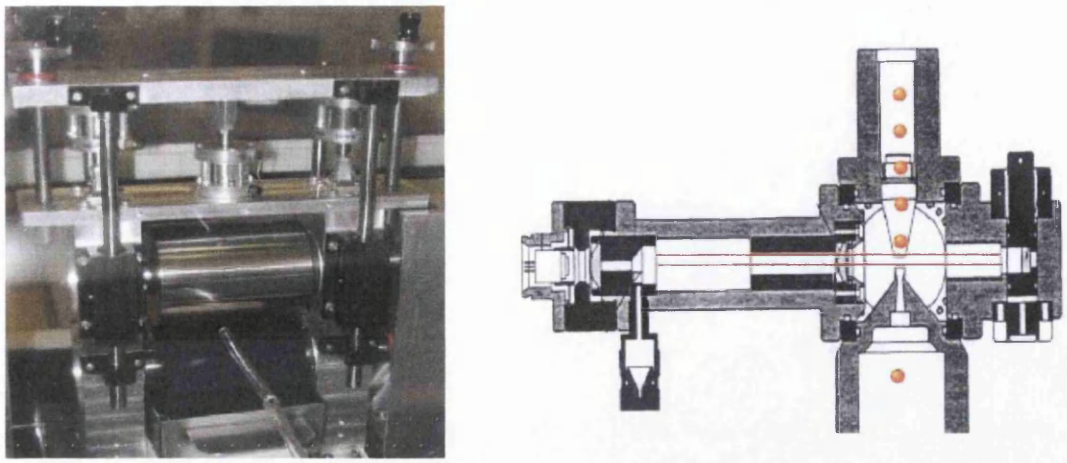

Figure 2-8 Owens (2005) used an Aerosizer DSP system to collect and calculate the misting droplets number and mass at the nip exit (right image). The droplets were analysed by the adapted laser beam through the droplets pass. The collection tube was set at 8cm away form the nip and had 17mm inner diameter (left image).

Owens was the first that focused on calculating the mass and the number of the misting droplets even for non-viscoelastic fluids or thin films. There was a significant effect of the parameters such as distribution speed, rollers size, temperature and viscosity. The increasing temperature decreased viscosity as found by others (Fuchs, Lindqvist and Wallstrom 1991). However, misting is not fully understood and studies on the complete profile, the characteristics and clear effects of the parameters have not been previously undertaken.

2.7 Rheological properties of lithographic inks

Inks are non-Newtonian viscoelastic fluids with complex formulation. Typical lithographic inks formulation involves binders (usually resins), colorants (pigments), solvents and additives (Thompson 2002) with the objective to produce a fluid that can be transferred between the rollers to provide a uniform transferred film thickness and adhesive with the substrate. Viscoelastic models use the polymer network to predict rheological behaviour. The deformation mechanism includes linear elasticity, plasticity and viscoelasticity. Viscoelastic models proposed by Maxwell and Kelvin consisted of a composed mechanism of a spring with a dashpot to study a variety of viscoelastic materials. However, these models do not predict results accurately when thin viscoelastic fluid films are applied (Zevallos et al 2005).

In 1965 Mill identified the importance of ratio between yield stress and viscosity and that ink film thickness was independent of the viscosity. Rheological characterisation usually examines fresh ink samples. This does not allow the identification of mechanical effects on ink from of the press (Oittinen et al 1992). Viscosity, yield value and tack appear to significantly influence to ink printability (Rosenberg 1991).

A number of authors deal with high shear of the ink in the nip region of the rollers (Chou 1992, MacPhee 1998). De Grâce (1988) claimed that there was no effect of pressure at the nip that affects ink. Most rheometers geometry does not allow measurements at high shear of viscous inks. The ink flows out during shear stress due to adhesive dynamics of the ink and centrifugal forces of the plate or cone rotation. This phenomenon is referred to as the Weissenberg effect (Zevallos et al 2005). The viscoelasticity and thixotropy of lithographic inks depend on the shear rate and time (Pangalos et al 1985). Chou et al (1990) stated that pseudoplastic fluids are independent of time at any shear and yield stress was defined as the minimum to induce the fluid to flow otherwise ink is behaved like solid. They also stated that viscosity decreases with increase temperature, shear stress or time in most lithographic inks and dispersions. Fuchs, Lindqvist and Wallstrom (1991) found that the viscosity of the ink decreases by about 50% with a temperature increase from 23°C to 30°C and it is constant over the entire shear rate. High shear rates also provide consistency to the viscosity. Blayo et al (1998) studied the effect and temperature on the formation of pigment-based network structure and found that the inks exhibited a higher viscoelastic character at 40°C than at 20°C.

MacPhee (1998) claimed the rheological properties of the ink that can affect the ink flow behaviour in the roller nips are tack, elasticity and viscosity. He reported also that tack was affected by speed. Film thickness and additives could also affect elasticity. Podhajny (2002) described tack by the adhesive dynamics between two surfaces during elongation when ink film exists. Mewis and Dobbels (1981) argued that viscoelasticity and bearing friction affect tack which is not constant through the period between the first to the last nip of the roller train. Banks and Mill (1977) altered Stephans equation to understand the factors that influence tack by the following:

$$P = A = 3\mu\eta r^2/h^3 \qquad (5)$$

Coco and Cockerline (1988) found that the equation was not accurate for complex fluids such as lithographic inks while tack varies inversely with the cube of ink film thickness and therefore an ink film that is half as thick as another has eight time its tack. They also stated that cavities extension was affected by surface tension and the factors that affect tack. Further studies such as Aspler et al (1996) showed that tack was not constant through the nips due to ink film thickness instability. Chou, Fadner and Bain (1990) found that ink viscosity decreases with the increasing shear forces. They also found that the internal structure of the ink immobilises the vehicle and the ink becomes more resistant to flow. The increasing strength of the internal structure may also increase viscosity.

The viscoelastic character of the lithographic inks shows a complex behaviour that changes with shear stress and temperature. Rheological properties of inks can explain variations on phenomena and it is important to calculate the complete rheological profile. However, there are no clear records comparing viscoelasticity to tack, or how thixotropy or other rheological characteristics affects the ink transfer mechanisms. Tack is related to the stickiness of the ink and it is usually referred to in the rheological studies of the printing inks but there is not a clear definition of the characteristic. The rheological profile of the ink becomes more complex with the effects of emulsification due to fountain solution at the printing mechanisms. Such interactions have also been studied in order to understand the printing mechanism of the lithographic printing process.

2.8 Ink water balance and interaction

The principles of the process involves the water with ink interaction. The fountain solution properties and its effects were first examined by Rosenberg in 1991. They used a "Litholab" printability tester of FOGRA and a densitometer detector. The results showed that water decreases the ink tack and affects its rheology. Hayasi and Amari (1992) used video and acoustic capture devices placed on a model press to record and analyse images and sounds. The ink/water balance was found to affect ink transfer and also trapping, dot sharpness, gloss and drying rate of ink. They assumed that emulsification was pigment's effect and that the length of the ink filaments

decreases as the amount of the water increases. Huang and Goodman (1995) used the contact angle measurements of the fountain solution on the plate surface to show that the components of the fountain solution provide undesirable effects on plate image areas in comparison with pure water. Wu, Auerbach, Catena (1998) measured the HLB (Hidrophile-Lipophile Balance) values of resins from the ink production industry. The resins hydrophilicity was found to affect rheological properties and the degree of shear thinning. Pineaux, Blayo (1999) used a Tack-o-Scope tester and found that the emulsification and ink water interaction was affected by the ink structure and system temperature. Wickman, Hallstensson and Strom (1995) measured the static and dynamic surface tension between ink and water. They stated that the proportion of isopropyl alcohol in the water and alkyd resins of the ink affect and decrease interfacial tension between ink and water. MacPhee (1998) described and divided the way that water comes in contact with ink by three ways:

1. Emulsification of the water with the ink in the nip
2. Evaporation of the water at the nip exit
3. Surface release from the ink during passage from the nip.

Coco and Cockerline (1988) used printability tester to examine effects such as mottling and pilling. Mottling is the uneven back splitting (back-trap mottling) to next printing unit blanket. The poor absorbency of substrate or the ink repellent effects by the water provide mottling effects. Pilling characterises the built-up ink on the blanket image areas. SAPPI refers a complete study of these effects that are owed to water affects and occurs to high dampening feed or additives that have not adapted to the ink.

2.9 Closure

The offset lithographic printing process consists of a range of mechanisms and materials. The ink distribution system and the presence of the fountain solution generate numerous dynamic phenomena that affect the uniformity of ink transfer mechanisms. Mathematical offset printing-press models failed to predict accurately the ink transfer and overestimated values based on symmetric splitting. The instabilities of the distribution system may be affected by the phenomena that are related to ink splitting mechanisms of the ink at the nip exit of the distribution rollers.

The findings of the literature review prove firstly that the research on misting and ribbing phenomena is inadequate and secondly that not much work has been done on film splitting in roller coating. As a result, ink splitting mechanism is not fully understood yet. Ribbing profile has not been taken into account by mathematical models although related to the split ratio. Misting mechanism is not fully described by previous studies. Also, it is not clear how the printing parameters and rheological properties of the inks can affect those phenomena. Therefore, the purpose of this project is to explore the ink splitting mechanism and to investigate related parameters and rheological properties that generate such dynamic phenomena. It attempts to examine the importance of ribbing and misting phenomena in distribution systems by understanding the background mechanisms. Furthermore, it establishes the methodologies and techniques required in order to identify these phenomena and characterise their profiles, and researches how these are affected or related to the rheology and distribution system parameters.

Lithographic inks are rheological complex fluids even without the presence of the fountain solution. Ink roller trains consist of complex mechanisms with different surfaces and geometries. Experimental techniques have to focus on shorter distribution systems but with similar configuration of an inking train. A closed loop distribution system allows studies on the distribution profile of system based on real inks. However, the use of different inks with different formulations and rheological profile complicates the results because of the effect of printed parameters. The methodology has to be established before a wide range of fluids can be tested.

This thesis focuses on experimental methodologies by using coldset inks (these are inks which set by absorption of oils into the substrate). The rheological threshold can be achieved by changing the viscoelastic character of an ink by modify its rheology with a Newtonian agent without affecting or complicate its primary formulation. A typical fountain solution usually includes other diluted fluids in order to provide low surface tension and high evaporation rates. Ink emulsification is also affected by the additives that are used in the fountain solution such as isopropyl alcohol or alcohol-free solutions and non-ionic surfactant that affects surface tension. However, the effects of the fountain solution properties are beyond the scope of this thesis.

Fountain solution also has high evaporation rates, making it difficult to study the emulsified ink from the press. Thus other components with lower evaporation rates were used to replace the aqueous fount solution in order to allow experimental study under stable conditions. A low evaporation rate substance was required such as Butyl-Diglycol in order to decrease viscoelasticity of the fluid.

The development of the methodology focuses on understanding the distribution profile of the viscoelastic character of the lithographic inks and the effects of the distribution configuration. The knowledge of the instabilities threshold provides information for modifications of the ink train.

3. Instrumentation and techniques

3.1 Introduction

A variety of different laboratory based equipment has been used to characterise the ink emulsions and to create a physical simulation of the ribbing and misting phenomena.

The methodology focuses on extracting fundamental information about the ink transfer mechanism that can describe the distribution nature on inking roller train in offset lithographic printing. Numerous experimental methodologies and instrumentation are required in order to retrieve detailed behaviour and responses of the ink transfer mechanisms through inking roller train. The ink transfer process is a complex procedure that demands a complex investigation in order achieve the most details of the actual mechanisms.

This chapter focuses on instrumentation description that been used to develop methodologies and analysis methods for ribbing and misting phenomena. The next section 3.2 looks at the rheological characterisation of the ink emulsions using shear rheometry, measurements of surface energy and tack. This does not include the development of extensional rheometry, which is covered in more detail in chapter 5 nor the use of the tack meter to simulate ribbing and misting a simple nip system, the development of which are discussed in more detail in chapters 6 and 7 respectively. Section 3.5 looks at the measurement techniques used in this study. Butyl-Diglycol was used to simulate the dilution of the ink by the fount solution and for controlled modification of the ink rheology. In order to establish whether this had any detrimental effect on the ink transfer which may have affected the results, a study was undertaken using an offset press simulator. This study is described with the results in section 3.4. Finally, confirmation experiments were run at the end of the study. The principles of the orthogonal array methodology used for the statistical design of experiments for this phase of the study are described in section 3.5.

Instrumentation selection focuses on building reliable methodologies and research philosophy around offset lithographic printing and other high speed printing or coating processes that do not allow real time measurements. Printing simulations are the basic instruments when a printing process is examined. Such devices allow the study of printing materials under a range of process conditions that affect printing quality. Rheological characterisation is an important process as it defines a number of fluid mechanical properties. Printing inks are complex fluids and rheological examination needs to be extensive in order to collect maximum information for their complex behaviour on roller distribution systems. Numerous devices have been developed by the industry in order to examine different rheological characteristics of the inks. The problem of each methodology is not only about which instrumentation to select but also how to use it to produce meaningful results.

3.2 Rheological characterisation

Rheological characterisation is the fundamental process to provide a detailed description about the ink that is the main fluid involved in the process. Shear and elongation viscosity is measured to identify the structural effects to the ink body under nip region circumstances. Tack and printing density is also involved with rheology. Tack describes the adhesive dynamics that are usually involved with the stickiness behaviour of the ink which affects the transfer mechanism between rollers. On the other hand, printing density determines the transfer properties of the ink into substrate or printability. Tack and printing densities are compared with rheological characteristics or profile of the ink. Thus, they provide a link between rheology and printability or transfer abilities.

3.2.1 Measurements of viscosity

The ink transfer mechanisms generate forces through the roller nip that are not possible to be measured in real time. Thus, rheological changes of the ink can be determined only by tests that explain the internal structure changes and behaviour of the ink solutions.

Bohlin Gemini HRnano-rheometer (Figure 3-1) is a cone and plate configuration rheometer with 1nNm torque resolution. The fluid sample is placed on a cone surface that rotates on a flat surface where it is sheared between the two surfaces and the rheometer calculates the negative torque that occurs due to the shear strain rate of the fluid. The pneumatic motor technology allows extremely low shear rates and can be measured accurately at extremely low or high viscosities. The motor configuration allows steady, transient and dynamic modes for strain or stress controlled tests (Malvern instruments 2007). Rheometry determines a wide range of fluid properties throughout standard tests. A large number of different tests can be undertaken such as shear viscosity, oscillation, relaxation and creep to creep recovery.

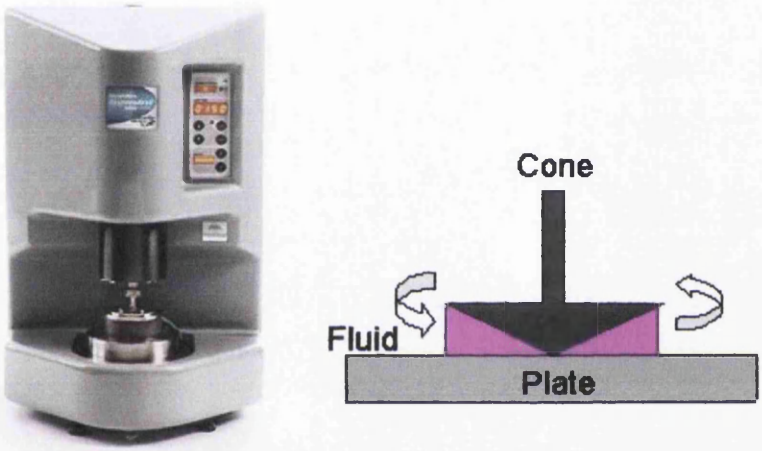

Figure 3-1 Bohlin Gemini HRnano-Rheometer manufactured by Malvern Instruments. The system uses the cone and plate configuration (right).

The viscosity of a liquid is characterised by its resistance to flow when a force is applied to it (Figure 3-2). Lithographic inks are complex fluids and so viscosity is one of the primary parameters to be examined. The test is included in order to determine viscosity under different shear stresses. The cone and plate configuration is a standard method that measures the viscosity of viscous fluids such as lithographic inks. The fluid sample is placed between a plate and a cone of the same radius with very small angle (Figure 3-3). The velocity profile is linear with respect to the θ position in the gap for a very small angle. The gap between truncated cone and plate is set such the virtual nip would make contact with the plate. Viscosity is proportional to the torque and inversely proportional to the rotational speed (rad/s). Viscosity (η) is determined as a function of shear stress (τ) under steady shear rate (γ), table of shear rates or complex shear rate.

Shear stress (τ)= $\frac{T}{\frac{2}{3}\pi r^3}$ (6)

Shear rate (γ) = $\frac{\omega}{Sin(\theta)}$ (7)

Viscosity (η) = $\frac{\tau}{\gamma}$ (8)

Where:

T is the torque

r is the cone radius

ω is the imposed angular rotational speed of the cone

θ is the cone angle

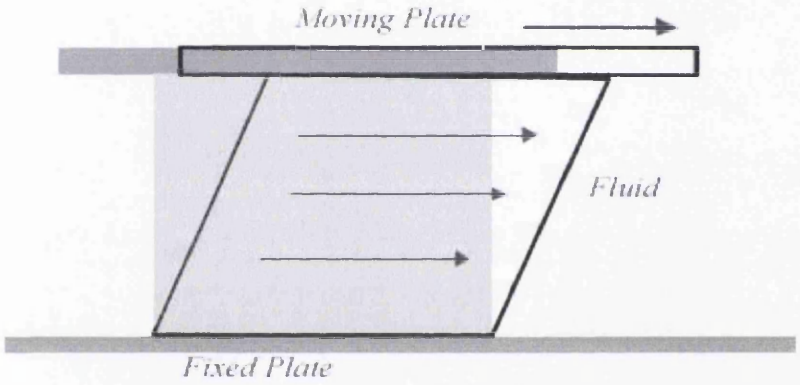

Figure 3-2 The moving plate forces fluid to move and shear stress is generated between the two plates.

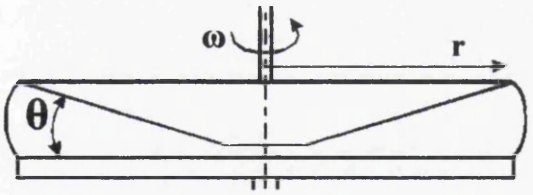

Figure 3-3 Cone and plate geometry

Relaxation modulus is calculated as a function of time by step change in strain. This uses the creep to creep recovery test where zero viscosity and yield stress can be also determined. This test examines the ability of ink polymer solutions to rebuild their structures when low or zero stress is applied. The ink viscosity drops with sudden high shear stress that exceeds yield stress. The ink structure recovery is determined by applying a low shear stress of 0.01 that allows restructure while strain is

monitored as a function of time (Malvern instruments 2007). This is used in order to examine the recovery rates of the ink polymers solutions when shear stress is applied at the rollers nip contact. This can show also the performance of the inks from the nip outlet and before the next nip inlet. The extremely high shear stress in short time provides also an example of the nip contact effect.

Rheometer accessories involve a wide variation of cones that are selected according to the viscosity of the fluid. Solvent trap is used when material is affected by evaporation. The trap generates a saturated environment that prevents solvent evaporation. Rheometer configuration allows also modification of experimental time and temperature. This flexibility of parameters allows the study of the performance of the fluids under different environments.

The Bohlin software uses a flexible interface that allows a wide range of parameters to modify a rheometry test. This is a most important ability of the system because the operator can design and perform extremely advanced rheological tests with steady or accelerating levels of the parameters such as table of shears. The program includes data analysis and viscoelastic analysis.

An overview of the experimental methodology deals with the following tests:

Hysteresis (Thixotropic loop)

Oscillation (Frequency sweep)

Relaxation (Creep to creep viscosity)

Shear viscosity (Table of shears)

3.2.2 Shear viscosity, viscoelasticity and recovery

Bohlin Gemini rheometer was used to examine characteristics such as shear viscosity, thixotropy, viscoelasticity and relaxation of the emulsions. The pre-settings were modified be selecting the parameters of temperature, time and torque or frequency. Cone geometry was changed manually. The selection of the cone geometry was based on the viscosity of the fluids. Small cones are recommended for

viscous fluids and thus the CP2/20mm cone geometry was selected for the tests. Plate temperature was selected in a steady mode for all the tests of 24°C. However, some of the parameters were modified in order to study the relations with the tack of the ink and the dilutions.

Precondition time (relaxation) plays an important role on rheological measurements for viscoelastic fluids. The fluid viscosity decreases rapidly due to generated stress by the compression of the ink sample between the cone and the plate. The viscosity decrease was independent of the placement method and compression dominated to this effect (Figure 3-4). The viscosity decreases 60% due to cone compress effect on the plate and that was independent on the placement method of the ink. The placement of ink by a pipette or a typical glass rod does not show any variation. The delay time indicates the shear stress effect due to systems compression. The precondition time is important in order to examine a relaxed sample, 10-minute precondition time was therefore used as this found to be the time required for the fluid to recover and reach a steady viscosity. The following paragraphs describe settings and procedures extensively for each rheological test.

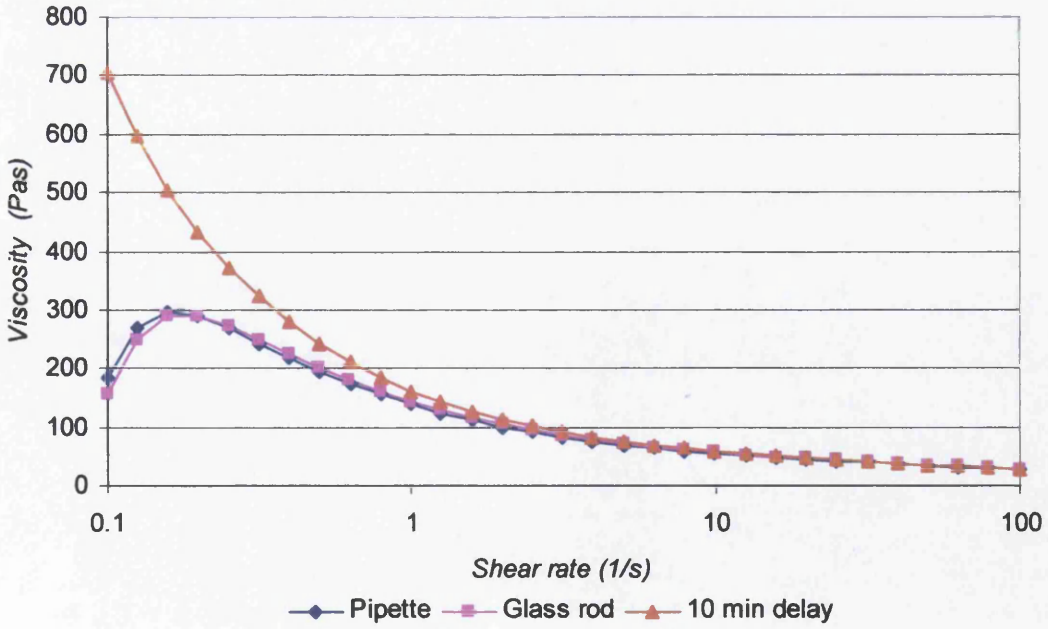

Figure 3-4 Shear viscosity curves with and without precondition process.

The viscosity of most dispersion including printing inks tends to decrease with increasing shear or time (Chou et al 1990). Table of shears determines the shear thinning behaviour of the fluids with gradual changes in shear stress.

The table of shears was carried out by step accelerating shear stress. The applied shear stress was gradually increased by 31 steps in a logarithmic scale. The shear stress sequence used a table from 0.1Nm to 200Nm torque, because that was the maximum torque that allowed sample consistency for the test. The higher than 200Nm extrapolated the sample due to cone velocity. The test was carried out three times for each emulsion. The 70 μm gap was selected for the shear viscosity test equal to the truncation gap value. Precondition time, temperature and cone geometry were set as described above. Viscosity values were plotted as a function of shear rate.

Thixotropy is a phenomenon of viscoelastic fluids that viscosity changes are time or shear dependent. It is characterised by the shear thinning behaviour of the fluids and the relaxation or recovery rates. Thixotropy is calculated by measuring the shear stress or viscosity while shear rate changes. The shear rate was gradually increased to the maximum torque value, then returned to the minimum torque level. The latter allowed recovery of the material microstructure. The difference of the viscosity curves generates the hysteresis loop where the loop area determines thixotropy of the material (Figure 3-5).

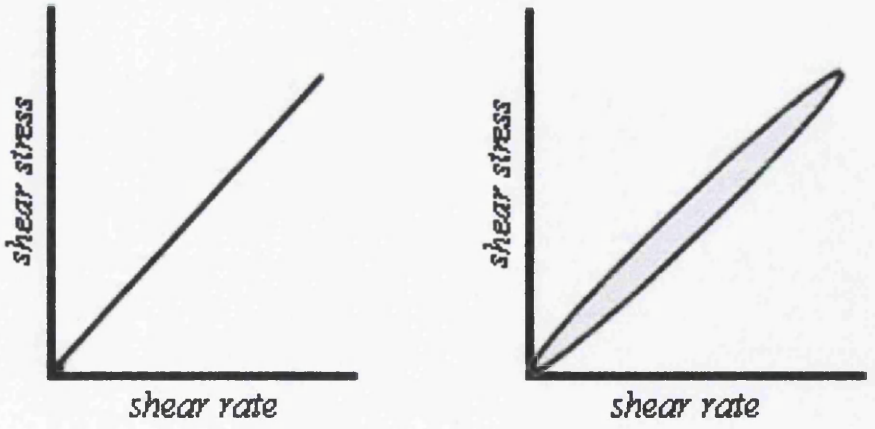

Figure 3-5 Ideal fluid does not show difference with increase or decrease of the shear rate (left). Thixotropy is determined by the difference area of the hysteresis loop (right).

Oscillation test examines viscoelastic properties as a function of frequency by using the cone and plate geometry with CP4/40mm truncated cone. This cone geometry increases accuracy of the measurement because fluid is spread and examined in a wider area. The test uses frequency sweep in order to determine the storage (elastic) modulus (G') versus the viscous (loss) modulus (G'') and the complex viscosity (η'). The storage modulus G' is proportional to the stress in phase with the strain, while complex viscosity (η') is proportional to stress 90° out of phase with the strain (Cook and Brockhurst 1980). The function G''/G' measures the relationship of the viscous to elastic modulus for a material at a given frequency. The complex viscosity (η^*) is defined by the complex strain rate ε^*

Stress (τ) = $\tau_0 \cos \omega t$ (9)

Strain (ε) = $\varepsilon_0 \cos (\omega t - \delta)$ (10)

Storage modulus $G' = \tau/\varepsilon \cos\delta$ (11)

Loss modulus $G'' = \tau/\varepsilon \sin\delta$ (12)

$\varepsilon^* = j\omega\varepsilon$ (13)

$\eta^* = G^*/j\omega$ (14)

Where:

$j = \sqrt{-1}$

ω is the angular frequency

δ is the phase angle

t is the time

The phase angle and amplitude ratio (τ_0/ε_0) will generally vary with frequency (Figure 3-6). The pure elastic materials store the deformation energy that is applied to it and the phase angle becomes 0 degrees. The pure viscous materials loose the applied energy and the phase angle is 90 degrees. Lithographic inks are usually viscoelastic fluids and their behaviour is expected between these two phases. The phase angle is an indicator of the degree of the viscoelastic behavior of polymers (Zeghal et al 2007).

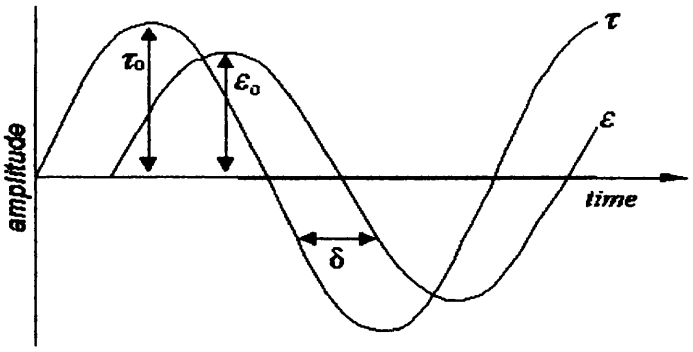

Figure 3-6 Stress and strain wave forms

Frequency sweep: Oscillation test determines the elastic (storage) modulus (G'), the viscous (loss) modulus (G'') and the complex viscosity (η^*) of the fluid. The characteristic modulus at each frequency indicates the dominant behaviour of the fluid between elastic and viscous. When phase angle between stress and strain approaches 90^0 viscous modulus dominates to elastic modulus (Ferry 1960). The dominant viscous modulus indicates not broken structure. The decrease in phase angle indicates elastic modulus as dominant to the viscous.

DAT1100 dynamic contact angle (Figure 3-7) allows measurements of surface tension and contact angle of fluids. Surface tension is the surface layer effect of a liquid to behave as an elastic sheet due to intermolecular dynamics. In the bulk of the liquid each molecule is pulled equally in all directions by adjacent molecules that cause a net force of zero. The molecules are pulled inwards at the surface of the liquid by other molecules inside the liquid. The absence of outside molecules generates an internal force of molecular attraction that generates a stretched elastic membrane with regard to the negligible forces of the outside air molecules. As a result, the liquid squeezes itself together until it has the locally lowest surface area possible.

The DAT1100 uses a precision pulse system to apply the droplet of the tested fluid (Figure 3-8). The fluid is supplied by a syringe (1ml) through a tube. At the other exit of the tube a droplet is formed. The surface tension measurement is carried out by the shape of the droplet that is pendent from the tube exit. The Pendant drop technique has been introduced by several authors for the simplicity and the accuracy

on surface tension measurements (Li et al 1996; Juza 1997). The shape of the pendant drop in a homogeneous gravitation field can be described through Young-Laplace equation, expressed as 3 dimensionless first order equations:

$(2+\beta z) = d\theta / dS + \sin\theta / X$ (15)

$\cos\theta = dX / dS$

$\sin\theta = dZ / dS$

$$\gamma = \frac{g\Delta p b^2}{\beta} \quad (16)$$

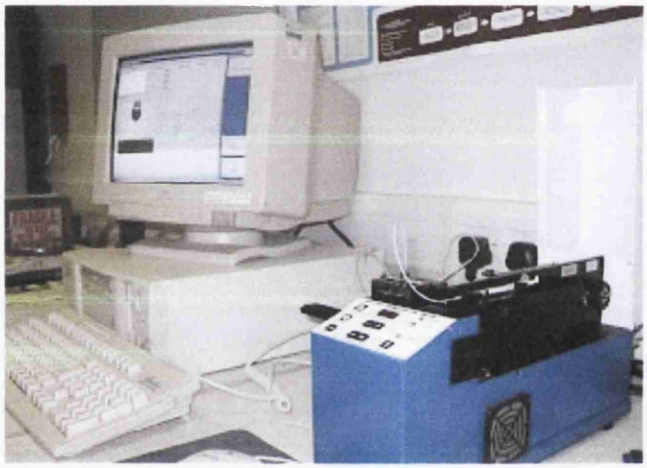

Figure 3-7 The Fibro Dat1100 dynamic contact angle. It was used to carry out the surface tension of the fluids through the pendant drop method.

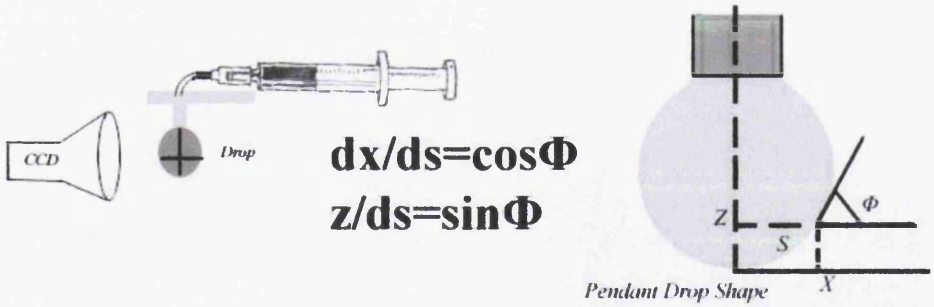

Figure 3-8. The DAT1100 uses a precision pulse system to apply the droplet of the tested fluid. The fluid is supplied by a syringe (1ml) through a tube. The surface tension is carried out by the shape of the droplet that is pendent from the tube exit.

Contact angle is the formed angle between a liquid drop in contact with the surface due to adhesive dynamics, and surface tension. Typical surface tension tests include Wilhelmy plate, Metal rod and Pendant drop shape analysis. The contact angle is carried out from the drop shape of a droplet on a substrate. Using the same process

with the syringe, a droplet applied on the substrate via the tube. The contact angle is carried out by the angle between droplet and substrate. A CCD camera captures the images every millisecond to calculate the contact angle or the surface tension of the tested fluid. The contact angle analysis specifies also the wetting rates of substrates with higher accuracy than other static methods.

The Pendant drop shape method was used to determine the surface tension of the emulsions through the Fibro DAT 1100 contact angle system. Surface tension was determined by analysing the dimension of the fluid drop that was formed while it was extruded from a thin tube. Lithographic inks are viscoelastic fluids. A modification was made to the system in order to accommodate these viscous materials. The steady pressure of the syringe compresses the ink in the tube. The ink structure gradually was relaxed due to viscoelastic character of the ink. As a result the ink flows and drops, instead of forming drops. The tube was shortened in length to decrease this effect and the syringe was operated in manual mode to control the pressure according to drop formation. The drop size was captured by a CCD camera where angle, horizontal and vertical dimensions calculated the surface tension through the interface of the software according to the horizontal and vertical dimension of the drop. Temperature control was not supported by the system configuration. Each ink emulsion was measured five times to determine surface tension.

3.2.3 Adhesive dynamics (Tack)

In order to understand the whole operation it is necessary, first of all, to understand the individual flows between pairs of rolls as mentioned by Carvalho (1997). Instrumentation is based on existing standard devices that are used extensively by the printing industry and techniques are modified in order to be modulated with the actual methodology. The extensive use made of this work instrumentation in industry and research validates its accuracy and repeatability. However, preliminary tests were important in order to examine quality process parameters.

Tack is described as the stickiness of a fluid. Tack describes the adhesive dynamics between two surfaces during elongation when fluid exists (Podhajny 2002) between them. Printing inks are examined by specific instruments that are called tack-meters.

Tack is the force that is applied on the measurement roller by the motor roller during rotation (Figure 3-9). However, there is not a clear description of tack and the rheological properties of the ink. The methodology focused on understanding and identifying how tack is related or affected by other rheological characteristics.

IGT Tack tester 450 (Figure 3-10) has three rollers train configuration in order to distribute the ink and measure its stickiness in gram meters units. The closed loop distribution system geometry of the IGT tack tester provides advantages such as controlled ink volume in order to investigate related phenomena with the ink splitting mechanism. The system geometry consists of three rollers in nip contact. The driven metallic roller is the core of the system. The two elastic rollers are rotated by friction with the metallic motor roller surface peripheral with 90^{o} degrees apart (Figure 3-9). The measure roller is supported on pressure sensors that calculate the change in friction applied to the measure roller during rotation by the motor roller. The other roller that supports the system by oscillation along the axis in order to equalise the ink film thickness across the rollers.

The ink is applied on the rollers by a pipette. The system allows control of temperature and distribution speed. The roller surface (distribution) speed can be varied from 50 to 450 meters per minute (m/m). The tack value, temperature and distribution speed were recorded predetermined intervals throughout experiment. The temperature was controlled by an external water cooling unit which supplied water through the internal drum of the motor roller. The operating interface allows also modification in oscillation frequency from 0 to 5 Hz.

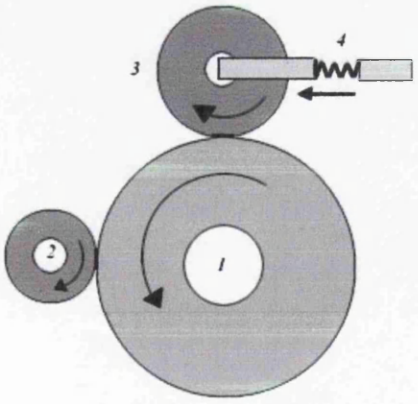

Figure 3-9 Tack Tester configuration 1 motor roller, 2 Measure roller, 3 Oscillator, 4 Press sensor

The temperature control was set at 25°C. This temperature was used throughout this and subsequent experiments such as the printing density test (section 3.3) and the rheology tests (chapter 4). The test was based on BS ISO 12634:1996. The sample was loaded by using IGT micropipette on the distribution rollers. The ink film thickness was defined according to the sum surface volume (742cm^2) of the system rollers, 0.3 ml ink 3.9μm average ink film thickness and 0.6 ml ink provided 7.8μm average ink film thickness. The applied ink was distributed on the system for 3 minutes at low speed to ensure uniform thickness. A relaxation of 10 minutes was applied to ensure viscosity recovery. The system speed was selected in four steps through the run. Each test began with 50m/min for 1 minute and speed was increased in two steps of 100m/min and 150m/min for every following minute. Finally, the speed was decreased again into 50m/min to compare tack difference through speed variations and shear effects. The tack measurements of the complete run were exported to a computer that was connected to the tack tester.

The rollers were thoroughly cleaned and dried between tests. Tack tester is very sensitive residual solvent from cleaning, which can produce up to 30% reduction in tack. A temperature variation test was also carried out in order to examine tack variations when temperature varies. The temperature test was varied from 25°C and 30°C at a constant speed. This temperature increase drops viscosity 50% as stated by Fuchs et al (1991). The same range was used in the shear rheometry investigation. Variation of ink dilutions in temperature allowed the comparison of responses between tack and viscosity. Measurements were carried out every 10sec. Tack values were averaged for each set of parameters and were plotted into graphs.

Figure 3-10 The Tack tester 450 manufactured by IGT testing systems

Potential sources of errors:

- Ink applying uniformity. The ink is applied on the system manually by a finite pipette. This process can be subject to operator variation. The elimination of this effect occurs in the distribution process before the test. The longer pre-experimental distribution time can provide higher ink uniformity along the rollers.
- Non equal film thickness between rollers. The concept of 50/50 split ratio indicates that the distribution process provides a uniform ink film thickness on a closed loop distribution system. This was measured and calculated through an ideal model, which does not differ considerably from how the system works. However, the stability of tack value indicates the uniform ink on the rollers. The distribution time was two minutes and was selected by preliminary tests.
- Cleaning process. The rolls were cleaned with solvent between the experiments. The required drying time could vary from one hour to five hours depended on the environmental conditions. Preliminary tests showed that an amount of solvent is deposited on the rollers surface and affects the ink rheology on the following test. An air dryer was used to ensure all the solvent was eliminated.
- Gap variation due to ink film thickness. The system does not provide a fixed gap. The increased incoming ink through the nip is possible to lift the roller and increase the gap between the rollers. This gap increases with the increased ink on the system. It is not possible for real time measurements of the nip gap.
- Gap variation due to rollers position. Both the two elastic rollers are in rolling with the metallic roller. The large measurement roller is positioned position on the top of the metallic roller while the small roller is attached at the side of the metallic roller. The weight of the measurement roller generates a level of pressure in the nip. The configuration of the small roller allows vibration that generates micro-oscillation effects during rotation.

- Roller slip. The increase film thickness floods the nip. The elastic rollers rotate due to surface contact with the metallic roller which is also the motor roller. Roller slip is present when the nip distance increases in such way that ink adhesive dynamics are not able to pull the surface of the roller. So the roller rotates slower than the motor roller and the forward roll system behaves like a reversed roll.

3.3 Print Characterisation techniques

3.3.1 Colour measurements

Gretag-Magbeth SpectroScan is a scanning spectrophotometer with 0/45 geometry. Spectrophotometers are instruments that measure colour and density by calculating the reflection and absorption rates of light. Spherical and 0/45 spectrophotometers are two basic categories that depend on the optical geometry (Figure 3-11). Spherical spectrophotometers are specific instruments that use an integrating sphere that diffuses the light from the source. The detector calculates the reflectance of the sample in a vertical angle. Spherical spectrophotometers operate in included and excluded mode and can calculate repeatable measurements in any direction. T sphere instrument uses a diffuse illumination and is generally used for advanced surfaces such as glossy and textured coating of materials (Mouw 1995). However, this is not required for the project. 0/45 provides accurate density measurements and fast process for calibration. This geometry is more suitable for mat papers and lithographic inks and it is extensively used by the printing industry.

Spectrophotometer used to measure colour and density values of ink on the substrates. The visible wavelength is measured in nanometers. Electronic filter is programmed to allow a specific wavelength of light to pass through it. The visible light spectrum ranges from the reds at 400 nm to the blues in the 700nm range. The device analyses Red Green and Blue colour values at every measurement. A colour C can be defined by the Rc units of red, Gc units of green and Bc units of blue according to Grassman's Law of the additive colour mixture.

$C = Rc(R) + Gc(G) + Bc(B)$

These values are converted into L, a, b values of the CIE colour system in a three dimensional model (Figure 3-12). The CIE is the system that classifies colour according to the human visual system. The L* axis represents the lightness and extends from 0 (black) to 100 (white). The other two coordinates a* and b* represent redness-greeness and yellowness-blueness respectively. It needs to convert the colour specification in terms of tristimulus values. Thus the three-dimensional colour space is defined by X, Y, and Z values. The chromatic coordinates x, y, and z are used to specify the colour by calculating the fractional components of the tristimulus values as follows:

$$x = X/(X+Y+Z) \qquad (17)$$

$$y = Y/(X+Y+Z) \qquad (18)$$

$$z = Z/(X+Y+Z) \qquad (19)$$

The XYZ convertion depends on illumination and the standard observer thus it is necessary to refer these parameters (Sharma 2003). SpectroScan uses 0/45 geometry that means 45 degrees between light source, measurement area and observer. The spectral range of the device is 380 to 730 nm and was operated under reflection mode. It allowed measurement with different illuminants such as D50, D65, A or C. The measurements were carried out on black backing surface by using D50 illuminant and D65 filter with 2 degrees standard observer. The device performs measurements in scanning mode according to the sample dimensions. The scanning range depends on the measurement analysis through the methodology and was modified as described in the paragraph above.

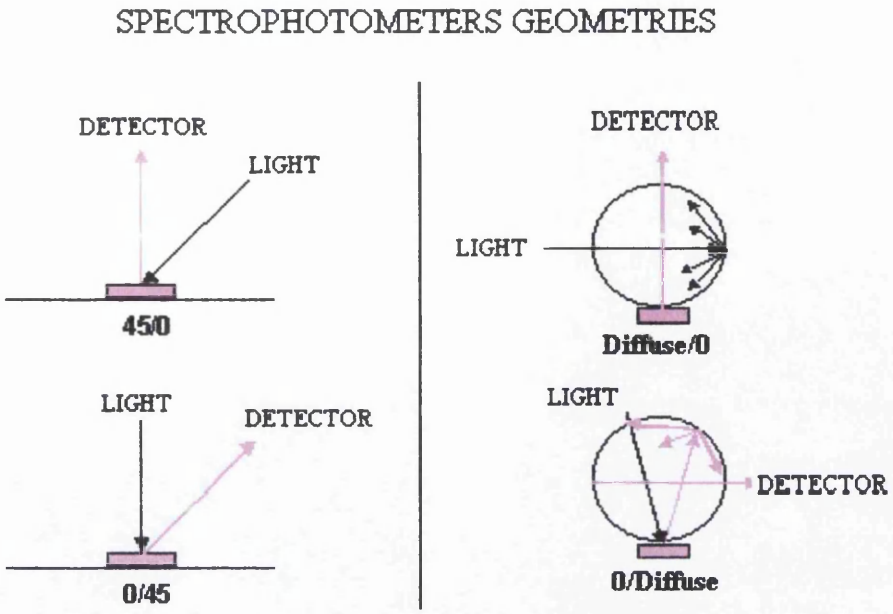

Figure 3-11 The geometry of a spectrophotometer specifies the optical geometry between light source, reflecting surface and detector. 0/45 (left) spherical (right).

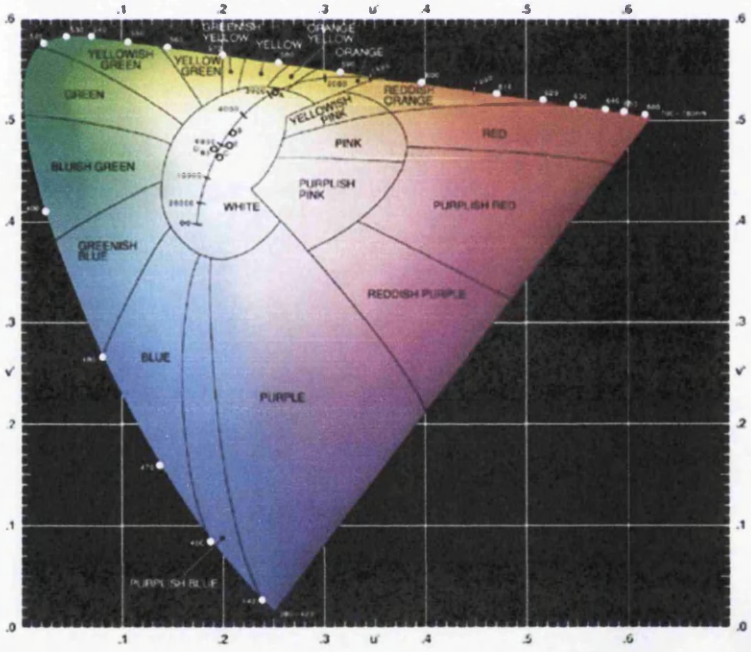

Figure 3-12 CIE Lab 1976 colour space. Image courtesy of Photo Research, Inc

3.3.2 Image Processing

Leica Wild M3Z stereomicroscope was used for image analysis. It consists of an optical system that allows 6.5x to 40x magnification. It can be used as analogue or digital capturing device. A CCD camera is used to capture the analysed image and it is saved on a computer as a digital image. Further images can be analysed by image analysis software. A ring light source is used to illuminate the measured sample that

allows light uniformity around the lens area. Stereomicroscope was used to define misting droplets dimensions and dispersion on misting trap. Misting trap and methodologies are described further in Chapter 6.

3.3.3 Surface topography

White Light Interferometer NT2000 (Figure 3-14) allows non-contact vertical scan of surfaces. The surface analysis is calculated by a sequence of images based on light reflection by the surface. The principles of the system are based on a single light beam that is split in two beams (Figure 3-13). The light is converted in parallel light through a system of lenses and lead to a beam splitter. The first light beam leads to the reference surface and the other light beam leads to the measuring surface. The reference surface (mirror) is usually set in a slight angle to produce the fringes. The two reflected light beams interfere and lead to the observer or the CCD camera (Blant 2006). The system scans vertically through focus at evenly spaced intervals. A CCD camera captures the frames of the interference data through vertical movement via a piezoelectric motion transducer. The surface differences come into focus at different heights. The fringe contrast (intensity) increases as the sample comes into focus, and decreases as the sample falls out of focus.

The system is supported by Vision32 analysis software which combines these patterns into a 3D image. The changes of the patterns determine the changes to the surface and the profile is plotted according to the changes of the fringes. The system allows Vertical Scanning Interferometry (VSI) and Phase Shifting Interferometry (PSI) or a combination of both modes. PSI is used for very smooth surfaces without steps such as optics and other polished surfaces. Phase shifting differs from the vertical scanning since is based on the analysis of the phase transition of the fringes; this method has a measurement range of few nanometers and is therefore limited to very smooth surfaces such as a polished mirror. It is unsuitable for surfaces found in the printing industry. Vertical scanning is a very flexible technique that allows the scanning of large areas and is only limited by the magnification lens used and depth limited by the movement of the objective versus the reference mirror (1 nm depth is easily achievable).

VSI is less accurate than PSI but is suitable for rough surfaces with up to 500nm minimum roughness that allows a depth ranging from few microns to around hundred microns. Its specifications are perfectly adequate for most of the surfaces used in printing and the measuring of thin ink film thicknesses on rollers (Figure 3-14).

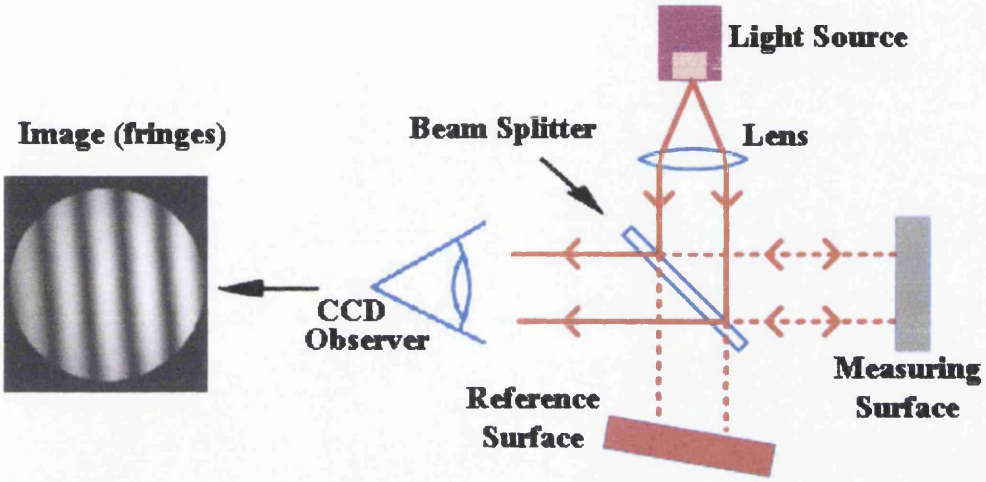

Figure 3-13 Schematic diagram of white light interferometer. A single light beam is separated into two light beams. The reflected light beams interfere and lead to a CCD camera that captures the image.

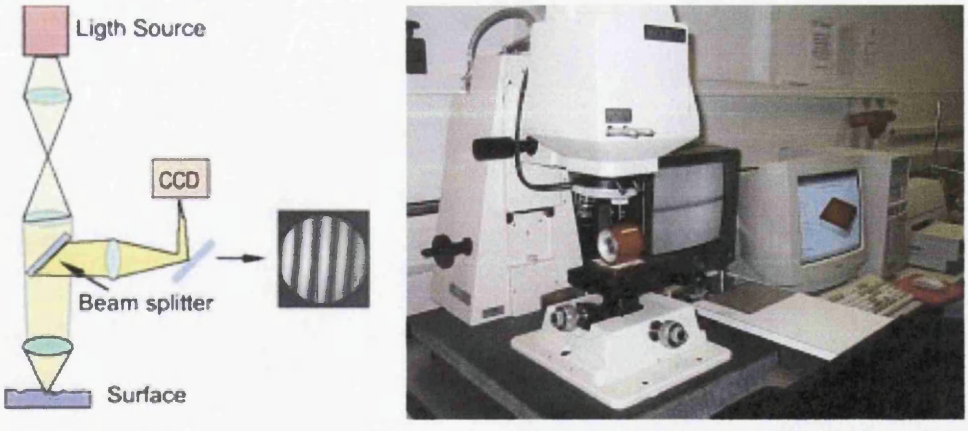

Figure 3-14 WYKO white light interferometer NT2000 configuration manufactured by Veeco systems. The system was used to measure ink film thickness on rollers surface.

3.3.4 Large area image capture

Epson Perfection 4990 Scanner is a flatbed configuration scanner that transforms 2D hardcopy images into digital files with high accuracy in dimensions and colour.

The hardware consists of a glass pane which functions as image carrier or frame. A bright light source illuminates the image under the pane and moves with the CCD that analyses and transfers the colour information (Figure 3-15).

The image is placed face down on the pane and an opaque cover is placed on the top to exclude ambient light of the environment. A white cold cathode fluorescent lamp is used as light source to illuminate the image through the pane. Alternate 6 lines colour Matrix CCD with micro lens is used to detect the light reflectance from the image. Light reflectance is transformed into RGB colour information and transferred to the computer. The supporting software combines the array of that information and generates the digital image from the original scanned image. The accuracy of the process depends on the quality of the pane, the uniformity of the light source and the quality of the CCD and the optics. The system allows up to 48 bit (281.5 trillion colours) with 50 to 12800dpi (dot per inch) image resolution. The increased resolution provides more detailed image information but also increases the image file, which means less flexibility especially for A4 (216 x 297mm) image size. The resolution of 1200 dpi is detailed enough to digitise misting dots of 20 to 100 μm accurately. Additional resolution of 300 dpi is applicable in order to digitise ribbing profiles. This methodology and scanner resolution is described further in Chapters 6 and 7 which deal with the development of techniques in misting and ribbing analysis.

Code and macros have been developed on software programming to complete the methodology and extract detailed information from the captured images. Octave software was used in order to examine ribbing profiles through fourier analysis. MatLab was also used to calculate elongation viscosity. Both codes have been developed by Davide Deganelo in the Welsh Centre for Printing and Coating of Swansea University. Image-J was used for digital image analyser of captured ribbing and misting images and converted them to grey scale numeric profile.

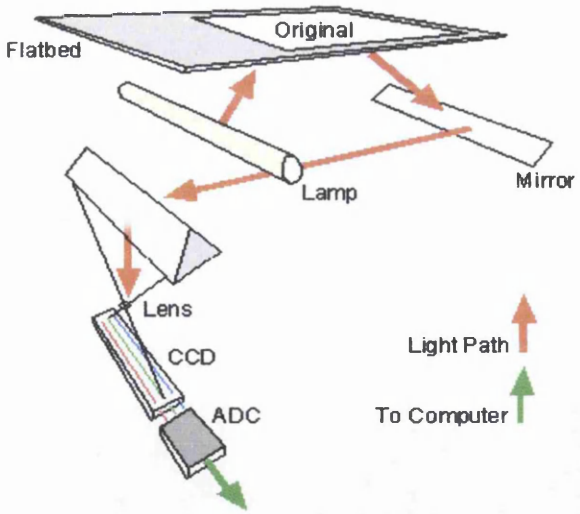

Figure 3-15 Typical geometry of a flatbed scanner.

Potential sources of errors

- Scanner light non-uniformity. Flatbed scanner provides increased light at the middle of the scanning area. As a result, values need calibration by using a specific profile for the actual substrate.
- Threshold limitations. The calculation of density according to grey values of the image is confused when the density is extremely high or low. In misting calculation, multiple dots in the same area are calculated as a single dot and very small dots disappear. As a result, average size increases significantly when misting provides increased coverage area on the misting trap. Similar errors are located with ribbing analysis when thin or extremely thick ink is present.

3.3.5 Measurements of print density

Printing density is determined by measuring the colour reflectance of the ink of the printed substrate according to the visible spectrum. This is described by Beer's Law where density is described by the log ratio of the reflected light from a surface and the transmitted light through the surface. There are a number of standard devices that are used to lay an ink film thickness on the substrate. The selection of those devices usually depends on the characteristics of the substrate and the ink. K-bar and printability testers belong to standard instrumentation that is used when printing density tests are performed. However, the purpose in this methodology was to define

transfer instabilities according to viscoelastic character and tack of the ink solutions and thus the printability tester was used. This allowed studying the printability performance (ink transfer) of ink solutions with different rheological characteristics when very thin film thickness applied. K-bar is used when opacity tests are performed in order to determine colour or opacity differences and that was out of the scope of the thesis. K-bar is not suitable for extremely thin film thickness such 2 μm. IGT printability tester can apply such thin film thickness of inks. The opacity of the dilutions was examined by printing on a leneta paper. Leneta paper is a test card substrate separated by black and white areas. The printed surfaces are measured separately and density and colour values averaged for the black and the white background. The colour difference characterise the transparency of the printed ink film thickness and the suspension. An ideal opaque ink has a difference of 0 between black and white printed surfaces. Printed density was determined by the light reflectance according to the ink film thickness. This is described by Tollenaar-Ernst equation which is used extensively by the printing industry (MacPhee and Lind 2002).

$$Dpr = Dsr(1-\varepsilon^{-mh}) \qquad (20)$$

Where:

Dpr = Print density at film thickness h

Dsr = Saturation density

Rsr = Saturation reflectance $=10^{-Dsr}$

m = Constant in square meters/gram

h = Print ink film thickness, in grams/meters^2

The printing density of the emulsions was defined by the density difference of the printed paper and the substrate density before print. The density and L, a, b values of the samples were measured by the Gretag-Magbeth 0/45 scanning spectrophotometer (Figure 3-16). Spectrophotometer was set with D50 light source and D65 filter with 2 degrees observer.

Fifteen measurements were carried out for each printed sample and values were averaged to define the average density of the sample. The average value did not show significant variations between 10 to 20 measurements across the substrate. Extended

measurements were also carried out with 200 density and L, a, b measurements per sample. The density and L, a, b values were carried out in scanning mode across the width and length of the printed substrates for each sample. This allowed detailed examination of the printed samples surface morphology and variations of ink transfer by variations into emulsions rheology and tack. ΔE L, a, b values were plotted into surface graph to visualise the ink transfer variations on the printed substrates. The colour difference ΔE was defined by CIE L, a, b colorimetric calculation formula of 1976 (Robertson 1977).

(CIE Lab 1976) $$\Delta E = \sqrt{(L_1 - L_2)^2 + (a_1 - a_2)^2 + (b_1 - b_2)^2} \qquad (21)$$

Figure 3-16 Printed strips are measured by a scanning spectrophotometer.

3.4 Evaluation of the effect of dilution of the ink with Butyl-Diglycol

Lithographic coldset cyan ink was selected for this research program as being a representative commercial ink. Butyl-Diglycol (BDG) was used to dilute the ink in different concentrations and to study the ink transfer performance and characteristics in relation to the rheological profile and tack. Butyl-Diglycol ($C_8H_{18}O_3$) is a clear, low-volatility, mobile liquid with a very faint, mild odour. It is miscible with many common solvents, e.g. aliphatic hydrocarbons, alcohols, ketones, aldehydes, ethers, glycols, glycol ethers and water and its typical viscosity is 5.9 Pas[i] and its density 0.955. It is soluble in water and it is used in industrial coatings, specialised coating and in lithographic printing fountain solution due to low vapour pressure and excellent dual functionality solvent properties in comparison to many other monofunctional chemicals. This allows suspensions with low evaporations rates and complex characteristics such as fountain solution of the press. The dilution with a low evaporation agent allows the long term study of controlled suspensions.

Six ink suspensions were produced in dilution with the lithographic ink, namely 0.5%, 1%, 2%, 5%, 10% and 20% of Butyl-Diglycol. The ink suspensions were compared with the industrial cyan ink properties as reference. The study related variations into ink viscoelasticity with variations to other rheological characteristics, tack and ink transfer effects. The controlled dilution is expected to decrease viscosity and tack.

However, before adopting this method of choice for varying the ink to simulate ink/fount emulsion on the press, it was necessary to evaluate it impact on the printability of the ink, i.e. would it be fair repraisenation of the ink behaviour in practise.

Printing was performed on IGT-AC2 printability tester using the IGT high speed inking unit for ink distribution and inking of the printing disc of the tester. The adjustments of the system were similar to IGT Tack tester. This was defined in such a way to compare tack values with printing densities. Any differences during the tests are the result of variations due to operation menu and rollers surface volume of the systems.

IGT AIC2-5 printability tester (Figure 3-17 right) was used to simulate the ink transfer in lithographic printing to evaluate the effect of diluting the ink with Butyl-Diglycol on the ink transfer. The system is based on a forward roll coating mechanism that allows studies on ink transfer mechanisms. The system consists of a main sector that carries the substrate and two printing discs that coat or print on the substrate. The sector operates as an impression drum of the press and the printing disc as form roller or the blanket. The printability tester is used to determine ink transfer phenomena on a wide range of materials that are supplied as thin films in order to be mounted on the sector. The inking process of the printing disc is carried out on an external inking unit.

The tester provides the operator ability to modulate settings such as printing pressure, and speed. Printing pressure is applied between printing disc and sector which can reach 1000 Newton. Printing speed can be set in accelerating or steady mode with low or high speed from 0.2 to 5 m/s. The sector is fixed on the motor of the system

and its surface is aluminium but also packing can be applied. The standard packing is a multilayer paper that is clamped firmly in the front clamp across the rotation and it is secured by the rear clamp of the sector. The printing disc type is supplied with different surface qualities such as rubber, blanket or aluminium coating. The rubber printing disc is recommended for offset inks and the hardness of the rubber is 85 shores which is close to a conventional printing blanket.

IGT high speed inking unit 4 (Figure 3-17 left) is the supporting system for the printability tester. The system consists of three rollers; two metallic rollers with rider and oscillation mechanism and one elastic roller that is placed on the top and rotates by friction with them. The system consists of four independent inking areas across the length. Each printing disc is placed on the top of the elastic roller for inking by the use of a brachium. The system is supported also by an external water cooling unit that allows control of the inking unit rollers temperature.

The ink is applied on the rollers by a finite inking pipette that allows fine control of the ink volume. The ink volume is calculated by the overall surface area of the rollers multiply by the desirable ink film thickness according to the concept of 50% ink splitting through the distribution system. The inking table illustrates recommended ink volumes according to printing disc type in order to transfer the desirable amount of ink for printing to the printability tester (Appendix 1). The table also recommends the amount of ink that is needed between prints in order to replace the ink volume on the system and to provide identical print through the printability tester.

Figure 3-17 The high speed inking unit (left) and AIC2-5 printability tester manufactured by IGT testing systems.

IGT ink settings table recommends 0.6ml ink volume in order to provide 4 μm ink film thickness on the printing disc and 2 μm to the substrate. The ink was applied on the rollers using a fine pipette (Figure 3-18). The temperature was 25°C at the high speed inking unit which also supported by an external cooling unit that circulated water through the rollers internal drum (Figure 3-19). The ink distribution and printing speed was 0.8m/s similarly to the speed that was used at the tack tester with 0.8m/s. The 135gr velvet paper was selected for printed substrate. This type of paper provided better printing quality for the actual inks (coldset) than other substrates due to surface quality and thickness. The process was divided into two steps. The pre-inking of the printing disc was carried on the IGT inking unit and was then transferred to the printing unit to print the sample.

The 10cm rubber printing disc was used for printing. The hardness of the rubber surface was 80 shores, similar to the hardness of a conventional blanket. The inking process was performed for 30 seconds which provided equilibrium to the four rollers system as was carried out by preliminary tests. The paper strip was mounted to the sector of the IGT-AC2 printability tester (Figure 3-20). After the inking process at the high speed inking unit, the printing disc was placed on the tester for printing. The impression force was selected in 300N as was defined by the preliminary printing tests, which also determined the best printing quality for the actual printing materials and the printing speed (0.8m/sec similar to 50m/min of tack tester) with the higher density and ink uniformity (Figure 3-21). The printed paper strip was placed for drying after printing. Coldset inks dry by absorption to the porous substrate and so drying was a time-consuming process that did not allow direct further process such as density measurements (Vlachopoulos 2003).

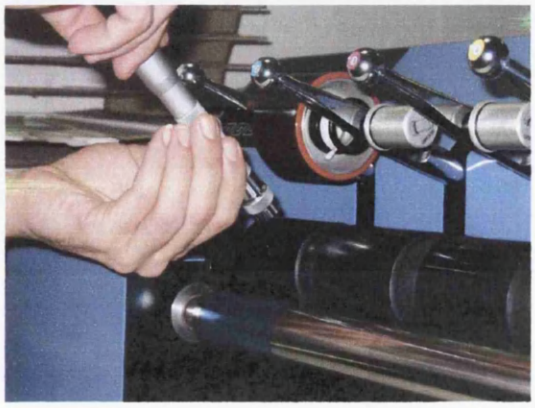

Figure 3-18 Ink volume is applied by a micrometer pipette on the IGT high speed unit

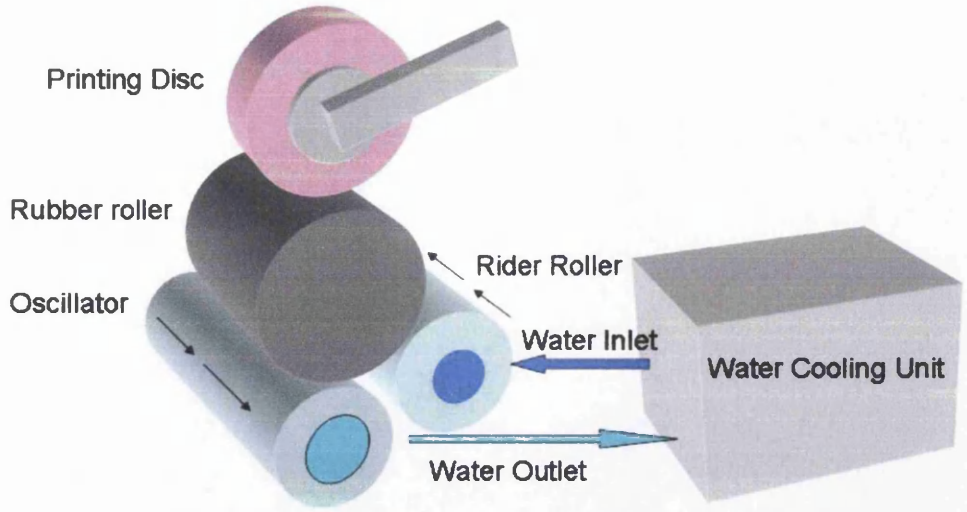

Figure 3-19 The IGT inking unit is supported by an external cooling unit that circulates cold water through the metallic rollers (rider and oscillator). This allows constant temperature on the ink distribution system.

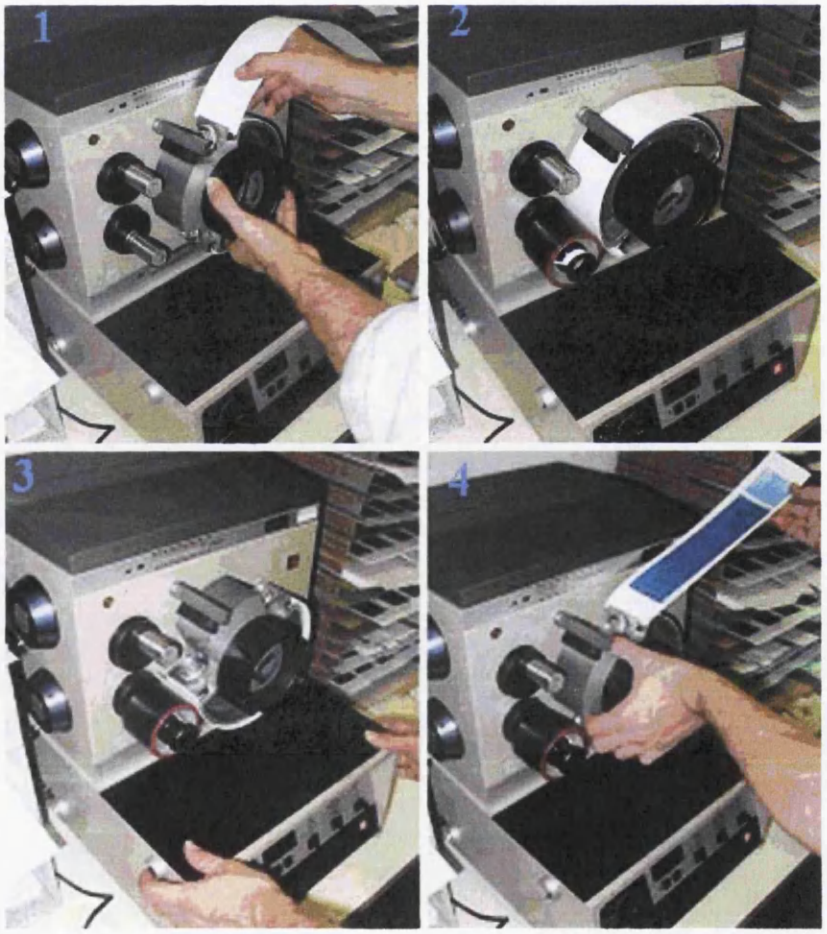

Figure 3-20 The substrate strip is mounted on the printing sector (1) and is set in printing position (2). Ink is transferred by impression with the inked printed disc (3). The printed sample is removed for drying (4) and further analysis.

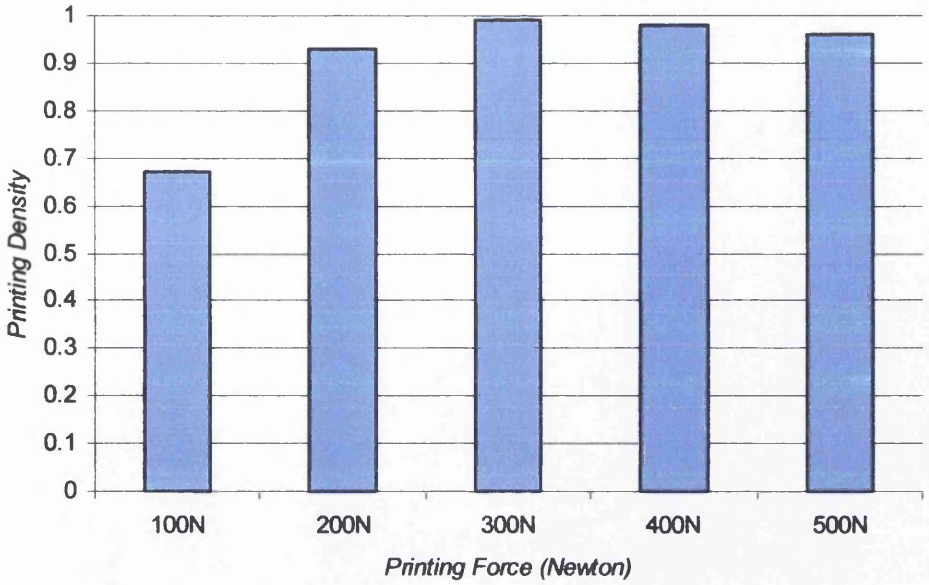

Figure 3-21 The printing force of 300 Newton provides higher printing density for the actual coldset ink and printing paper.

Four printing runs were performed for each ink dilution. Each printing run produced five sequenced samples. The inking – printing process was repeated five times. Finally, 28 samples were produced to carry out colour density and 72 samples to establish ink transfer effect according to ink film thickness. Paper strips were also measured by a five digit balance before and after printing process to determine ink transfer rates between prints according to ink weight of the ink solutions.

3.4.1 Printing density results

The printing density was measured by a scanning 0/45 spectrophotometer. It was calculated as an average of four printing samples on IGT printability tester. Each printing sample is an average of 15 (3 across the width, times 5 along the length) density measurements across the width and the length of the samples. Topographic analysis of the samples was calculated by 50 density measurements across the width and the length to investigate ink transfer quality. Printing density does not illustrate significant variations up to the 5% increase in concentration of Butyl-Diglycol. A significant decrease of printing is determined by the 20% Butyl-Diglycol diluted ink sample. On the other hand, the printing density increases significant by the 10% diluted ink sample. Figure 3-22 illustrates densities values of ink suspensions in dilution with Butyl-Diglycol according to cyan density that is measured by scanning

spectrophotometer. Printing density increases 3% with a low dilution of the 0.5% Butyl-Diglycol. This may occur due to ink transfer variation on the printed substrate or even ink distribution effect of the inking unit as shown in Figure 3-23 and Figure 3-24.

The ink is applied on the rollers by a micropipette as described in the methodology section. Such variations are accepted with a short distribution system such as the inking unit. Density decreases again with increase in dilution but indicates negligible density variations. Averaged density of samples indicates a significant increase with 10% dilution in comparison with the remaining measured densities in dilution with Butyl-Diglycol. The constant printing parameters affect the printing results. Different ink viscosities demand different printing parameters for the production of similar densities. The ink transfer consistency may be affected by the free rotation of the printing disk on the inking unit where there is no gap between the nips. A real inking train consists of rigid and elastic rollers at every nip. The IGT inking unit involves two elastomeric surfaces at the inking process, namely the printing disk and the form roller. As a result, ink transfer instabilities may was a result of rollers deformation at the nip.

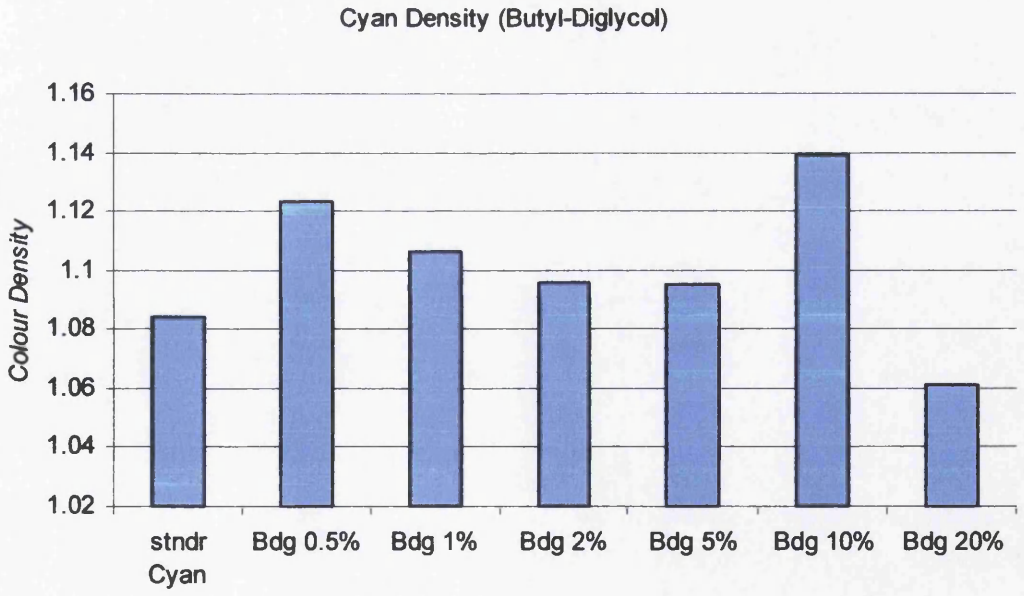

Figure 3-22 Printing densities of ink suspensions in dilution with Butyl-Diglycol

Values vary from 0.01 to 0.05 densities by measuring printed samples in sequence while the amount of ink decreases on the printing disc (Figure 3-23). Consistency of

the ink decreases with dilution of Butyl-Diglycol. Printed samples with low dilution from the 0.5% to 5% indicate significant instability and non-uniformity on printed density (Figure 3-24). Printing density instability does not vary between 10% and 20% dilutions while the average printing density of the 20% dilution significant decreases compare this of the 10% dilution. Ink opacity decreases with increase of Butyl-Diglycol dilution and that difference is significant between the 10% and 20% dilution (Figure 3-25). As a result, viscosity changes do not indicate significant ink transfer variations. Viscosity affects the absorption in the porous surface of the substrate due to low printing speed. Higher printing speed may show negligible effects. On the other hand, printing pressure was modified for the original cyan ink, which showed high consistency of density between runs with 0.2 density difference. As a conclusion, ink transfer instability increases with decrease viscosity and tack when the impression and the printing speed remain constant. This assumes that ink transfer is independent of the dilution and instabilities that occur to the printing process.

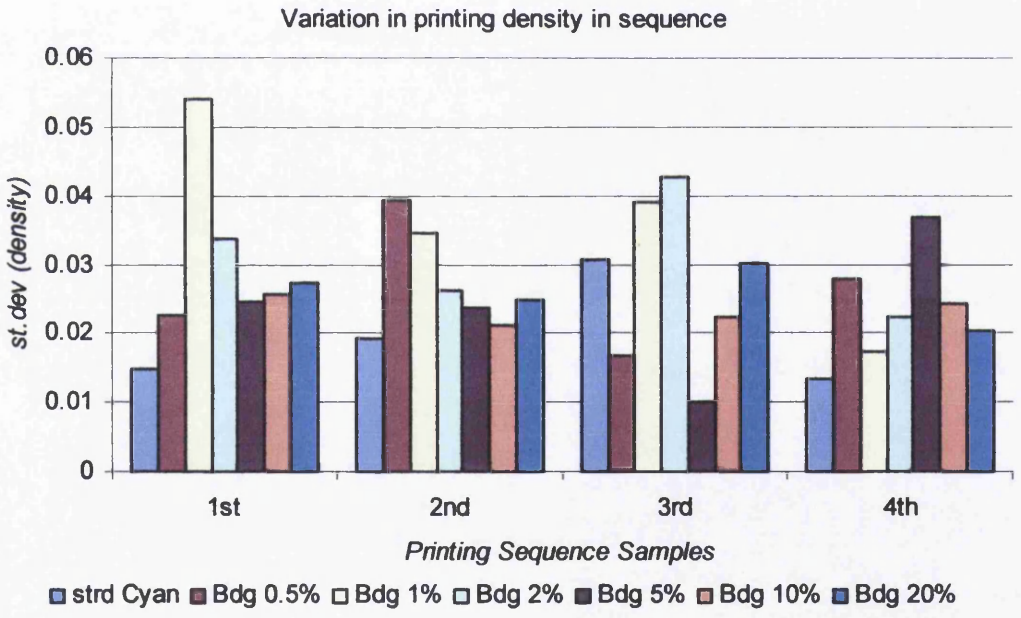

Figure 3-23 Variation in printing density between printed samples in sequence according to standard deviation of density values.

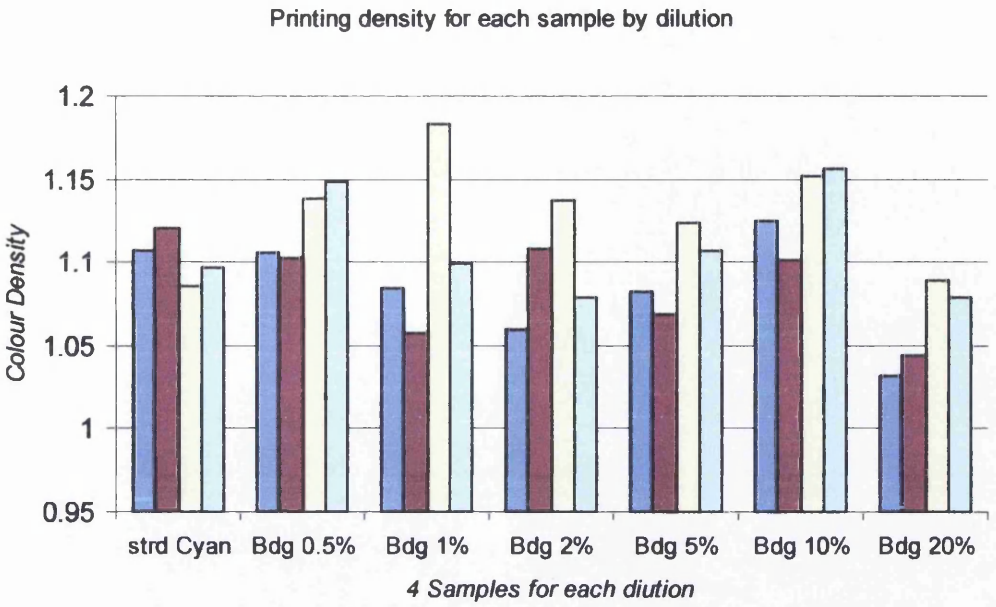

Figure 3-24 Density variation between samples averaged for density by dilution of Butyl-Diglycol.

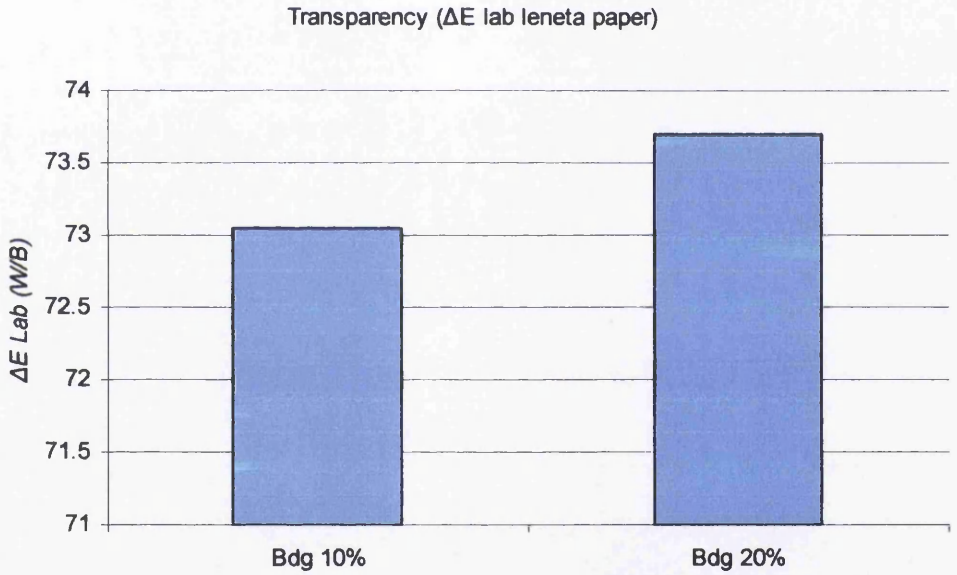

Figure 3-25 Transparency increases with dilution of Butyl-Diglycol in litho Cyan ink from 10% to 20% dilution. Transparency was calculated by printing on a leneta paper.

3.4.2 Ink transfer performance

The viscosity decrease affects ink transfer uniformity. The printing density decreases with more than 10% dilution because of the pigments dispersion in the mix and the weak ink structure. Colour density decreases with increase in dilution of Butyl-Diglycol with a significant increase of 10% suspension.

Topographic analysis of printed samples shows a significant instability of the transfer mechanism. This was carried out by increased and detailed density measurements across the width and the length of the printing samples. The difference between colour areas was adjusted at 0.2 ΔE Lab to illustrate variations on the printed substrate. Densitometer averages measured areas and calculates the printing density respectively to the ink film thickness. The variation depends on the transfer mechanisms and the steady state of the IGT inking unit. Figure 3-26 illustrates topographic analysis of printed samples with 10% and 20% Butyl-Diglycol dilution. Each of those verifies the transfer instability that affects colour density according to the transferred ink film thickness on the substrate.

Viscosity decrease indicates higher absorbency levels from the substrate. However, density variation of ink with increase in dilution does not indicate significant differences on density values. Density difference between 10% and 20% is a clear effect of dilution that increases transparency of the ink as density values indicate by printing on leneta paper as described in section 3.4.1.

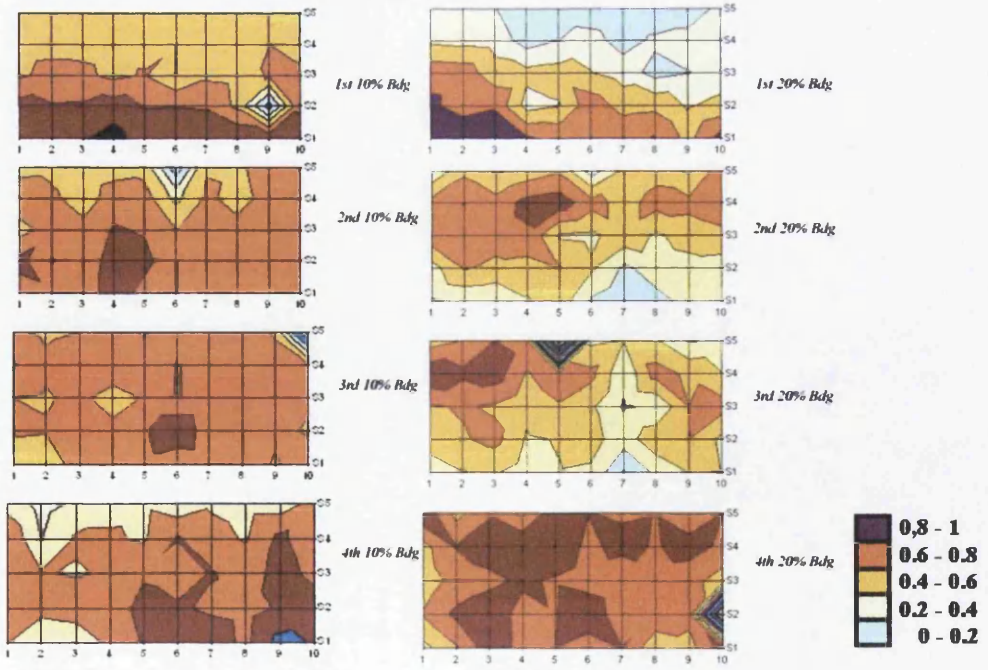

Figure 3-26 The ink transfer uniformity drops with the viscosity decrease. The above images illustrate ink transfer instabilities of printed samples with 10% and 20% Butyl-Diglycol concentration with litho ink. The difference between colour areas is located to 0.2 ΔE Lab.

Printing density shows transfer instabilities with a decrease in viscosity. This agrees with Rosenberg (1991) who found that viscosity and tack affect the printability performance of the inks. Further to the results of this thesis, the transfer performance of the ink can be improved due to absorption effects but the 20% dilution drops density dramatically due to the increase of ink transparency.

3.4.3 Design of the experiments

The action of ribbing and misting is dependent on several parameters which affect the rheological characteristics of the ink. A validation experiment was performed in which several parameters were varied to evaluate both their overall contribution and interactions. In order to undertake this in a meaningful timescale a design of experiments was used based on orthogonal arrays (sometimes referred as "Taguchi method").

Orthogonal arrays are highly fractional orthogonal designs proposed by Dr. Genichi Taguchi. This method can be used to estimate main effects using only a few experimental runs without sacrificing accuracy of a full factorial experiment. The proper orthogonal array can be selected by the known number of parameters and the number of levels to be studied. The objective function in the orthogonal array technique is the Signal to Noise ratio (S/N) which is a function of the signal (mean) and the noise (variation). Orthogonal arrays are an effective simulation aid to evaluate the relative effects of variation in different parameters on the response with the minimum number of experiments. Orthogonal arrays allow also the study of interactions between parameters. Interactions indicate the effect of two parameters where the combined effect is greater than the sum of the two parameters considered individually. The orthogonal arrays and their use in experimental design and optimisation are described by Phadke (1989).

The data from the orthogonal array based on experiments and the relative parameter effects can be analyzed by advanced statistics such ANOVA (analysis of variance). Half-normal plots use the magnitude of the response of each column from the orthogonal array (Grove et al 1992). The response is plotted against a set of half-normal scores from the positive portion of a normal distribution curve with a mean of

zero. The positive portion of the normal distribution curve is used as it is the magnitude of the responses that is important and not the direction of the response. The plot of the responses against the half-normal scores would produce a linear relationship and a normal distribution in case of no parameter had a significant effect on the process. Therefore, any parameters that have an effect on the process may be identified, as its point on the half-normal plot will be on the non linear part of the curve.

3.5 Closure

This chapter focused on the instrumentation and methodologies that were used throughout the experiments and analysis work of this thesis. Table 3-1 summarises the instrumentation use according to the experimental setup for each investigation. It described devices that were used to examine phenomena related to the ink transfer mechanisms in lithographic printing. The Printability tester, high speed inking unit, and tack tester provide systems that simulate roller trains similar to a lithographic press. The short trains and controlled parameters allow flexibility on tests such as those described in the following chapters. It also discussed the meaning of rheological characterisation the following chapters. Conventional rheological characterisation was described. Extended rheometry is presented in a separate chapter it includes the development of this process. Similarly, the methodologies on misting and ribbing phenomena are also dealt with in separate chapters in order to describe in detail the techniques that have been developed for capturing and analysing such phenomena.

Table 3-1 Instrumentation use according to the experimental setup for each investigation.

	Rheology	Tack	Density	Ribbing	Misting	L18 OA
IGT Tack tester		✓		✓	✓	✓
IGT inking Unit			✓		✓	
IGT AIC2-5			✓			
Bohlin Rheometer	✓					
Ext. rheometer	✓			✓		
Scanner			✓	✓		✓
Spectrophotemeter			✓			
DAT1100 P-Drop	✓					
Leica M3Z					✓	
White Light Interf.				✓	✓	

4. Viscoelasticity and tack

4.1 Introduction

Characterisation of the rheological properties of ink suspension provides a detailed description of their internal structure and can help to explain behaviour in the printing process. Lithographic inks are complex non-Newtonian viscoelastic fluids with a shear thinning behaviour. Inks are characterised by their profile that is related to their specific formulation. Commercial inks have a range of ingredients. These can include rheology modifiers which generate a different structure. Therefore, to avoid experimental errors due to variations in the additives a lithographic coldset cyan ink was used with controlled rheology modification by the addition of Butyl-Diglycol.

Section 4.2 deals with the methodology used for rheological characterisation. It analyses the production of ink suspensions in dilution with Butyl-Diglycol in order to produce a variety of suspensions while keeping a similar ink formulation. The rheology of the inks was examined by a variety of rheological tests such as shear viscosity and recovery, oscillation, extension, surface tension, tack and printability. While those characteristics have been examined extensively by previous researchers (Mewis et al 1981; Rosenberg 1991; Blayo et al 1996; 1997; Podhajny 2002), however they did not report any relation remarks between rheology and tack on ink transfer mechanisms.

Results are given in Section 4.3. This section examines the results of the viscoelasticity and recovery of the structure. The last paragraphs of this section analyse tack characteristics when changes occur to rheology of ink suspensions and distribution system parameters.

Section 4.4 discusses the results and indicates the relations between rheological characteristics and tack. It also deals with responses between the factors that affect rheology and tack and explains the importance of rheology on a printing press.

4.1.1 Characterisation of printing inks and suspensions

This study focuses on understanding the rheological changes of coldset lithographic ink suspensions. It deals with relations between rheological profile and printing characteristics such as tack and printability performance. A series of viscoelastic fluids was produced by the use of a commercial lithographic ink in dilution with a Newtonian agent.

4.2 Methodology

Lithographic coldset cyan ink was selected for this study. Coldset inks are recommended due to the environmental profile with good recycling abilities, low Volatile Organic Compounds (VOC's 0-20%) and lower energy cost for printing applications instead of UV and heatset inks. Coldset ink dry by absorption and partly oxidation and do not demand extra curing for drying such UV-lamps or heat. Butyl – Diglycol (BDG) was used to dilute the ink in different concentrations and to study the ink transfer performance and characteristics in relation to the rheological profile and tack. Butyl-Diglycol ($C_8H_{18}O_3$) is a clear, low-volatility, mobile liquid with a very faint, mild odour. It is miscible with many common solvents, e.g. aliphatic hydrocarbons, alcohols, ketones, aldehydes, ethers, glycols, glycol ethers and water and its typical viscosity is 5.9 mPa.s and its density 0.955. It is soluble in water and it is used in industrial coatings, specialised coating and in lithographic printing fountain solution due to low vapour pressure and excellent dual functionality solvent properties in comparison to many other monofunctional chemicals. This allows suspensions with low evaporations rates and complex characteristics such as fountain solution of the press. The ink dilution with a low evaporation agent allows the long term study of controlled suspensions.

Six ink suspensions were produced in dilution with the lithographic ink, namely 0.5%, 1%, 2%, 5%, 10% and 20% of Butyl-Diglycol. The ink suspensions were compared with the neat cyan ink properties as reference. The study related variations into ink viscoelasticity with variations in other rheological characteristics, tack and ink transfer effects. The controlled dilution was expected to decrease viscosity and tack.

4.2.1 Table of shears

The shear table test was carried out by increasing accelerating shear stress in 31 steps in a logarithmic scale. The CP2/20mm cone geometry was selected for the test due to the high viscosity of the ink. The shear stress sequence used a table from 0.1Nm to 200Nm torque. The test was carried out three times for each emulsion. The 70 μm gap was selected for the shear viscosity test according to the value of the truncated tip of the cone as described in section 3.2.1. Precondition time, temperature and cone geometry were set as described in Section 3.2.2. Viscosity values were plotted as a function of shear rate (Figure 4-1).

4.2.2 Creep to creep recovery

The recovery rates were measured after the compressive forces of sample loading and after an applied shear stress. The rheometer's ability to measure with extremely low torque enabled the measurement of the recovery of the ink with time. The ink sample was loaded on the plate for the test. The cone was gradually placed down on the top of the sample to generate the preset gap (70μm) between cone and plate so as to form the ink volume that was tested. This procedure ensures the uniformity between samples and different tests. The cone applied pressure to the ink affecting the internal coherence of the fluid and hence the "loading" viscosity. The recovery calculates the time in which the ink viscosity was fully recovered from the compression of the sample. Steady shear stress was applied for 300 seconds with 0.01Nm torque and recovery rates were measured at 5-second intervals. The low shear rates allowed recovery of the suspension structure over 60 measurements.

To examine recovery from applied shear, a steady shear stress of 200Nm torque was applied for 30 seconds where 30 measurements of viscosity were carried out. This was the shortest time in which the rheometer could calculate an accurate measurement. Shorter times generated noise because of the instant change in torque value. In the final step, low steady shear rate was applied once more with 0.01Nm and recovery rates were measured again by 60 viscosity measurements in 300 seconds. These settings were selected in order to estimate the inks viscosity effect under sudden changes of shear rates. Printing inks experienced such changes of shear rates within a very short time at the inlet to outlet passage of the printing nip. Similar techniques have been followed by other researchers (Cohu and Magnin 1995; Al-

Ganainy and Mostafa 2004). The viscosity values are plotted as a function of time to visualise recovery rates (Figure 4-2). CP2/20mm cone geometry was also selected for the test due to ink samples high viscosity. Recovery was carried out by the hysteresis of the thixotropy loop under steady shear stress.

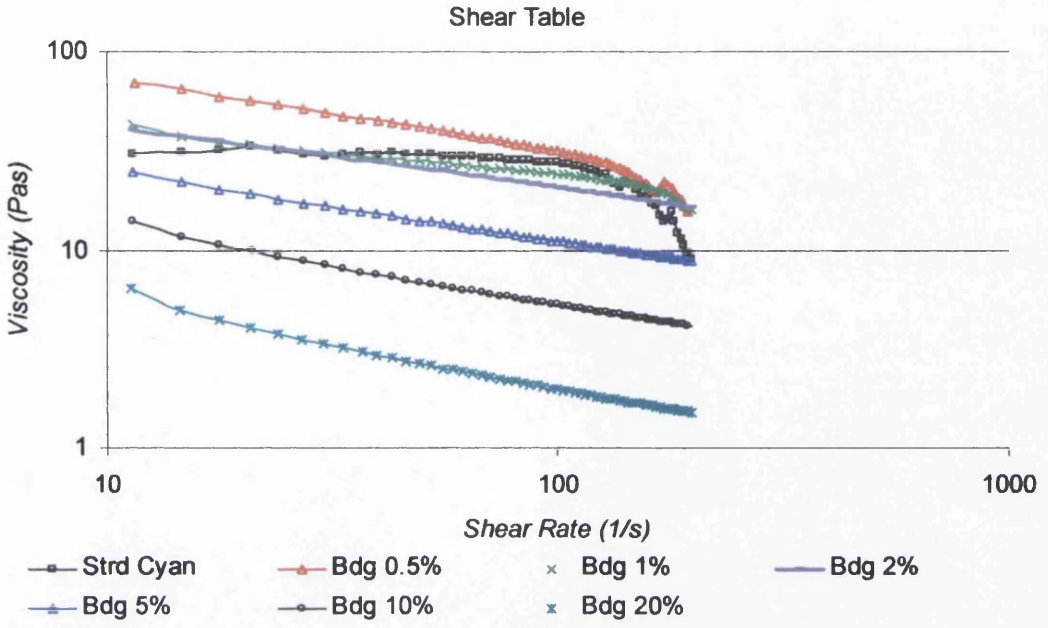

Figure 4-1 Plotting graph for viscosity / table of shears for ink suspensions in dilution with Butyl-Diglycol (Bdg%). Results in section 4.3.1

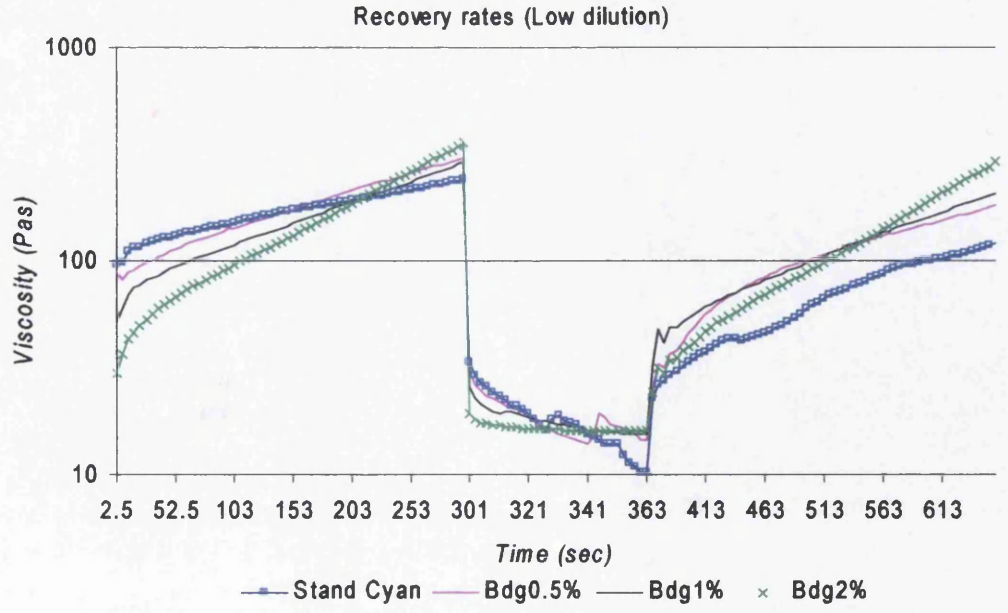

Figure 4-2 Plotting graph for viscosity recovery rates of ink suspensions in low dilution with Butyl-Diglycol under step shear test. Results in section 4.3.1

4.2.3 Thixotropy

Thixotropy was carried out using a shear table on a cone and plate configuration. The test set in a logarithmic scale with minimum shear rate of 0.1Nm torque and maximum 100Nm torque value. Higher torque caused the cone to expel the ink. The measurements were determined every 30 seconds with every 10 seconds integration time. The thixotropy loop was determined by increasing the shear rate in steps and then decreasing it by a series of steps. The shear table was calculated by 31 steps in forward and reverse order which conclude sum time test for 456 seconds. The CP2/20mm cone geometry was selected with 70μm gap for all the suspensions. The thixotropic loop was also evaluated with temperature variation. Two more temperatures were used, the 28°C and 30°C degrees. The thixotropy curves were plotted as a function of shear stress versus shear rate (Figure 4-3). The thixotropy of the suspensions was carried by the hysteresis loop area in Watt/m^3. Three tests were carried out for each suspension and test protocol.

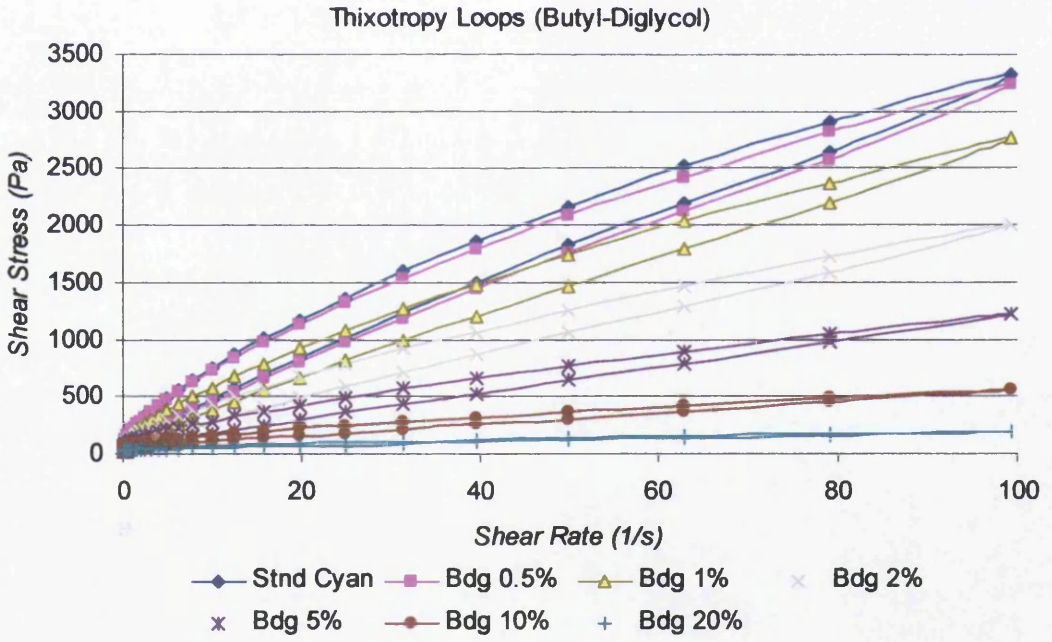

Figure 4-3 Plotting graph of thixotropy loops for ink suspensions in dilution with Butyl-Diglycol (Bdg%). Results in section 4.3.1

4.2.4 Frequency sweep

The viscoelasticity of a material was calculated in the frequency range that phase angle was steady. Preliminary tests were carried out in order to avoid such experimental errors and select an individual frequency sweep range for each

suspension Those tests showed that higher diluted suspensions required a shorter frequency range as Figure 4-4 illustrates.

The oscillation test is carried out by using CP4/40mm cone geometry as described in chapter 3 with frequency sweep test and stress control. The wider truncated cone geometry increases accuracy of the measurement. Frequency sweep is calculated by preset of the maximum frequency of 10Hz and minimum of 0.01Hz as found by the preliminary measurements. The frequency sweep is carried out by 31 measurement steps with 5 seconds delay time and 2 periods integration which result in 3380 seconds summation test time.

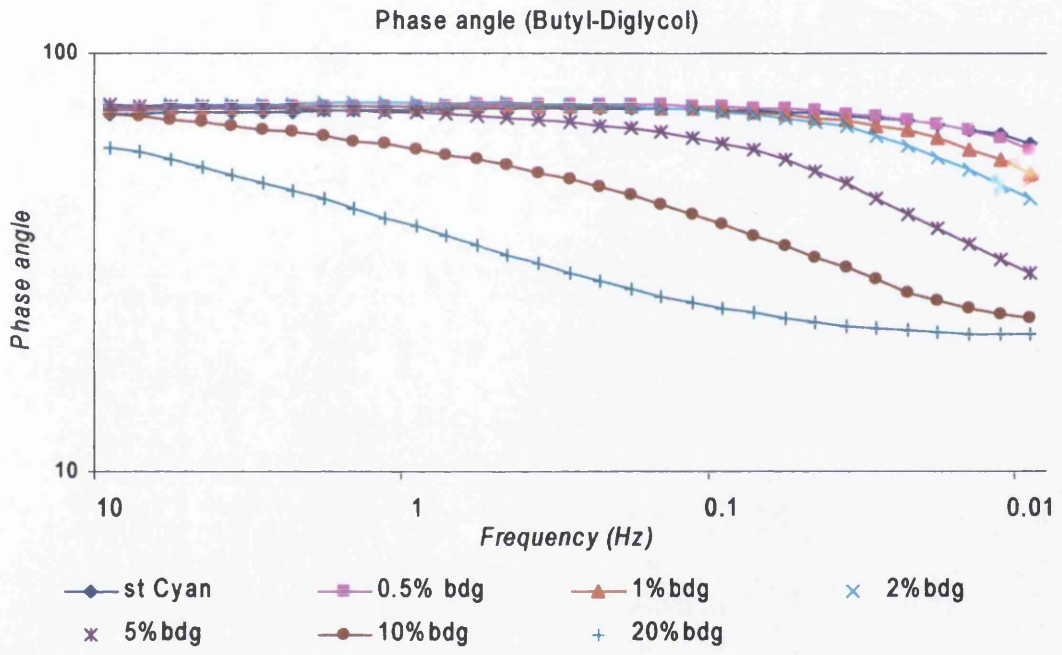

Figure 4-4 Phase angle decrease in low frequency range and the effect is higher with increase in dilution of Butyl-Diglycol. Results in section 4.3.2

4.3 Results

4.3.1 Viscosity and thixotropy of suspensions

The ink dilutions recovery rates increase by the concentration of Butyl-Diglycol in the ink. It indicates a slightly faster but rapid recovery step when shear stress decreases back to minimum value with 0.01Nm torque. The recovery time is not significantly affected by the increase of Butyl-Diglycol dilution when this reaches

2% but it indicates an increase in static viscosity when no shear is applied. The increase of dilution from 5% to 20% indicates a significant effect and tends to follow Newtonian behaviour. This decreases rapidly the viscosity with shear but also provides faster recovery rates with significant increase of static viscosity (Figure 4-5). The neat cyan ink shows shear time dependence behaviour while diluted samples show constant and Newtonian behaviour under steady shear especially with more that 5% dilution (Figure 4-6). Cyan ink viscosity decreases rapidly with shear stress and reaches viscosity levels of 2% dilution with 10.17 Pas in a short shear time. The viscosity decreases even more with the increase in shear stress and reaches viscosity of 5% dilution. The viscosity shows consistency through time and depends on the shear stress rates as Butyl-Diglycol increases in the ink.

Changes of the polymers behaviour are indicated by the shear viscosity and recovery responses. The elastic modulus dominates to the viscous modulus during relaxation. The structure becomes viscous and increases significant static viscosity. However, this effect shows a threshold between 10% to 20% suspensions, because the static viscosity tends to decrease again with 20% dilution.

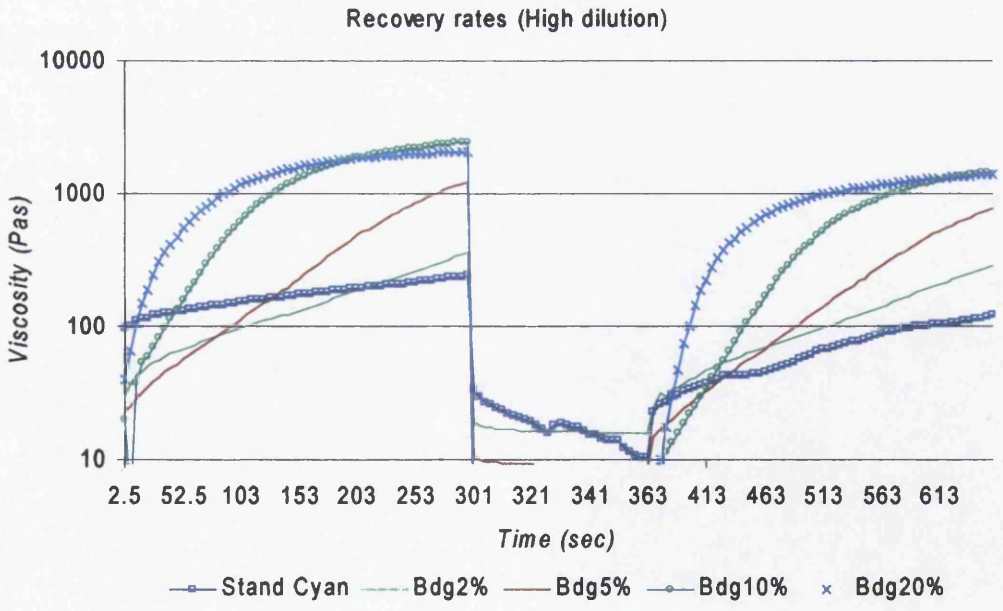

Figure 4-5 Recovery rates of ink suspensions in dilution with Butyl-Diglycol under steady shear.

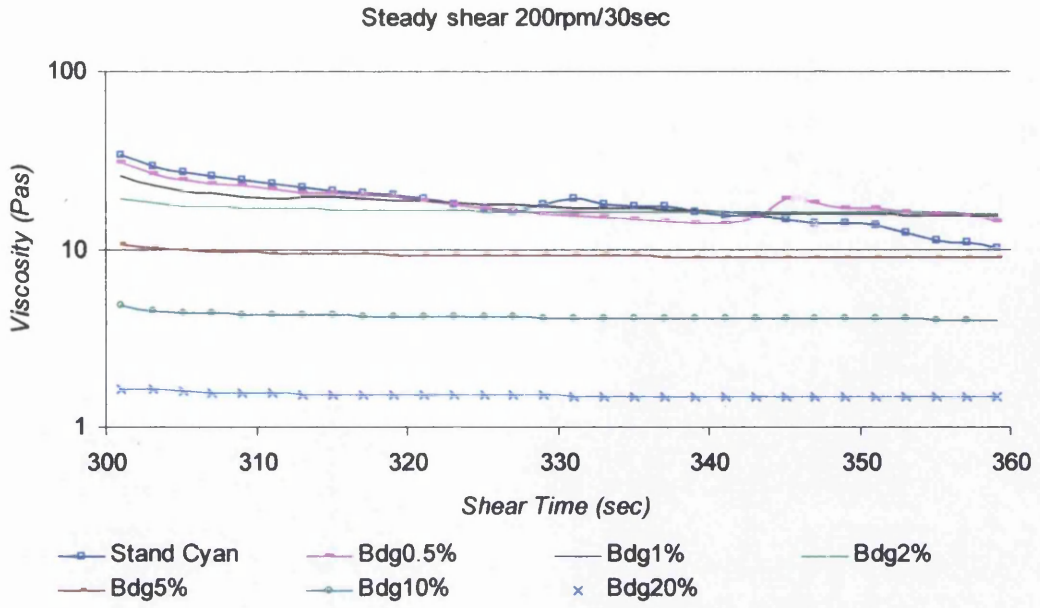

Figure 4-6 Viscosity of ink suspensions through steady shear rate (200rpm) across shear time (30sec).

Figure 4-7 illustrates hysteresis loop area of steady shear stress to recovery by Butyl-Diglycol dilution. It shows that thixotropy decreases with the viscosity. Relaxation time decreases with increase in dilution and that decreases also the thixotropy of the ink (Figure 4-8). Those results indicate a hysteresis decrease of 50% for the 1% dilution that gradually reaches a hysteresis decrease of 92% with 5% dilution. Hysteresis decrease was calculated between Cyan ink hysteresis versus each sample hysteresis in percentage.

Hysteresis Decrease = [(Hcyan – Hsample)/Hcyan]% (23)

Where:

Hcyan is the Hysteresis value of the neat cyan ink as reference

Hsample is the Hysteresis value of diluted ink sample that is compared

Decrease in thixotropy is also verified by flow curves and thixotropy loops of the suspensions by following similar calculations. Butyl-Diglycol decreases 24% hysteresis area for the 1% suspension and reaches a decrease of 93% for the 20% suspension (Figure 4-9). The difference in low concentrations occurs to the difference between high shear stress and acceleration shear stress by same calculation as described for hysteresis decrease above. The hysteresis variations on the test process between steady shear and shear table. The steady shear test

instantaneously applies the shear rates that rapidly decreases the viscosity rapidly. The recovery of the ink is slow on relaxation. However, the shear table test increases and decreases gradually the shear rates which, as a result, allow the same recovery time of the ink when lower shear is applied from step decrease of shear.

Thixotropy is also affected by ink temperature. A significant decrease in thixotropy occurs with a slight increase in temperature from 25° to 28° and 30° Celsius (Figure 4-10). The increase of temperature decreases viscosity as stated also by Fuchs et al (1991) and affects polymers. The Butyl-Diglycol concentration indicates that the effect to the coldset ink is similar to that of temperature. The 1% diluted sample present similar hysteresis with the temperature increase from 25°C to 28°C. Hysteresis loop decreases with increase in temperature as much as with Butyl-Diglycol concentration. The significance decreases approximately 25% with 1% dilution with Butyl-Diglycol. Temperature shows also similar effect while significant decreases 24% in 3 degrees of temperature from 25°C to 28°C. As a result, inks thixotropy is affected significantly by these two parameters. The hysteresis decreases more 20% with 2% diluted ink almost as much as with increase in temperature to 30°C with 26% hysteresis decrease. This indicates a linear decrease in thixotropy of the ink across dilution and temperature increase. It indicates that the effect of temperature in the ink structure is similar with this of the dilution with Butyl-Diglycol.

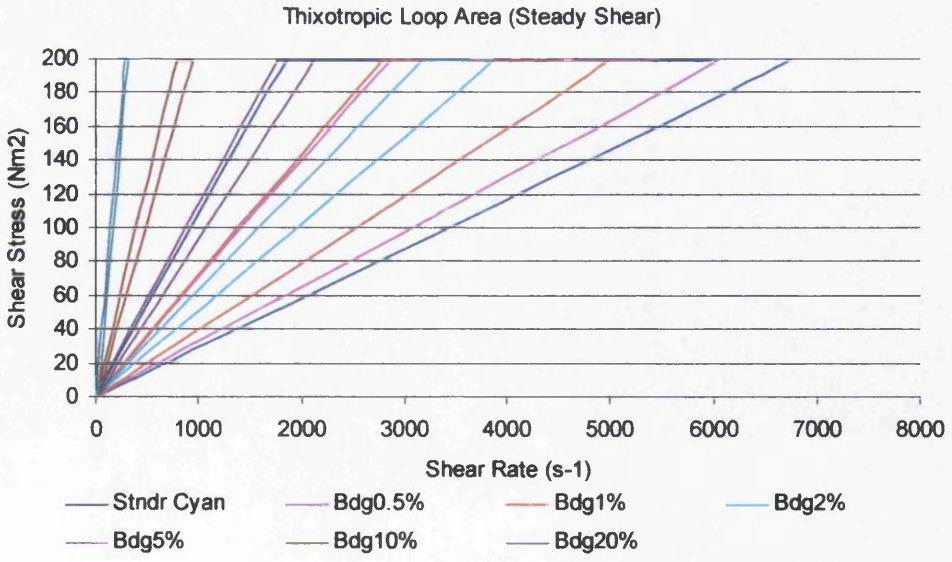

Figure 4-7 Hysteresis Loop area decreases with increased dilution of Butyl-Diglycol. It shows that thixotropy decreases with the viscosity of the inks.

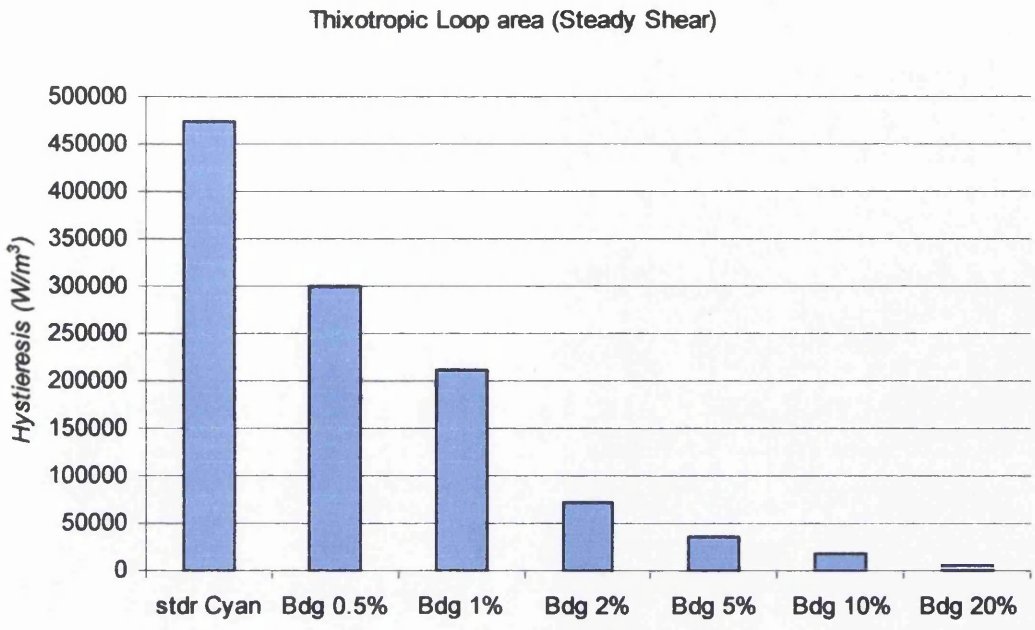

Figure 4-8 Thixotropy decreases as Butyl-Diglycol increases dilution in the ink.

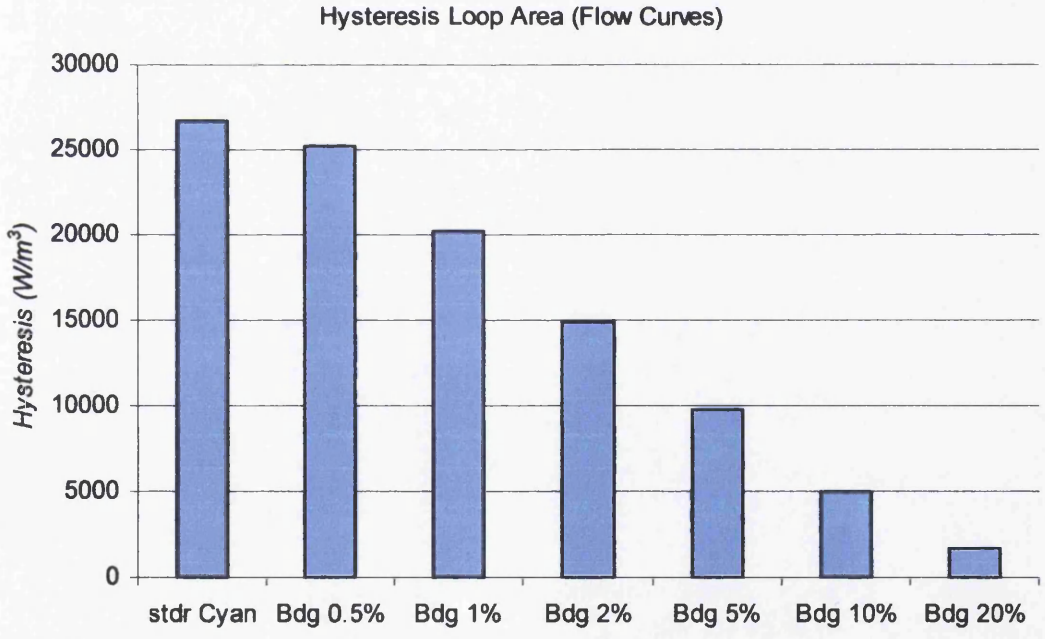

Figure 4-9 Hysteresis loop area differences of ink suspensions in dilution with Butyl-Diglycol.

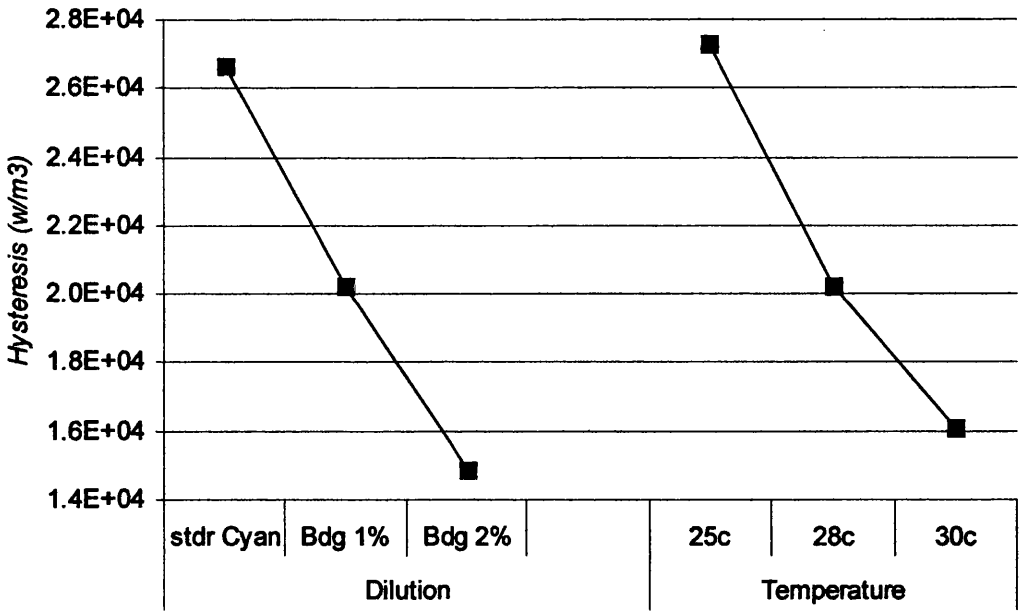

Figure 4-10 Hysteresis loop area variation between temperature and dilution effect.

4.3.2 Viscous and elastic modulus

An oscillation frequency sweep test was used to determine the viscoelastic character of the ink dilutions with Butyl-Diglycol. Oscillatory measurements in which the frequency was varied (0.01-10 Hz) showed that the viscous modulus (G'') dominates in higher frequencies, while the elastic modulus (G') dominates in lower frequencies. This indicates that the viscous component is more dominant than the elastic component. The effect increases with the Butyl-Diglycol concentration.

Viscoelasticity of ink decreases with high levels Butyl-Diglycol dilution but does not present significant variations when dilution is kept low (up to 5%) between the dilutions (appendix 2). Phase angle increases with increase of Butyl-Diglycol dilution as frequency increases. Ink suspensions show frequency dependent viscosity and viscoelasticity decreases slightly with the increase in dilution (Figure 4-11). Viscous modulus G'' dominates to elastic modulus G' and both increase while viscosity decreases. Viscous modulus dominates against elastic modulus through dilutions up to 10% of Butyl-Diglycol (Figure 4-12). The elastic modulus of the ink increases with the dilution and indicates dominant effect especially on 20% Butyl-Diglycol dilution at low frequency range (Figure 4-13). Viscous modulus dominates

to elastic modulus with frequency increase and becomes significant also with increase of Butyl-Diglycol concentration.

The elastic modulus and the viscous modulus increase with increases in the concentration of Butyl-Diglycol. At lower frequencies, no significant effect of concentration on elastic modulus was observed. The rise in the elastic modulus was observed at low frequencies (less than 1Hz) especially for the dilutions with more than 5% Butyl-Diglycol (Figure 4-12; Figure 4-13). Viscous modulus increases with the frequency. On one hand, the increase in the viscous modulus seems independent of the Butyl-Diglycol concentration (appendix 2). Elastic modulus increases also with frequency but seems to be dependent on the Butyl-Diglycol concentration. It remains constant with frequency while viscous modulus increases for the 10% and 20% concentrations of Butyl-Diglycol.

Those results indicate a weakly structured system with possible agglomeration. Elastic modulus dominates to viscous modulus with decrease in frequency and also increases with dilution in the ink. This is further verified by the decrease of the phase angle with the increase in Butyl-Diglycol. The increase of the elastic modulus dominates over to the viscous modulus decreases the phase angle between strain and stress signal as described in chapter 3.

In conclusion, the viscous modulus increases with frequency and dominates versus elastic modulus. The difference between viscous and elastic modulus increases with frequency and so with shear stress. Butyl-Diglycol increases elasticity in viscoelastic structure in relaxation and decreases with shear.

The pendant drop method was used to calculate surface tension. The surface tension decreases with Butyl-Diglycol concentration. The ink suspension with 20% dilution indicates almost 50% decrease in surface tension versus the no diluted litho ink (Figure 4-14).

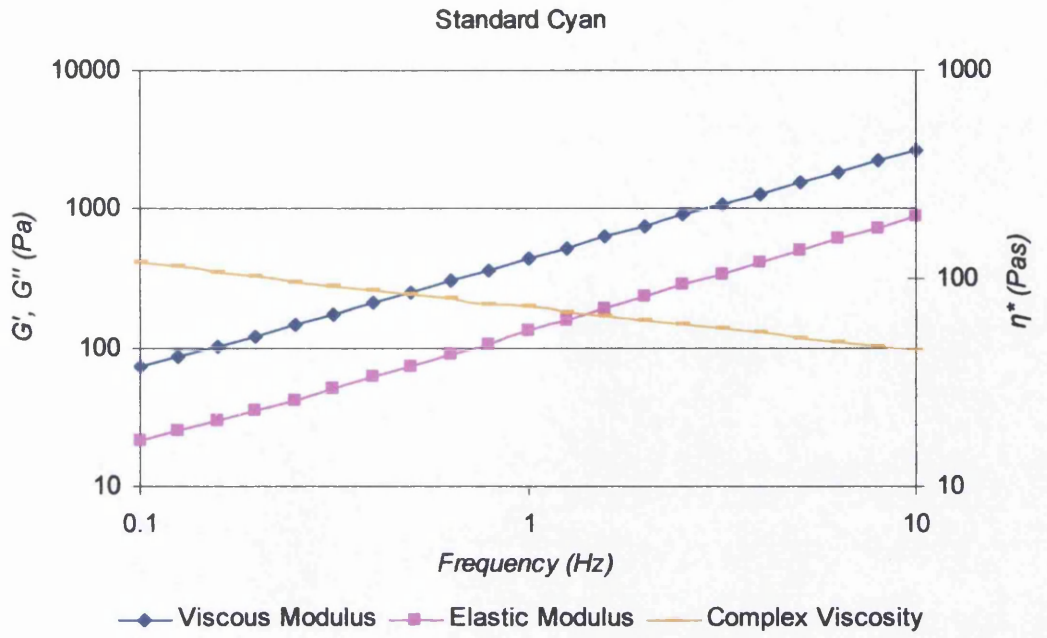

Figure 4-11 Viscous modulus dominates to elastic modulus with viscosity dependent on frequency

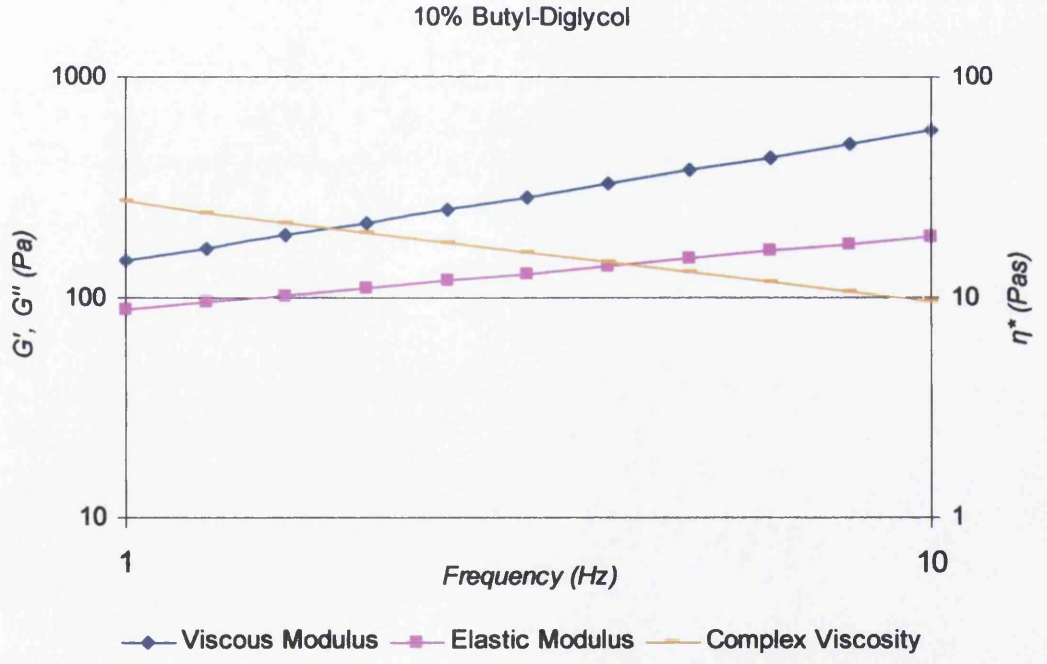

Figure 4-12 Viscous modulus dominates to elastic modules with viscosity dependent on frequency in 10% Butyl-Diglycol dilution.

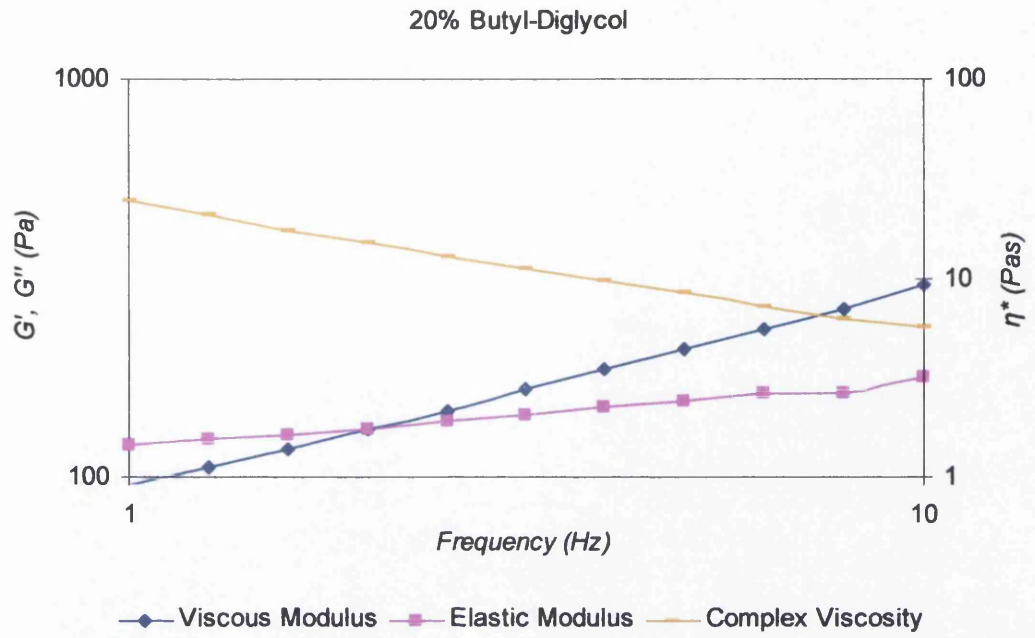

Figure 4-13 Elastic modulus dominates to viscous modulus at low frequencies in 20% Butyl-Diglycol dilution with viscosity depending on frequency.

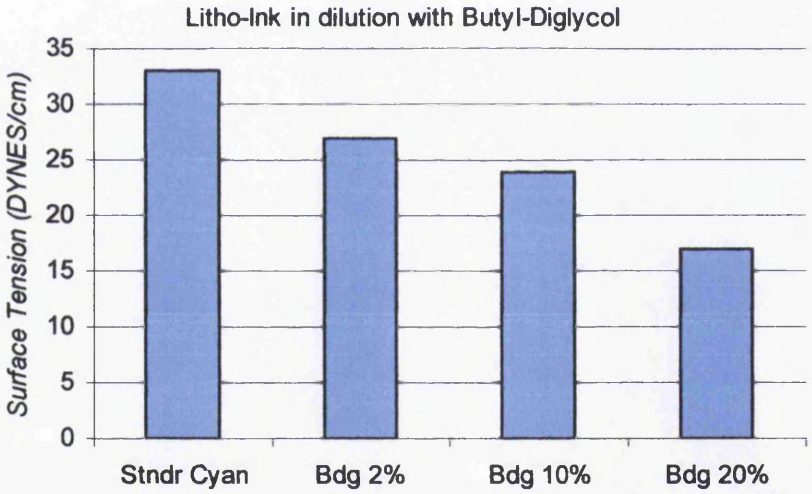

Figure 4-14 Surface tension of the ink suspensions in dilution with Butyl-Diglycol (Fibro DAT 1100).

4.3.3 Tack measurements results

Speed, ink film thickness and dilution significantly affect the tack value of the ink (Figure 4-15). It increases to 20% higher values from 0.8 to 1.6m/s (50 to 100m/min according to tack tester interface) and by 10% from 100 to 150m/min. Tack is not affected significantly by step change in distribution speed. Similar tack values are indicated by low to high speed steps and step back to previously low speed. Figure

4-15 illustrates speed bars for each diluted ink. The first and last bars represent the lowest speed of 50m/min (0.8m/s). The tack values are affected also by ink film thickness. The 7.8 μm film thickness has up to 20% higher values than 3.9 μm film thickness especially between 100 and 150m/min. This difference is dominant for the 20% dilution which shows 20% tack difference even at 50m/min. However, the lower concentration dilutions produce insignificant difference with 5% to 15% maximum tack difference with respect to the parameters to be studied.

Temperature affects tack with speed, ink film thickness and dilution (Figure 4-16). Tack decreases 20% from 25° to 30°C for the standard litho Cyan ink. The increase of Butyl-Diglycol dilution increases gradually the effect of temperature the 20% dilution produces a 65% decrease in tack. Increase in temperature produces 50% less tack for 5% dilution and 55% decrease for 10% dilution. The effect slightly decreases with increased speed. Eight times higher speed decreases the effect to only 10%. An increase in temperature from 25° to 30°C decreases tack by 20% for the standard ink, 30% for the 5% dilution, 34% for 10% dilution and reaches 50% decrease in tack with 20% dilution with speed up to 450m/min.

Figure 4-17 illustrates tack variation with the average responses of the parameters. Tack increases with increase of ink film thickness and increase of speed but decreases with increase in temperature and dilution of Butyl-Diglycol.

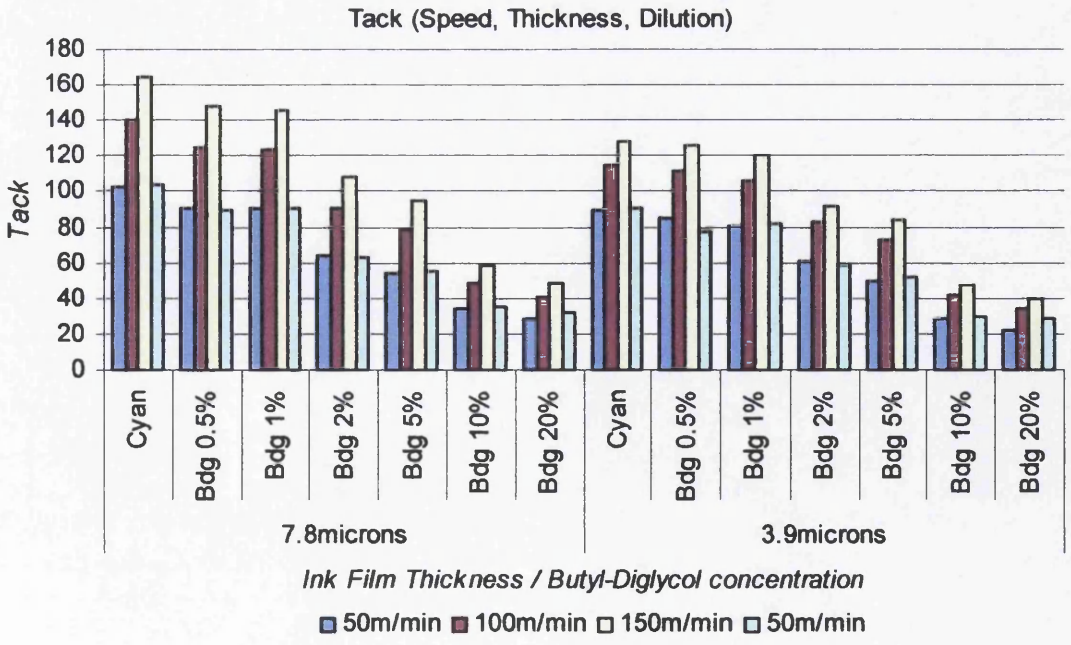

Figure 4-15 Tack values of ink suspensions in dilution with Butyl-Diglycol in variation of ink film thickness and distribution speed.

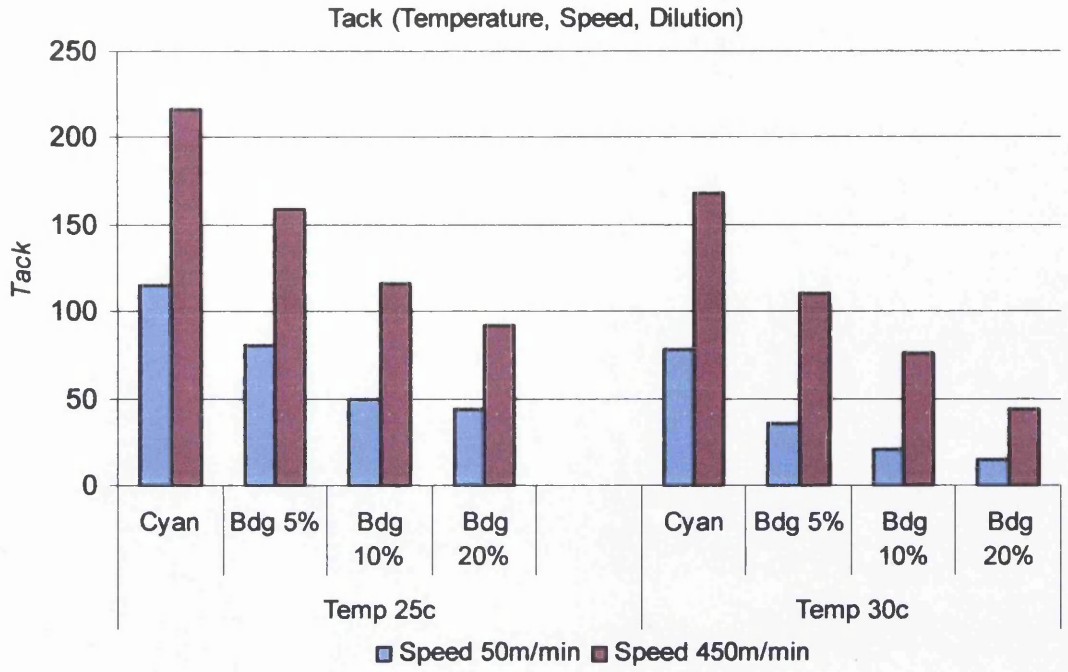

Figure 4-16 Tack values of 3.9 µm according to variations in speed, dilution and temperature.

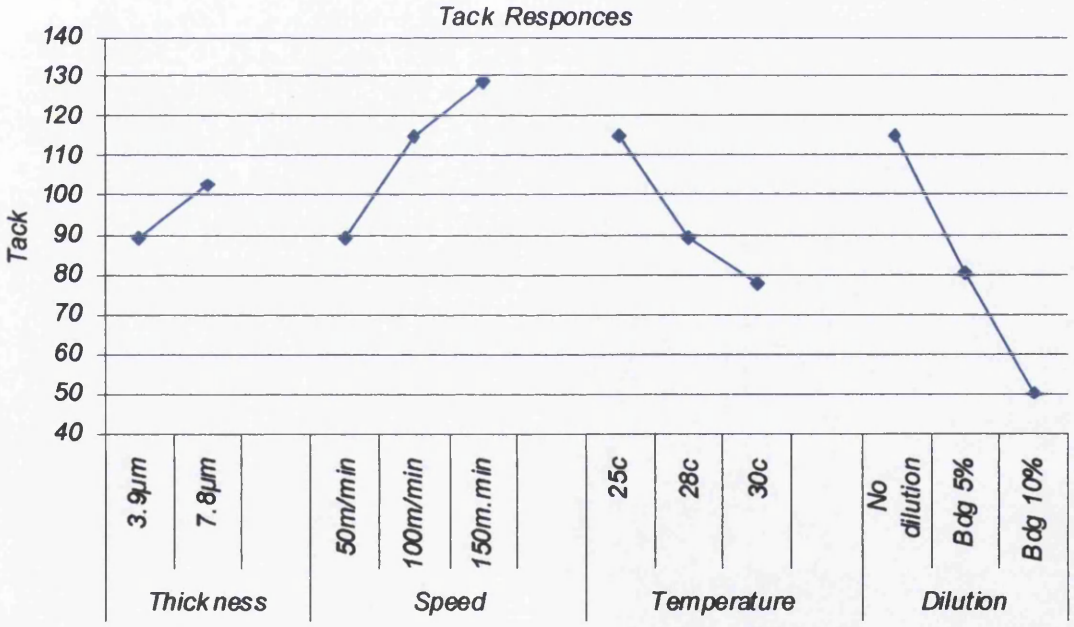

Figure 4-17 Tack variation according to responses of thickness, speed, temperature and Butyl-Diglycol concentration.

4.4 Discussion

The Butyl-Diglycol allows a successful decrease of viscosity of the coldset ink as was expected. The decreased viscosity of the suspensions also decreases also

viscoelasticity, surface tension, extension viscosity and tack value. Increased temperature decreases tack and viscosity through all of the diluted inks suspensions. Butyl-Diglycol in the non-Newtonian structure of the ink decreases thixotropy and affects polymers chains. The increased concentration breaks down the polymers network and ink indicates Newtonian behaviour. Dilutions of ink with 10% Butyl-Diglycol affect ink transfer mechanism and increases printing density. However, the significant increase of more than 10% Butyl-Diglycol concentration destroys the structure of the ink and tack value repeatability becomes unstable. The 10% suspension in dilution with Butyl-Diglycol illustrates a significant increase in printing density. This determines further investigation and verification on printing density due to transfer instabilities. Such study was not undertaken because it was beyond the scope of this thesis. The significant increase of 20% Butyl-Diglycol in dilution concedes with ink complex structure with a trend to Newtonian behaviour. Viscosity increase on relaxation is verified by elastic modulus domination versus the viscous modulus at low frequencies. While elastic modulus dominates, it seems that storage modulus dominates the loss modulus and so the structure increases in storage energy and increases viscosity.

4.4.1 Tack and viscosity

Tack tester configuration is affected by the adhesive dynamics of viscous fluid through forward roll process. The decrease in viscoelasticity and film thickness decreases tack value due to the decrease of the adhesive forces. The viscosity decrease of the suspensions shows a decrease of the structure elasticity as described in Section 4.3.2. Tack also decreases with increase in system temperature which affects viscosity as found in Section 4.3.3. However, it increases with increase ink film thickness and distribution speed. Transients in tack indicate transients in distribution time of the system to achieve uniform ink film thickness on the rollers.

Tack is affected by the adhesive dynamics of the fluid that is distributed between the rollers. Tack decreases when the contact area along the nip is not uniform. Thus, changes in tack indicate variation of ink uniformity on the system. Tack is steady when the ink is uniform on the system and measuring roller is pulled forward uniformly across the roller length. The variation in film thickness decreases the ink

coverage area and also the contact area of the nip. The contact nip area of the measure roller decreases the average adhesive dynamics decrease and so does the tack value. Tack is affected by viscosity, ink film thickness and temperature. Those results agree with previous authors (MacPhee 1998, Blayo et al 1998).

Dilution of Butyl-Diglycol decreases viscosity and also decreases tack. Viscosity and tack decrease with increase in temperature. Podhajny (2002) reported similar results through his work and he stated that tack is affected by ink elasticity, printing speed, film thickness and additives. The results of this thesis show that distribution speed increases tack significantly but the increase in shear stress and shear rate decreases viscosity with time. The cone geometry and plate configuration do not allow viscosity measurements in extremely thin film thicknesses such as 2 or 4μm. Such thicknesses can be studied accurately by a tack tester or other similar roller configuration. Unfortunately, tack tester presents measurements instabilities such rollers slip when too much ink is applied. Tack value or adhesive dynamics of the fluid can be related to viscosity effects (Figure 4-18). Temperature and dilution parameters produce similar responses in tack and viscosity as determined. The difference between tack and viscosity occurs to the instrumentation that they are carried out. Tack tester determines the adhesive dynamics of the ink while shear rheometer measures the viscosity changes under shear stress. However the results show that fluids with high tack value occur to high viscosity fluids.

4.4.2 General discussion and printing process

The comparison between tack values and shear viscosity of the ink suspensions does not indicate high shear stress at the rollers nip. Viscosity of lithographic cyan ink decreases with shear rate and produce shear thinning behaviour. Its viscosity decreases significantly when high shear stress is applied and thins further over time. The increase in dilution decreases viscosity and generates a structure independent of time effect. Tack measurements determine gradually decrease of tack with increase of dilution with Butyl-Diglycol and also decrease in viscosity. Figure 4-19 illustrates variations of viscosity and tack effects with increase in speed for tack and shear rate for viscosity. Speed increase does not affect responses of suspensions with variation into viscosity due to Butyl-Diglycol dilution. On the other hand, shear thinning effect

indicates less than 150/s shear rate. This is estimated by the tack value of ink over the viscosity response according to the dilutions. The tack value does not change through distribution time. The viscosity drops with time and the non diluted ink presents lower viscosity than the 2% concentration of Butyl-Diglycol (Figure 4-1; Figure 4-6). This indicates low shear effect on forward roll distribution systems under the assumption that tack is related to viscosity. The non diluted ink viscosity drops rapidly under sudden shear stress and reaches the lowest value of the samples between 0.5% and 2% Butyl-Diglycol concentration. Tack decreases with decrease in viscosity and so a significant decrease in tack was expected if increased shear stress was applied through the nip region. Similarly, De Grâce (1988) reported that there was no effect of pressure at the nip region that affects ink. However, Chou (1992), argued that high shear rates affect the ink rheology at the nip region which was subsequently supported by other authors such as MacPhee (1998). Therefore, the nip region between an elastic and rigid roller indicates negligible shear stress.

The decrease in viscosity affects capillary number of the dilutions. The capillary number decreases with tack and produce similar responses (Figure 4-20). As a result tack and viscosity decrease with the capillary number of the fluids.

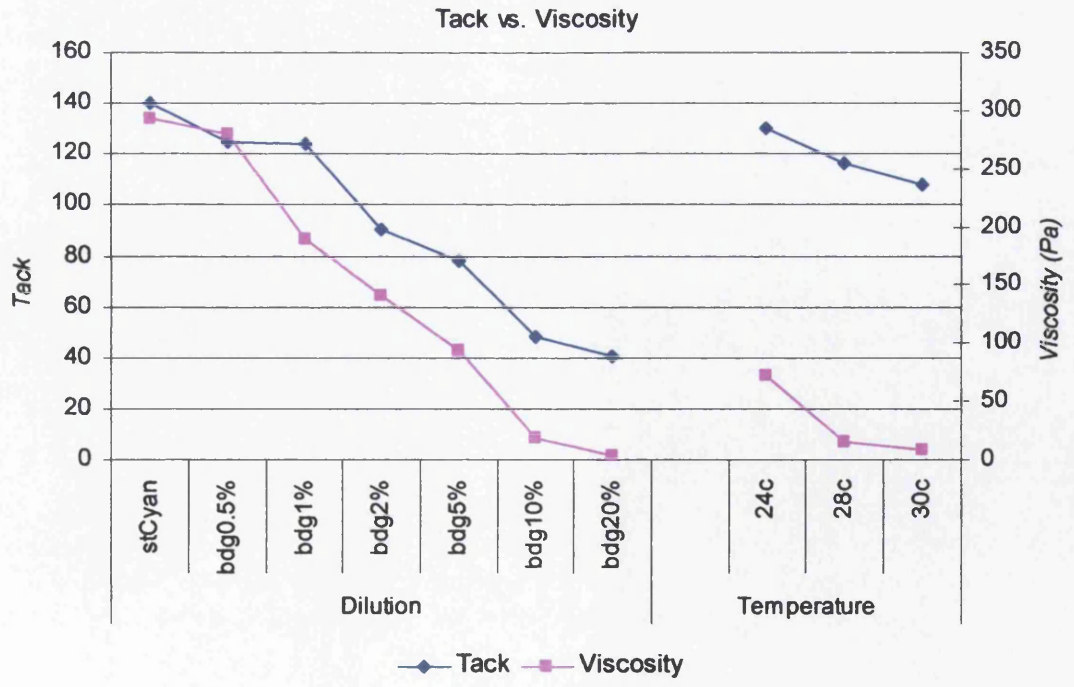

Figure 4-18 The effects on tack value versus viscosity, with increase in temperature and dilution of Butyl-Diglycol.

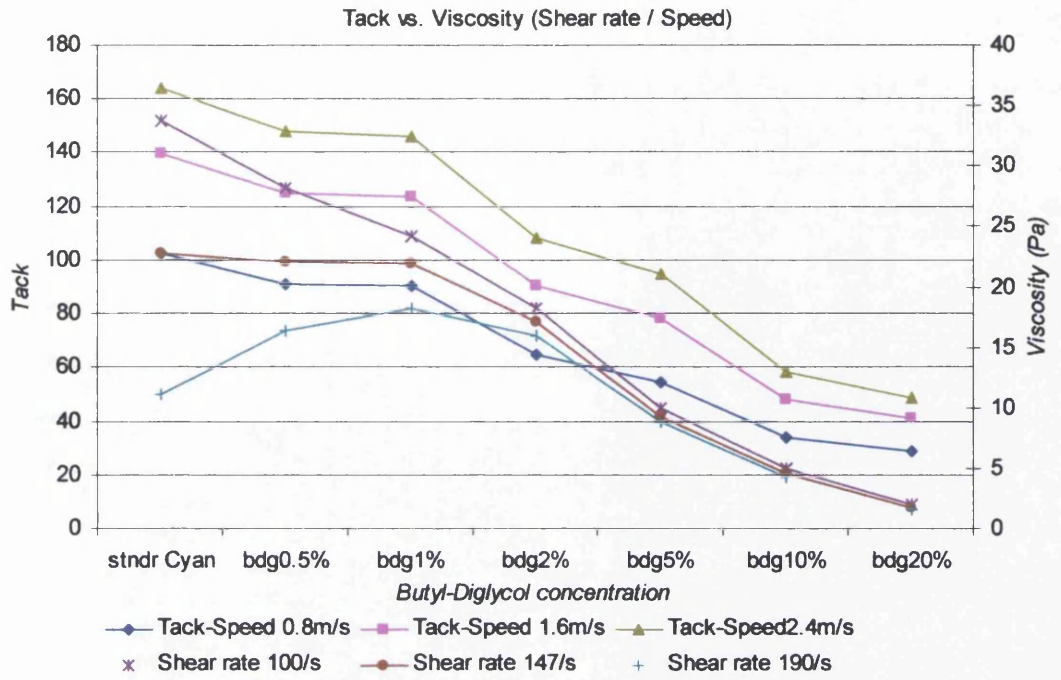

Figure 4-19 Responses of fluids with viscosity variation indicate similar responses in a particular range of shear rate. Tack responses do not vary by speed.

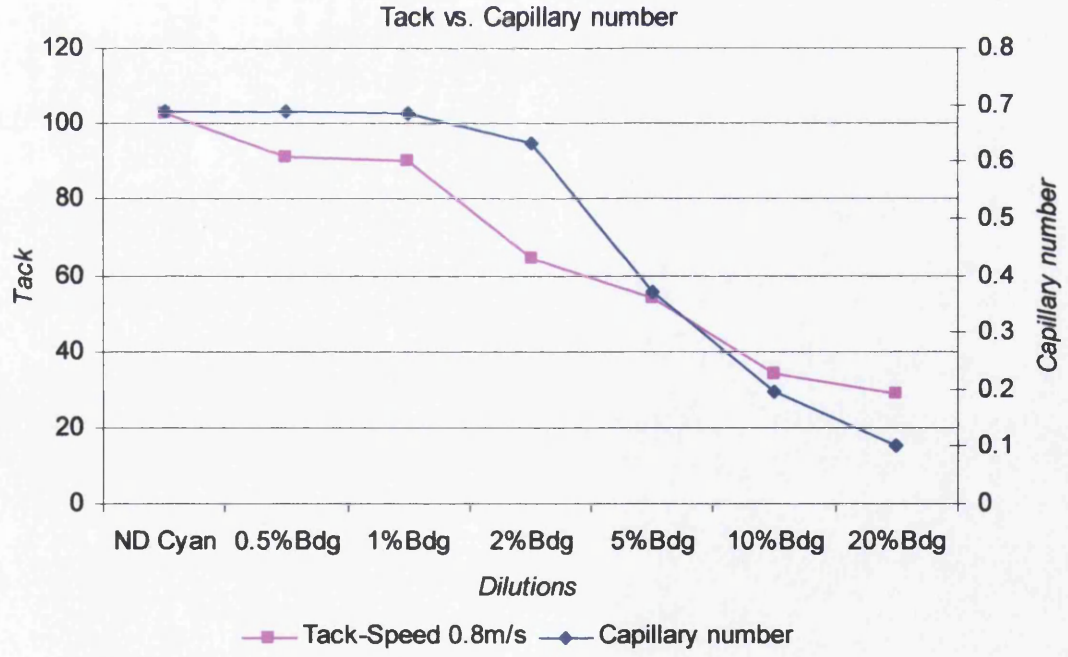

Figure 4-20 The tack decreases with the capillary number of the dilutions which also decrease with the viscosity.

4.4.3 Understanding tack and rheology on the printing press

Tack value on a press has a significant variation through the ink train. The ink film thickness decreases through the train and also the tack. However, different roller circumferences provide different rotational speed and as a results different separation rates. The tack can increase on smaller rollers and decrease on wider rollers as claimed also by Mewis and Dobbels (1981). Furthermore, Aspler et al (1996) argued that tack is not constant due to ink film thickness instability at the nip. As a result, the tack can be mainly important for the printing process and the actual ink transfer on the paper. However, the ink absorption can decrease or increase the tack and this depends on the ink film thickness and the paper surface qualities.

Tack is strictly related to the ink and the rheological profile of the ink. The current results of this study indicate how the tack varies with viscosity, ink film thickness and distribution speed. While the viscosity has similar responses with the tack, it is possible to be estimated by the tack under constant conditions. Tack can decrease 0.8 times when the ink film thickness decreases at the half. Coco and Cockerline (1988) stated also that the tack varies inversely with the cube of ink film thickness and therefore an ink film that is half as thick as another has eight times its tack. This is affected by viscosity and temperature changes as found through the experiments and by others (Fuchs et al 1991; Blayo et al 1998; MacPhee 1998). The results of this work show that an ink that has half the viscosity can show the same tack with a different one that is two times viscous but with half the rollers velocity. That is referred to the printing press application where the ink train is consisted by a series of rollers with various circumferences as described in chapter 1. The ink tack can change by the printing speed of the press and the ink train configuration. Short variations can occur also due to ink loss of the system and this is discussed through Chapter 7 that deals with misting phenomena.

4.5 Conclusions

This chapter examines the rheological characterisation that was carried out to establish behaviour and relations between complex fluid ranges based on a coldset lithographic ink formulation. Butyl-Diglycol was used as a low evaporation solvent to decrease primary viscosity and flux of the viscous ink. Variation of rheological

test was carried out on those diluted inks in order to establish relations and identify behaviour of inks on lithographic process.

- The ink profile is characterised by increased tack, shear thinning but also extension thickening behaviour. This affects the ink transfer mechanisms on rollers trains where printing parameters such as ink film thickness, temperature and printing speed are not constant.

- Shear thinning behaviour decreases with concentration and that also reduces thixotropy and relaxation. Hysteresis loop area decreases significant with increase in temperature. The viscosity decrease rapidly 40% to 60% with shear stress and temperature increase similar to the diluted ink with 1% and 2% Butyl-Diglycol concentration. The decrease in viscosity of lithographic ink indicates also a decrease in thixotropy, viscoelasticity and surface tension. Temperature and dilution can increase or decrease viscosity and affect the rheological profile of the ink.

- Viscoelastic profile decreases with Butyl-Diglycol concentration. The viscoelasticity decrease is determined by the increased difference of the viscous modulus versus elastic modulus with frequency increase. In low frequencies elastic modulus dominates and this effect increases with Butyl-Diglycol dilution.

- Tack decreases with the elasticity of the inks. Tack increases with increase of ink film thickness and distribution speed. The tack decreases with the rise of the temperature or the Butyl-Diglycol concentration similar to the viscosity. Relations between tack and shear viscosity determine a shear window of low shear rate in the nip region that is also independent of distribution speed on forward roll system.

- Tack and viscosity are affected by the capillary number of the fluids. The forward roll distribution system does not affect tack when temperature, speed, ink film thickness and viscosity are constant. This study does not verify shear

thinning effects on roller distribution system and the nip region. When viscoelastic fluids become extremely thin indicate pseudoplastic behaviour.

However, the increase in concentration affects the ink structure with undesirable effects such as increased misting phenomena and destruction of the ink structure network. Such phenomena are examined through developing techniques for extensional rheology and studies of ink misting and ribbing profiles in the following chapters.

5. Developing techniques on Extensional Rheometry

5.1 Introduction

Extensional deformations play a very significant role in many processing operations. Printing inks and coating fluids are all essentially extensional deformations. Shear flow measurements are not sufficient to characterise the deformation behaviour of a fluid. In many industrially important processes extension (elongation or tension) is the more critical characteristic of deformation than shear deformation. Trouton (1906) realised through his study that torsion was not exactly proportional to the shear by measuring the viscous flow rates of pitch and waxes. The torsion experiments did not relate to variables because the rate of flow in a twisting rod was not the same everywhere; it varies from zero at the centre to a maximum at the surface of the rod. More experiments included the flow produced in a rod under traction and under axial compression and the flow of a free stream of material. He simply thickened the rod at each end so that it fits exactly into a metallic box and then he attached weights to the box to produce the desired traction. That was also the principles of the extensional rheometry. Numerous configurations have been developed for unaxial and biaxial stretching testing of materials. The actual configuration of extensional rheometer came later under the work of Bazilevsky et al (1990). The first industrial configuration was appeared to the market by the Thermo Electron Corporation as CaBER (Capillary Break-up Extension Rheometer) test and the developing work of Entov (1997).

The elongation, filamentation and splitting of inks are critical phenomena in printing processes. Characterising these extensional behaviours will greatly improve our understanding of inks and coating. Extension viscosity is based on fluid stretching along elongation axis that generates tension across the direction due to viscoelastic structure. Stretching is the mechanism that through progressive elongation over time forces the fluid to split. The principles of the ink transfer mechanism described in chapter 2 refer to the ink transfer being divided into three stages, the entrance of the ink at the rollers nip, the compression at the rollers nip and the exit from the nip. The ink is elongated at the nip exit which tensile forces generate cavitations. Cavities

expand into filaments that are elongated between the two rollers and finally the filaments split. This is described also as ink splitting mechanism by Banks and Mill (1954). Figure 5-1 illustrates an ideal ink splitting at the rollers nip exit in relation with the extension rheometer with parallel plates and the viscocapillary thinning effect. The tension is proportional to the elongation and also to the shear rate (Bird et al 1987). Numerous variants of such systems are currently being developed by research groups around the world. An analytical description of those systems can be found in the Handbook of experimental fluid mechanics (Tropea et al 2007) However, the most promising system for fluids is the extension rheometry by using parallel plates. This configuration allows higher accuracy of measuring fluids extension characteristics and has been extensively studied and developed the last twenty years by numerous of authors (Bazilevsky et al 1990; Entov 1997; McKinley 1999; Anna et al 2001).

5.2 Methodology on extension rheometry

The concept of Extensional Rheometer (Figure 5-2) was developed to calculate extension properties of fluids. The original design of the instrument based on microfilament rheometer of Bezilevsky et al (1990) as was suggested for determining the viscosity of Newtonian fluids and the relaxation time of viscoelastic fluids. They developed a system configuration where a captive liquid drop was placed between two parallel plates. The plates are gradually separated vertically by a spring mechanism in a distance of two to three times of the initial separation and the filament is formed. The progressive thinning of the filament was captured during time until rupture. They fitted the experimental data to flow model based on Oldroyd-B equation to extract relaxation time.

$$R_{(t)}/R_p = (\eta_p R_p/\lambda\sigma)^{1/3}\exp(-t/3\lambda) \qquad (24)$$

The extensional rheometer used in the current work was built-up in the Welsh Centre for Printing and Coating and the Centre of Complex Fluids Processing of Swansea University. The system uses two electric motors that can move individually the plates up and down by individual adjustments of elongation speed and distance. The

elongation speed and elongation distance can be preset by the computer individually for each of the parallel plates. The fluid sample is loaded between the two plates in order to form a fluid cylinder. Either one or both plates can be moved apart at a set distance and the fluid is stretched to generate a single filament. The progressive thinning of the fluid filament is recorded by an external high speed CCD camera in a digital video system. Analysis is carried out by the captured images sequence. The filament neck thinning rates (Dmid) is calculated as a function over time. Finally, the extension viscosity is carried out by the stress versus strain rate. This test is based on development on CaBER rheometer (CaBER tests).

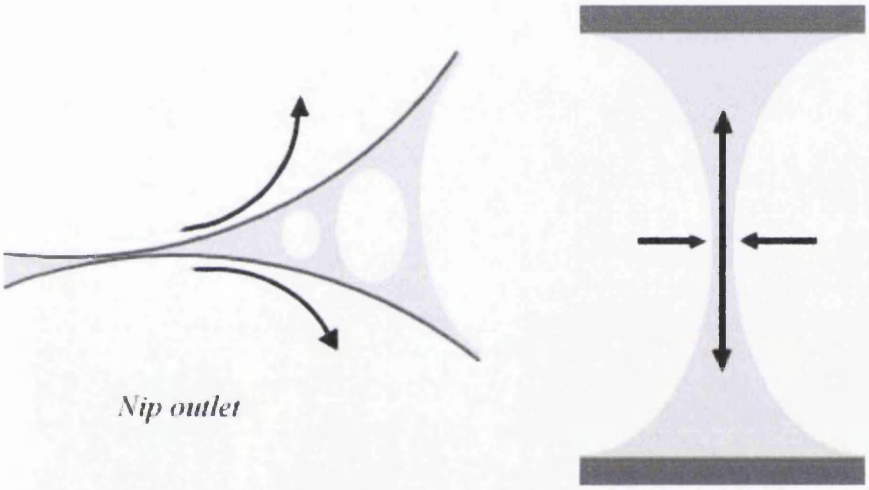

Figure 5-1 At the left image, ink filaments are formed at the nip exit due to cavities (Banks and Mill 1967). Extension of fluid cylinder forms a filament that progressively thins in the middle area (right).

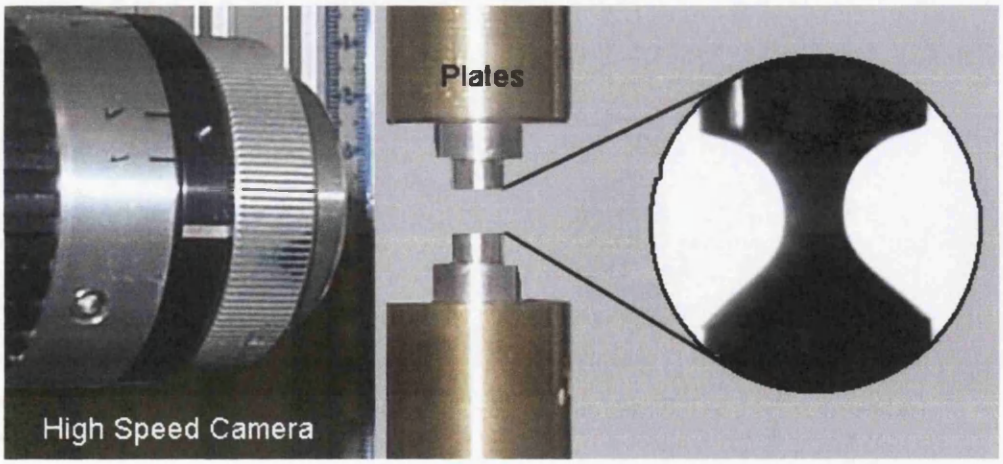

Figure 5-2 The extension rheometer was built-up by the Centre of complex fluid processing (Swansea University). The fluid sample is elongated between the two plates and a high speed camera captures the progressive thinning of the filament.

The current study and methodologies focused on investigations of repeatability and accuracy of the extension process for viscoelastic fluids summarized as follows:

The precondition times of the test

The temperature control of the fluid

The magnification rates by the capturing device

The performing of the main experimental process

The Cyan coldset lithographic ink was used for this work with high viscoelastic and thixotropic character. More ink dilutions were tested by using Butyl-Diglycol as a solvent. The rheological profile of all the dilutions was examined in details in Chapter 4. Preliminary studies were carried out by the use of model viscoelastic fluid in order to visualise fluid motion or gravitational effects during capillary thinning and break-up time.

5.2.1 The CaBER test approximation

The CaBER test was developed by the work of Bazilevsky, Entov and Rozhkov (1990). It consisted of a fixed bottom end plate and a moving top end plate. During a Caber test, the tested fluid is "instantaneously" stretched between two plates to a specific distance, creating a filament between the two plates. Extensional viscosity is defined as the ratio of the extensional stress and the extensional strain rate. The problem with the analysis of a capillary-thinning geometry lies in the accurate determination of the strain rate and stress. The filament is analysed only at its thinnest point, i.e. the mid filament, where it is assumed to have a cylindrical shape. Assuming that the axial velocity does not vary by the radius of the filament and the extension rate can be defined as follows:

$$\dot{\epsilon} = \frac{-2}{R}\frac{\vartheta R}{\vartheta t} \qquad (25)$$

Where R is the mid-filament radius

The stress equation as proposed by Szabo et al (1997) in differential form is

$$\rho\frac{\vartheta v}{\vartheta t} + \rho v\frac{\vartheta v}{\vartheta z} + \rho g = \frac{1}{R^2}\frac{\vartheta R^2}{\vartheta z}\tau_E - \frac{\sigma}{R^2}\frac{\vartheta R(1+RR'')}{\vartheta z} \qquad (26)$$

Where τ is the extensional stress, σ the surface tension and ρ the density. Imposing the cylindrical approximation and neglecting the effect of inertia, curvature and gravity, the stress equation becomes:

$$\tau_{\varepsilon} = \frac{\sigma}{R} \qquad (27)$$

The extensional viscosity is defined by integrating those equations

$$\lambda_{ext} = \frac{\tau_e}{\dot{\epsilon}} = \frac{\sigma}{-2\frac{\partial R}{\partial t}} \qquad (28)$$

Theoretical work has been carried out by Lubansky et al (2006) in collaboration with the Welsh Centre for Printing and Coating to extend the capabilities of extensional analysis including effects of inertia, gravity and surface tension on the whole profile of the filament (Deganello and Lubansky 2007).

The extensional rheometer configuration allows a wide modification of the fluids test due to flexibility of different elongation speeds, diameters and surface qualities of the used plates. This provides the ability of using the rheometer for capillary break-up rheometry either for filament stretching rheometry. The current study focuses at the capillary break-up rheometry to investigate the viscoelastic character of the lithographic inks.

5.2.2 High speed capturing process

Kodak EktaPro 4549mx imager is a digital high speed camera that can record up to 4.500 frames per second. It uses a 256x256 CCD sensor that allows 256 grey levels. Captured images were loaded in a VCR (digital video) for playback that allowed up to 24.500 full images. The images were saved in a computer in independent images or video format such as TIFF, JPG or AVI for further analysis. The use of high speed video allowed extensive analysis of the fluid viscoelastic deformation through tensile mechanisms. The camera records nearly 17 images for every second at 500fps (frames per second) or 100 images in one second at 3.000fps (the video frame of a standard recording camera is usually 30fps.

5.3 Process on extension rheometer.

The current work target was to understand the extensional flow of a viscoelastic fluid. The progressive Dmid thinning was measured by image analysis. The capturing quality depends on the operator and the lens characteristics. Low lighting lenses decrease capturing quality of filaments thinning neck but are affected also by the image and the angle or quality of the external lighting. The lens had to be in such position that it was orthogonal to the filament. The capturing speed and mode could also be varied.

5.3.1 Precondition times and temperature

Extension rheometry measures the progressive filament thinning to the break-up. The fluid sample has to be completely relaxed before being subjected to an applied tensile stress. Viscoelastic fluids are extremely difficult to be placed between the narrow gap of the two plates. The ink sample was loaded by a syringe which formed a fluid cylinder between the two plates. Plates of 6mm diameter were placed with a loaded gap of 2mm. These plates allow loading the fluid with the syringe by forming a good quality fluid cylinder for the experiments. A fluid cylinder was formed with 56.5 mm^3 ink volume. The fluid placement method generates shear stress in the ink causing the viscosity to decrease. Unfortunately, no other method had been developed to load the viscous fluid between the narrow gap of the plates. The fluid needs to recover completely before any further process. The recovery time of the fluid was set as the precondition time (relaxation) for which the fluid sample has to remain between the plates before the measurement. A precondition time of 10 minutes was defined by the Gemini shear nano-rheometer through creep to creep recovery test in Chapter 4.

A handheld infrared gun was used to establish the temperature of the fluid sample across each experiment. The IR gun could measure to 320°C in 0.5° resolution that covers the range of the temperatures that a fluid sample can reach. The measured ink temperature was found to be 23°C ±1. This reflects the constant temperature maintained in the laboratory.

5.3.2 Studies on repeatability and further aspects

The top plate moved a part in one step with 0.03m/sec separation speed. The capillary action between the plates formed a fluid filament. The progressive viscocapillary thinning of the filament was recorded by the Kodak EKTAPRO 4540mx camera. The capturing rate was 60 frames per second because the filament of the viscous emulsions had low progressive thinning rates. More detailed capturing did not provide further information but increased the captured file. This capturing speed generated more than 4.000 frames per test dependent on filament thinning rates. Three tests were carried out for each diluted ink with Butyl-Diglycol concentration by three different elongation distances of 6, 8 and 10 mm (Figure 5-3).. Those distances provided 3, 4 and 5 times elongation of the volume in order to examine variations of the process Extension was tested also under three different volumes of ink at the same elongation speed and distance to identify gravitational effects (Figure 5-4). Such effects were determined by the increase of contact angle at the bottom end plate which indicated fluid flow. Each test was repeated three times for each test protocol.

There has not been much work reported on viscoelastic fluids except those of Anna et al (2001). Therefore, tests were carried out in order to examine the elongation mechanism. These tests included elongation of one plate independently or both plates simultaneously (Figure 5-5). The filament thinning rates were examined under different extension configuration process at steady elongation speed of 0.03m/sec. The effect of tensile stress under progressive elongation speeds was also examined by moving only the top end plate up (Figure 5-6). This test was necessary in order to examine the repeatability of the process and to develop the extensional rheometer, optimising magnification, lighting and volume loading techniques to improve accuracy. Each individual parameters test was repeated three times to obtain reliable values.

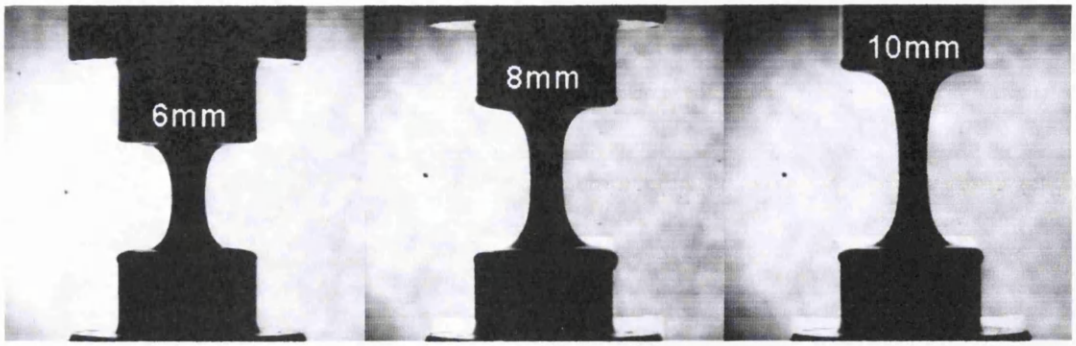

Figure 5-3 Capillary break-up test was performed by 3 different elongation distances of the top end plate named 6mm, 8mm and 10mm. These provided an extension of 3, 4 and 5 times the ink volume.

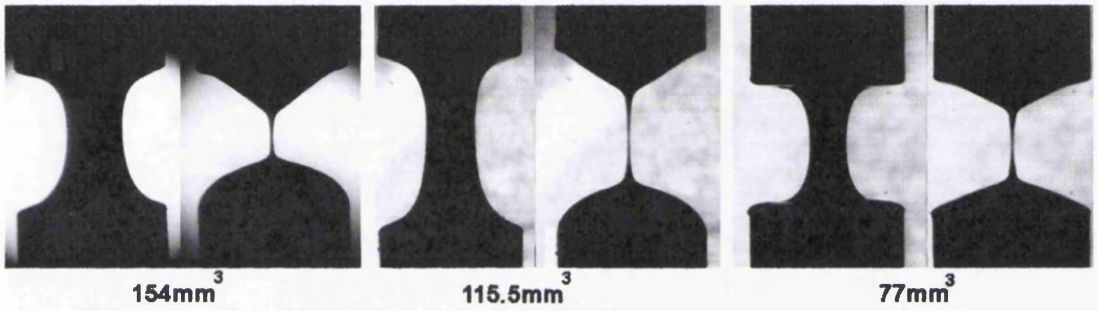

Figure 5-4 The volume of the fluid was also examined to identify gravitational effects. The parameter of the start gap was tested by increasing ink volume between the preliminary tests in order to establish the effect of gravity on the extensional rheometry for viscoelastic fluid and lithographic inks.

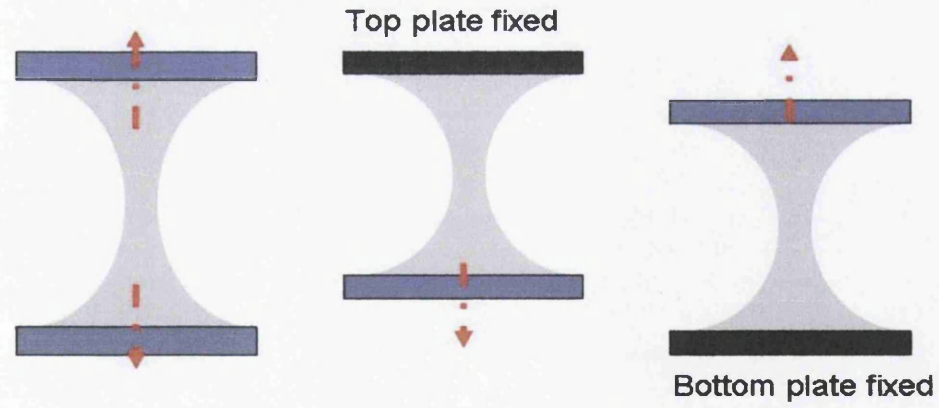

Figure 5-5 The filament thinning rates were studied moving the two end plates simultaneously or each of the plates independently. The effect of the end plate was also examined by performing tests with three different moving geometries of end plate. The test examined the effect of the both two end plates extension, the bottom end plate extension and the top end plate extension geometry.

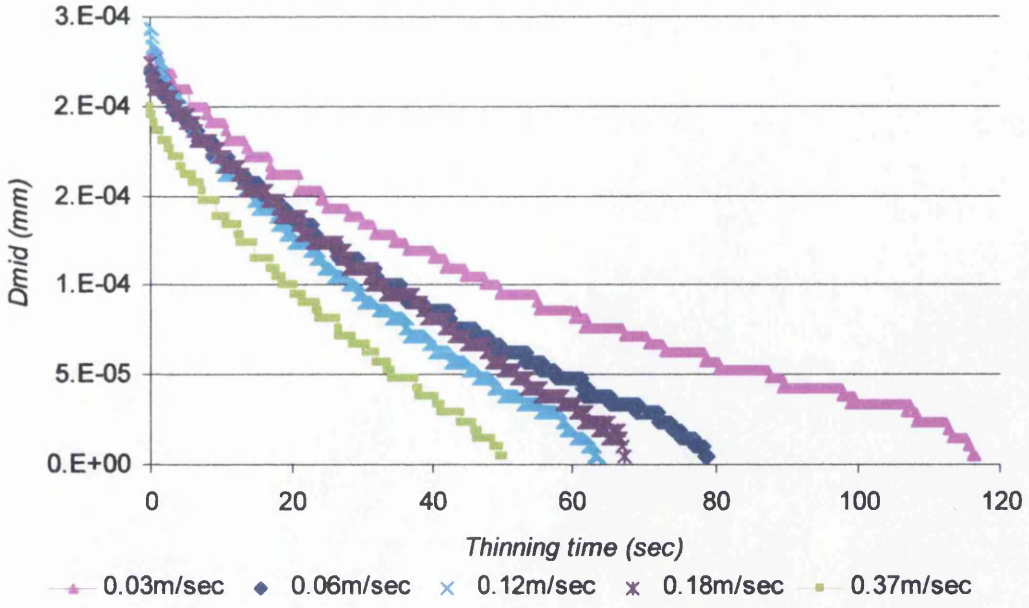

Figure 5-6 Five progressive elongation speeds have been examined at the extension rheometer by examining the speed effect. The filament thinning time decreases with the elongation speed.

5.3.2.1 Internal flow and model fluids

This section involved also the study of two model fluids in order to examine the internal motion. It was not possible to verify this on complete transparent or opaque fluids. The model fluid consisted of a viscous or a viscoelastic material with dissolved pigments in low concentration. This allowed the light to reflect the particles through the transparency of the viscous liquid (Figure 5-7). The high speed camera captured the particles moving during the fluid elongation and the progressive thinning of the filament providing detailed imaging of the elongation mechanism. Those tests were examined by elongation distance of three times the volume and progressive elongation till filament rupture at 0.03m/sec separation speed. Toothpaste was used for the preliminary experiments, before a model fluid was developed which consisted by glycerine (49.5 mPa-s) with 2% dispersed metallic pigments in it. The high speed video allowed monitoring the pigments flow during filament thinning time. Results of model fluids are discussed in section 5.5.1.

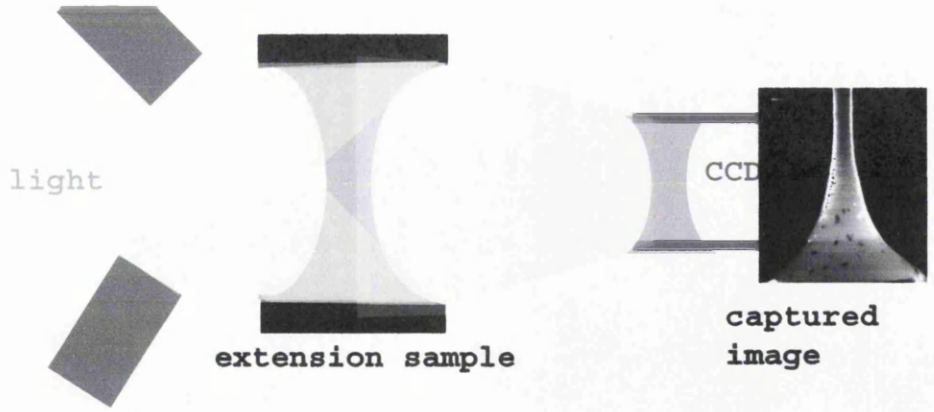

Figure 5-7 Backlighting for extension rheometer used to illuminate model fluid in order to capture the fluid flow during capillary thinning and break-up. The right light angle illuminates the transparent fluid and highlights the particle movement in the fluid during the extension. The process is captured the high speed camera for the capillary thinning analysis.

5.3.2.2 Simulating a printing nip on extension rheometer

The configuration of the extensional rheometer was used also to determine filaments formation in the rollers nip exit. Wider parallel plates of 65mm were used to simulate a printing nip. A linear ink film was applied across the diameter of the plates in order to form a linear nip (Figure 5-8). The end plates came in contact to generate a nip with narrow gap. This gap was set to 500 μm and the ink volume was approximately $40mm^3$ at a line of 20mm. That generated nip dimensions of $80mm^2$ nip contact area (4mm wide nip) at 500μm gap. The extension process followed the capillary break-up protocol. The test was carried out by two different speeds namely 0.03m/s and 0.6m/s. Higher speeds was not possible to applied due to limitations of the extension rheometer but also the critical vibrations by higher speeds. The capillary break-up was captured by high speed camera and filament thinning rates calculated to examine such mechanisms. This is important for roll inking and coating systems where high speed recording states limits due to narrow gaps and vibrations.

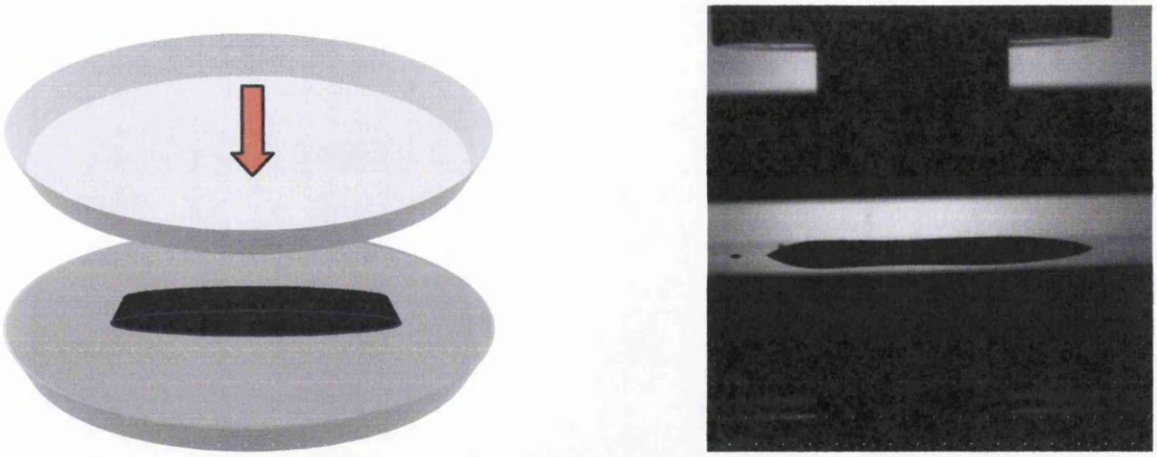

Figure 5-8 A single printing nip was formed between the parallel plates of 65mm diameter.

5.3.3 Extension viscosity analysis protocol

The captured images were analysed by Image J software in order to calculate the progressive Dmid of the filament neck thinning (Figure 5-9). The macro analysis of the Dmid was modified by Dr.Alex Lubansky. The extracted data of the Dmid were plotted into charts to visualise the progressive filament thinning time (Figure 5-10). The extension viscosity was calculated in MatLab programming code developed by Dr. Davide Deganello (Deganello et al 2007) based on CaBER approximation as described in instruction manual HAAKE CaBER, as follows:

$$\text{Stress} = \tau = (2 \times \sigma)/\text{Dmid} \qquad (29)$$

$$\text{Strain rate} = \varepsilon' = -2/\text{Dmid} \times (d\text{Dmid}/dt) \qquad (30)$$

$$\text{Extension Viscosity} = \text{Stress} / \text{Strain rate} \qquad (31)$$

The charts plot extension viscosity versus strain rate in a logarithmic scale (Figure 5-11). The interest was focused on the middle of the filament and high magnification was selected to eliminate lighting effects (Figure 5-12). The low magnification determines lower thinning times due to conflict of the grey background.

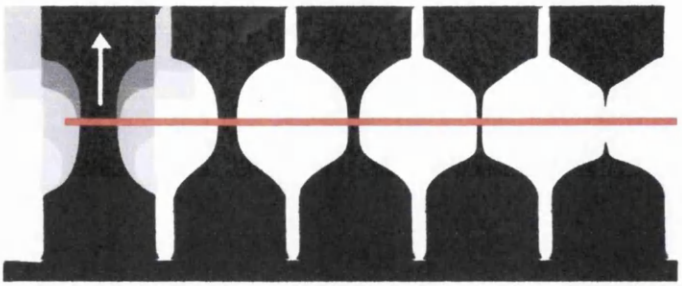

Figure 5-9 Elongation to failure after the plates have been moved a preset distance. The images are captured by a high speed photographic camera and are analysed by image analysis software in order to determine the D-mid filament thinning over time.

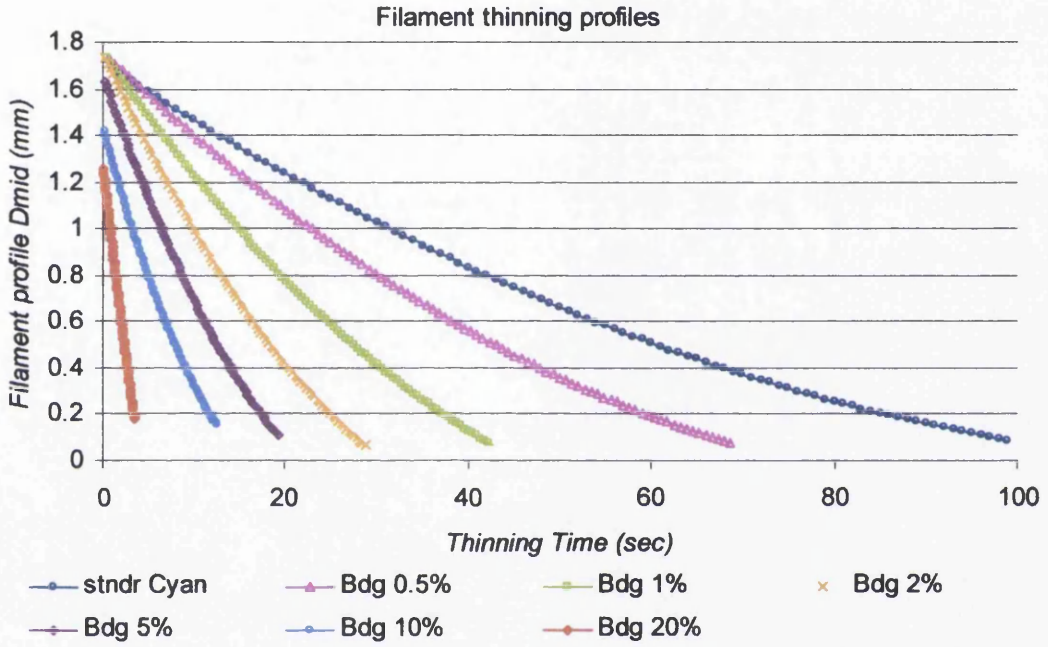

Figure 5-10 Progressive filaments Dmid thinning profile over capillary break-up time by ink in concentration with Butyl-Diglycol. Results are discussed in section 5.4.4

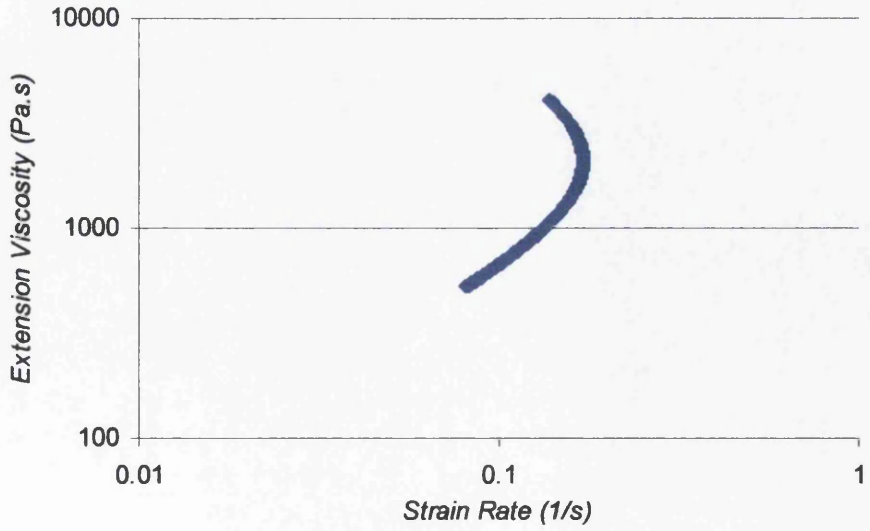

Figure 5-11 The apparent extension viscosity over strain rate was plotted on a logarithmic scale chart.

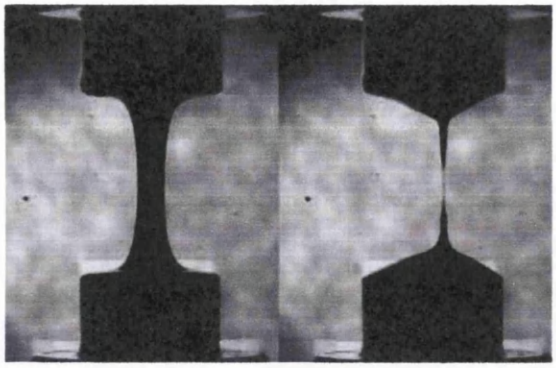
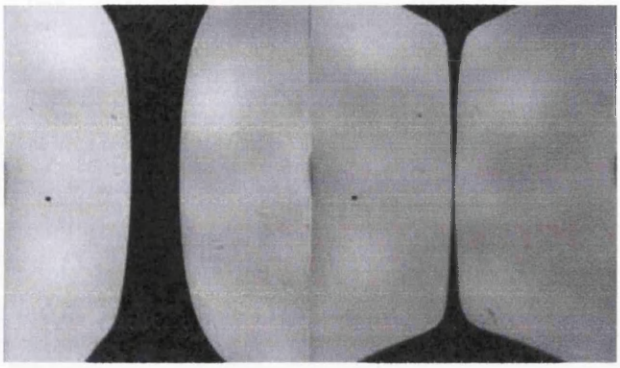

Figure 5-12 The magnification at the middle of the filament allows of capturing the critical stage of the extension and break-up (app. VCD V1-V2).

5.3.4 Trouton ratio

Trouton's ratio is determined by the extension viscosity over the zero-shear viscosity. The Trouton (1906) theoretical results concluded that the elongational viscosity is three times the shear viscosity for the most Newtonian liquids while for non-Newtonian fluids it is usually greater than three. Trouton found that in all cases the rate of flow was faster immediately after application of the force and the time rate of elongation per unit length (dv/dx) was proportional to the force of traction (extension viscosity) per unit area (F/A) which described as follows:

$$\lambda = (F/A)/(dv.dx) \qquad (32)$$

The experiments with a stream falling under its own weight allowed Trouton to determine the differential equation of the shape of the stream. Trouton was able to develop the following equation for calculating the value of the extension viscosity.

$$\lambda = (\rho g\, \pi K^2)/2M \qquad (33)$$

The coefficient of viscous traction must be equal to three times the coefficient of viscosity, μ, that is, $\lambda = 3\mu$.

The resistance of the elongating fluid filament to this deformation is the tensile force on one of the plates and was referred as a transient Trouton ratio (Bird et al 1987). Trouton ratio (Tr) is defined as the ratio between the time-dependent extensional viscosity and the zero-shear viscosity (Spiegelberg et al 1996). Trouton ratio

provides a good indicator of polymers conformation. The Trouton ratio increases when the extensional viscosity increases relative to the shear viscosity. This increase is indicative of an increase in hydrodynamic size due to polymers stretching. If the Trouton ratio is constant and low (minimum 3 for Newtonian fluids) then the time scale (inverse of the strain rate) is too long to influence the polymers shape. If the Trouton ratio is constant and high, it is an indicator that the polymer is fully stretched. The absolute magnitude of the Trouton ratio in the upper plateau (if measurable) is an indicator of how much the polymer can be stretched out. A large difference between the ratio at low and high strain rates indicates that the polymer is very flexible and can be extended to a high degree. A large polymer will show a greater Trouton ratio than a small one.

5.4 Results on Extension and Capillary break-up rheometry

The current work used a capillary break-up rheometer to analyse the extensional behaviour of dilutions. A range of tests were performed to determine the accuracy of the process because not much studies have been reported before for non-Newtonian highly viscoelastic fluids such as lithographic printing inks. The tests used to establish the experimental conditions in order to compare the dilutions of offset ink and Butyl Diglycol. Extensional tests were also used to simulate fluids behaviour at the printing nip. The extensional viscosity was based on standard mid-filament theory following the measuring process described in work of Deganello (2007).
Furthermore, preliminary studies were performed testing a specially developed model fluid, which allowed examining the internal flow of fluids under tensile stress. Modifications on the extension rheometer provided also the ability to study multi-filament formation, typical of the printing nip.

5.4.1 Ink volume effects

The effect of ink volume on the measurement of the extensional properties of the fluid was investigated. The test was carried out with an elongation distance named three times the examined ink volume. The symmetric splitting and the negligible change in contact angle over the filaments thinning time showed that gravitational effects were negligible in a low concentration of Butyl-Diglycol and did not affect

the experimental results even when the ink volume was as low as 77mm^3 (Figure 5-13). Higher ink volumes illustrated increase of contact angle during break-up time. The increase of contact angle indicates the increase of surface tension through relaxation of the fluid. This can also assumes fluid flow due to gravitational effects. Gravitational effects are significant in low viscosity fluids due to decreased adhesion or tack as determined in Chapter 4.

The ink volume is critical for the extension viscosity. The capillary break-up time decreases at lower volumes. This represents an extension distance of more three times the reference ink volume between the plates. The test was at low speed 0.03m/s. The formed filament thickness increased with the ink volume as was expected indicating there was a faster break-up. This could also be due to a gravitational effect which increases with the volume and affects thinning rates (Figure 5-14). The extension viscosity increases with decrease in ink volume due to the increased filament thinning rates (Figure 5-15). As a result the apparent measured extensional viscosity is depends on variation in ink volume. Therefore it is essential to use same fluid volume and set of parameters for comparative analysis.

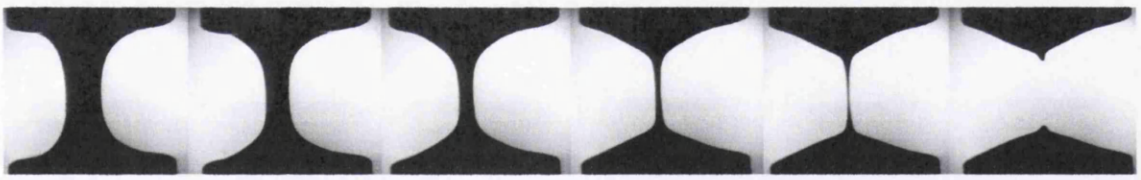

Figure 5-13 The low ink volume (77mm^2) does not appear any gravitational effect. This was carried out by the equal splitting between the end plates and the negligible change of the contact angle (appendix video cd V3).

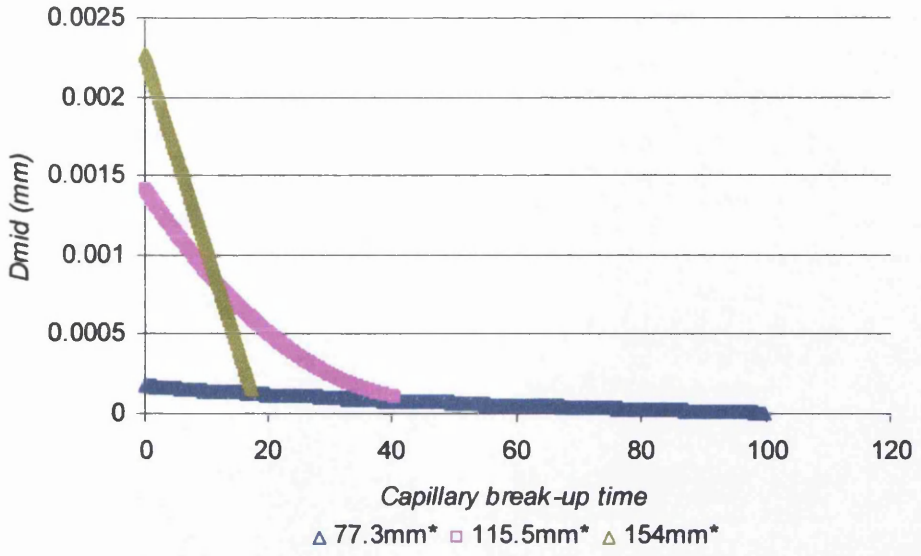

Figure 5-14 The increase ink volume decreases the capillary break-up time as an effect of gravity. The capillary thinning is affected by the inertia of the ink volume. The weight increases and the break-up time decreases. Each of the samples were extended three times the start gap with the same speed of 0.08m/sec

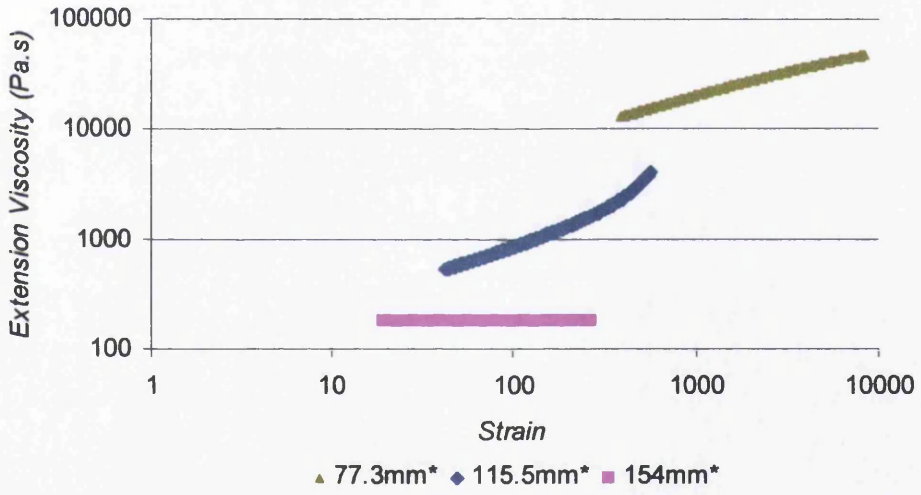

Figure 5-15 The apparent extension viscosity increases with the decrease in ink volume. The effect of gravity determines lower extension viscosity.

5.4.2 Elongation speed effect

The elongation speed affects tensile stress of the materials. The break-up times decreased significantly with the increase in elongation speed. The decrease was approximately proportional to the speed and the surface tension of the fluid. Capillary-break-up time decreased with the increase in elongation speed (Figure

5-16). Higher speed increased inertial effect and affect thinning rates caused almost instantaneous break-up of the filament.

The extension viscosity increased at low strain rate indicating thickening behaviour. However, high strain rates indicate Newtonian behaviour which was determined by consistency in extension viscosity over strain rate (Figure 5-17). The inertia increase capillary break-up and extension viscosity does indicate thickening effects. Between these speeds there was linear increase of the thickening effect with the decrease in elongation speed. Thus, extension viscosity was also affected by the elongation speed.

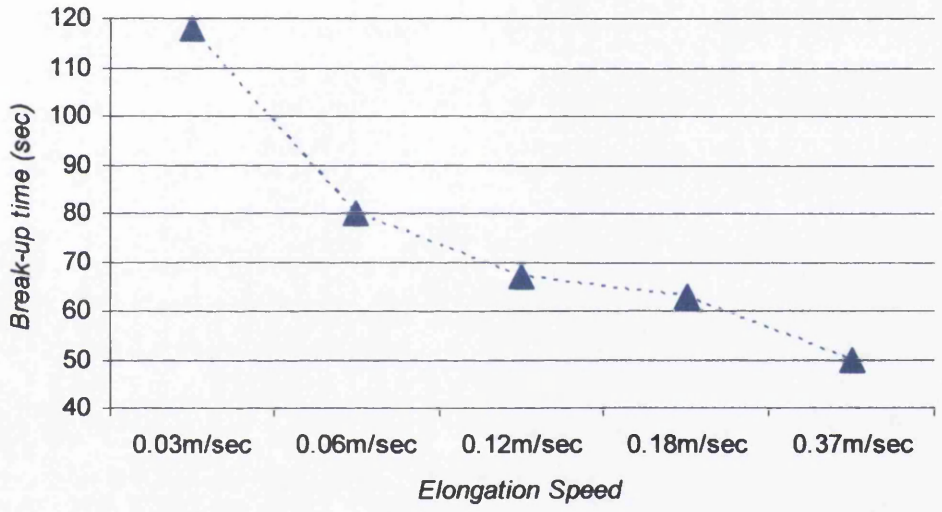

Figure 5-16 The capillary break-up time decreases with the increasing of the elongation speed.

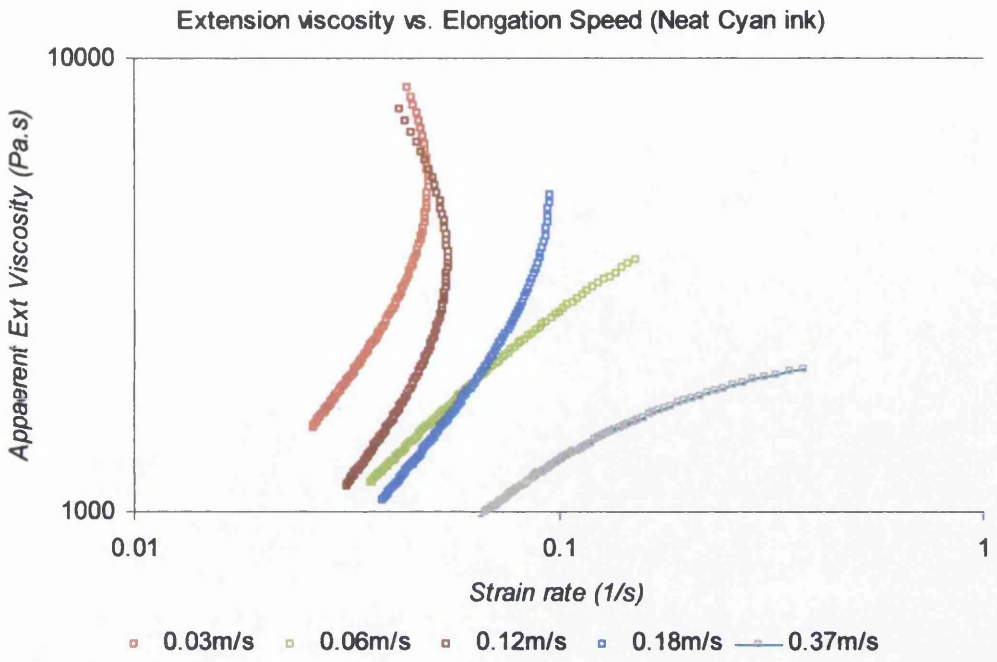

Figure 5-17 The extension thickening effect decrease with the increase in elongation speed.

5.4.3 Plates configuration effect

The test examined the end-plate effect on the capillary break-up time effect and extension viscosity of the ink dilutions. The capillary break-up time was not significantly varied which ever plate moved at low speeds of extension (0.03m/s). Figure 5-18 illustrates the middle diameter of the filament over the capillary break-up time for different end plates movement. Moving the top plate only increased the filament thinning time. Moving the bottom plate only slightly decreased the thinning time. Moving both plates produced a faster thinning effect in comparison of the two other configurations. Both plates moved with same speed and the overall separation speed was same as the independent plates with 0.015m/s. There was extension thickening of the viscosity over strain rate especially when the top or the bottom plate were moved independently (Figure 5-19). The both plates lead in lower extension viscosity with lower thickening effect. The elongation speed increases with the both plates uniaxial elongation.

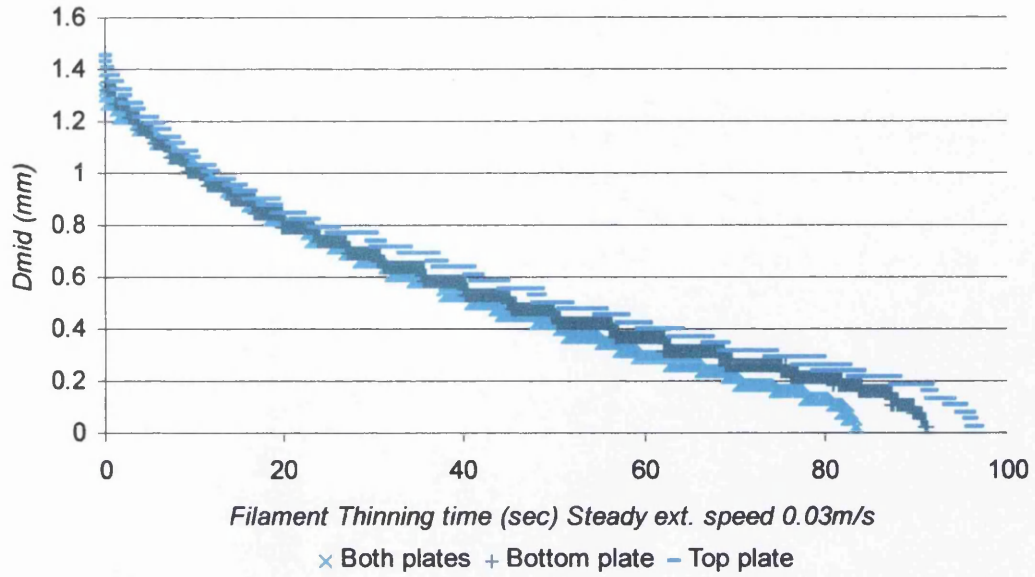

Figure 5-18 The effect of the both end plates is higher than the effect of the top or the bottom plates configuration.

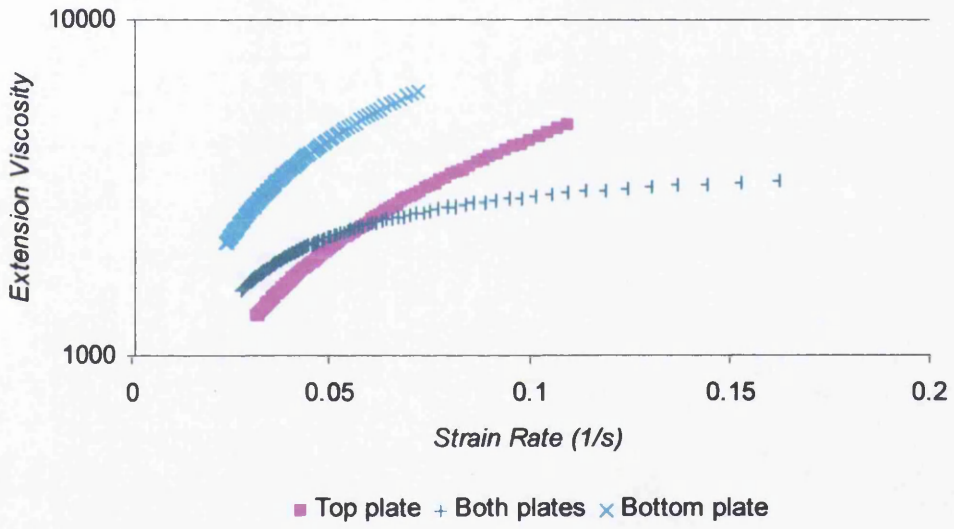

Figure 5-19 The extension viscosity increased with the strain when the bottom or the top plate used. The both plates uniaxial separation multiply the elongation speed and minimises the thickening effect.

5.4.3.1 Magnification

The capturing magnification was adjusted by the lens use of the high speed camera. The light's intensity showed that can burn the image of extremely thin filament during recording. As a result this carried out lower filament thinning rates. Reflected light was used to decrease intensity of the back light. Low magnification allowed the capture of the whole profile of the extension process including the contact angle at

the end plates. However, the extension viscosity calculation is based on the mid filament diameter. Focusing closer to the mid filament and capturing the narrow area of thinning with high magnification improved this was critical aspect for the accuracy of the measurement. The extension viscosity was significant higher at the low magnification than the high magnification (Figure 5-20). Both magnifications determined extension thickening rates over strain with higher trends from the low magnification. The lower magnification captures with lower resolution and a result the image becomes unstable with faster break-up time. The high magnification focuses on the critical area of the thinning neck and captures more accurate profile in longer break-up time and different thinning rates.

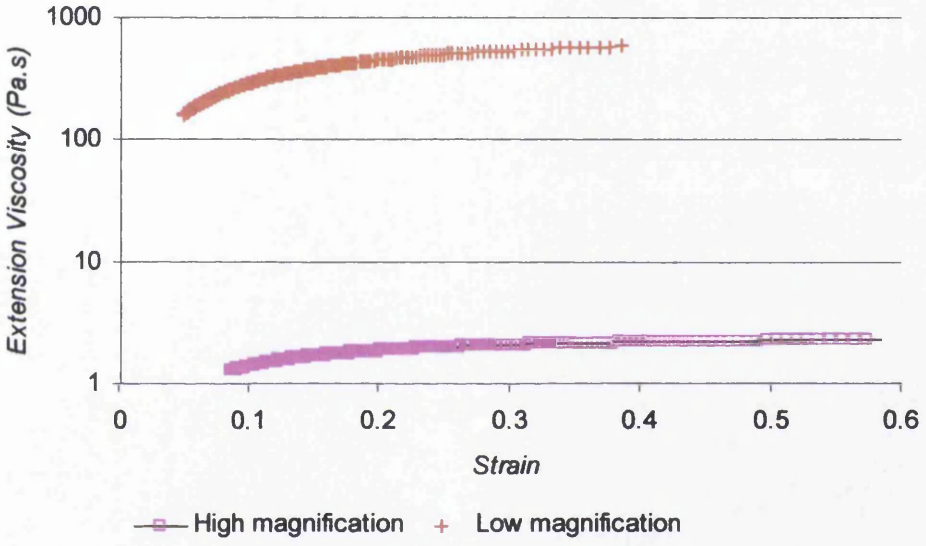

Figure 5-20 Higher extension viscosity is carried out by low magnification of the capturing filament thinning

5.4.4 Viscosity effects by Butyl-Diglycol concentration

The capillary break-up time decreased with increased concentration of Butyl-Diglycol (Figure 5-21). Dilution with only 0.5% Butyl-Diglycol decreases the break-up time of the filament by 30%. The break-up time continues to decrease by 80% with the increase of 5% Butyl-Diglycol concentration in comparison with the original coldset ink. The 20% concentration reaches almost 3 seconds of break-up time that concludes to approximately 95% decrease in comparison with the coldset Cyan ink as reference.

The extension rheometry results indicated an extension thickening behaviour over strain stress of the lithographic ink dilutions. The extension thickening effect persisted with increase in dilution independent to Butyl-Diglycol concentration. The extension viscosity increased with the decrease in Butyl-Diglycol concentration. The ink dilution of 20% decreased significantly the extension viscosity and tends to Newtonian with a steady behaviour over strain (Figure 5-22). The viscoelastic fluids indicate extension thickening effect over strain rate. The decrease in shear viscosity affects also extension viscosity which decreases with the Butyl-Diglycol concentration.

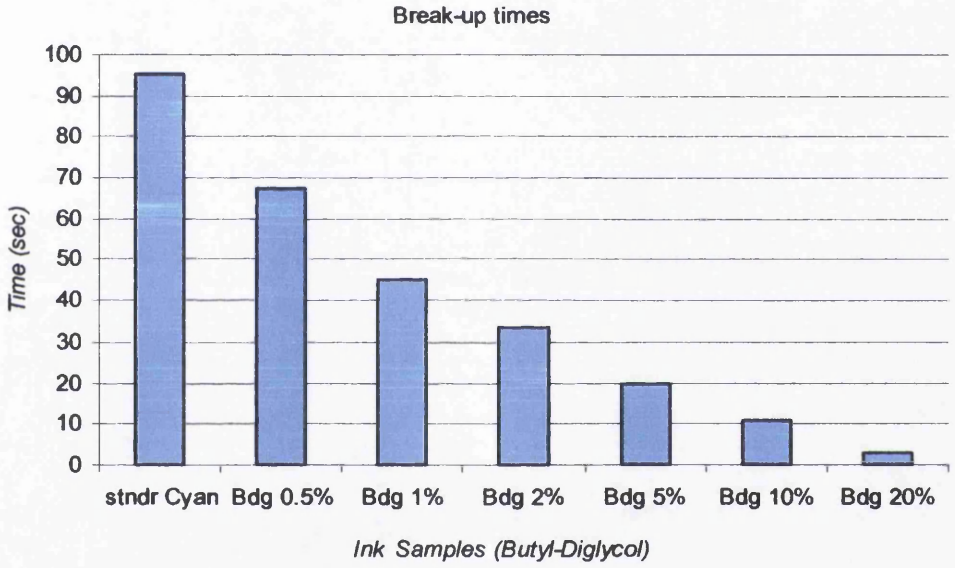

Figure 5-21 Break-up time decreases with increase of Butyl-Diglycol dilution in Cyan ink or decrease in viscosity. The results indicate similar rates with tack

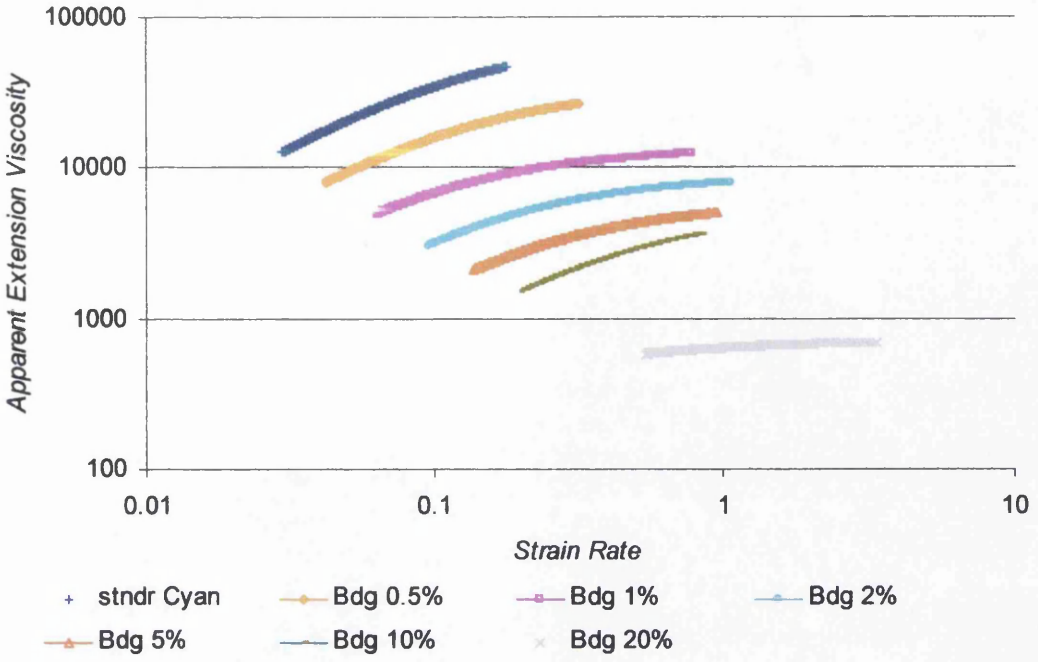

Figure 5-22 Apparatus extension viscosity of lithographic ink with dilution of Butyl-Diglycol versus strain rate.

Trouton ratio was calculated by the apparent extension viscosity over the zero-shear viscosity. The zero shear viscosity was determined by the relaxation viscosity in Chapter 4. Trouton ratio of ink dilutions indicated linear extension effect over strain. Trouton ratio becomes less than 3 for the high diluted ink samples such as 5%, 10% and 20% Butyl-Diglycol concentration. The cyan determined also 1 to 3 Trouton ratio at longer strain. The 5% dilution showed higher Trouton ratio from 2 to 4 while 10% and 20% dilutions determined lower than 1 Trouton ratio. On the other hand, the low concentration diluted ink samples illustrated higher ratio than 10. The lowest dilution of 0.5% Butyl-Diglycol lead to higher Trouton ratio. The ratio decreased with the dilution and 1% determined 50 while 2% dilution approximated 8 to 20 Trouton ratio. The Trouton ratio range decreased linearly with the Butyl-Diglycol over strain. Highest polymers stretching over strain is illustrated by the neat cyan ink.

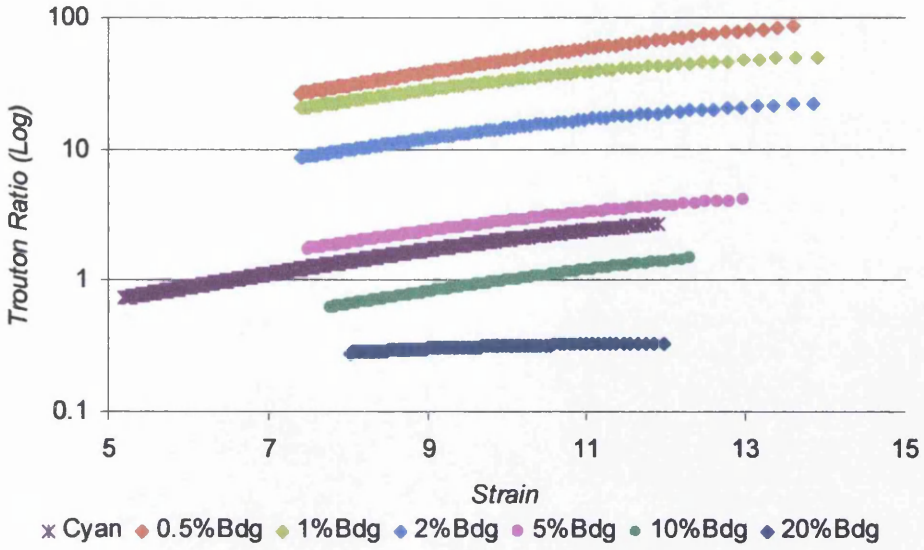

Figure 5-23 Trouton ration was calculated by the extension viscosity over the zero shear viscosity.

5.5 Discussion

Increased Butyl-Diglycol concentration decreases viscoelastic character of the ink and this also decreases surface tension and tack value (Chapter 4). Capillary break-up results indicate similar behaviour. The filament thinning time decreases with the viscosity and tack. This affects extension viscosity which decreases as a function of the tack and the capillary number based on the current results of this work as discussed in chapter 4.

The Trouton ratio increases when the extensional viscosity increases relative to the shear viscosity. The increase in Trouton ratio is an indication of an increase in hydrodynamic size due to molecular stretching (Spiegelberg et la 1996). The Trouton ratio of ink dilutions indicates the linear extension effect over strain. The viscoelastic polymer chain extends linearly with the strain. The variation in viscosity determines weak polymers with increased concentration of Butyl-Diglycol. Cyan ink indicates highest extension rates over strain. This drops with the shear viscosity of the dilutions. Trouton ratio is usually 3 for Newtonian fluids and can be much higher for non-Newtonian fluids with viscous and viscoelastic character (Bird et al 1987). Trouton ratio was found to be low (less than 3) for the cyan and the high concentration diluted ink therefore, the time scale is too long to influence the polymers shape. The low Butyl-Diglycol concentration inks are show higher than 10

Trouton ratio which indicates that polymers are fully stretched during extension. The higher plateau of the Trouton ratio indicates extension rates for the inks. The large difference between the ratio at low and high strain indicates that the ink polymers are very flexible and can be extended to a high degree.

The calculation of the extension viscosity over the characteristic shear viscosity at 147/s determines different ratio plateau. The characteristic shear viscosity was determined from the ratio between viscosity and tack. The Trouton ration becomes more accurate when characteristic viscosity is applied. The Trouton ratio climbs significantly higher than 10 (Figure 5-24). This suggests that ink polymers are fully stretched during extension. This also indicates that the Butyl-Diglycol does not significantly affect the extension of the polymers and these do not lose flexibility with strain. The variation over strain determines that dilution can form shorter filament over uniaxial extension or filaments that break-up faster. This was determined by the results on capillary break-up. Therefore, the Trouton ratio for printing ink becomes more accurate by the extension viscosity over the characteristic shear viscosity at 147/s shear rate as was determined in chapter 4.

The filament break-up time results indicate influence of the test by fluid volume, the elongation distance and elongation speed. This can also affect the determination of extension viscosity. However, the diluted ink samples were tested under the same protocol of parameters and magnification in order to eliminate such effects.

The elongation speed affects extension viscosity which decreases with increase in elongation speed as shown in Section 5.4.2. The decrease is higher between extreme speeds of 0.03m/sec to 0.4m/sec. The effect of high elongation speed may also be due to inertia effects. The high tensile stress affects the polymers extension and generates plasticity to the structure at the formed filament. Thus the polymers stress exceeds deformation rates and break faster. Extension viscosity was calculated in much lower elongation speed (0.06m/s) but elongation speed rates determines that break-up time can approximate values close to zero.

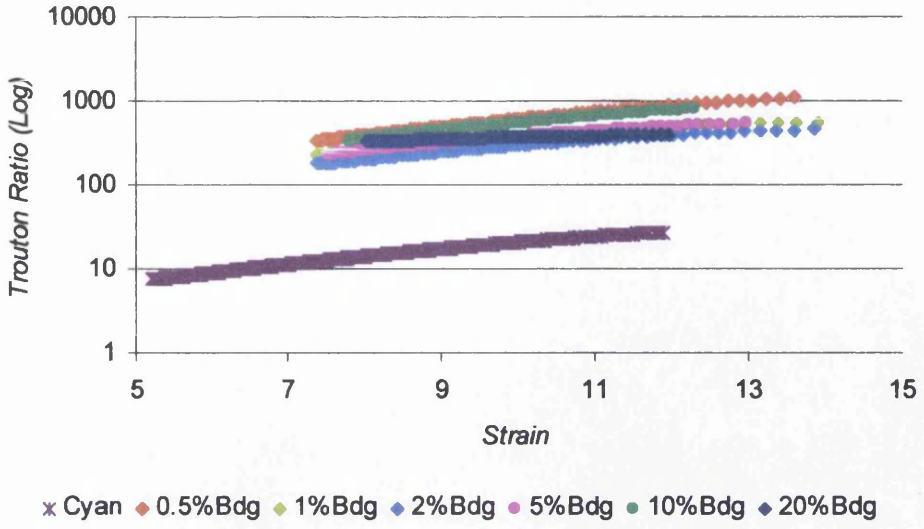

Figure 5-24 Results of the Trouton ratio in a range of shear viscosity characteristic of the nip region. The overlapping of the results indicates that independently from concentration the polymer present similar flexibility.

5.5.1 Recovery and extension thickening effects

The apparent extension viscosity decreases with the increase of Butyl-Diglycol dilution which results to decrease with the capillary number. Lithographic ink shows an extension thickening effect on viscosity. Results indicate a transit extension process with deformation due to elongation. Polymer chains are extended and reach the maximum deformation. A hardening effect is generated through the break-up of the polymer chain of the ink. This was determined by extension analysis of glycerine with pigments dispersion. Three steps are established during elongation (Figure 5-25). First, the fluid cylinder is deformed by linear motion, the mass concentration between the end plates at the start position to the extension position. Second phase is the longest where fluid begins to flow from the upper volume to the bottom plate under the effect of gravity which increases with the recovery of the surface tension. This phase is determined by the increase of contact angle at the bottom plate. In the final step, the fluid extends in two directions and finally splits. The last step is characterised by a short extension delay which provides differences between the viscocapillary thinning of the glycerine and that of pigments dispersion (Figure 5-26). The last step seems to be critical for the extension behaviour of the fluid while this is the only time scale of the observation where actually the fluid is stretched uniaxially.

Butyl-Diglycol decreases elasticity of the ink and increases flow through extension and thus thinning time decreases. As a result, the thinning time increases with elasticity which also affects the ratio between flow thinning and extension thinning. Similar results were determined by using toothpaste as a model fluid (Figure 5-27). The viscous fluid begins to flow after the upwards movement of the top plate. During uniaxial extension the fluid is deformed like a rod. If the filament does not break during extension, then it starts to flow to the bottom plate. While the fluid volume decreases from the top plate the adhesive dynamics of the fluid becomes equal and the fluid filament is extended uniform in both directions and finally splits.

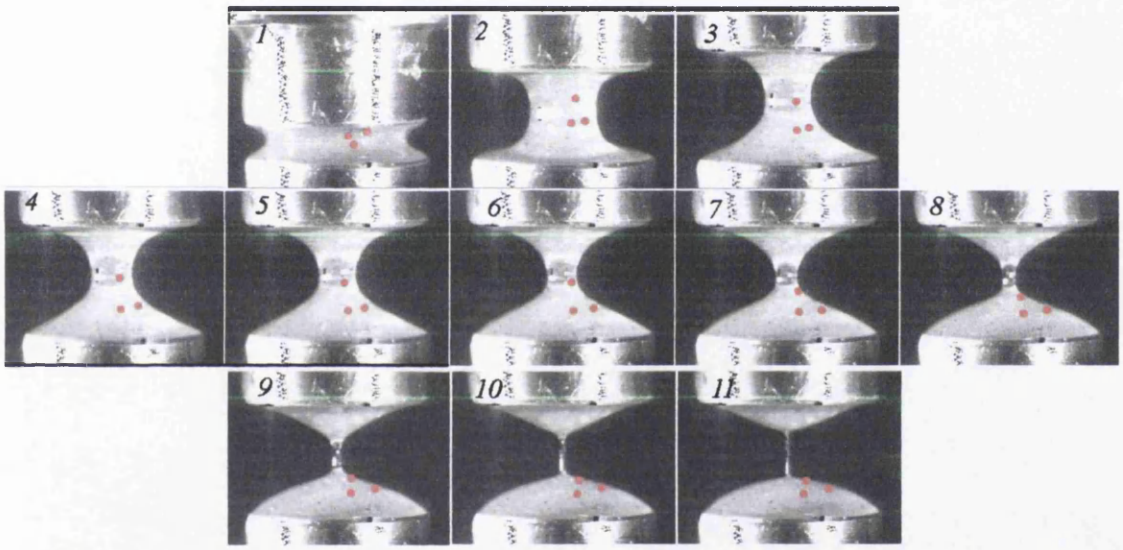

Figure 5-25 The extension analysis of glycerine with pigments dispersion indicates three steps of extension thinning, a) tensile deformation b) internal flow c) tensile break-up. The increased elasticity of the structure decreases internal flow and increases extension (app. Video cd V4).

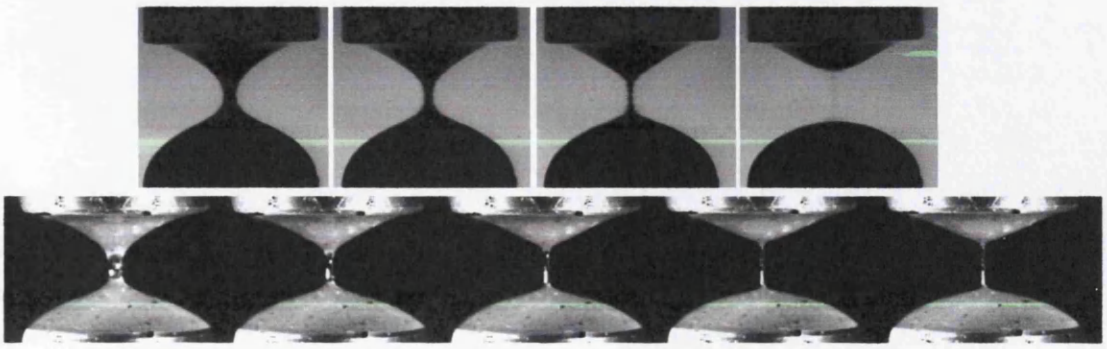

Figure 5-26 The glycerine with silver pigments (bottom figure App.VCD V5) illustrate significant extended thinning and break-up time than the pure glycerine (on top figure App.VCD V6).

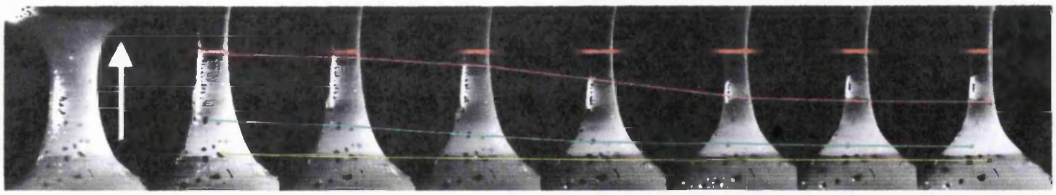

Figure 5-27 The filament failure occurs to both directions flux due to surface tension recovery. Lines highlight particles motion in viscous fluid through filament thinning time. Each colour highlights certain particle movement in the fluid during the extension process (App.VCD V7).

5.5.1.1 Relaxation

Butyl-Diglycol affects dielectric constant of polymers and the extension viscosity, which decreases with the shear viscosity. The thickening effect is steady between dilutions with lower viscosity. The extension thickening behaviour may be due to relaxation of the material after the tensile stress step during the elongation process. McKinley (1999) also purported a theory of relaxation during filament thinning. The results of this thesis show indications that the thickening rates of extension viscosity are combined with the relaxation rates of the zero shear viscosity (Figure 5-28).

The ink polymers are deformed through tensile stress but without filament failure due to elasticity and the low progressive elongation speed. Surface tension and adhesive dynamics pull each part of the ink equally. As a result, the free area between the two plates thins. This is followed by internal flow which is verified by the increase of contact angle with the plate (Figure 5-27). The internal flow increases fluid volume and structure on the plates. This also increases the adhesive dynamics while the free surface decreases in volume due to surface tension recovery. Finally, the filament fails but the split parts illustrated step recovery with increased elasticity due to relaxation. The Trouton ratio shows that the polymers chain can extend extremely long over strain. As a result, the polymers relaxing and going back to the previous stage during the flow of the capillary break-up process. Extension viscosity depends on the deformation and relaxation rates of the material according to its viscoelasticity and elongation velocity. As a result, extension viscosity decreases with decreased structure elasticity and increased tensile stress. This can be determined as a thickening effect by the equation but actually is proportional to relaxation due to polymers viscoelastic recovery, similar to a spring after tension.

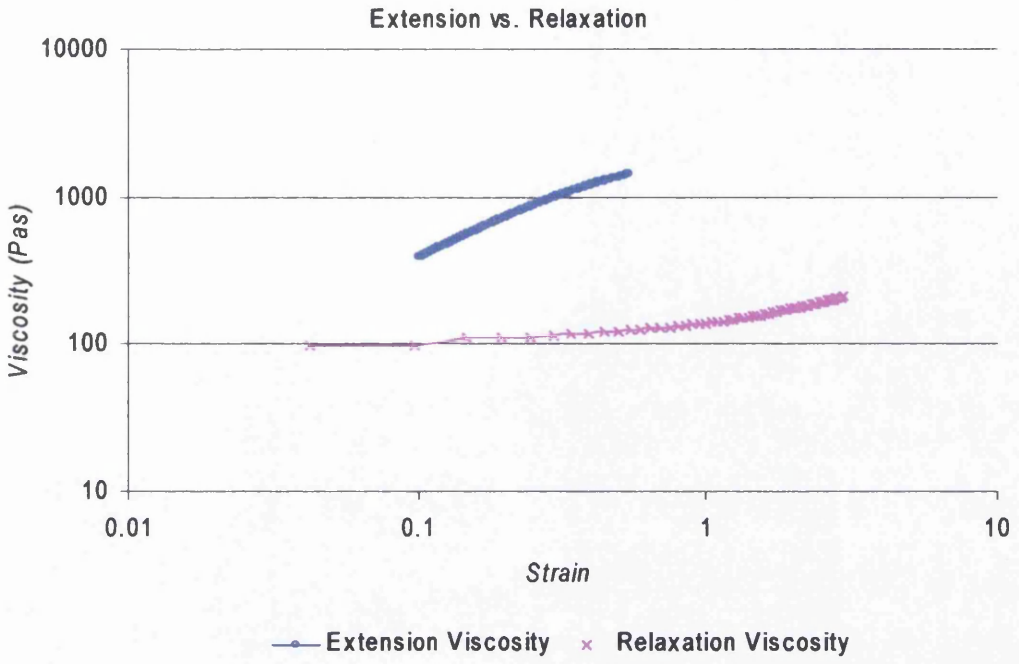

Figure 5-28 Apparent extension viscosity is affected by the relaxation of the material. Recovery curves determine similar trends with the extension viscosity.

5.5.1.2 Extension at the nip

The printing nip uses extremely thin ink films at the printing press. The extensional rheometer was used to determine how the filaments are generated at the nip exit. Cavities at the printing nip can vary as a function of the ink volume and the separation velocity at the nip exit and the capillary number of the fluid. The capillary number is determined by the shear viscosity over the surface tension. Owens (2005) discussed the effect of the capillary number on the capillary break-up rheometry an extension viscosity. The results of the current work also determined that apparent extension viscosity decrease with the capillary number while Butyl-Diglycol concentration decreases shear viscosity and surface tension of the ink.

The velocity is critical for cavities where form filamentation. Figure 5-29 illustrates a printing nip simulation under continuous extension at constant speed. The applied low speed of 0.03m/s extends slow the ink volume between the nip. The filament is formed by both direction capillary actions during axial tension. This generates a single filament that expands without perturbation over strain. However, an applied

high velocity of 0.6m/s generates multiple cavities along the nip which expand to filaments. The polymers expand along the axial tensile stress. The structure deforms to ribs and ruptures at the middle area points where the free surface becomes thinner during tension. The rupture releases energy and generates cavities which expand to filaments. The filaments deform under same strain rate but form different volume filaments. The filament axial extension increases with the ink volume area that finally split at longer break-up time (Figure 5-30).

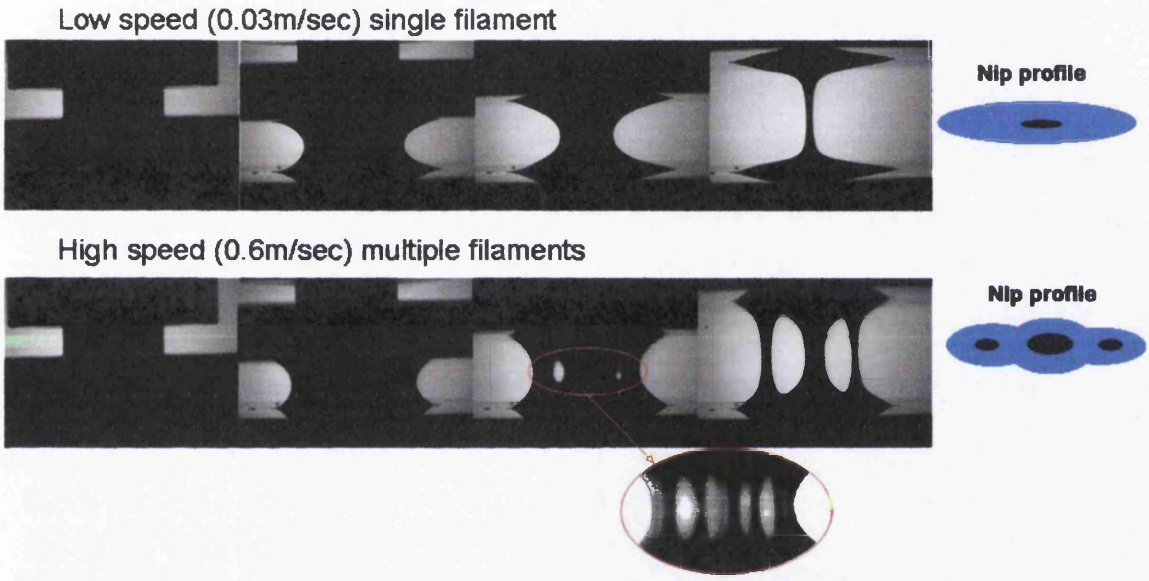

Figure 5-29 The low speed generates a single filament which is elongated uniaxial and thinning over time (App. VCD V8). The higher speed deforms the structure of the extending ink and ribs are generated along the ink nip (App. VCD V9). The areas between the ribs with lower ink volume break and cavities are formed that finally expand into multiple filaments along the nip. The final profile of the split filaments highlights the areas with lower ink film thickness between the filaments. The figures on the right side of the movie slides illustrate the final image of the ink nip with blue colour. The black colour illustrates the thickness and the position of the formed filaments. The bottom image in red frame focuses at the moment where ribs and cavities are formed. The movie slide shows two cavities during extension. The analysis of this image shows that more than two filaments were possible to be generated by higher extension speed than the used one named 0.6m/sec.

The final profiles of the nip (Figure 5-29) indicate the areas where tensile stress deformed the ink at the nip during the axial extension. The capillary break-up time varies by fluid volume. This determines that the filaments at the roller nip exit split at multiple point depend on the filament volume and the cavities patterns. This confirms ribs during extension which is related to *ribbing* phenomena as Chapter 6 discusses. Printing presses use much higher printing speeds but it was not possible to apply such extension speed on the extension rheometer.

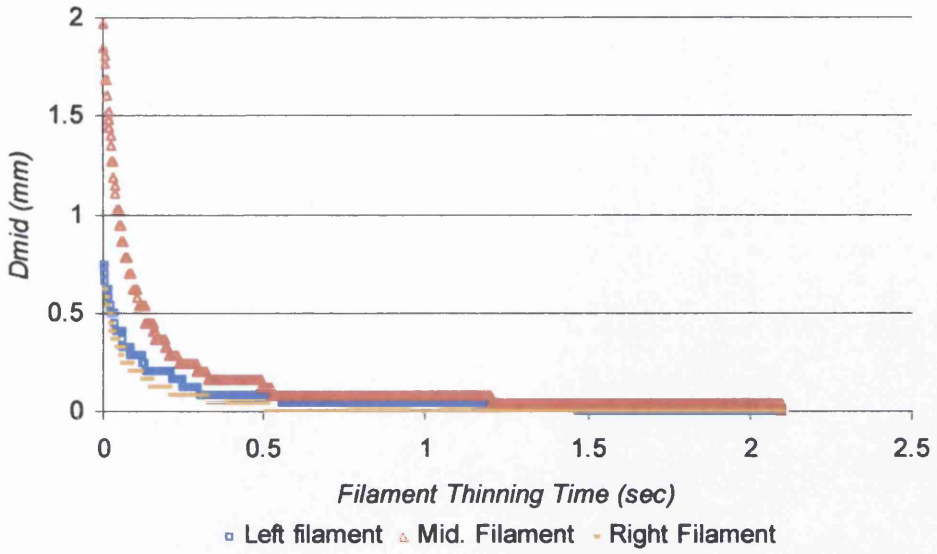

Figure 5-30 Multiple filaments along the nip illustrate variation in capillary thinning time.

5.5.1.3 Filament instability

The capillary break-up action is determined by fluid extension to a reference distance. However, the filaments are deformed till rupture at the printing nips and do not relax after that. The filaments can show instability by performing an axial extension. This indicates that filaments are expanded but do not split equally every time. The filament is deformed linear by following the longest expanding of the polymers till its break-up. However when the filament are too long an instability is generated along the axial distance (Figure 5-31). This is focused usually at the middle of the filament where free surface is away of the end plates. The adhesive dynamics at the free surface between the two end surfaces is decreased with the uni-axial distance. Aggregation can be formed at the middle filament where polymers do not expand linear or expand faster due to internal flow and generate perturbation of the filament structure. This parts follow the one of the two end surfaces independent of the gravitational direction after filament split in extremely low rates This causes a viscoelastic deformation to the filaments that is characterised by slow relaxation rates (Figure 5-32). As a result high volume droplets are formed which can flow away by following the velocity of the moving surface after split. This can cause high droplets effect to the *misting* mechanisms which is discussed in Chapter 7.

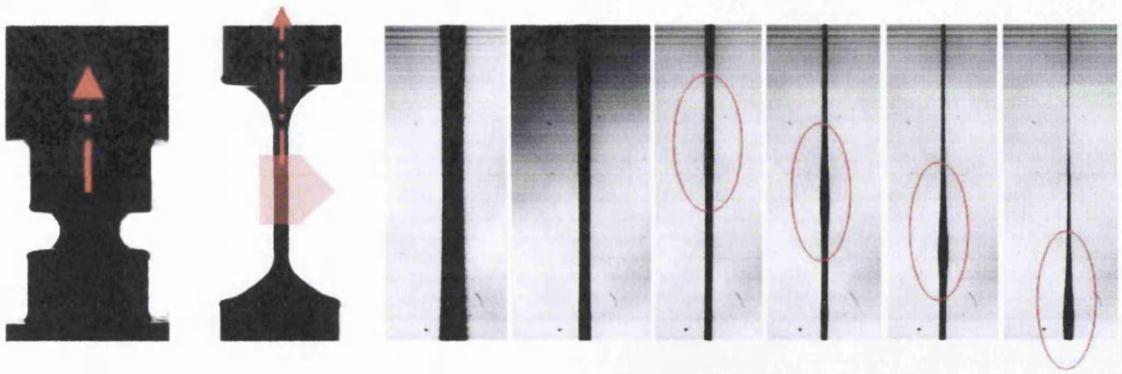

Figure 5-31 The axial elongation generates instability to the filament shape. Aggregation is generated along the filament which follows one of the two end plates directions (App. VCD V10).

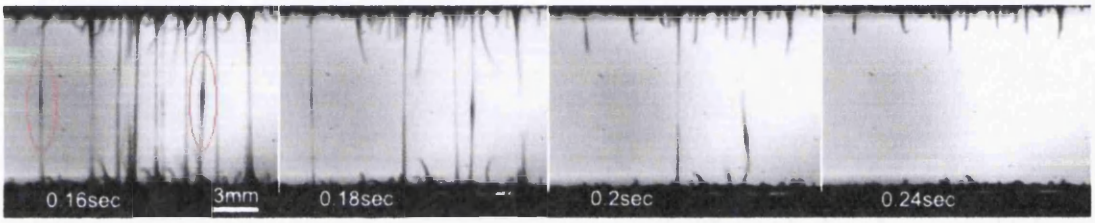

Figure 5-32 The high axial tensile stress generates also aggregated parts along the filaments where are characterised by a viscoelastic deformation with extremely low recovery rates (App. VCD V11).

5.5.1.4 Repeatability aspects

The temperature control using the IR shotgun showed not significant variations on the temperature between the tests except these of 24^0c to 26^0c degrees which conclude +-1 degree. This variation is usually acceptable but shear viscosity measurements determined that this variation in temperature affects viscosity and can be critical. However, it was not possible to control temperature due to room temperature limitations and storing environment. As a result, transient effect and experimental variation may occur due to the slight temperature variation.

The process between plate separations showed interesting results about methodology limitations. The extension process by using the two end plates provides lower break-up time than end plates independently as shown in Section 5.4.3 which indicates increase stress. While the top plate separation provides slight increase break-up time, the bottom plate separation shows critical increase of break-up times. This result shows that separation and extension are affected by gravitation. However, further

study can show more details about this effect but was not performed during this work due to time limitation.

The study on the model fluid transparent fluid with reflective particles was not completed due to time limits of the current work. Difficulties encountered were poor lighting and creating a fluid with similar viscoelastic characteristics with ink that provides also transparent structure. A good model fluid developed specifically for this application would provide information about fluid behaviour during extension and also on gravitation effects.

5.6 Conclusions

This chapter discussed the capillary break-up action by axial extension of viscoelastic fluids. Variation in two parameters was examined in order to increase the understanding of extension viscosity and capillary break-up action at the nip exit of the inking rollers on a printing press. This also extends the study of the rheological characterisation of diluted ink in concentration with Butyl-Diglycol of discussed in Chapter 4. The conclusions of this chapter can be summarised as follows:

- The capillary break-up is divided by three periods of extension thinning, a) tensile deformation b) internal flow c) tensile break-up. The viscoelasticity of the structure decreases internal flow and increases extension rates. The last period seems to be critical for the measurement of the extension viscosity.
- The extension viscosity indicates extension thickening effect during capillary break-up and filament thinning rates. The thickening effect occurs due to relaxation of ink structure.
- The thickening effect decreases with increase in tensile stress as an effect of the elongation speed.
- Extension viscosity decreases with tack value and it also decreases with decrease in shear viscosity and surface tension as a function of the Capillary number.
- In order to minimize the gravitational effect the ink volume has to be proportional to the viscosity.

- Zero viscosity can be determined by the relaxation viscosity and not the shear viscosity
- The Trouton ratio for printing inks is more accurate by the extension viscosity over the characteristic viscosity at 147/s shear rate. That shear rate estimated that is applied at the nip region between rigid and elastic surfaces of the rollers on the tack tester. Trouton ratio indicates that ink viscoelasticity forms polymers that expand linear over the strain.
- Capillary break-up (time) is proportional to Surface tension, viscosity, velocity (tensile stress) and extension axial rate as a function of the ink volume over the extension distance.
- Cavities are occurred to ribs formation which generates ink thickness variation along the axial deformation.

6. Developing techniques and establishing ribbing profile and mechanisms

6.1 Introduction

Splitting instabilities force the ink film thickness to form a wave-like profile, ribs, across the width of the roller. These wave patterns have been related to the rheological profile of the fluid and the capillary number by numerous authors (Savage 1984, Coyle et al 1990, Carvalho 1996, MacPhee 1998, Lopez et al 2002, Owens 2005).

Ribbing on the roller train is related to the ink film splitting mechanism at the nip exit. It is a result of a decrease pressure generation at the nip exit while tensile forces create cavities. Cavities expand and form filaments between them. These break resulting in the final splitting of the ink film. Banks and Mill (1954) established this phenomenon during investigation of the splitting ratio using oil and printing inks. They located the split ratio nearly to 0.5 between rollers and also the ribbing pattern due to cavities by the rollers rotation at the nip exit. Ribbing was described as a function of the ratio of the gap between rollers (nip region) and the rollers radius. They observed also that the oscillator roller randomises ribbing pattern which also randomises the cavities of the splitting mechanisms and the split ratio. Additional research (Savage 1992; Coyle 1984-1992) on ribbing instability focused on the formed meniscus at the nip exit that depends on the capillary number and not on the ribbing profile. Coyle (1984) investigated the onset of ribbing instability experimentally and theoretically. He studied the properties of surface tension and viscosity of the coating the speed ratio and the gap. He found that a critical capillary number Ca increases with the gap between two rolls. Carvalho (1996) concluded through his theoretical study the deformable forward roll delays the onset of ribbing and stabilizes the coating flow studied.

The ribbing pattern is created due to cavities across the nip. When the oscillator is not present, negative pressures at the nip exit create cavities which form a meniscus-shaped fluid flow. Earlier, Banks and Mill (1954) stated that cavities expand to

filaments that split at the nip exit. After a theoretical study, Zevallos et al (2005) concluded that filaments are formed due to meniscus perturbation.

However, ink filaments are more visible during ink splitting than the actual meniscus which is generated close to the nip region. As lithographic rollers trains operate at high speeds, the perturbation theory is more dominant than the actual meniscus shape due to capillary number. This is because ink transfer mechanisms focus on the splitting mechanism of the ink between the rollers, which generates filaments at the nip exit.

The ribbing patterns on forward rotating rollers are related to the ink film thickness and the rheological profile of the ink. The effect of varying the main process parameters, such as ink film thickness, viscosity, distribution speed, distribution time and rollers ratio, were obtained on the ribbing patterns profile. There are no published studies on the instabilities and their relationship with fluid properties or parameters that can affect the ribbing phenomenon. The identification of the ribbing mechanism can support studies on ink transfer mechanism on roller trains. The methodology focuses on establishing study parameters that can affect ribbing phenomena and also variations on profile characteristics.

There are several techniques to study the phenomenon depending on the fluid viscosity, such as rotating plates, flow surfaces and internal drums.

An overview on experimental methodology is explained in Section 6.2 with references on instrumentation, capturing techniques and analysing procedures. Additional techniques were also performed as tools on software development and video capturing in order to investigate and understand the actual phenomenon before design and set parameters of an actual experimental trial.

6.2 Experimental methodology

The ribbing patterns were studied on IGT tack tester (chapter 3) with the support of digital imaging analysis processes.

The methodology of the ribbing patterns analysis can be divided into three basic steps (Figure 6-1):

- The ribbing generation
- The imprinting and capturing techniques of the ribbing
- The ribbing profile analysis

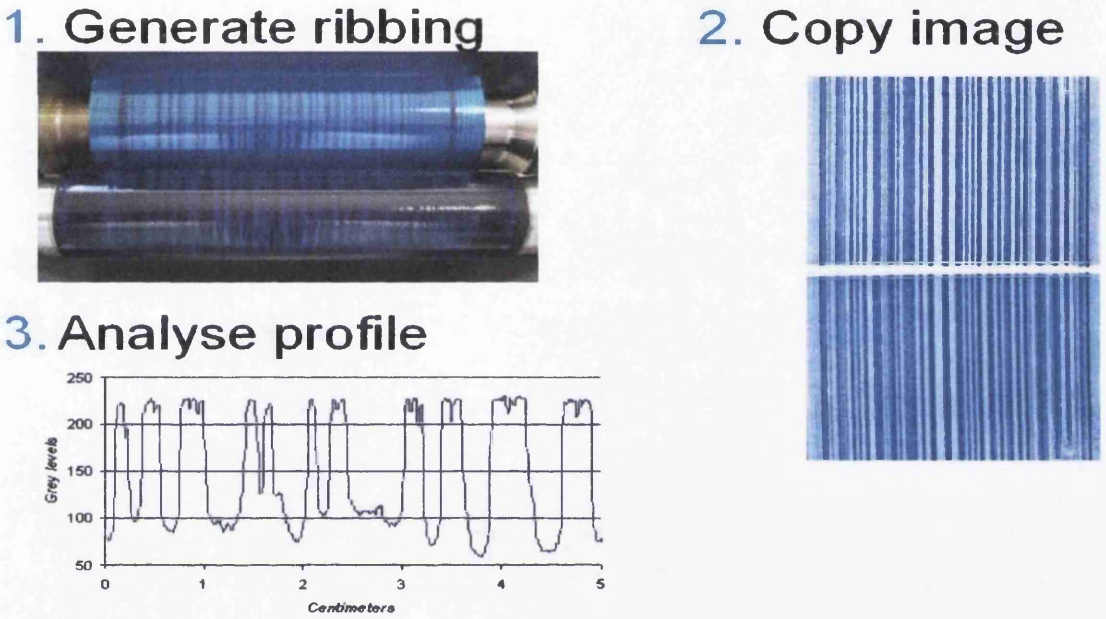

Figure 6-1 Ribbing generation is carried out on Tack tester (1). The pattern is captured by imprinting process on paper (2). The ribbing sample is scanned and transformed into power of grey levels (3).

The results of this investigation were focused on establishing the following ribbing characteristics across the rollers width:

- Frequency of ribbing
- Mean ribbing width
- Variations of ribbing width
- Mean values of lines/cm across the roller length
- Ink surface coverage area on roller

The ribbing is related to ink transfer mechanisms and thus parameters that affect distribution or printability were selected to investigate estimation on ribbing

mechanism. The parameters of rollers ratio, viscosity, distribution speed and time are selected for preliminary tests. The parameters vary by levels as described below. Distribution time was examined by 3minutes and 6 minutes. This was set in order to examine the effect of distribution time by comparison to the onset of ribbing profile by increase twice the variation of the study parameter.

Rollers ratio was varied by the use of the oscillator and the measure roller as riders in contact with the independent motor roller. The oscillator is smaller than the measure roller and that difference gives a peripheral ratio of 1.48 for the oscillator – motor rollers and 1.85 for measure-motor rollers. This generates a difference in angle separation of the roller with 18 degrees for the oscillator and 22 degrees for the measure roller.

The repeatability of the experiment is highly dependent on the pre-distribution process to form a uniform ink film thickness through the rollers. The most uniform ink film thickness on the rollers leads to the most repeatable experiment. The system has to be completely dry before any experiment. The solvent which is deposited into rubber rollers surface requires more than two hours for complete evaporation. The cleaning process between experiments is important because solvents or cleaning agents decrease the ink viscosity. This was concluded by tack measurements where solvent effect demonstrated a critical decrease of ink tack value. Different cleaning agents can require more than 5 hours for complete evaporation and this depends on solvent evaporation rates. Rollers drying time was decreased by the use of an air gun after cleaning.

The ink was applied into the system by a fine pipette. The volume of the ink for the exact ink film thickness was calculated from the IGT manual that recommends 0.3ml ink to provide 3.9 μm ink film thickness and 0.6ml ink to provide 7.8 μm ink film thickness. This assumes an even distribution of ink and is based on the surface volume of the roller train. The ink was applied on the rollers in fine ink lines across the width to improve the uniformity of the distribution ink film. The system speed was then adjusted to lowest level of 50m/min (approximately 0.8m/sec) for distribution to avoid misting effects and ink loss. The ink volume was distributed for 2 minutes on the system by using the full system geometry with the measure roller

(rider) and oscillator. The distribution time was increase to 5 minutes at higher ink film thicknesses. After the distribution process, the Tack meter was stopped for a relaxation time of 10 minutes. The relaxation time was calculated by the shear tests on the shear rheometer as described in the rheology section. While rheology measurements did not calculate any high shear effects at the nip region although high shear stress was applied by the finite pipette use. Ink viscosity decreases during the application process. The ink is applied on the tack tester rollers via a micro pipette with a 2-millimetre opening. This applied high shear stress to the ink and decreased viscosity. The relaxation time was important in order to eliminate viscosity decrease effects during the experimental study.

Ribbing was then generated by operating the tack meter with only two rollers in contact and no oscillation of the rollers. The ink volume, ink viscosity and distribution speed were set for the required distribution time. The system was stopped after the distribution run and the ribbing image was captured (Figure 6-2).

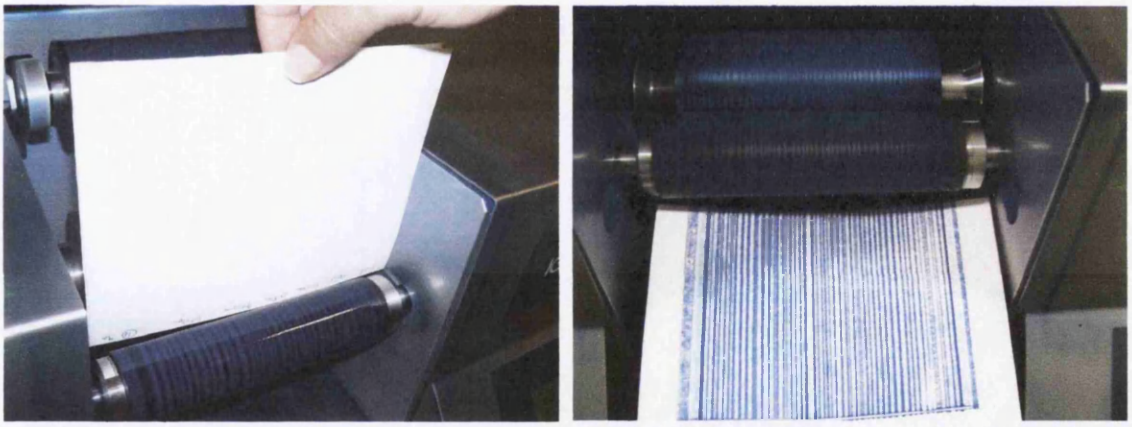

Figure 6-2 The ribbing image was captured by using the rollers nip as a printing nip after the ribbing run on tack tester. The paper was folded in two in order to capture separately image for each one of the two rollers at the nip.

The ribbing was captured using an imprinting technique with the rollers as a printing nip. The substrate had to be porous and thin in order to absorb the inked image without smearing due to increased ink film thickness. A substrate was placed between the two rollers after the end of the run while system was stopped. The substrate was a photocopy paper and folded in two. The purpose of folding was to capture the ribbing image of each roller simultaneously so the images were not imprinted double-faced. Rollers were coming in contact again with the substrate

through the nip. The system rotated again and a ribbing imprint was produced. Two separate ribbing images were produced of the metallic and rubber rollers on the unfolded substrate. Those two images were captured also by the same nip in order to provide information about the ink on the rollers at both rollers side of the same nip.

The Kodak high speed camera was used to capture images of the ink film splitting at the nip exit of the rollers (Figure 6-3). Variation in magnification was used to capture the ink splitting process between the two rollers. The video was captured at the nip exit of the rollers. The visualised splitting mechanism was examined in slow motion by using the frames sequence (Figure 6-4). The capturing process required high speed recording with good lighting. The narrow gap did not allow a wide range of parameters and thus the nip was flooded. This allowed better light and high recording speed with f8 apparatus which provides wider focusing area. The distribution speed was 0.8m/s which also allowed higher quality images with the 4500 frames per sec recording speed.

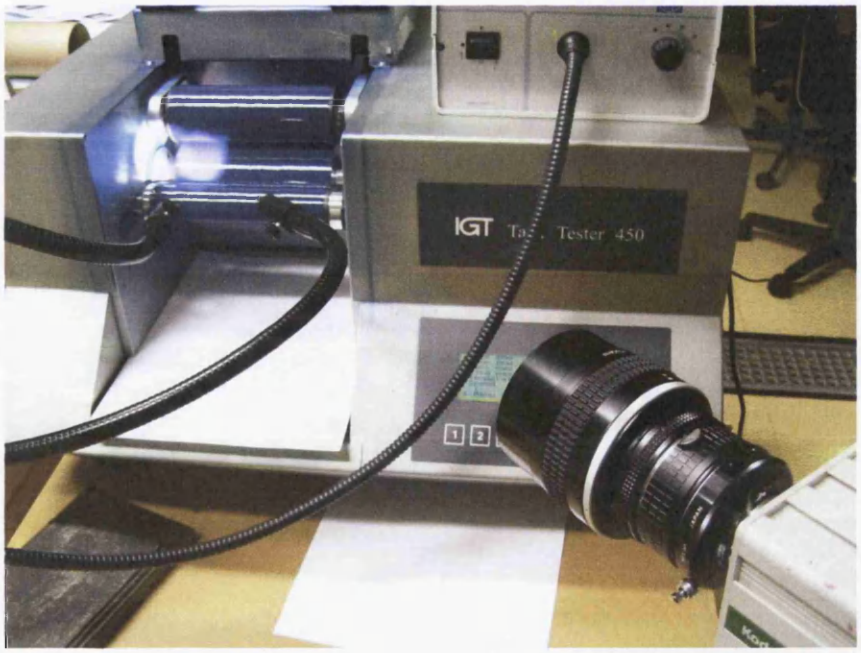

Figure 6-3 The high speed camera was used to record the onset of ribbing at the nip exit.

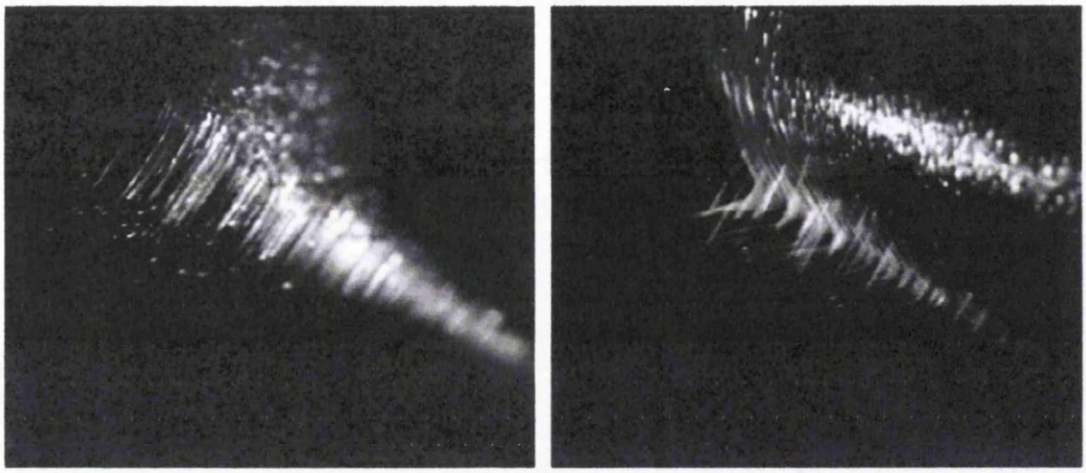

Figure 6-4 High speed video capturing techniques were performed on the IGT tack tester in order to examine the splitting mechanism and the onset of ribbing at 0.8m/sec distribution speed and 4500 frames per second recording speed. The two images show the ink filaments at the nip exit of the rollers nip. Multiple filaments are generated by following the ink film thickness along the nip exit (App. VCD V12a - V12b).

6.2.1 Accuracy and repeatability

The repeatability of the methodology was examined by repeating two random sets of parameter tests 5 times. The two sets of parameters were chosen according to the observations during the preliminary studies. Table 6-1 illustrates the parameters for the test on repeatability.

Table 6-1 Test parameters for repeatability examination on ribbing patterns

	IFT	Speed	Time	Ink	Temperature
Sample 1	3.9μm	1.6m/s	3min	Cyan ND	20Celsius
Sample 2	15.6μm	1.6m/s	12min	Cyan ND	30Celsius

The repeatability test focused on establishing variations that occurred to ink film thickness. Instabilities occur due to the non uniform ink film thickness on the roller surface due to preliminary distribution of the system. The increased ink volume on the system required increased distribution time in order to form uniform ink film thickness along the roller surface. When the ink volume is low, there is high repeatability of the ribbing pattern due to faster equilibrium of the system. However, when the preliminary distribution increases from 2 to 5 minutes, results show high repeatability even on high ink volumes (Figure 6-5). The ribbing instability occurs to non uniform ink across the roller length. The ribbing pattern between the two sides of

the roller show if there is uniform ink film thickness across the surface. Decreased variations in ribbing width are characterised by a uniform ink while high width variations show also that ink is unstable across the roller length. Those instabilities are raised with increased ink volume that floods the nip region (Figure 6-6). This error occurred due to oscillator dimensions that slid because of the ink flood and did not spread or transfer the ink uniform when the distribution time was short.

The amount of ink between the two rollers provides a significant effect on the ink transfer mechanism. The gap between the rollers can affect that mechanism and oscillation frequency is also important to instabilities such as increased ink film thickness variations across the rollers length. However, increased pre-distribution time can eliminate the non uniformity such instabilities and increases the accuracy and repeatability of the experimental process (Figure 6-7). The doubling the pre-distribution significantly reduces the variation of the ribbing while it increases average ribbing width. The non-uniform ribbing illustrates higher variations than the average ribbing width along the rollers.

Figure 6-5 Ribbing instability occurs to non-uniform ink across the roller length. The ribbing patterns depend on the ink film thickness along the rollers. The ribbing patterns are not uniform at the left image because ink film thickness was higher on the right side of the rollers. The right image illustrates a uniform ribbing pattern which was a result of a uniform ink film thickness along the rollers of the distribution system.

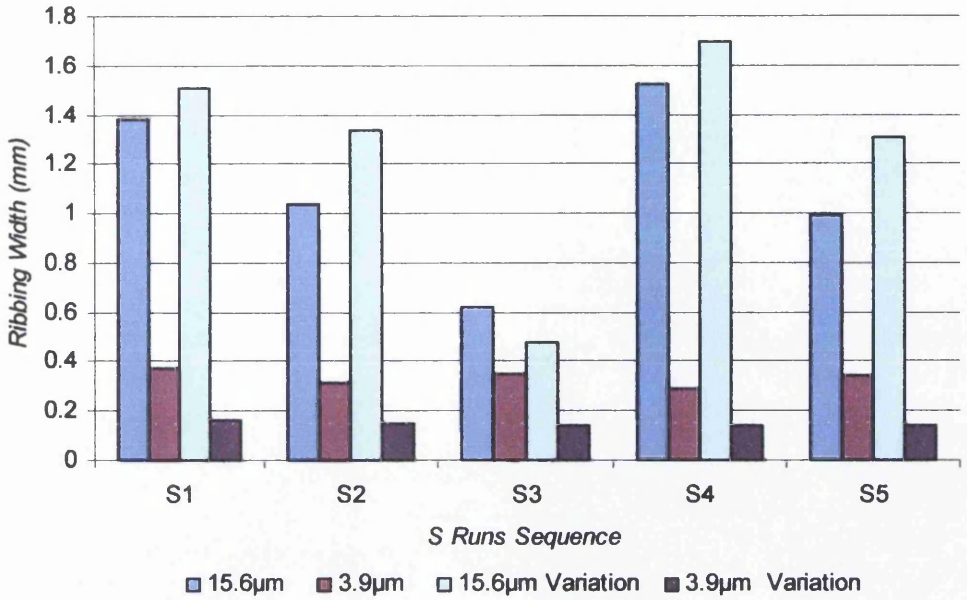

Figure 6-6 Increased ink film thickness generates instabilities on ribbing width with increased variations. This indicates also an effect on transfer mechanism due to ink flood at the nip region. Colour bars represent the ink volume along the roller length by five measured areas named S1, S2, S3, S4 and S5. The ink ribs width variation increases with the ink film thickness on the rollers.

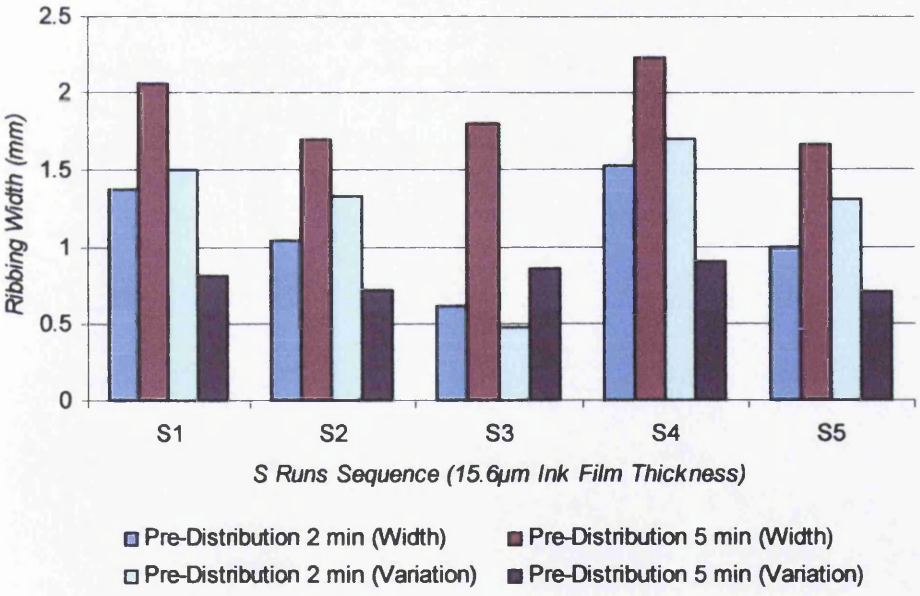

Figure 6-7 The increase of pre-distribution time increases uniformity along the rollers and provides higher repeatability between the runs. Colour bars represent the ink volume along the roller length by five measured areas named S1, S2, S3, S4 and S5. The variation of the ribbing pattern decreases with the longer pre-distribution time of 5min.

6.2.2 Ribbing analysis

Analysis was carried out by scanning the ribbing images with a flatbed scanner at 350dpi resolution, which provided a sufficiently detailed image for subsequent

analysis. The digitised images were analysed by the Image-J software. Each image profile was plotted into a graph of grey density values across the length of the ribbing pattern. The grey balance of the complete image was also calculated. The graph visualised a cross profile of the ribbing pattern that illustrated significant variations of the ink film thickness through the roller length in grey levels.

A programme was developed in Visual Basic for the analysis of the ribbing images. The moving average of the grey values was calculated (Figure 6-8). The edge of each rib was determined from the point at which the grey value profile crossed the moving average. The calculations extrapolated the ribbing wave and clearly determined the ribbing profile. The logic of the programming was developed as follows by simplified the Fourier transform for square waveform:

If $Px > Sav(1 \text{ to } 100)$ then $Px = 255$ (34)

If $Px < Sav(1 \text{ to } 100)$ then $Px = 0$ (35)

Where:

Px = Ribbing Peak value

Sav = Moving Average along the ribbing profile

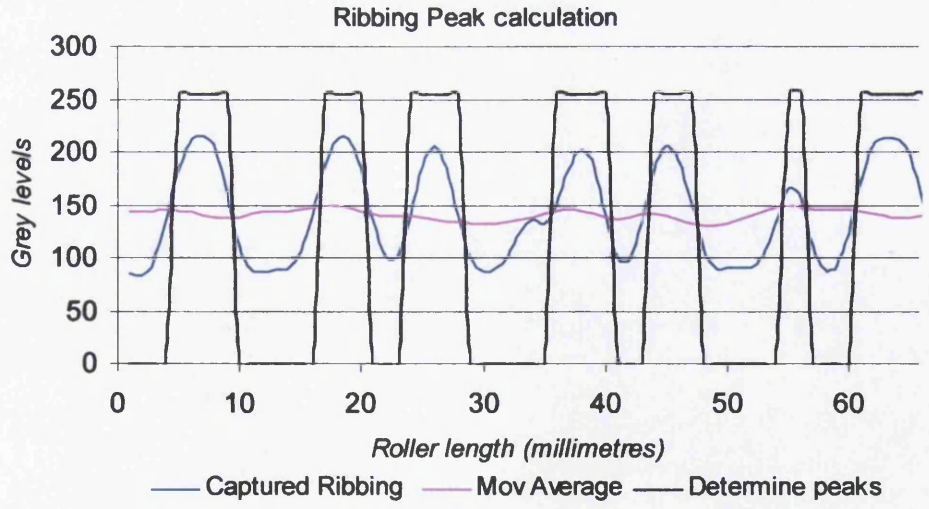

Figure 6-8 The number and width of the peaks is determined by the moving average axis cross to the captured ribbing profile according to grey levels of the digital image.

The programme calculated the thickness of the ribs, the number of ribs and the mean ribbing width in pixels (Figure 6-9). The values were transformed into millimetres

according to the pixel aspect ratio of the digital image of 73.8 pixels per millimetre for 350dpi.

Counting peaks: **if Pn = Sav then Count Pn + 1**

Counting pixels per Peak: **if Sav < Pw >Sav count Pw + 1**

Where Pn the number of Peaks and Pw the Peak Width

The Fourier analysis was also used to extract frequency directly from the ribbing profile. The power data of grey levels were transformed into frequency domain (Figure 6-10).

Power = abs $(Y(1:N/2)^2$ (36)

Frequency = (1:N / 2) / (N / 2) x (1/2) (37)

Period = 1 / Frequency (38)

Ribbing signal = period / power (39)

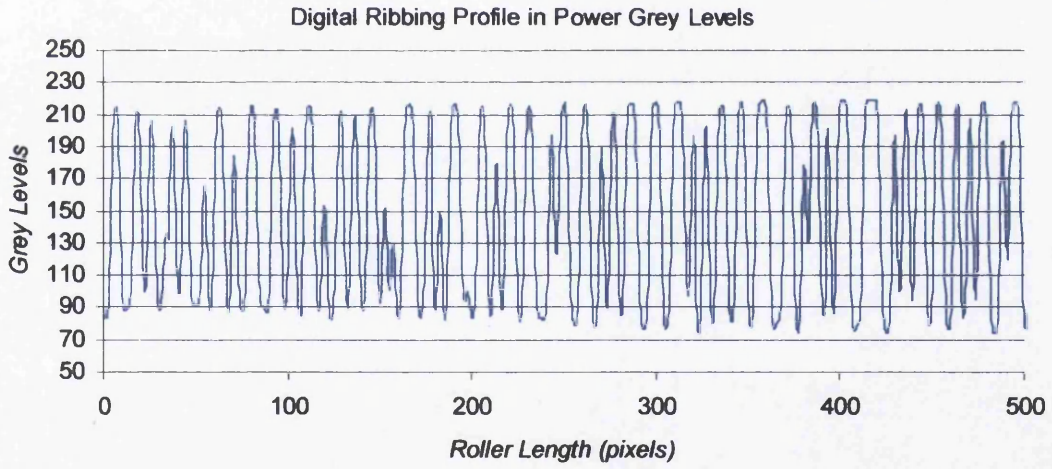

Figure 6-9 The numeric profile consists of values of grey levels power

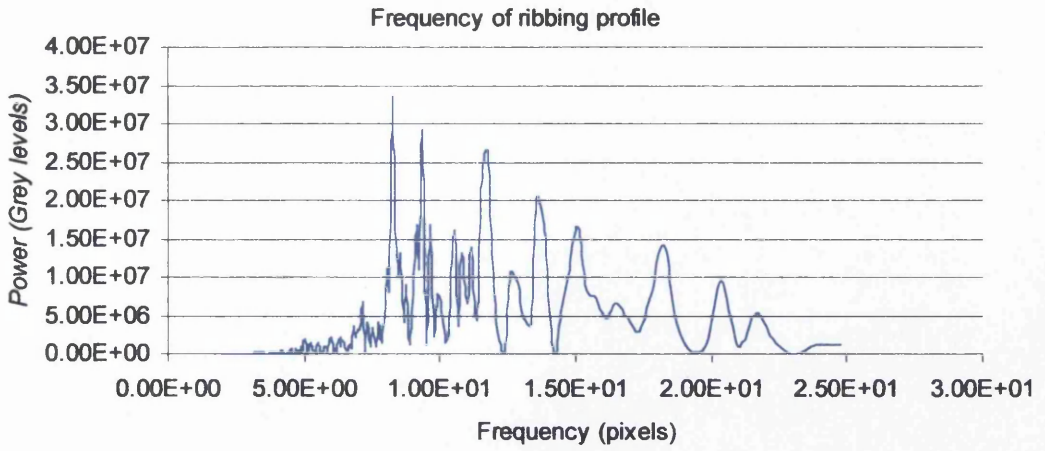

Figure 6-10 Fourier analysis extracts frequency domain from ribbing profile according to power of grey levels of the profile.

6.3 Results and discussion

Previous authors have used photographic techniques to capture a short area along the nip and focused only on the profile variation (Carvalho et al 1994, Lopez et al 2002, Owens 2005). Their studies involved thick film thicknesses and low viscous fluids. This thesis focuses on establishing the ribbing profile across the width and the length of the rollers under conditions approximating to an offset printing nip.

6.3.1 Ribbing profile and characterisation

The onset of ribbing generates visible line patterns on the parameters settings. The ribbing profile cannot be attributed to one parameter alone; e.g. the same ink viscosity can generate ribbing variations on individual characteristics such as lines width or frequencies (Figure 6-11). Fine patterns can appear in lower or higher frequency, with variation also in ink film thickness or distance across roller length that generate variation of inked surface coverage on roller.

Preliminary tests showed that ribbing frequency was significantly influenced by parameters such as temperature, viscosity, distribution speed, and distribution time. Table 6-2 illustrates printing parameters of preliminary tests. It uses two ink film thicknesses of 3.9 and 7.8 μm under low and high parameter levels of distribution speed and time, temperature and viscosities, namely neat Cyan and 5% Butyl-

Diglycol concentration. This established the dynamic formation of the ribbing patterns. The same ink film thickness generates ribbing patterns with different frequencies. The ribbing frequency decreases with the high level of parameters at 3.9 μm of ink film thickness (Figure 6-12). Similar changes are carried out with the ink film thickness increase at 7.8 μm. Figure 6-13 illustrates ribbing profile variations by changing the level of parameters from low to high with lower viscosity, higher distribution speed in higher distribution time and higher temperature. This concludes that ribbing frequency variation is highly dependent on the interaction between process parameters.

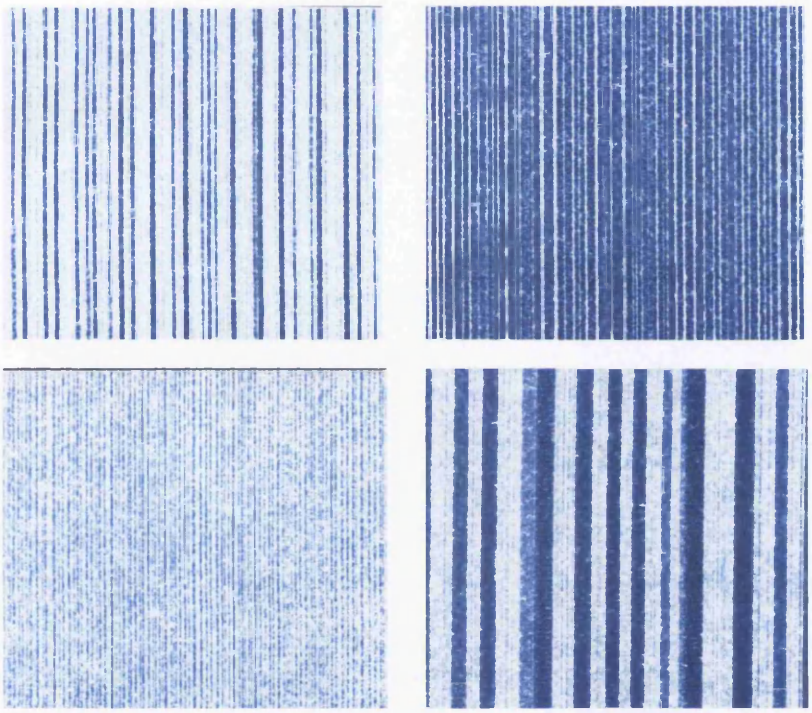

Figure 6-11 Ribbing patterns are not uniform and can vary by the parameters on the frequency of the appeared width. Higher ink film thickness can increase the ink ribs width and decreased ribbing frequency like the bottom right image. The lower ink film thickness increases ribbing frequency and ink ribs are much thinner as bottom image at the left side illustrates.

Table 6-2 Preliminary tests parameters.

Test	Ink thickness	Viscosity	Temperature	Speed	Time
1	3.9μm	Cyan	20celsius	1.6m/s	3min
2	3.9μm	5%bdg	30celsius	3.2m/s	6min
3	7.8μm	Cyan	20celsius	1.6m/s	3min
4	7.8μm	5%bdg	30celsius	3.2m/s	6min

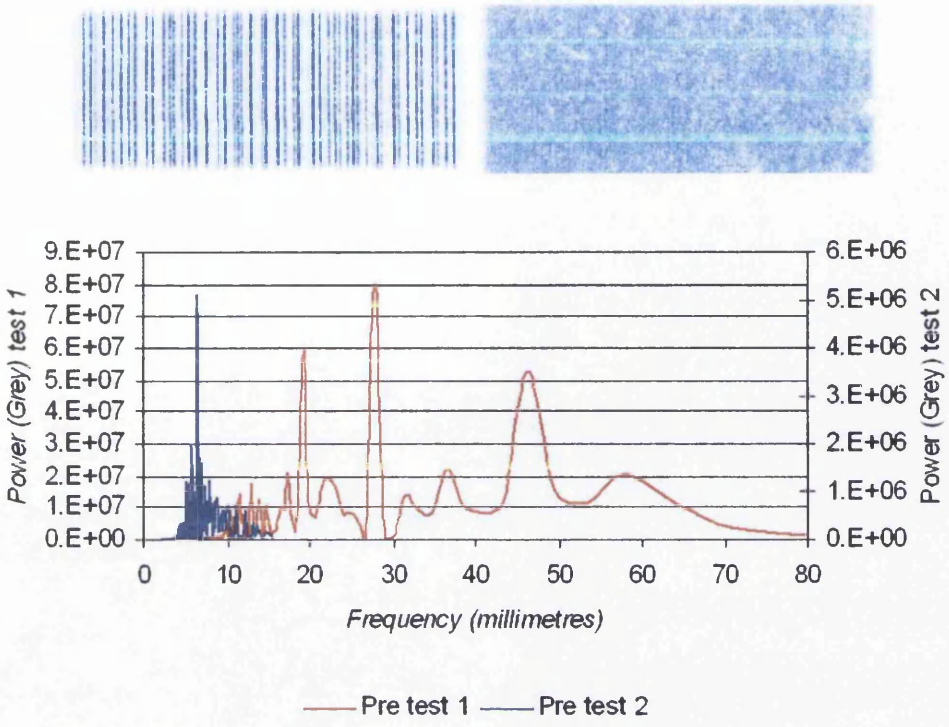

Figure 6-12 The ribbing frequency indicates significant changes with the same ink film thickness (3.9 µm) but with different printing parameters. The second test parameters are characterised by lower viscosity, in higher speed with higher time and at higher temperature in comparison with the first test as table above illustrates. This determines that parameters can affect significant the ribbing patterns on roller distribution systems.

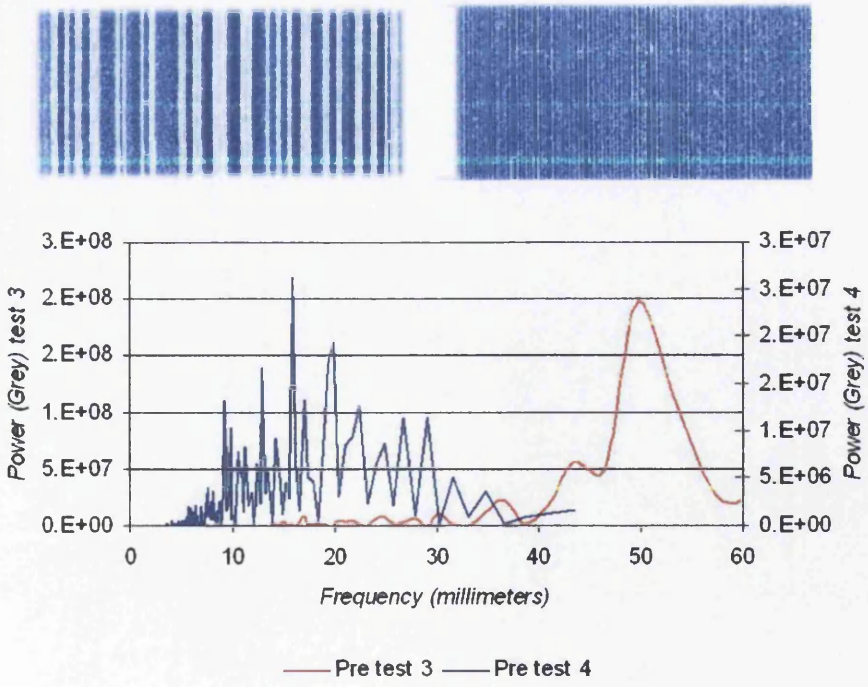

Figure 6-13 The increase of the printing parameters influence the ribbing frequency even with the increased ink film thickness of 7.8 µm.

The height of ribbing is generated equally between the two rollers i.e. the same minimum level of grey. However, there is a higher contrast on the metallic roller (Figure 6-14), which suggests the rubber roller transfers ink evenly from the areas between ribbing patterns due to surface deformation at the nip with the substrate. This is the amount of the ink that was immobilised on the roller surface and did not participate in the ink transfer mechanism. This was confirmed also by high speed video capturing at the nip exit. It was not compared to scumming because no image existed at the system. Scumming is usually generated by corrosive areas of the printing plate that accept ink instead of fountain solution.

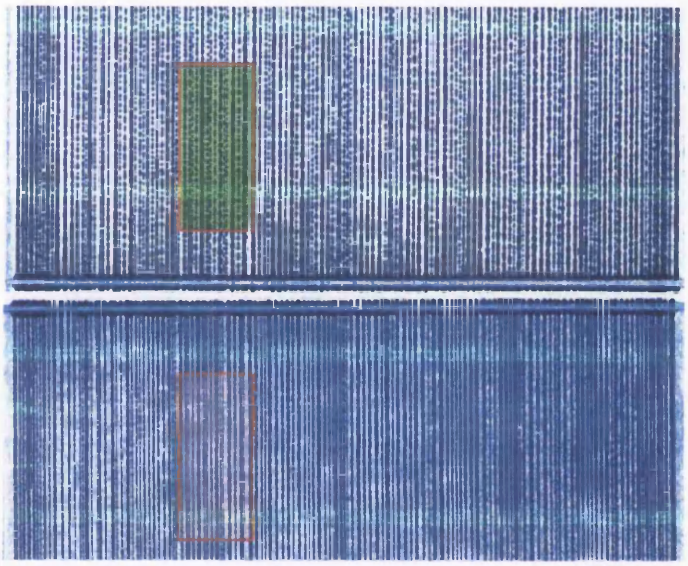

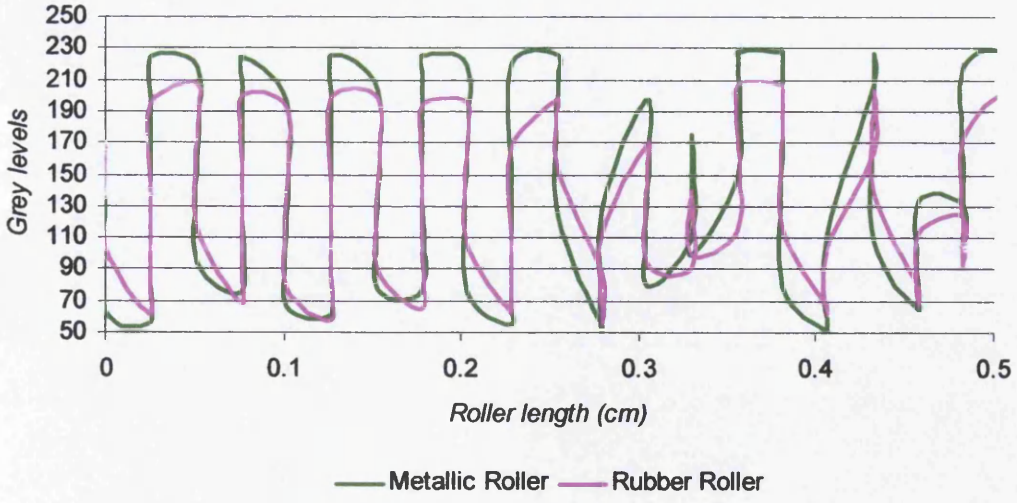

Figure 6-14 The Metallic roller transfer clearer image and provide slightly higher contrast of ribbing lines and gaps. This decreases noise of the profile especially in fine patterns (image) and gives a more detailed and clear image. This suggests that ribbing width is formed equally between the two rollers. The green line at the graph indicates the grey levels of the metallic roller ribbing image of the image above. The red line indicates lower grey levels at the areas between the ink ribs in regards with the green line. Both graph and image illustrate that the elastic surface roller transfers ink from the both areas and confuses the image analysis.

The ribbing is wider out on the sides of the roller (Figure 6-15). The ribbing is formed faster at the sides of the roller where free surface at the sides increases air pressure. Therefore, wider ribbing is formed at those areas which determine an increase to the nip gap. The ribbing patterns are affected by the ink film thickness that existed along the roller. This affects the thickness and the width of the actual pattern. Wider ribbing patterns are generated when the ink film thickness increases along the rollers. As a result, the uniformity of the final ribbing pattern is affected by the ink uniformity across the rolling and along the nip direction.

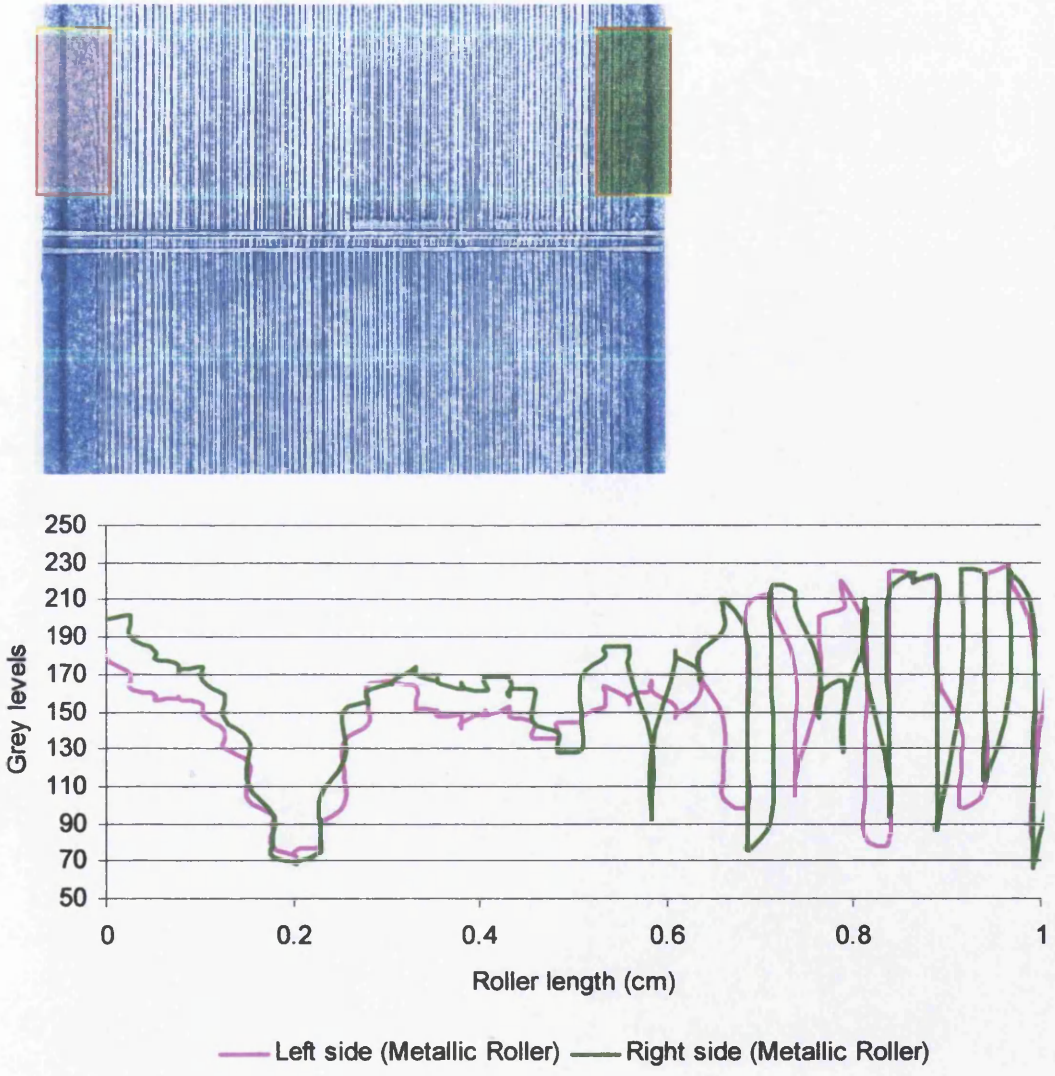

Figure 6-15 Ribbing increases locally at the sides of the roller which determine a lateral flow and gap generation according to the ink film thickness (graph at 0.2cm rollers length). The graph suggests that ribbing width is formed equally between the two sides of the same roller. This indicates that the nip gap is the same along the rollers nip length. The top image illustrates the captured ribbing image. The bottom graph visualise the grey levels of the green and red areas of the top picture in order to compare the density of the lateral areas of the rollers. The green area is rotated in order to match the two grey levels lines into the same graph.

The ribbing patterns were examined also by white light interferometer in order to establish the profile on the roller surface (Figure 6-16). The measure and the oscillator roller were removed from the tack tester after the run and placed at the white light interferometer for surface analysis. Five measurements were carried out along the rollers and 5 across the rolling direction in VSI mode (Figure 6-17). The ink film thickness of the ribbing increases according to the ink thickness that was at those areas from the preliminary distribution process. The thickness increases also with the rise of ribbing width. The gap generation affects the ribbing patterns due to lateral ink flow at the roller sides which becomes negligible when ink film thickness decreases to values such as 3.9 μm (Figure 6-18).

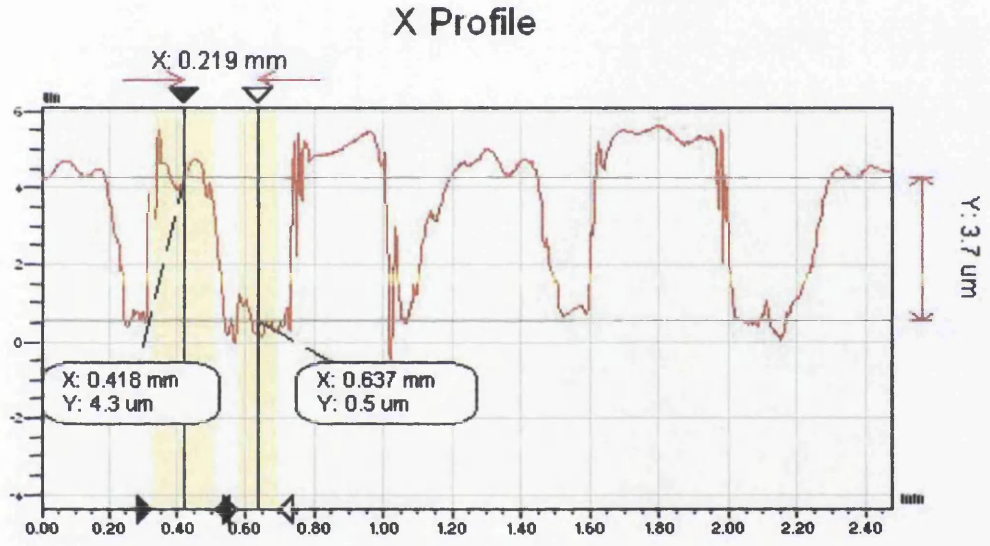

Figure 6-16 The ribbing surface was measured by the white light interferometer after the run. The roller was removed from the tack tester and was set for measurement at the WLI table. The ink film thickness of the ribbing increases according to the ink film thickness that was at those areas from the preliminary distribution process. The ink ribs width increase as the ink film thickness decreases at the areas between the ink ribs.

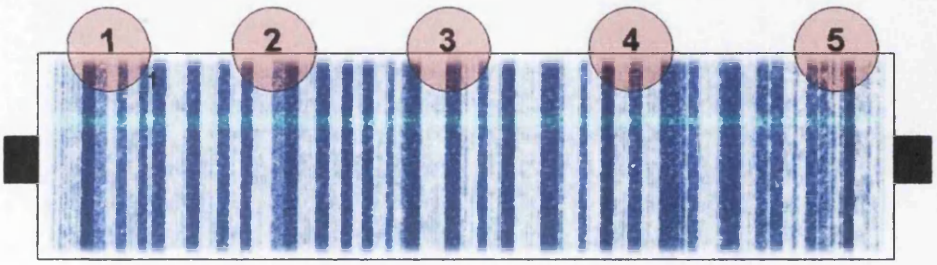

Figure 6-17 Five measurements were carried out along the rollers by the white light interferometer. The rollers were removed from the tack tester and placed on the white light interferometer table for surface analysis in VSI mode. This allowed measuring the ink film thickness variation between the ink ribs along the rollers length as above figure illustrates..

The ribbing is increased on the sides and affects ribbing patterns in between due to gap generation. Low ink film thickness indicates negligible effects and ribbing uniformity along the rollers. The ink film thickness increases at the sides and ribbing tends to increase. This is affected by lateral flow of the oscillation mechanism through the ink distribution process as was reported by Chou (1997). Ribbing is affected by the distribution process in order to spread the ink film thickness uniformly and this also verifies the ink transfer instabilities of the distribution systems. Ribbing is related to the ink film thickness that exists across the rollers length. It is also possible to monitor what ink film thickness is on the system according to the appeared ribbing patterns. The ribbing analysis determines not only the ink film thickness is critical but also the uniformity levels of the distribution system due to oscillation mechanism and the gap at the nip. Coyle (1984) stated that ribbing is affected by the capillary number which increases with the gap at the nip.

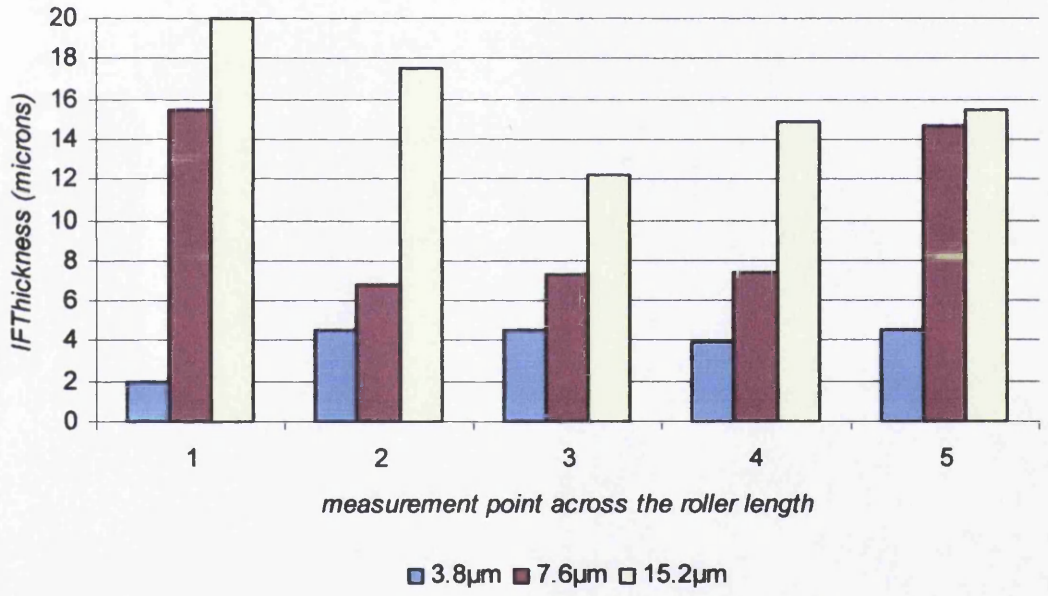

Figure 6-18 White light measurements across the roller length. The ribbing is increased on the sides and affects ribbing patterns in between due to gap generation. Low ink film thickness indicates negligible effects and ribbing uniformity along the rollers. The x axis indicates the five measurements point along the roller.

6.3.1.1 Ribbing peaks

Ribbing forms parallel to the rotating direction. The ink volume can be estimated from the grey levels of the captured image, where 0 indicates black or high ink volume and 255 indicates white or negligible ink volume. The plot profile visualises this pattern in a wave-like profile. The grey troughs indicate the number and width of

the ribs. The number of troughs indicates how many lines are generated per certain area but does not provide a detailed description of the ribbing pattern.

The width of ribbing lines is related to the ink film thickness along the roller by the effect of the air pressure. The ribbing can be characterised by the averaged line width that is generated per cm. This also indicates the average gap (troughs) of the ribbing pattern. The average ribbing width provides a good indication of the ribbing generation according to ink film thickness on rollers.

The ribbing width changes with the ink film thickness. The variations in ribbing lines width across the roller surface indicate variations of the ink film thickness. This is because the same ink film thickness is forced to decrease in coverage area along the roller. The coverage area decreases while the ink volume increases periodically and forms the ribbing patterns similar to the present ink film thickness. This variation characterises the instability range according to the ink film thickness. The uniformity of the ink film thickness leads to low ribbing width instability. The width instability increases when ink film thickness is not uniform along the rollers as shown in section 6.2.1. The variations increase on ribbing pattern with the increase of the ribbing width. This is not linear with the distribution time and it also depends on other process parameters such as distribution speed and viscosity as described in section 6.3.2.

Inked coverage area can vary on the rollers surface by the ribbing lines width and variation. Thin ribbing patterns do not indicate necessarily fine patterns or increased ink coverage area along the roller surface. The ink coverage area determines the ink free surface across the roller length. The average gap is similar to the average ribbing width in respect to the variations due to ink film thickness instabilities along the rollers. The ink along the rollers is divided into uniform ribbing across the roller length due to cavities when ribbing derives from uniform ink film thickness. The cavities variation depends on the ink film thickness along the nip. The onset of ribbing decreases the ink at the areas of cavities and ribbing lines are formed with increased volume between them. As a result, coverage area decreases as the cavities expand or the air canals increase between ribbings lines.

Frequency increases with finest patterns that tend to be formed with low ink film thickness. A typical ribbing profile of fine patterns is represented by high frequency and low amplitude that derives from low ink film thickness along the rollers. On the other hand poor ribbing patterns are represented by lower frequencies with higher amplitude that derive from higher ink film thickness (Figure 6-19). As a result, ribbing frequency increases with ink film thickness while there is a decrease in ribbing amplitude. The extracted domain does not represent a steady frequency because ribbing does not generate variations only along the nip but also along the rolling direction (Figure 6-20). The variation increases with the ink film thickness. The grey values are affected by the substrate and noise is generated that affects the frequency domain due to low contrast when ink film thickness is low. The contrast increases with the ink film thickness and the extracted domain presents higher consistency. However, ribbing instability along the rollers length and the rolling direction seems to be directly related to the ink film thickness. The analysis of the rolling direction shows that the ribbing frequency does not vary significantly with the ink film thickness.

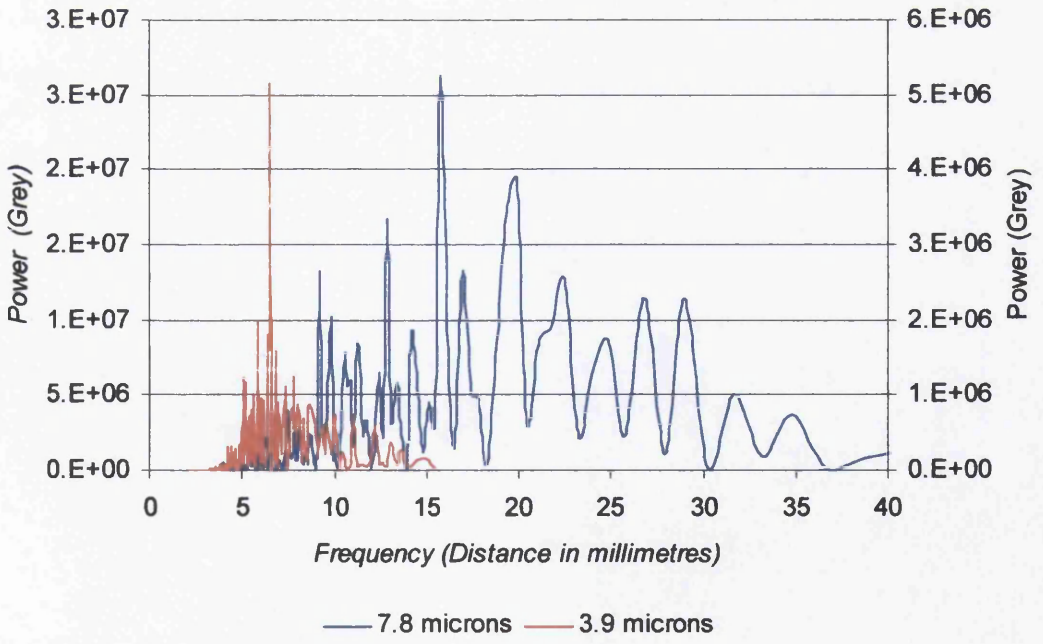

Figure 6-19 FFT analysis illustrates dominant pattern of ribbing. High frequencies derive from finest ribbing patterns. The frequency decreases with the ink film thickness increase.

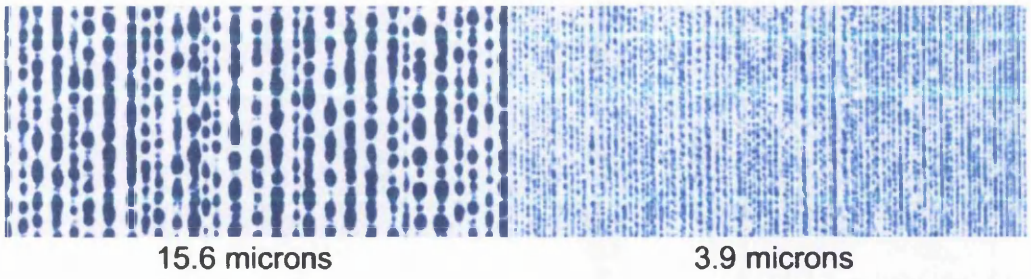

Figure 6-20 Ribbing presents variations across both directions that decrease to the rotating direction. Thus frequency does not indicate a clear domain through the profile.

Figure 6-21 illustrates ribbing frequencies between different ink film thicknesses. The frequency tends to decrease with the increase of ink film thickness. On the other hand, the ribbing frequency illustrates higher instabilities with the same ink film thickness and on the same run (Figure 6-22). This indicates that the ink film thickness along the rolling direction is not uniform. The ink film thickness instability causes also cavities instability along the rolling direction.

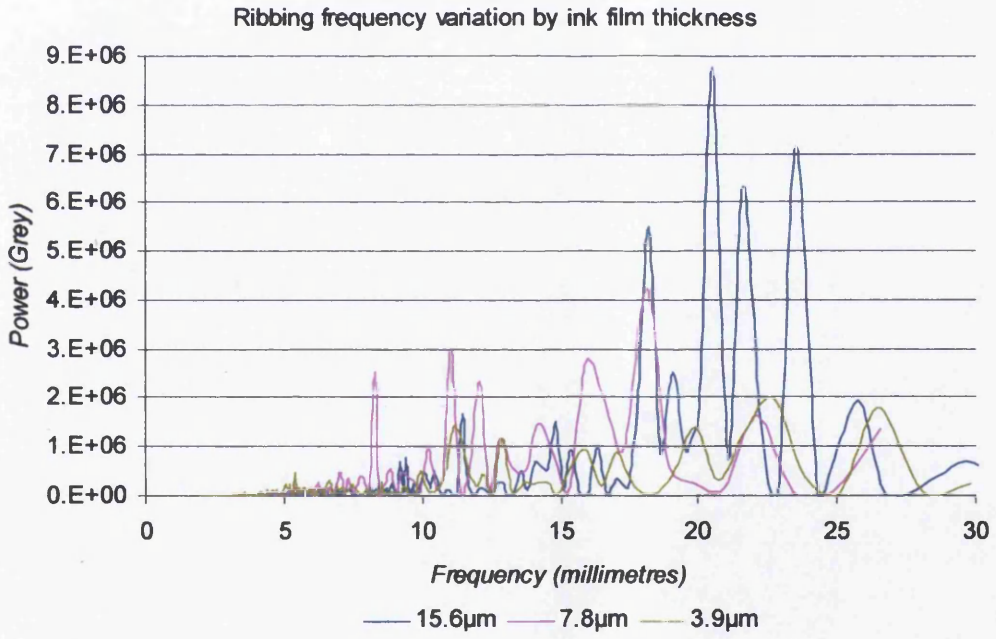

Figure 6-21 The ribbing frequency does not decrease significantly along the rolling direction with the increase of ink film thickness.

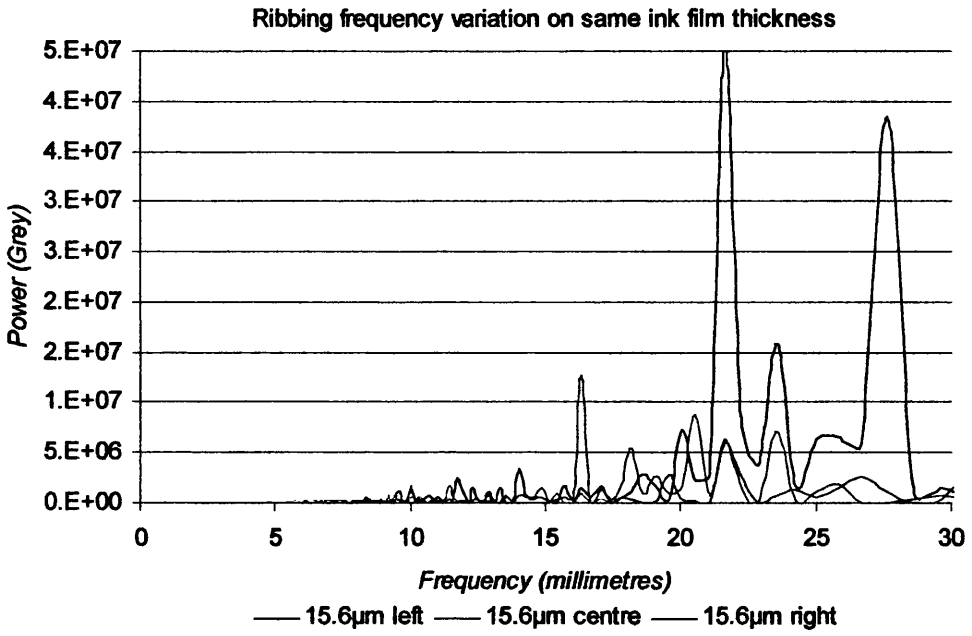

Figure 6-22 The ribbing frequency illustrates higher instabilities along the rolling direction with the same ink film thickness.

6.3.2 Mean of ink distribution parameters

The distribution conditions of the system have a significant influence on ribbing patterns. The changes in parameters affect the ribbing width and variations along the rollers length and also across the rolling direction. The patterns increase in variations by the effect of rollers ratio, distribution speed, distribution time and viscosity of the ink according to film thickness. When the ink film increases the separation angle becomes wider at the nip exit and filaments are formed away of the nip exit. The increase of the separation angle due to ink film thickness increase can define an ink-flood nip. The ink-flood nip decreases the effect because of rollers slipping and the significant increase of filaments length at the nip exit that lay back after splitting. Ribbing is formed even in ink-flood nips when the roller does not slip during rotation. The increased ink film thickness does not highlight the ribbing thickness variation by scanning due to the ink density saturation. The adhered ink is not affected by cavities when the ink film thickness significantly increases on the rollers. The higher ink transfer instabilities may occur to the stabilised ink film thickness on the rollers surface as an effect of ink surface immobilisation. The stabilised layer may also increase with the ink film thickness on the rollers. The stabilised ink was discussed by Melia (1974) and MacPhee (1998) but they did not report variations

with the ink film thickness. They conclude that stabilised ink is affected by the microstructure of the surface. Melia (1974) stated that the immobilised ink is highlighted by the non transfer performance. No study has been reported yet on such effects by the elastic rollers of the ink train. This is a supposition of the current work and was not studied extensively.

6.3.2.1 Low importance parameters

Rollers ratio and distribution time indicate low influence on ribbing formation (Figure 6-23). This was concluded by comparison of tests between measure-motor roller ribbing and oscillator-motor rollers ribbing. The distribution time also has little effect but increases with the influence the roller ratio. However, the ribbing peak number is slightly decreased with increase of roller ratio that generates lower separation angle. The separation angle affects the extension of filaments due to effect of elongation speed. The decrease of separation angle decreases capillary action which decreases further with increase of ink film thickness due to decrease of tensile stress at the nip exit.

The time for which the ink is distributed affects rotation of the same nip on different roller circumferences. A small circumference roller runs more times at a nip in comparison with a wider roller at the same distribution time. The roller pair transfers an equal amount of ink and ribbing generates cavities. This is related to distribution speed due to rotations and as a result increased splitting sequence. Ribbing formation becomes visible through distribution time and instabilities depend on the number of rotations with an influence of distribution speed. The low ribbing variability across distribution time determines that ribbing is formed faster than it actually appears by observation. As a result, the increased rotations increase difference between high and low peaks of ribbing lines.

6.3.2.2 High importance parameters

Ribbing patterns are strongly influenced by distribution speed, ink film thickness and viscosity (Figure 6-24). Peaks number of ribbing profile is decreased with increase of distribution speed and ink film thickness or decrease in viscosity.

Ribbing is affected by viscoelastic properties of the ink with significant influence of ink surface tension that affects contact angle. This was calculated by the effect of non diluted ink and the ink with 5% concentration of Butyl-Diglycol. The dilution decreases surface tension and viscosity as reported in Chapter 4. The decrease in viscoelasticity affects ribbing where longer filaments generate finest ribbing patterns. The decrease in viscosity decreases plastic deformation and ribbing appears in longer time than for the higher viscosity fluid. The filaments split faster when viscosity is decreased as established in the extension rheometry test in Chapter 4. The formed filaments exhibit plastic deformation when the viscosity is high. Higher ink volume is transferred to a filament that lays back opposite to the rotating direction of the rollers. The filament loses instantly the ability to recover. As a result, the ink volume is inserted to the next nip in variation in ink film thickness due to filaments deformation.

Ink film thickness has a significant effect on ribbing formation. The surface area increases with ink film thickness due to surface tension and so ribbing with increased width is formed. The increase in ink film thickness generates fewer filaments and ribbing follows that decreases in lines and width.

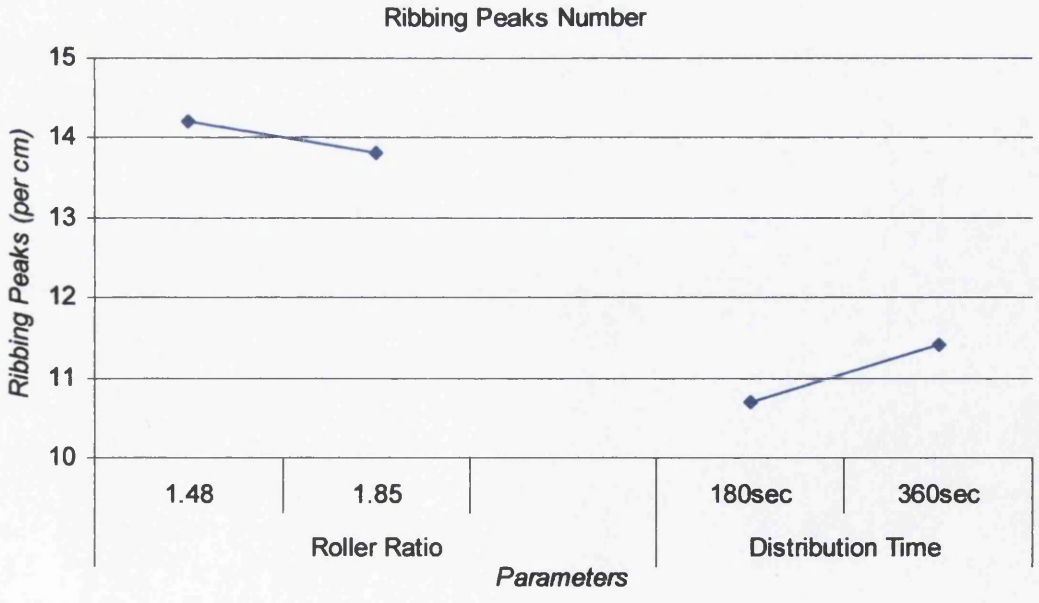

Figure 6-23 The increase of roller ratio decreases separation angle and decreases ribbing peaks. The longer distribution time increases ribbing peaks.

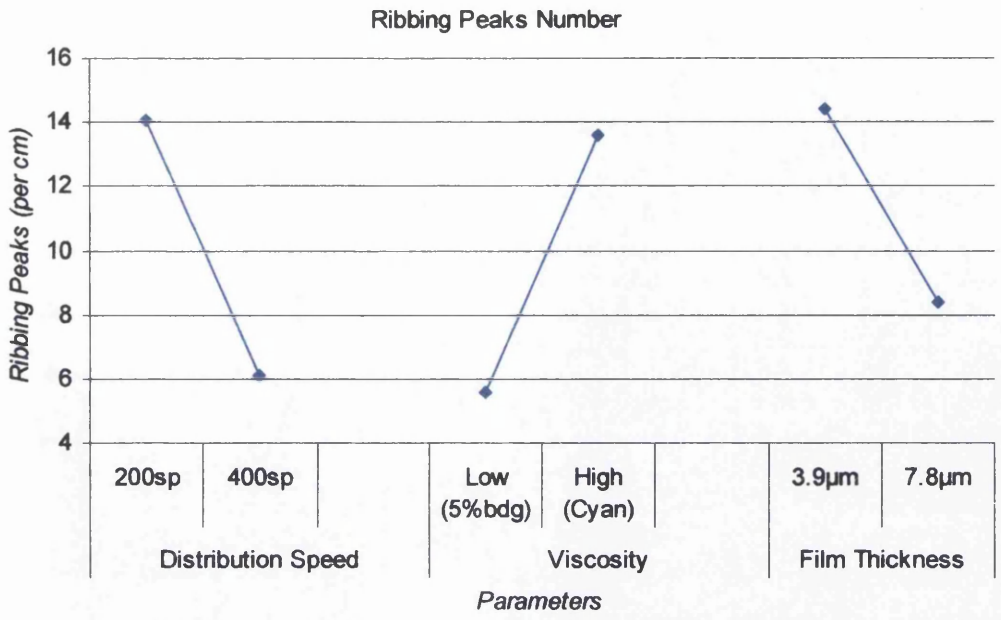

Figure 6-24 The increase of ink film thickness, viscosity and distribution speed increase ribbing peaks.

Ribbing is formed faster with an increase in distribution speed which increases cavities across the nip length. Distribution speed depends on ink viscosity and its effects increase with increase in viscosity. A given viscosity ink at high rotation speed can possible generate similar ribbing patterns with higher viscosity ink at lower distribution speed. This gives a similar ratio of filament break-up time and recovery of structure network before the following splitting. The increased distribution or rotation speed increases the amount of air that is forced to pass through the nip. As a result, wider air canals are formed which lead to a wider peak that concludes lower ribbing peaks. Air canals can be defined as the negative ribbing or the space between two ink ribs along the roller length. These are formed due to cavities and allow the air pass during rotation.

6.3.2.3 Ribbing width and instabilities

Ribbing is not uniform along the roller width or length. Ribbing across the rotating direction is also affected by patterns on the rolling direction. These two generate instabilities that affect the ribbing profile. While peak number indicates the generated pattern, it does not provide detailed information about ribbing width due to non uniformity. The increase of the peak number indicates finest patterns but does not calculate the actual width. The average ribbing width can be estimated by the

division of the roller length with the peak number divided by two because of the gap between the ribbing peaks. However, this does not illustrate instabilities along the roller but a average estimation of the ribbing width.

The width of ribbing decreases with the increase in roller ratio and distribution time (Figure 6-25). The increase in roller ratio increases separation angle at the nip exit. As a result, increased separation angle decreases ribbing width and also instability and more uniform ribbing is formed as shown on measure roller. This depends on the ink film thickness which demonstrates the opposite effect. The separation angle can increase as ink film thickness increases. This forms longer filaments that split away of the nip exit (Figure 6-26)

The distribution speed has a major effect on ribbing width and variations. The ribbing width increases with increase in speed but there is also an increase in width variation along the nip (Figure 6-27). This effect agrees with the reducing of peaks of the profile. However, higher speed was expected to generate more peaks and thinner ribbing. However, a conflict with increased rotations due to higher speed is possible. Higher distribution speed increases the pressure of the air canals and thin ribbing is forced to slide along the nip by increasing the air corridors. The air canal increases in area while at the same time wider ribbing is formed (Figure 6-28). As a result, ribbing width increases with increase of width variations.

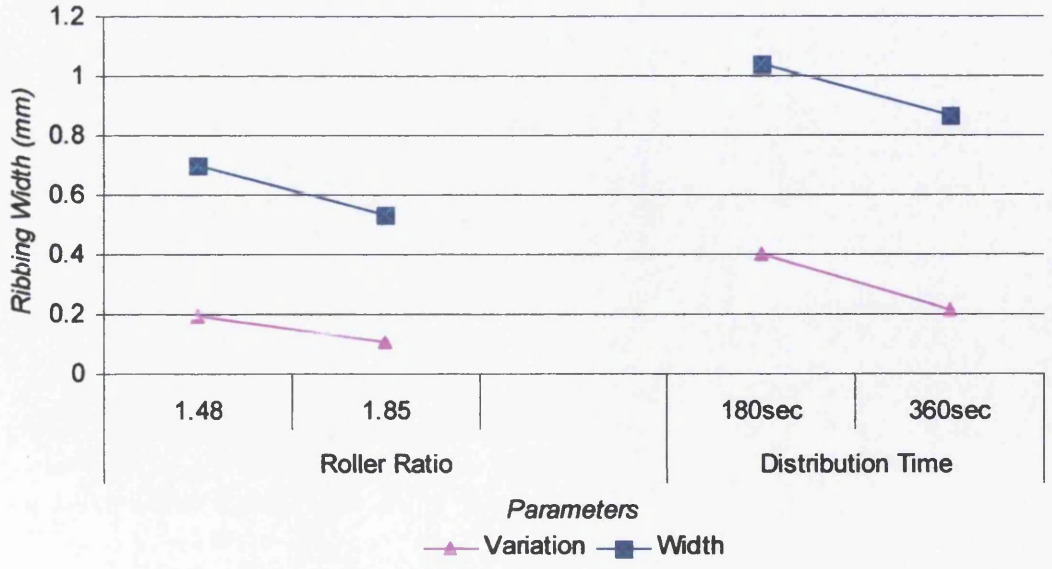

Figure 6-25 Ribbing width and variations decrease with increase distribution time and roller ratio

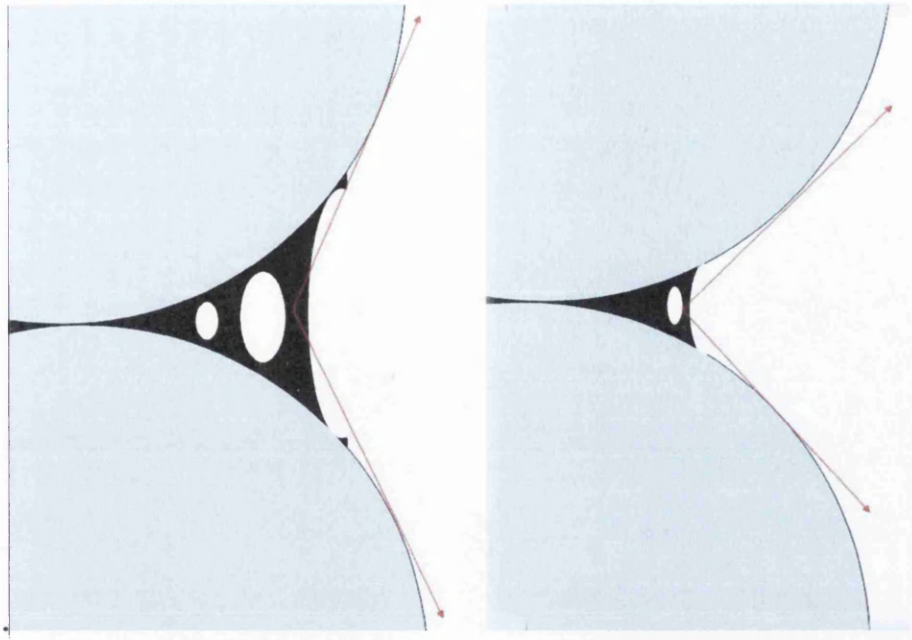

Figure 6-26 The seperation angle increases as the ink film thickness increase between the rollers. Longer filaments are formed that split further away of the nip exit. Similar effect has the decrease of the rollers perimeters.

The decreased viscosity increases ribbing width and generates high ribbing width instability (Figure 6-27). The ribbing increases when viscosity becomes higher and ribbing becomes finest and thus profile decreases in variations. This indicates an effect of intermolecular dynamics of the ink structure and elasticity. The ink film is stretched at the nip exit and longer filaments are formed that generate increased cavities. The increased number of cavities forms an increased number of filaments. When viscosity drops, ink loses elasticity and splits faster in shorter filaments. The ribbing becomes wider in width where deformation of ink filaments is lower and decreased surface tension spreads in a wider area across the rotating direction due to decreased contact angle. The ribbing width increases but also the variations in width.

An influence on ribbing is also indicated by ink film thickness. The ribbing peaks decrease significantly with increase in ink film thickness where slightly wider ribbing is formed with significant effect on width variations. The increase of ink volume at the nip exit decreases capillarity and negative pressures. This forms thicker filaments that extend and split further away of the nip exit. As a result, the contact area of the ink on the rollers increases with the volume of the ink at the nip exit and wider ribbing is formed across the roller rotation. The increased instabilities

occurred by a flood nip where rollers rotate under micro slip mechanism. The effect can be compared to the roller ratio effect where decreased negative pressures are generated at the nip exit. The ribbing width increases with roller ratio or ink film thickness where nip flood is determined.

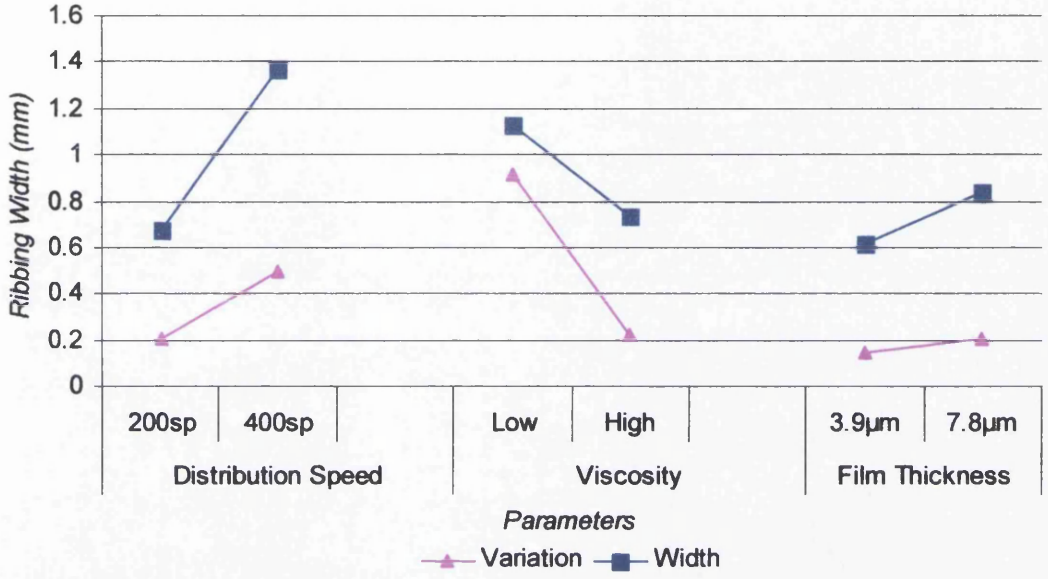

Figure 6-27 Ribbing width and variations increase with increase in distribution speed and ink film thickness or decrease in viscosity.

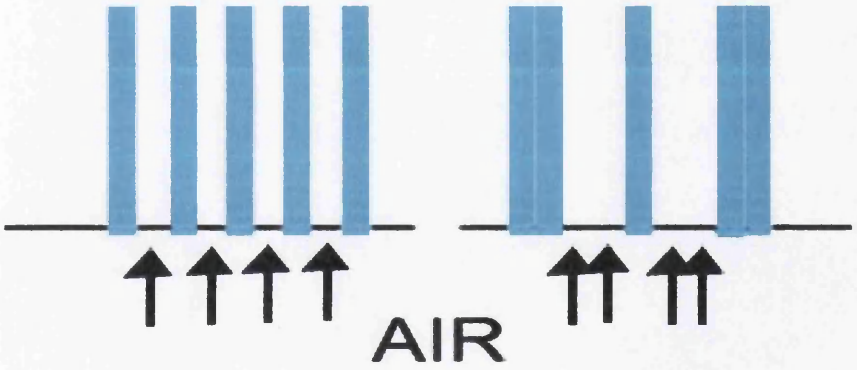

Figure 6-28 The higher distribution speed increase air pressure through the nip. The air pushes by the thinner ribbing and wider ribbing is generated

6.3.3 Observations and general discussion

The ink is squeezed to the surface of the rollers at rollers separation mechanism because it passes through the narrow gap. The separation meniscus is formed at the nip exit due to negative pressures. This is due to the fluid structure that is deformed

at the nip exit and generates capillary action as also discussed by Savage (1984), Coyle et al (1990), and Carvalho (1996). The free surface of the ink is pulled in three directions and the meniscus is formed. Cavity is generated by meniscus failure when the tensile forces at the ink volume increase by the two rollers and exceed the pull back strength at the nip exit. The cavity expands and filament is formed as discussed also by Bank and Mill (1956). Those evidences are based on video analysis that was captured on tack tester distribution rollers (Figure 6-32).

The sequence of this mechanism increases the thickness on specific points and generates a wave-like pattern across the length of the roller. The ribbing pattern is formed by continued step splitting. The wave pattern becomes uniform across the perimeter of the roller. The generated gap between the ribbing lines provides air canals during the rotation. The ink volume increases in thickness while it decreases in width and so the areas of the negative pressure increase in two dimensions.

Ribbing occurs to ink deformation due to cavities and the filaments elongation. Photographic analysis of distribution rollers illustrates how ribbing is formed through distribution time (Figure 6-33). Ribbing begins from the first minute, although it is not visible due to decreased variations on ink thickness and saturation density. Experimental simulation of a linear nip was examined on extension rheometer. An inked nip was formed along the parallel plates as described in Chapter 5 (Figure 6-29). The elongation mechanism applied tensile stress that formed a single filament when the elongation speed was low (Figure 6-30). On the other hand, the increased elongation speed applied higher tensile forces that generated cavities which expanded to multiple filaments as demonstrated by the video capturing (Figure 6-31). The elongation speed at the nip exit exceeded the higher speed that was applied at the extensional rheometer. Those results show that the cavities are generated by the ink structure failure. After that the surface tension forces generated filaments during the elongation mechanism that expanded until they split.

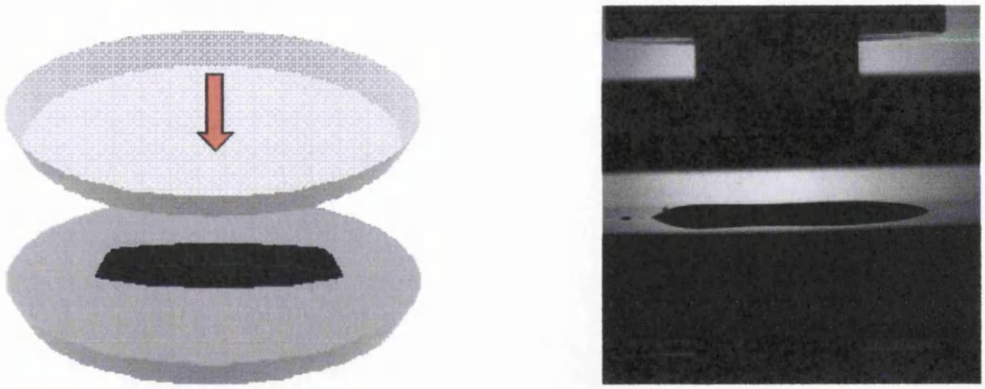

Figure 6-29 A virtual nip was formed between the parallel plates of the extensional rheometer in order to examine the filaments generation.

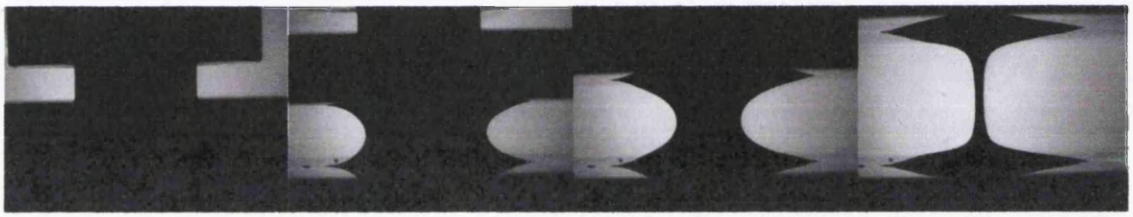

Figure 6-30 The low elongation speed (0.03m/sec) generates a strong structure that expands to a single filament due to the surface tension (App. VCD V8)

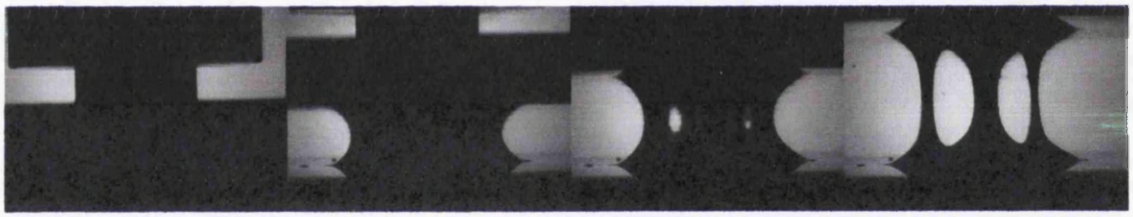

Figure 6-31 The extension mechanism of a virtual nip showed that filaments occurred to cavities. The cavities generation depends on the elongation speed and as a result the tensile forces that break the structure of the ink along the nip in multiple areas. The high speed of extensional rheometer (0.6m/s) does not exceed elongation speeds that are usually applied on real presses or coating processes by roller trains (App. VCD V9).

The ribbing pattern appears when the ink film thickness difference increases. High rollers difference (oscillator/motor roller) generates visible ribbing between the first and second minutes of distribution while lower roller difference (measure/motor roller) generates visible ribbing slightly later with finest pattern (Figure 6-34). The ribbing increases in contrast through distribution time while it increases in width. The gap increases between ink ribbing lines and allow air to pass by the nip through those canals. Air pressure increases between ribbing and forces thinner ink to move close to higher volume ribbing. As a result, wider ribbing is formed at certain areas according to ribbing ink volume.

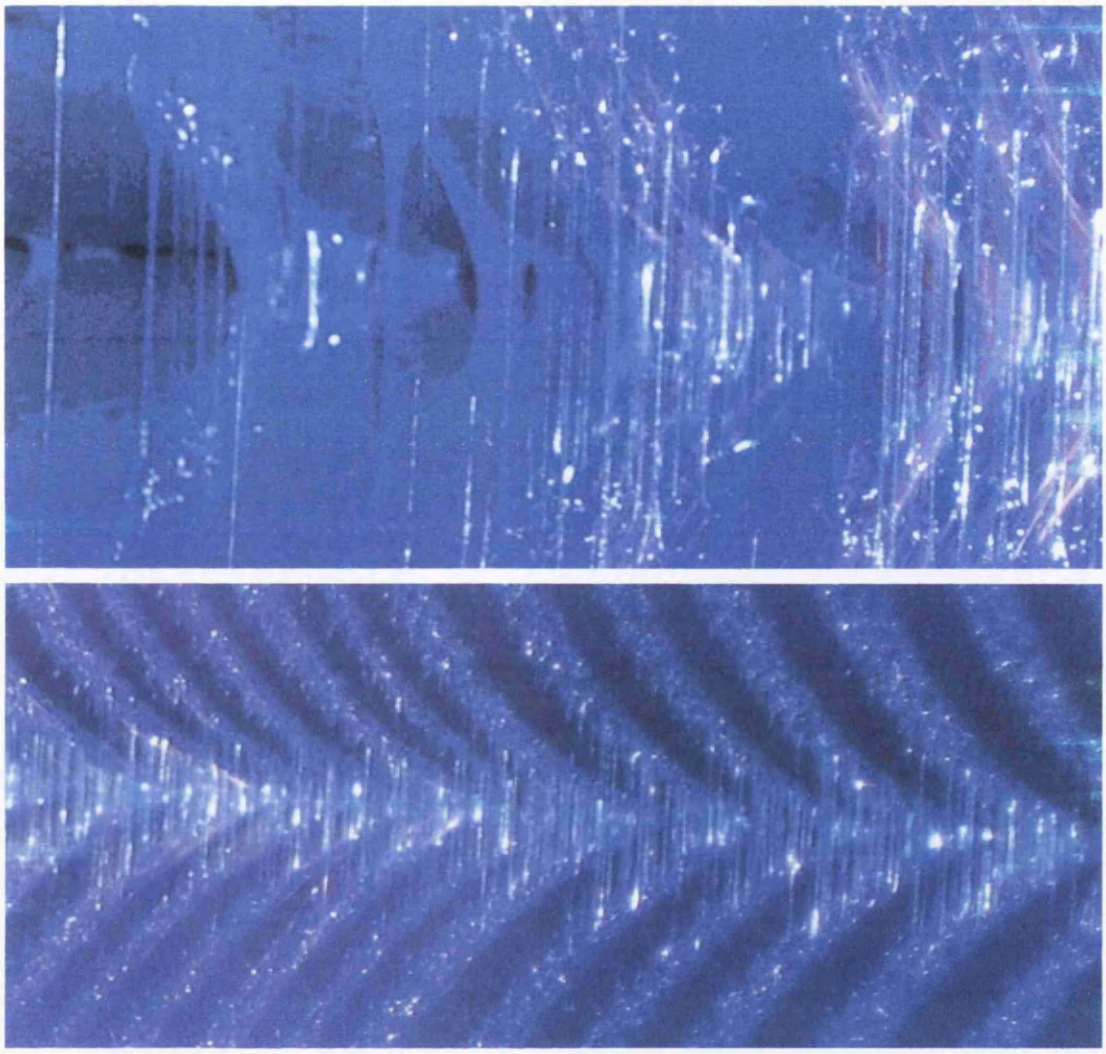

Figure 6-32 Cavity is generated when the forces increase between the rollers due to increase of ink volume. The pull back strength is exceeded and cavity expands to a filament. The variation increases with the ink volume decrease. The curent picture was captured by a digital protographic camera at a flood nip of the IGT tack tester where ribbing was generated by a single rollers nip The top high magnification picture shows how the formed filaments depend on the amount of the ink volume at the nip exit. The bottom picture shows that mulltiple ink filaments are formed in a single ink rib area. Darker areas indicate the areas between ink ribs.

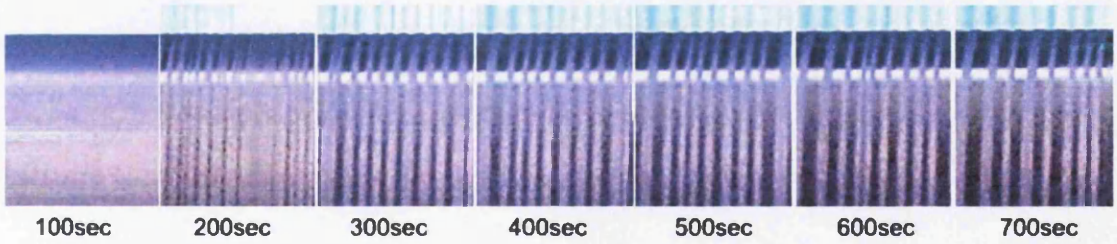

Figure 6-33 Ribbing increases in width through distribution time and becomes more visible between ink and non-ink areas. The ink ribs width increase with time but also increase the distance between them and change the ribbing patterns. The decrease in ribbing frequency with time generates areas with significant lower ink film thickness between the ink ribs with increased ink film thickness.

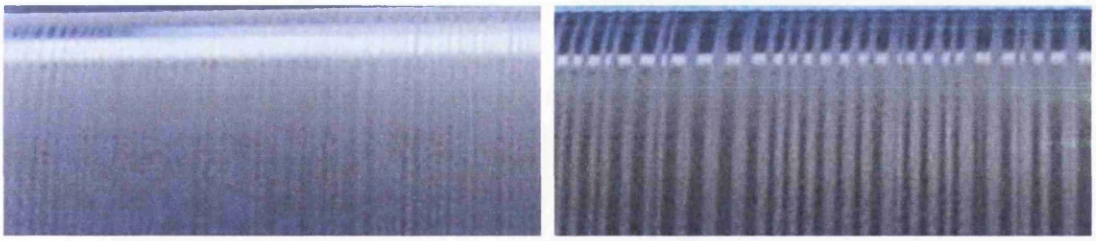

Measure Roller (400sec) Oscillator Roller (400sec)

Figure 6-34 Measure roller generates finest ribbing pattern versus oscillator roller in 400 sec due to variation in rollers ratio with the motor roller. The elastomeric material of the rollers was the same and they were varied only by their geometry.

This phenomenon increases with increase in roller ratio and is responsible for variations of the ribbing width. The roller ratio difference does not only affect separation angle and speed but also generates variation in rotations at the same time (Figure 6-35). The ribbing effect according to coverage area increases on both rollers through distribution time with higher rate to the oscillator roller. The number of ribbing peaks increases with the measure roller and finest ribbing is formed. The oscillator decreases the number of peaks and wider ribbing is formed (Figure 6-36). The ribbing width remains steady at the measure roller and increases at the oscillator across the time. The ribbing peaks decrease at the oscillator roller while increase on the measure roller. The ribbing coverage area increases similarly along the rollers over the time.

Process parameters significant affect ribbing patterns but also show some interactions. It is not possible to characterise the ribbing profile by only one parameter where variations are not always linear with the parameters variation. While parameters conflict between each other, it is important that the interactions and responses are examined under detailed experiments. The effect of the process parameters and interactions are studied through experiments using orthogonal arrays techniques at Chapter 8.

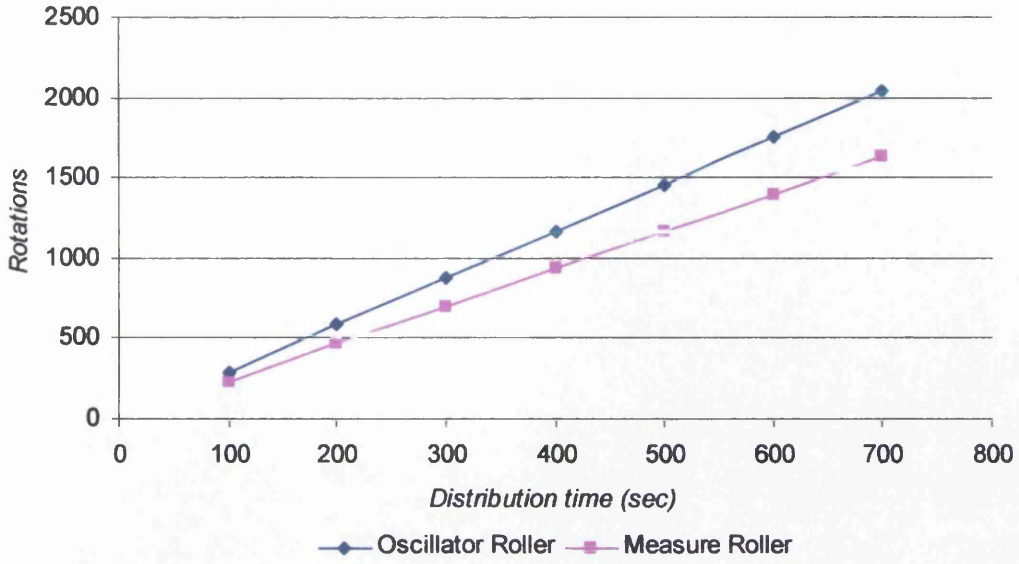

Figure 6-35 Oscillator roller generates more rotations than measure roller at the same time. This indicates how ribbing is affected by rollers rotations number and the splitting sequence at the nip.

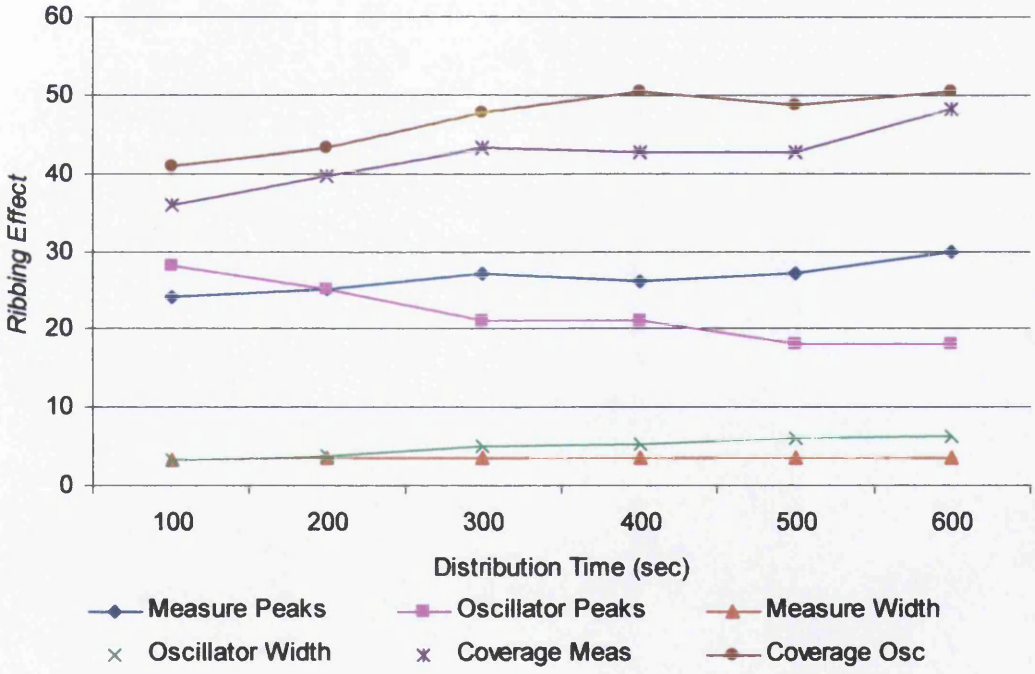

Figure 6-36 Ribbing coverage area increases across distribution time while ribbing peaks and width vary by roller ratio. The ribbing width remains steady at the measure roller and increases at the oscillator across time. The ribbing peaks decrease at the oscillator roller while increase on the measure roller. The ribbing coverage area increases similarly along the rollers over the time. As a result, oscillator forms faster ribbing with fewer peaks with increased width over time.

6.4 Conclusions

The ribbing phenomenon is critical to the forward rolling train. The ribbing pattern appears faster at thin films and the period decreases as a function of distribution time and ink film thickness. The low ink film thickness generates finest patterns but became unstable in period across time. The onset of ribbing occurs due to cavities at the nip exit which generate ink film thickness variation across the roller length but also across the rolling direction.

Cavities are an effect of the negative pressure and the stretching mechanism across the ink volume of the actual region due to capillary action at the nip exit as found by studies on extension rheometer and the high speed video analysis. Ribbing is affected by the sequence of splitting that generates cavities. Cavities generate a decreased ink volume in areas that allows air to pass through the nip during rotation. The sequential splitting continues to decrease ink volume in air canal areas while it increases between them and forms the ribbing patterns. Ribbing appears faster with the speed where ink filaments lose elasticity and generate plastic deformation between nips.
This chapter described analysis of ribbing phenomena by extracting information from the generated patterns that are related to the ink transfer mechanism. Some previous researchers focused on the formed meniscus at the onset of ribbing, although none of them analyses the complete patterns as an ink profile and the variations due to printing parameters. Concluding remarks of this study indicate how ribbing patterns are related to the distribution process. The profile analysis determines dominant characteristics of the distribution process. Methodology locates experimental threshold for high accuracy and repeatability through profile analysis. Video and capturing techniques support additional theories of ribbing phenomena on roller distribution system. The conclusions of this experiment can be summarised as follows:

- Ribbing is primarily generated due to the elongation mechanism at the nip exit, where ink is deformed in filaments due to cavitation and splits.
- The elongation mechanism affects elasticity of the structure and generates deformed thin filaments that lay back to the nip direction after splitting. The rotation rates do not allow ink to recover its elasticity before the insert at next nip inlet. Ribbing is formed due to sequential splitting through nips. The

ribbing width is a matter of rotations due to filaments deformation and ink contact angle. This is affected by distribution time, speed and rollers ratio.

- Ribbing width increases with decrease in ink viscosity and surface tension. The ribbing formation is affected by viscosity changes and as a result by temperature that affects viscosity.
- The cavities are generated between areas with lower ink film thickness along the roller length at the nip exit due to decreased intermolecular dynamics and viscoelastic failure of the ink structure. The filaments depend on cavities that expand at the areas where ink film thickness decreases. This generates perturbation of the formed meniscus at the nip exit.
- Ribbing can vary by its profile on ribbing peaks and width, surface ink coverage on roller surface that affect appeared frequencies. The ribbing amplitude is affected by ribbing width while frequency is affected by number of peaks.
- Ribbing amplitude and frequency across the rollers width and length increase with the ink film thickness. The detailed ribbing profile demonstrates the amount of ink film thickness along the roller length. The onset of ribbing is affected by separation angle, and rheological profile of the ink. The separation angle is a function of rollers ratio and the ink film thickness.
- Fine ribbing patterns are characterised by high ribbing frequency and high amplitude. Weak ribbing patterns generate low ribbing frequency with low amplitude. This concludes that ribbing can be described by the mean frequency versus the mean amplitude for a given set of printing parameters.

7. Developing techniques and establishing analysis of misting profile and mechanisms

7.1 Introduction

Misting affects the ink transfer quality and ability to print. It occurs in offset lithographic printing at the rollers rotation where ink film splitting and tangential forces causes the ink droplets to fly away, forming a mist of micro-droplets that interferes with the printing process and environment. As a result ink volume is reduced on the distribution system and the air is contaminated with fine droplets. No solution has been reported on such phenomena although there have been studies on the misting phenomena (Blayo et al 1998; Owens 2005). Owens (2005) used an Aerosizer system in order to calculate droplets dimension. However, his study focused on viscoelastic fluid properties at the narrow exit of the nip without establishing any relationship to the printing parameters. Blayo et al (1998) focused on ink film thickness and speed variations by calculating the amount of the ink that create misting by using tack-o-scope tack meter. Neither reported a complete profile of misting or effects of rollers properties or droplets movement.

The work reported in this chapter looks to establish the relations with the ink transfer mechanism looking on printing ink properties and the effects of the printing parameters. A methodology developed for the study of the misting phenomena is described. It uses trapping techniques on the tack-tester to understand misting mechanisms. The aim of the methodology was to investigate misting with respect to ink film thickness, rheology, tack and process parameters such as distribution speed and temperature. Trapping techniques characterise the misting phenomena on a short closed loop distribution system. Such systems eliminate dynamic effects of incoming and outgoing ink volume. The modified techniques and the detailed methodology are presented in section 7.2. The trapped misting is analysed in order to establish distribution variations along the roller's nip. The Section 7.3.1 deals with the printing parameters that affect misting phenomena. The misting profile is characterised according to droplets mass, dispersion rate and variations with respect to the ink film thickness and other printing parameters. The misting varies according to rheological

properties. Misting is not typical for viscoelastic fluids and so inks are not designed to produce such phenomena.

Numerous authors have reported that misting is related with the splitting mechanism, the ink film thickness and the distribution speed on rollers (Voet 195; Bisset et al 1959; Blayo et al 1998). The current work attempts to establish the amount of ink on the roller's surface through the relation between ink film thickness and misting rates. In order to establish this relation, it is necessary to investigate the misting rates along the roller's nip. No study before used the misting phenomena in order to determine the ink film thickness on ink distribution systems.

7.2 Methodology

The misting was determined by using the IGT Tack tester as a closed loop distribution system of three rollers. The trapping techniques were developed to collect misting droplets and to establish variations in the misting phenomena. The capturing methodology modified the concept of Blayo et al (1998) on misting studies that used a tack-o-scope tester to determine misting. Preliminary investigations were undertaken of parameter effects on misting during the development of the techniques. Dispersion directions and morphology used to determine misting mechanisms. Repeatability of misting effects indicates repeatability also of ink transfer mechanisms on roller distribution system. The ink film thickness, distribution speed, temperature and rheological properties were varied through the study to determine relations of ink film thickness with misting phenomena and also to establish and characterise those variations.

7.2.1 Misting generation and trapping techniques

The misting trap comprised a smooth flexible substrate placed at the bottom, side or surrounding the distribution system of the IGT tack tester. Tiny droplets can be lost on very rough or absorbent surfaces. Misting trap geometry was varied according to the aspect to be studied. A flat misting trap was used to determine average misting effects and film thickness profile on the rollers (Figure 7-1).

This was placed at the bottom of the tack tester and under the vertical direction of the nip exit of the motor roller and the oscillator. The oscillator frequency was 5,5 Hz in order to capture the ink film thickness and distribution speed effects. None of the rollers was disengaged and misting was captured as an average effect of the system. The second method used a curved surface in order to determine the misting effects of the individual rollers nip according to rollers geometry (Figure 7-2). The roller that was not being studied was disengaged from the motor roller contact area and so a single nip was formed. The oscillator frequency was also disengaged and was used as a rider. As a result two roller nips were generated with variation between rollers ratio as described in Chapter 6 on ribbing methodology.

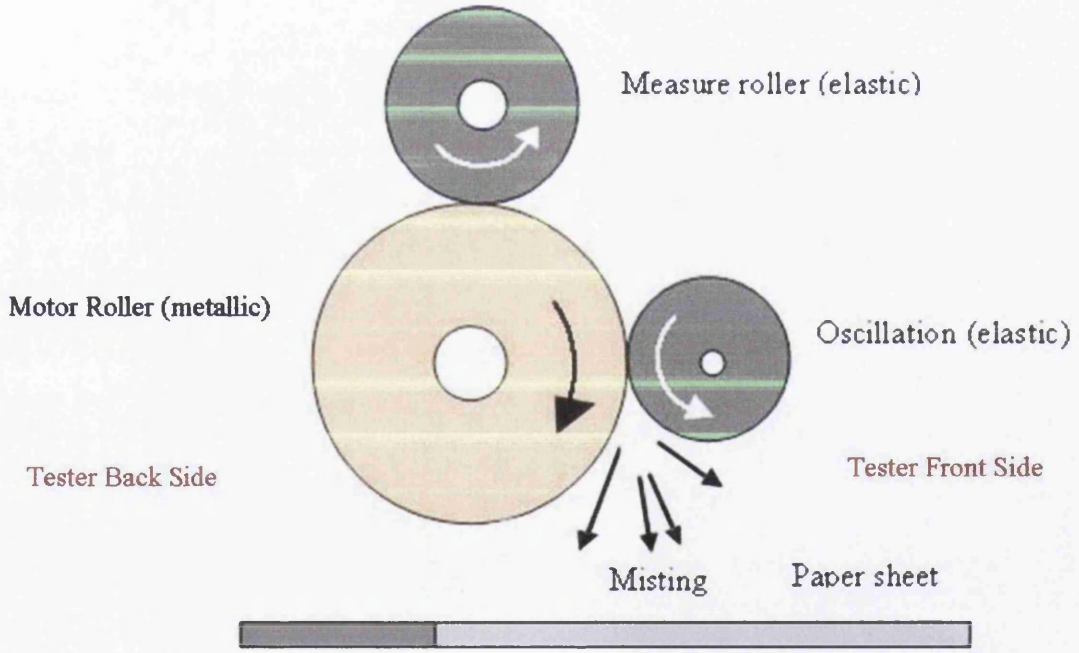

Figure 7-1 Flat misting trap (paper sheet) was placed at the bottom side of the IGT tack tester to collect the expected droplets of misting.

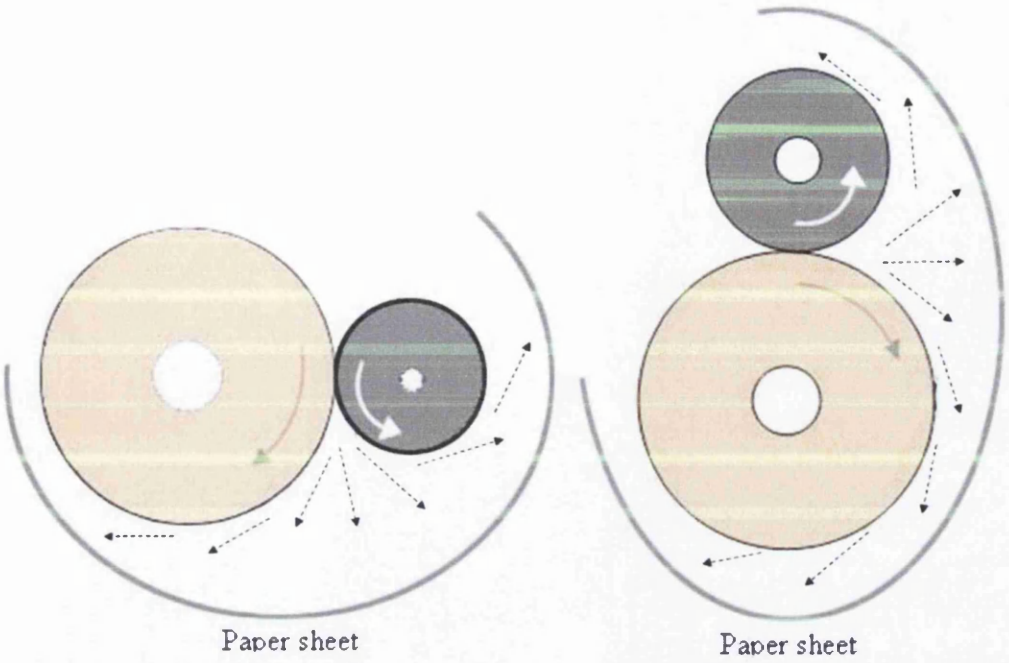

Figure 7-2 Misting trap on curved configuration by surrounding each independent nip. The arrows indicate directions of the expecting misting.

The surface quality of the substrate is important in terms of absorption and drying of dispersed droplets. Coldset inks dry by absorption of the surface so a porous surface is required. High porous substrate produces increase absorption or spread effects and droplets appear with increased area or linear shape. However, coated substrates do not allow quick drying time and the misting image is sensitive to storage and flexibility. The substrate with best qualities was determined to be a velvet quality paper of 170gr/m^2. Figure 7-3 illustrates misting images qualities between coated, photocopying paper and velvet substrate qualities that were examined during the preliminary experiments. Velvet quality provides high contrast and very good droplets shape in comparison with photocopy and coated substrates. The photocopying paper allows high absorption of the ink and as a result fast drying. It is suitable to establish misting on roller trains but the misting trap is very low quality. The substrate absorption does not allow accurately measurements of droplets shape due to blurring of the image quality. The coated paper allows very good quality of droplets. Unfortunately, the coated surface does not allow fast drying due to low absorption surface. As a result, the image of the misting trap is still wet after three days especially for high misting effects not allowing contact measurements such as

density and scanning. The velvet quality proved to be the best compromise. The good surface quality allows the ink drying in very short period of time (30 minutes to 1 hour). The low porosity of the substrate does not absorb or spread the ink and droplets are presented as sculptured image on the paper surface (Figure 7-4). The ink is absorbed by the porous surface of the photocopying paper and presents dissolved shape due to substrate fibres. The velvet quality paper provides high surface energy and ink misting remains in droplets shape on the substrate. This allows surface measurements of droplets with white light interferometer. Also, the fast drying allowed contact measurements in the same day thus accelerates the experimental time.

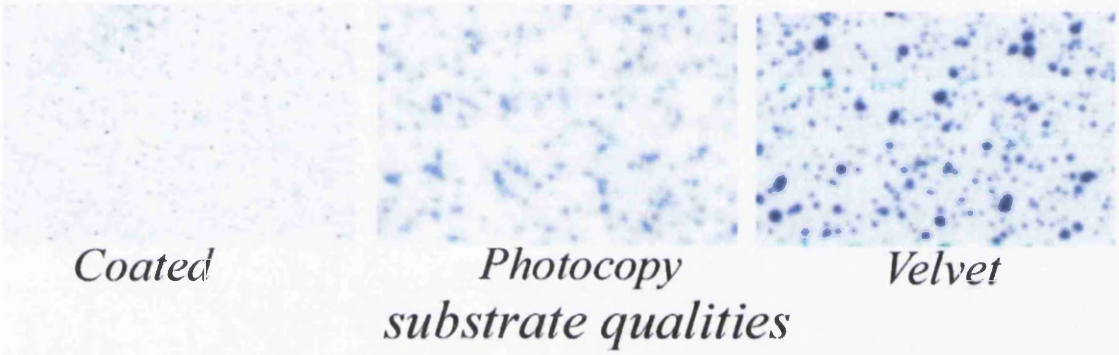

Figure 7-3 Substrate qualities for misting trap. Velvet quality provides high contrast and very good droplets shape in comparison with photocopy and coated substrates. The photocopy paper has low quality and high absorbance surface. The coated paper surface does not allows quick drying of the ink droplets and is flexible for further analysis.

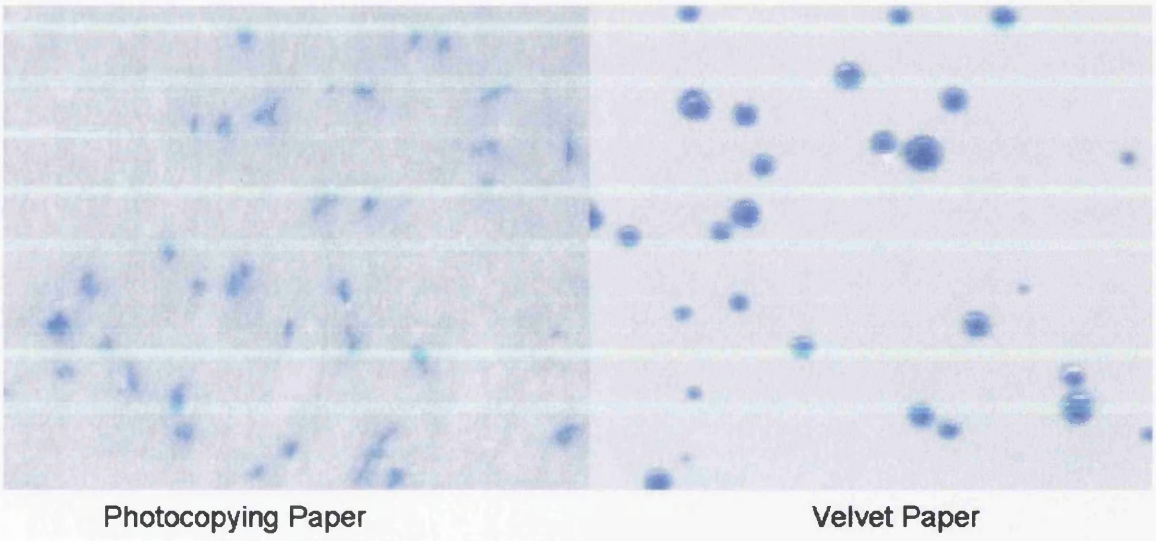

Figure 7-4 Comparison of dot shape with photocopy and velvet paper. The ink misting droplets are absorbed and change shape on the photocopy paper surface and is not possible analysis. The ink droplets dry fast and give very good image on the velvet paper surface which is excellent for further analysis.

The parameters that were expected to influence misting were the ink rheology, the roller diameter, the distribution speed and the ink film thickness.

Effects of viscosity on misting were examined by varying the viscosity of cyan ink by dilution with Butyl-Diglycol. Butyl-Diglycol dilution decreases viscosity and viscoelasticity, surface tension and tack with concentration. The seven dilutions were used 0%, 0.5%, 1%, 2%, 5%, 10%, and 20%. These correspond to the dilutions used in the study ink rheological properties in chapters 3 and 4 (Table 7-1).

Table 7-1 Illustrative table of rheological characteristics

Dilution	Shear Viscosity	Extension Viscosity	Hysteresis Loop Area	Tack	Printing Density	Surface Tension
ND Cyan	22.75	9.89E+02	2.67E+04	115	1.08	33
0.5%BDG	22.06	6.60E+02	2.52E+04	111	1.12	32
1%BDG	21.86	1.45E+02	2.03E+04	105	1.11	32
2%BDG	17.03	9.31E+01	1.49E+04	82	1.10	27
5%BDG	9.28	5.47E+01	9.76E+03	72	1.10	25
10%BDG	4.524	9.72E+01	4.94E+03	41	1.14	23
20%BDG	1.728	4.61E+01	1.66E+03	34	1.06	17

The *temperature* increase also affects rheological profile of ink by decreasing rheological properties similarly to dilution with solvent. System temperature was supported by external water cooling device that supplied water through the cylinder drum. The temperature was set to 25°C and 30°C in order to identify variations in droplets formation.

Two *ink volumes* were used through the examination. The 0.3ml 3.9mμ and the 0.6ml that provided 7.8mμ ink film thickness correspondingly on the system.

The *distribution speed* was varied between a low speed of 50m/min (0.8m/s) and high speed of 450m/min. Also accelerating speed was used every 30sec of time from 50m/min to 100 and 150m/min distribution speed (approximately 0.8m/s to 1.6 and 2.5m/s) and then back to 50m/min. This allowed examination of tack by changes in shear rate due to changes in distribution speed

The *distribution time* effect was determined by two tests. First, the misting trap was removed after a complete run of 3 minutes of time. The second one was determined

every minute for 3 minutes test. The misting trap was removed every minute in order to determine misting effects with time.

The *oscillation frequency* was examined by three levels, these of 0-0Hz, 3-3Hz and 5-5 Hz.

The *viscosity* effects were examined by using coldset ink diluted with Butyl-Diglycol.

The *surface qualities* and configuration effect were estimated by the use of IGT inking unit system as an alternative close loop system for misting analysis. The system consisted at three rollers, two metallic and a rubber roller as Figure 7-5 illustrates. The ink was applied as described in chapter 4 for the printing density experiments. A misting trap was placed at the bottom area of the rollers similar to the tack tester. The test was carried out for 3 minutes with 8μm ink film thickness and 1.6m/s distribution speed.

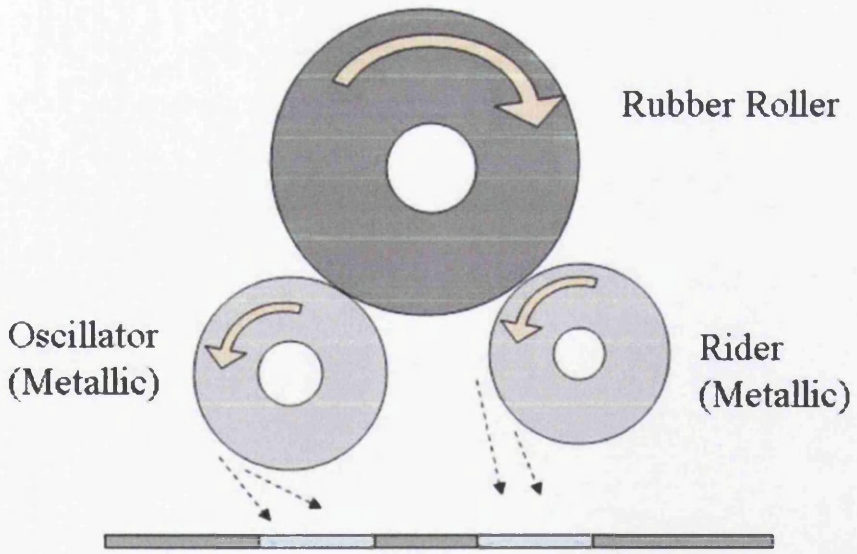

Figure 7-5 The High Speed inking unit was used as an alternative configuration to study surafec qualities effect on misting mechanisms.

The misting uniformity and numerous of misting characteristics were determined through this study as follows:

- Droplets area characterised as the average micro-droplet that was formed due to splitting instability. The shape of a droplet was related to the examined rheology of the fluid.
- Droplets area distribution characterised the generated droplets area range. This allowed a full description of the droplets range.
- Surface coverage determines the amount of misting generated. The ink density varies with the misting and also the coverage area on the misting trap.
- Spread variations determine misting trends of droplets directions. This analysis highlights relations with the ink transfer mechanism and describes the ink film thickness profile along the rollers surface.

7.2.2 Measurements and calculations

The surfaces of the misting traps were analysed by measuring densities and scanning with a flat bed scanner at high resolution. Selective areas were also analysed by white light interferometer in order to verify calculations on droplets shape and dimensions. The ink droplets generated a raised image on the missing trap. This allowed a detailed surface analysis with the white light interferometer.

Gretag Magbeth scanning spectrophotometer was used to scan misting samples. The measurements were carried out by using D50 light source and D65 filter with 2^{o} degrees observer. The average measuring area was 5mm and two scanning resolutions were used. The low resolution used 20 measurements through the width and 30 through the length of the misting image that gives 1 measurement per square centimetre. The high resolution used double analysis in each direction with 4 measurements per square centimetre which produce almost 100% coverage of the misting trap. Density values were averaged across the length and width to generate misting profile trends for each direction of the rollers nip. The ΔE L, a, b values were plotted as a contour plot in order to create a topographic analysis of the misting trap and misting spread distribution across the width and the length of the misting trap (Figure 7-6).

The Epson flatbed scanner was used to digitise the misting images. High resolution scanning enabled more detail to be resolved but also generated an extremely large file that was not flexible for analysis with the current system. The images were scanned with 350dpi for surface analysis which provided a flexible file with adequate resolution. The middle area across the trap's length was scanned with 1200 dpi which generated a high resolution image and medium size file for droplets analysis.

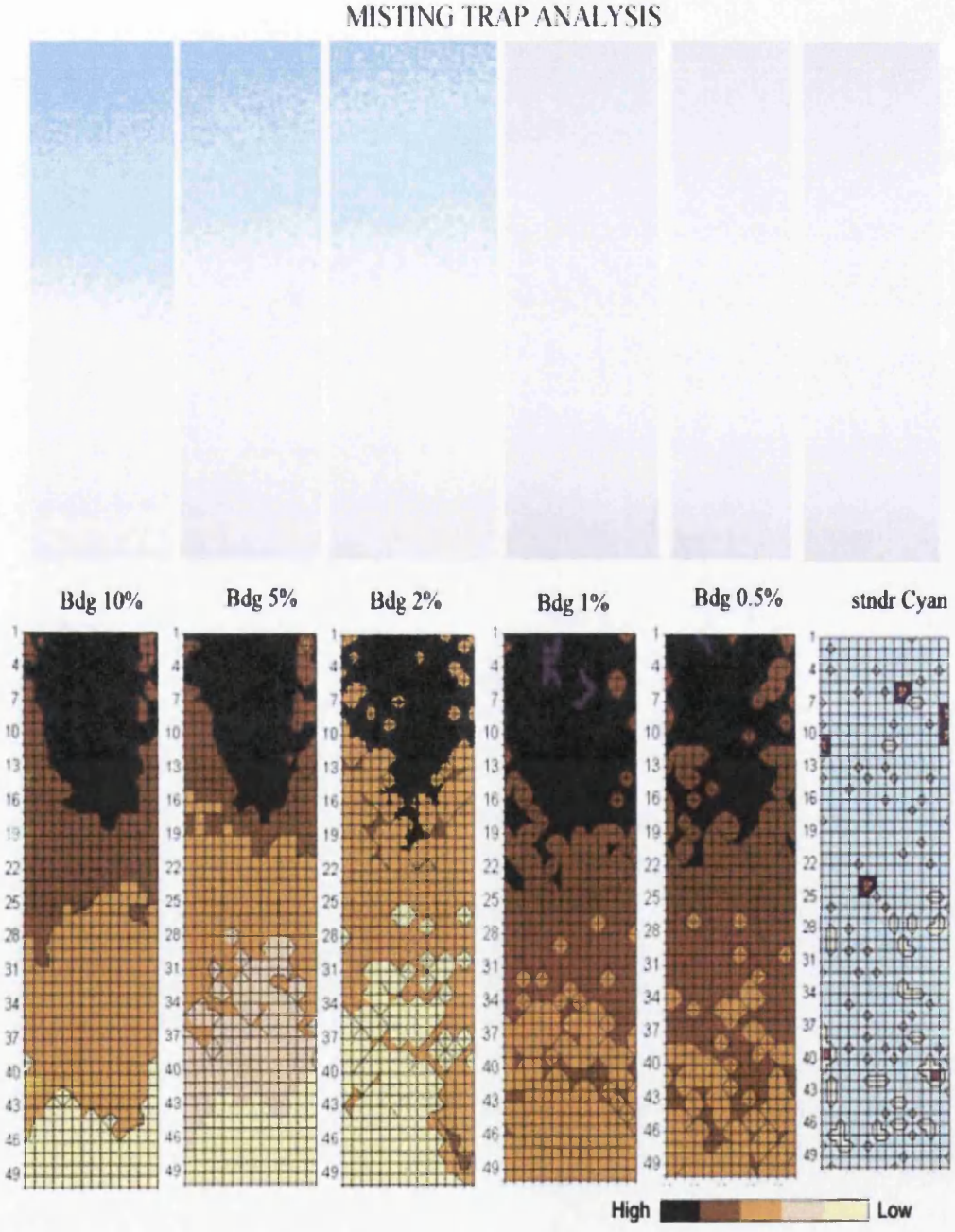

Figure 7-6 Misting traps were analysed by the measuring colour density values across the width and the length. ΔE L, a, b values were plotted on a surface plot (misting topography) to determine droplets spreading variations. The top figure is consisted by digitised images of the real misting trap samples. The bottom figure is consisted by the contour plots of the scanned top samples in order to visualise the areas with increased misting effects.

The Leica image analysis microscope was also used to capture selected parts of the misting image throughout the length of the trap for higher accuracy and verification of scanning and measured droplets geometries results.

The flatbed scanner did not provide uniformity of light source and a result a calibration process of the grey values was required to eliminate lighting instability. Calibration values were carried out using the white paper surface as a reference that was then used for the misting trap. The digitised image was converted into grey scale values from 0 to 255. The grey values of the scanned (digitised) white paper surface (velvet quality) were eliminated from the profile (Figure 7-7). The values were then inverted in order to demonstrate the actual profile of misting. The 0 grey value illustrated the black colour (no light) while the 255 grey value illustrated the white (highest light). Thus, an inked area appeared with lower grey values than a non-inked area after scanning, calibrating and inverting the values. The grey levels inversion demonstrated the areas where misting was increased (Figure 7-8).

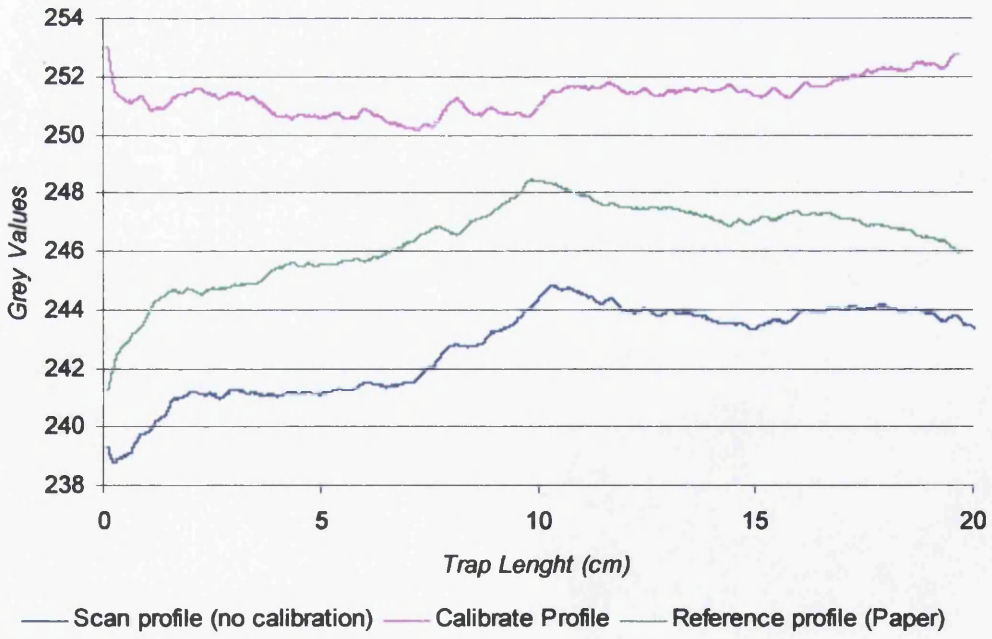

Figure 7-7 The scanned profile was calibrated by the grey values of the white paper as a reference in order to eliminate lighting effects of the scanning process.

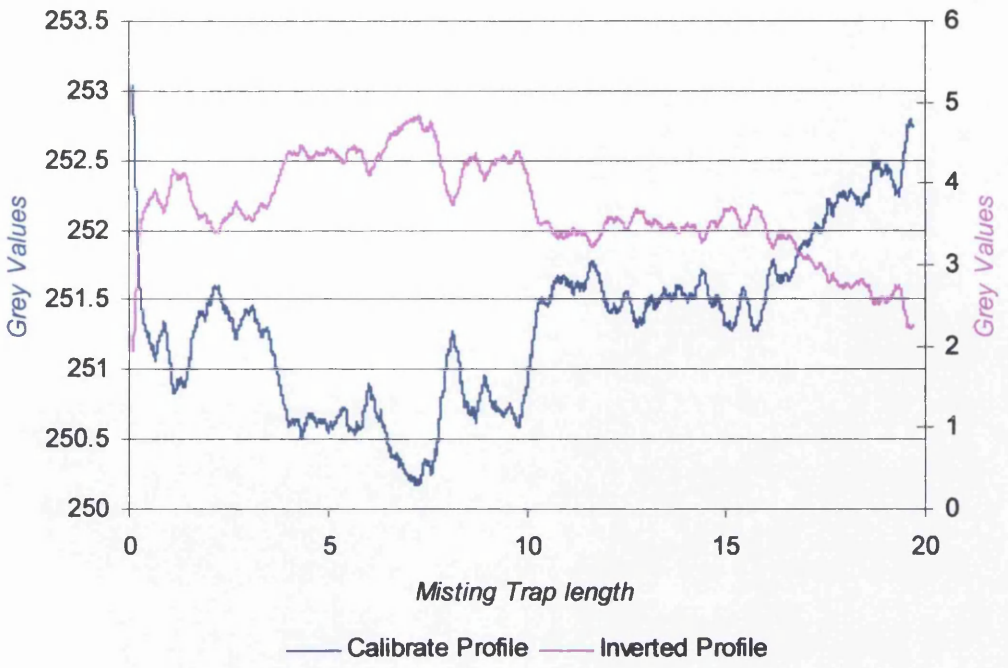

Figure 7-8 The calibrate profile values were inverted in order to illustrate the actual areas that misting appeared. The inversion was important because scan calculates the inked areas as zero value (no light) and the paper surfaces close to 255 as presence of light.

The droplets area and distribution were also calculated. The images were transformed into an 8-bit image that generated high contrast between substrate and droplets. Intensity threshold was used to adjust the grey levels that belong to the ink. This highlighted the ink droplets and eliminated the substrate grey values. The analysis summarises coverage area, number of droplets and average droplet surface. The images were analysed by the particles analysis macro of the ImageJ software.

White light interferometer was used to examine droplets area range. The substrate quality did not absorb the ink droplets due to high viscosity. A negligible part of the ink carrier can be absorbed by the substrate but is insignificant as found by the measurements. The ink droplets generated a sculpture image on the smooth surface of the misting trap. This allowed a surface measurement of the misting trap in order to achieve more three dimensions information about the droplets that consisted misting (Figure 7-9). The misting trap was examined by using VSI mode (Vertical Scanning Interferometry). This allows measurements of the droplets on the paper surface of the misting trap. The low volume droplets (less than 20μm) were of the same scale as the substrate roughness. However, the higher volume droplets (more

than 20μm) were easily located and calculated by a single interferometry scanning process.

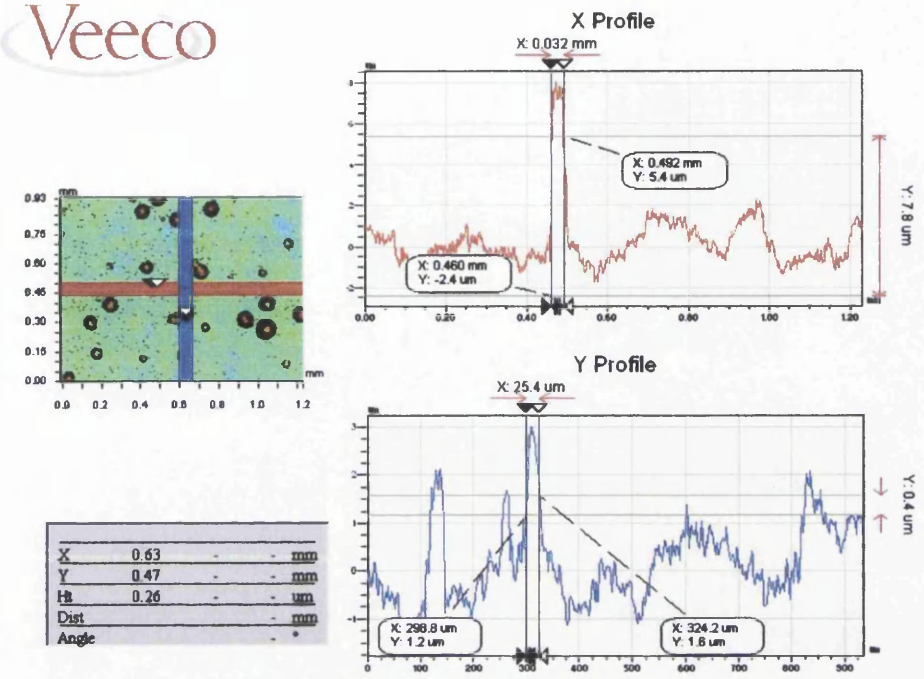

Figure 7-9 Surface analysis of ink droplets on misting trap using white light interferometer. The paper surface is consisted by areas with morphology between 20μm, as a result droplets less than 20μm are conflicted by the surface roughness to due to surface- ink immobilisation.

7.3 Results on misting analysis

Misting was examined under a series of parameters on the IGT Tack tester. These included the viscosity, ink film thickness, distribution speed and system temperature. The analyses attempted to establish the relations between misting rates with the ink film thickness along the rollers of a distribution system at the nip exit.

7.3.1 Parameters

Misting is a phenomenon related with the ink film thickness. Thus, ink film thickness is a parameter studied to identify a relation with misting mechanism. Printing speed is also an important parameter in such studies. The inking roller trains rotate by friction and this increases system temperature. The temperature affects the rheological characteristics of ink. Finally, roller surface qualities and geometries vary through out the roller trains. All these parameters compose the complex mechanism

of the ink distribution system with respect to distribution time or the time where the ink circulates through the rollers train.

7.3.1.1 Rheological properties effect

Butyl-Diglycol concentration decreases viscoelasticity, tack and surface tension of the ink. Misting results indicate that ink misting increases with the increase of Butyl-Diglycol concentration. The ink dilution range with Butyl-Diglycol indicates an increase of the misting effects with concentration. Figure 7-10 illustrates average densities of the flat misting trap (as described in Section 7.2.1 and Figure 7-1) with variation in Butyl-Diglycol concentration in the ink. The trap surface density of misting increases significantly after 2% dilution and dominates at 10% dilution. The lower concentrations do not indicate critical misting rates especially at low speed. Finally, the 20% dilution decreases in comparison with the 10% dilution which dominates statistically to the misting levels. This was established as colour density variation that was affected by the current analysis. Further examination on misting demonstrates that 20% dilution generates significantly higher misting effects.

The misting was varied by the direction axes of the nip. Misting densities were increased at the tangential direction of the motor roller away of the nip and decreased at the vertical axis of the nip exit (Figure 7-11). The misting trap was located under the nip exit between the metallic roller and rubber oscillator (Figure 7-12) as described also in Section 7.2.1.

7.3.1.2 Ink film thickness effect

The misting was examined between two ink film thicknesses these of 3.9mμ and 7.8 mμ. Misting increased significantly with ink film thickness as was also found by Blayo et al (1998). The ink film thickness effect increases with concentration and rises from 10% for low concentrations to almost 200% compared with the neat ink (Figure 7-13). Low concentration up to 1% indicated a slight increase with double the ink film thickness. When concentration increases from 2% to 20%, the difference gradually increases the misting effect from 50% to 100%. The dilution with 10% Butyl-Diglycol dominates the effect of ink film thickness. The low ink film thickness

such 3.9mμ indicates a lower effect with concentration than the 7.8 mμ as was expected. A significant decrease is indicated by 20% dilution where misting density drops almost 30% in comparison with the lower concentration sample this of 10% dilution which explained as colour density variation of the dilution.

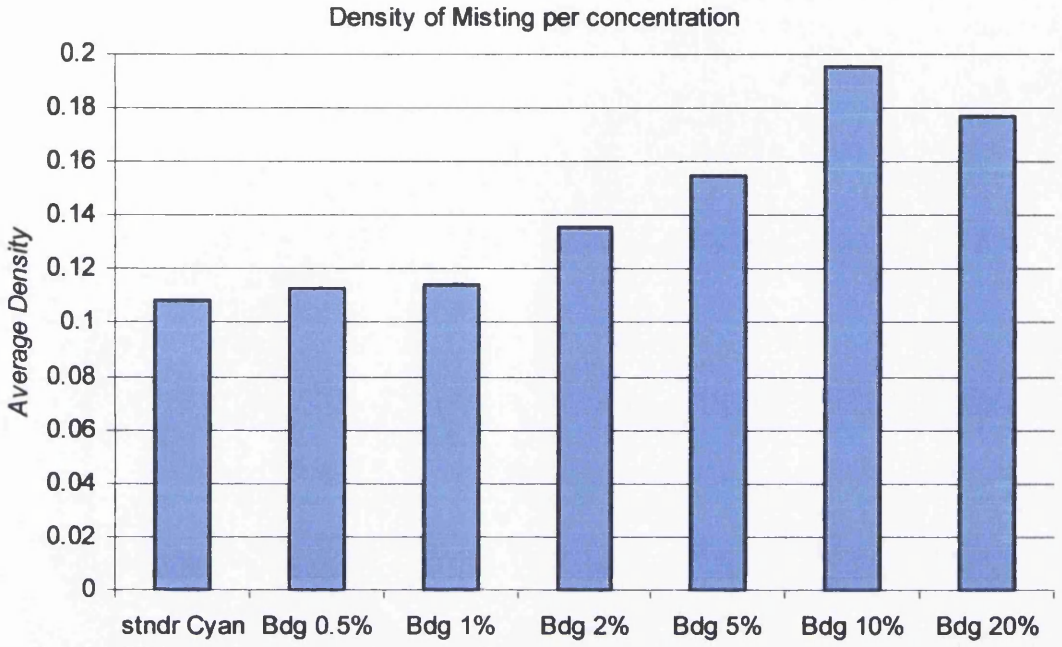

Figure 7-10 Average densities of misting effects on misting trap by ink samples with variation in concentration of Butyl-Diglycol.

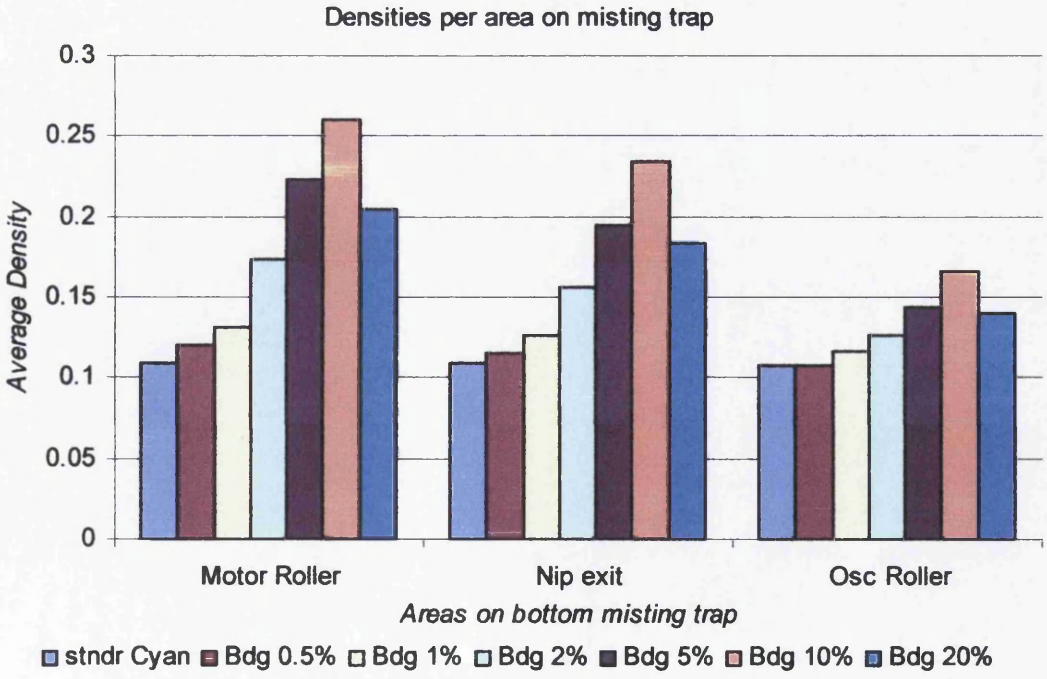

Figure 7-11 Misting increases at the back side of the trap where motor roller is and decreases at the nip exit.

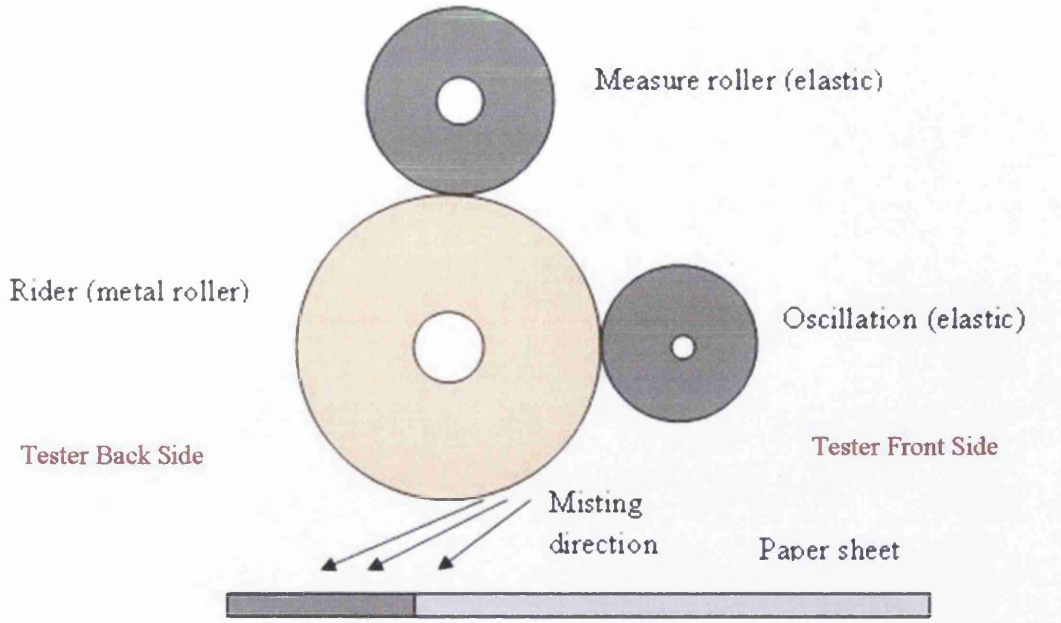

Figure 7-12 The misting increases at the tangential direction of the metallic roller away of the nip exit.

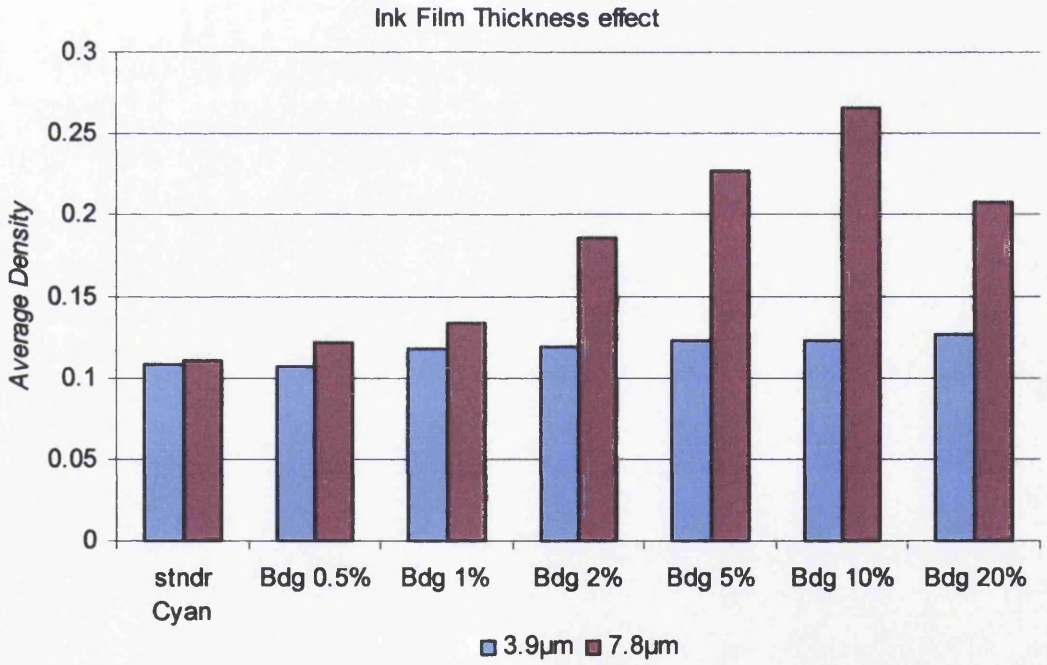

Figure 7-13 Misting effects according to variations in ink film thickness and concentration.

7.3.1.3 Distribution speed effect

Misting is affected by distribution speed. There is a significant increase between low, medium and high speed, especially with decreased viscosity. Distribution speed does

not increase significant misting of high viscosity fluids (less than 2% dilution) at low ink film thickness (Figure 7-14). The difference is very low between 5% to 10% dilution especially in speeds between 50m/min to 150m/min. It becomes critical with 20% dilution and the higher speed of 450m/min even with 3.9 mμ ink film thickness

7.3.1.4 Distribution time effect

The distribution time effect was evaluated by changing of the misting trap every minute for three minutes. The misting rates decrease through distribution time due to ink loss of the system. Misting density decreases per minute because ink film thickness decreases across time. This effect is significant with increased dilution of 20% Butyl-Diglycol at high speed of 450m/min (7.2m/s) (Figure 7-15). The decreased viscosity of the ink at high speed produces misting rates that decrease rapidly the ink film thickness on the rollers. Misting generates ink loss from the roller system thus the decrease in misting may be attributed to a decrease in ink film thickness. The low concentration samples do not indicate significant variability on misting with distribution time. This is because the amount of ink loss is negligible through time especially when low distribution speed is applied on the system.

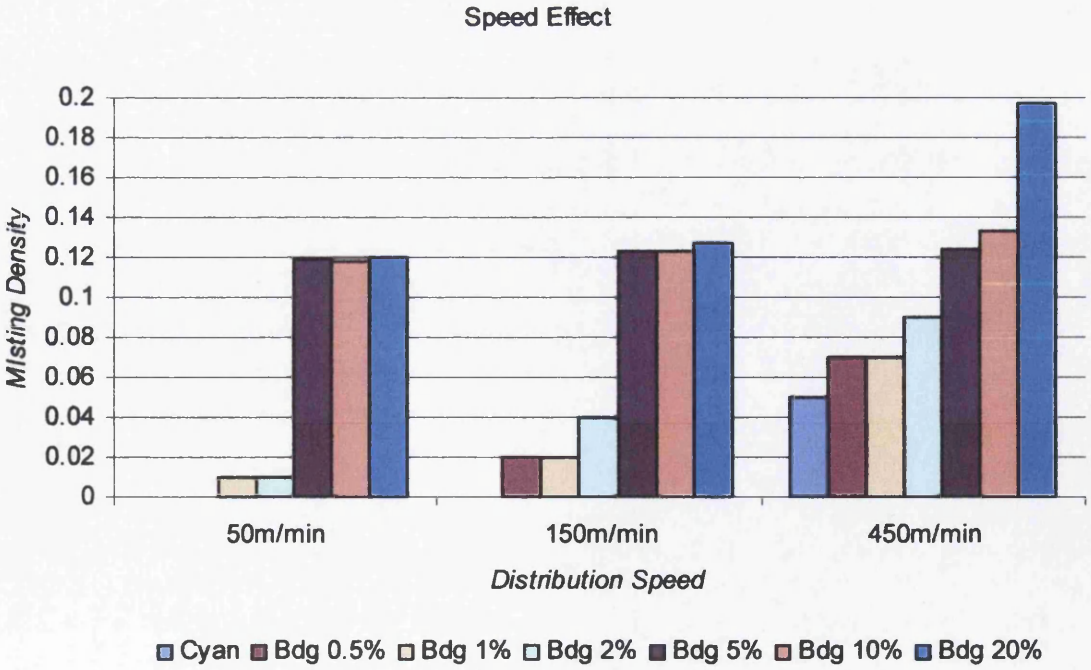

Figure 7-14 Misting effect variation by speed increase and concentration of Butyl-Diglycol.

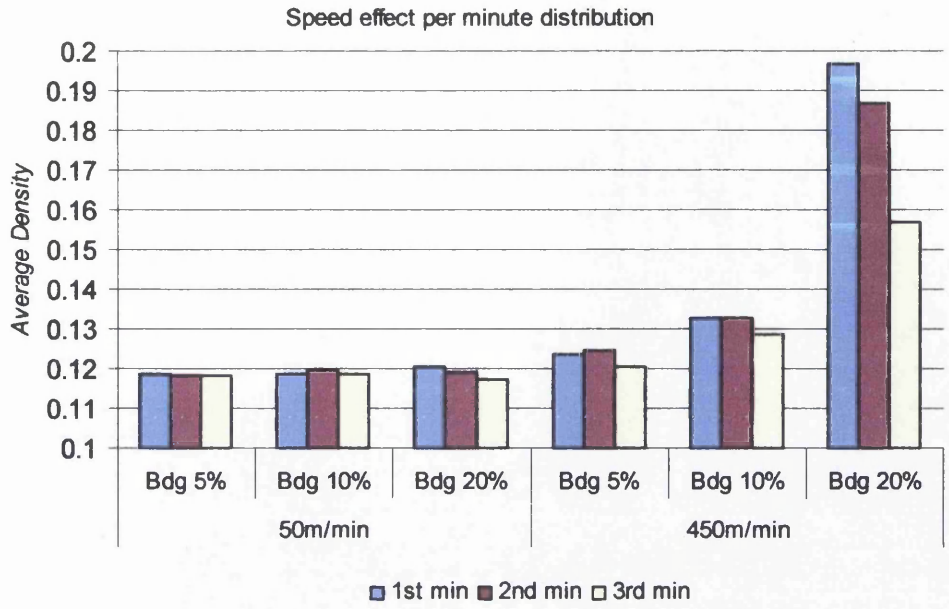

Figure 7-15 Misting effect decreases through time and this is higher with increase in dilution and speed.

7.3.1.5 Temperature effect

The temperature was changed on the system by an external cooling unit that supplies water through the drum of the motor roller. The system was described in Chapter 5 through the tack tester configuration. The rise of temperature increases the misting rates while the viscosity is reduced as found in Chapter 4 and also was reported by Fuchs et al (1991). The thin ink film thickness does not show significant variations especially when the viscosity is kept higher than 17.2 Pas (below 2% Butyl-Diglycol concentration). The misting varies slightly with time and this effect increases with decrease in viscosity due to rise of dilution and temperature (Figure 7-16).

7.3.1.6 Effects of rollers properties

Misting increases at the bottom area of the rollers where the misting trap is located and significant away from the nip exit (Figure 7-12). Profile analysis of misting trap indicates that misting increases on the motor roller side (Figure 7-17). The geometry of the misting profile does not change with decrease in viscosity. The misting significant varies between the two rollers sides at the nip exit. However, the misting profile does not show significant variations parallel to the direction of the rollers and nip.

The misting trap topographic analysis was created by plotting the ΔE L, a, b values to visualise the misting and highlight the misting direction (Figure 7-18). Misting spreading dominates at the motor roller area compared to the oscillator area. The effect is independent of film thickness. Ink samples of different dilution indicate similar results. Figure 7-6 illustrated topographic plots for each sample by dilution. The topographies are plot by variation in density range in order to visualise similarities on misting effects. Low misting effects do not generate significant misting images such as the neat Cyan ink. The misting decreases slightly with the distribution time. However, the misting samples do not exhibit significant variations in misting spreading and directions through 3 minutes distribution time. Figure 7-19 illustrates high resolution topographic analysis for 20% dilution sample per minute for the first 3 minutes distribution with 450m/min distribution speed. The tangential area of the motor roller area dominates the misting effects compared with the oscillator area at the bottom of Figure 7-19.

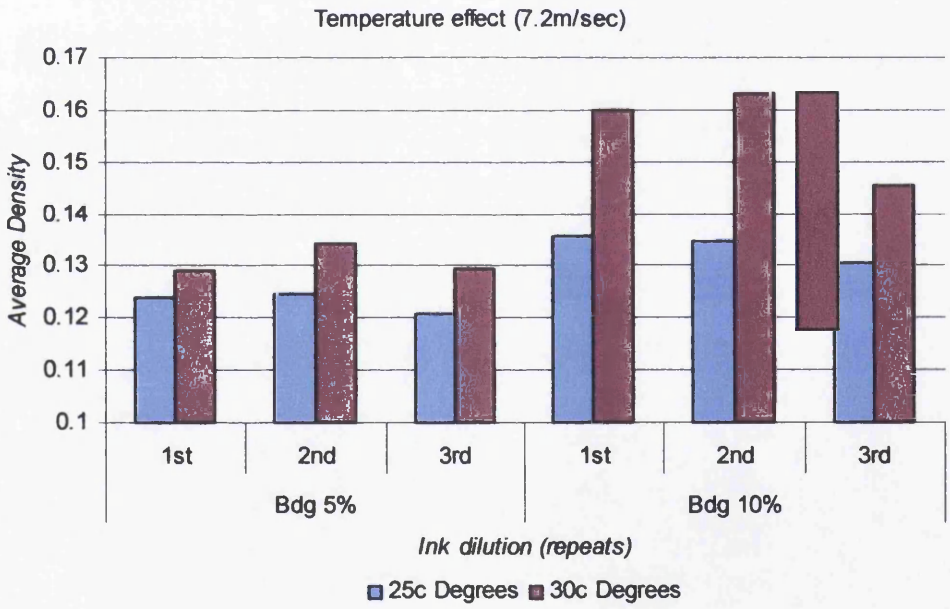

Figure 7-16 Misting increases with viscosity decrease. The misting effect of temperature increases as the viscosity decreases.

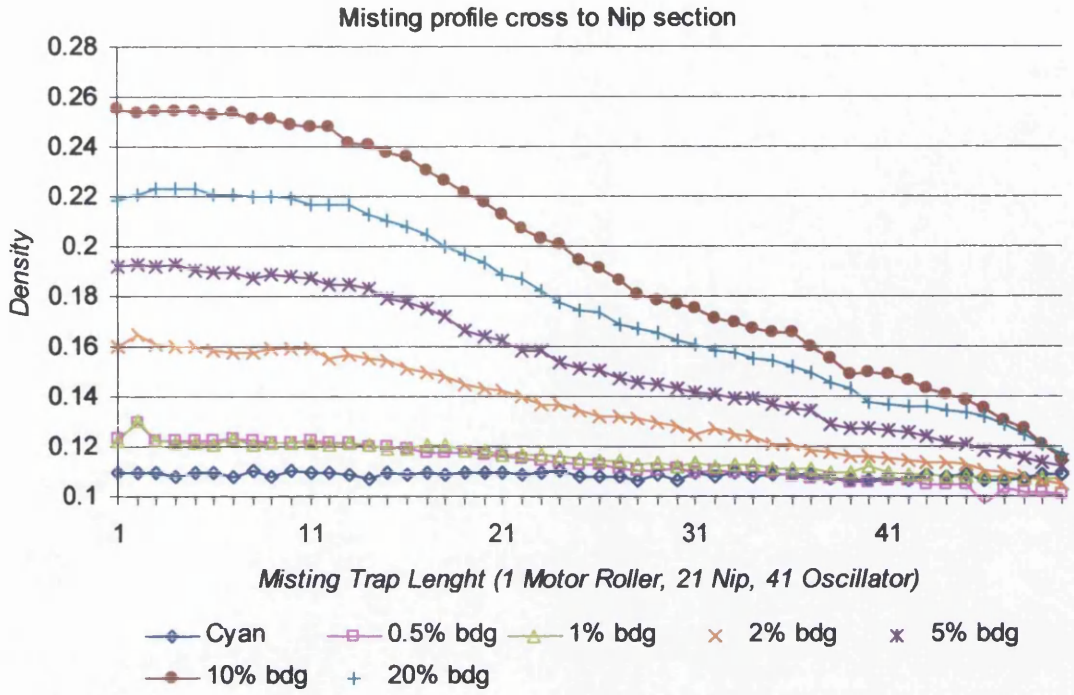

Figure 7-17 Misting profile cross to nip direction indicates increased misting effect to the motor roller area on the left of the nip on the graph. The misting effect increases with the decrease in viscosity after ink dilution with Butyl-Diglycol (%bdg).

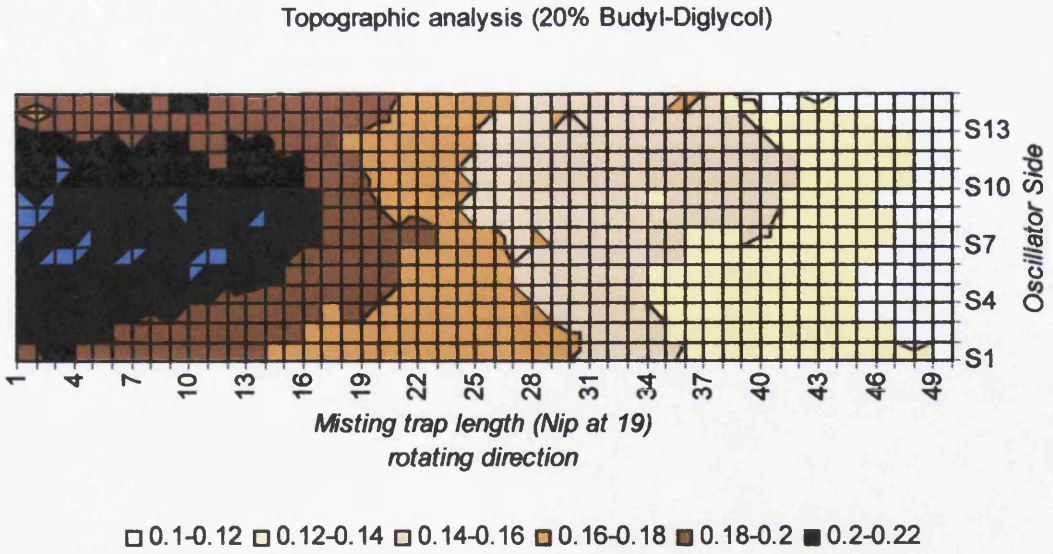

Figure 7-18 Topographic analysis is plotted by single density measurements on the misting trap surface. It illustrates the variation between the two sides of the nip where left is the motor roller and right the oscillator.

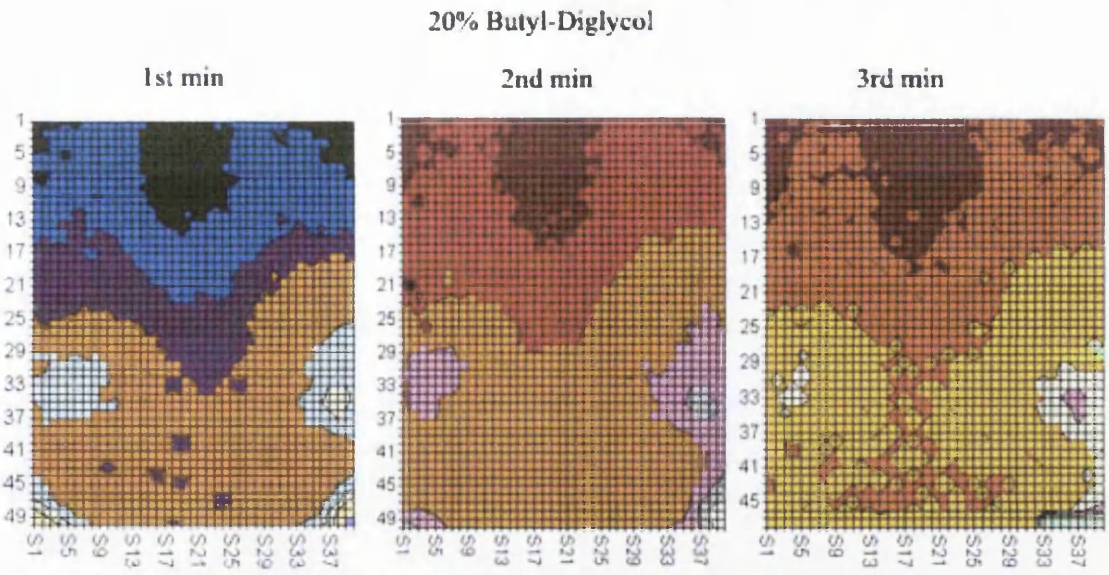

Figure 7-19 Surface analysis of the misting trap. Nip at 21, Motor roller area on top. The left misting surface analysis shows that misting is higher in regards with the second minute at the middle image. The effect is decreased also at the 3rd minute on the right image. The misting droplets are similar on spreading trends through distribution time.

7.3.2 Misting profile and characterisation

Misting produced no smaller droplets than a range from 4.5μm^2 to 7μm^2 dependent on the dilutions as were measured by surface measurements with the white light interferometer. The decrease in viscosity increases the average droplet area on the misting trap to 130μm^2. The overlapping effect is possible but was not monitored at real time and as a result was not determined. The misting determined at minute intervals was consisted with those obtained with the longer tests of 3 minutes. There is evidence that increased droplet area occur to overlapping phenomenon of droplets. High volume droplets appear to be generated by lateral flow and not from distribution along the rollers (Figure 7-20). This is because ink tends to flow laterally during rotation and this effect increases with oscillator roller.

Oscillation frequency provides high amplitude to the ink volume profile across the roller surface and generates symmetric misting phenomena across the rotating direction. Misting increases from the middle and sides of the roller due to oscillation mechanisms that increases ink film thickness on those areas. This was carried out after the misting test where ink uniformity examination along the rollers length was carried out by using the ribbing test. The ribbing generation showed a delay formation at those areas while ribbing was present at the areas between across the

roller length. That mechanism affects spreading rates and flow away angle due to tangential forces and gravitational effects. Droplet area does not significantly change with variations of the film thickness or the viscosity of the ink (Table 7-2). On the other hand distribution of droplets increases with ink film thickness or viscosity which also affects spreading and variations of droplets which is determined by analysis of the trapped misting.

Figure 7-20 The droplets size increases at the sides of the roller due to lateral flow of the ink distribution.

Table 7-2 Illustrative table of misting droplets analysis

Dilution	Count Croplets	Coverage Area	Aver.Size	Occurance
ND Cyan	93	0.59%	5.49E-03	1.69E+04
0.5%Bdg	117	1.28%	5.91E-03	1.98E+04
1%Bdg	213	1.40%	5.97E-03	3.57E+04
2%Bdg	1267	11.92%	7.63E-03	1.66E+05
5%Bdg	1127	6.79%	1.26E-02	8.96E+04
10%Bdg	2621	16.59%	1.28E-02	2.04E+05
20%Bdg	4086	27.99%	1.16E-02	3.53E+05

7.3.2.1 Droplets area

Droplets area was calculated by white light interferometer measurements. Droplet area does not vary significantly with ink film thickness between the lowest and the highest droplet area. The whole range of ink viscosities generates droplets between 4.5μm^2 to 130μm^2 on the misting trap. However, droplets less than 20μm in diameter are not visible or possible to be indentified due to surface roughness of the misting trap substrate. Substrate contrast allows grey values to be used to determine greatest range of droplets due to colour difference with the ink. Figure 7-21 illustrates a typical analysis for misting droplets. The occurrence describes the droplets average volume per number of droplets. The measurements of minimum volume do not indicate significant difference on misting effects but droplets of 4.5μm^2 dominate

across the length and width of the misting trap surface. Droplets maximum volume increases with decrease in viscosity (Figure 7-22). This also increases with ink film thickness but the effect becomes more significant with a decrease in viscosity. Decrease of viscoelasticity forces leads to shorter filaments with increase effects on satellite droplets due to high speed elongation of the ink body. The elongation rate is a function of speed ratio dependent on rollers size and rollers speed (Owens 2005). However, the misting is affected by the onset of ribbing that varies with number of parameters as has already been discussed in Chapters 6.

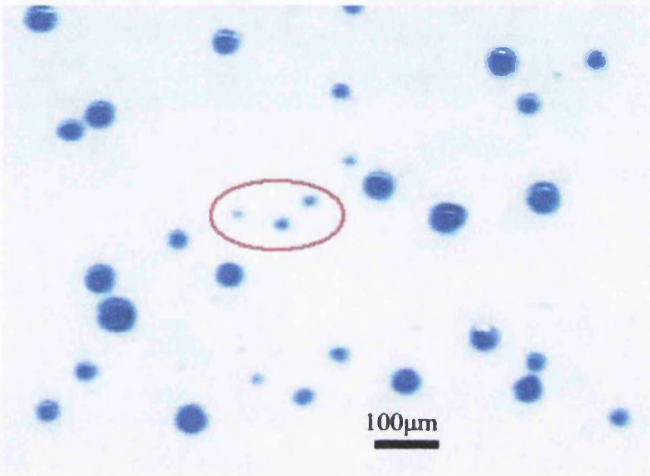

Figure 7-21 Tiny droplets less than 20µm are identified only by grey values difference between substrate and ink due to high contrast.

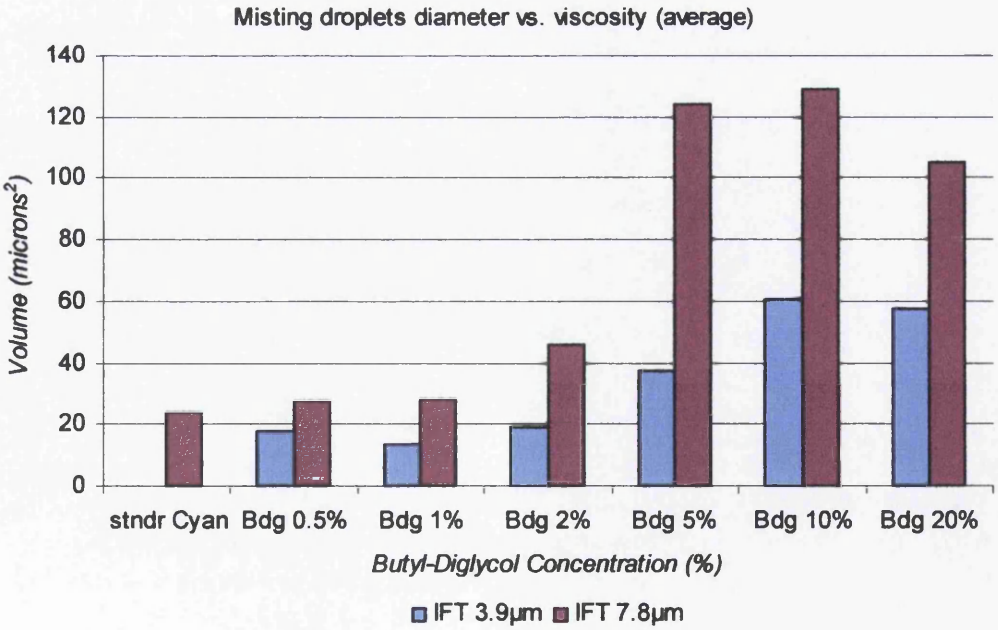

Figure 7-22 Average droplet diameter increases with decrease in viscosity. Increase of ink film thickness also increases droplets diameter where the effect is dominant when viscosity decreases.

The average area is affected by the number of droplets that is generated by misting. The results of average droplets size are affected by the dominated number of tiny droplets with random directions (turbulence). The results are affected by transit effects during ink distribution on the rollers. Droplets with higher volume are formed because of lateral flow at the rollers sides. The ink film thickness is also unstable during distribution with variations of ink film thickness on certain areas and as a result variations in filaments are formed which lead to variations of filaments width. The break-up instability forms higher or lower volume particles depenings on filaments thickness and length. This leads to form higher or lower volume droplets at the nip exit depending on ink film thickness, the roller's velocity and the separation angle at the nip exit. Droplet volume can increase at the nip exit with the increase of parameters such as speed and ink film thickness. Misting character shows an influence on viscosity, rollers ratio and seperation geometry of rollers nip with the axis of gravity. The Capillary number decreases with the Butyl-Diglycol concentration as a function of the viscosity versus the surface tension (Figure 7-23).

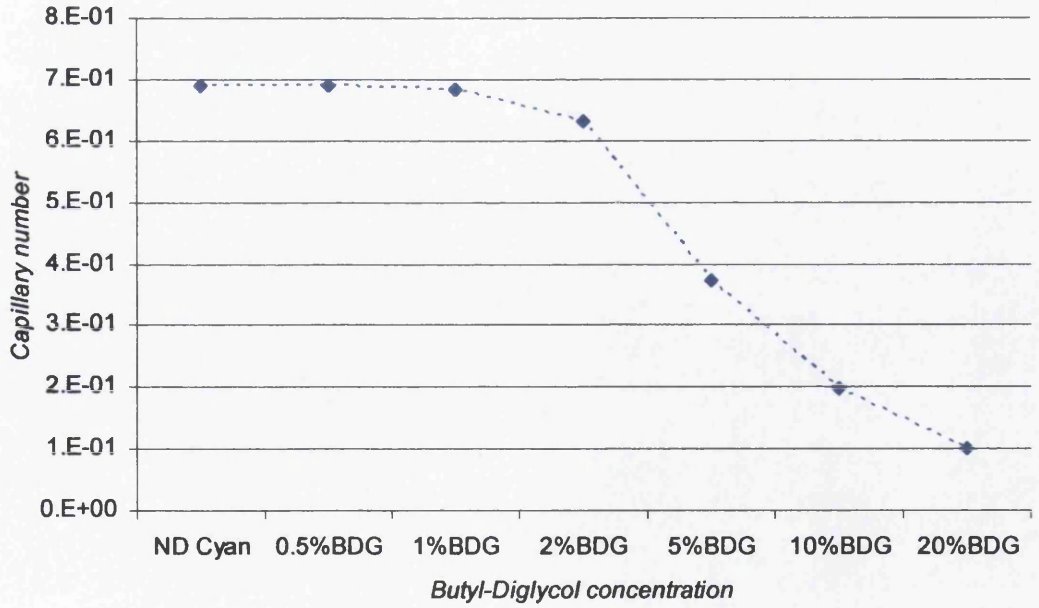

Figure 7-23 The decrease of the viscosity and surface tension indicates a decrease to Capillary number. This concludes that misting increases with the decrease in capillary number.

7.3.2.2 Droplets threshold variation

The range of the droplets variations comes to complete the misting profile of a fluid. The average area of droplets does not completely describe the misting effects due to variations as discussed. The average area is affected by the number of droplets variations. The standard deviation of droplets area determines the average difference between the droplets area variations. This describes also the range of droplets size that varies with the parameters such as fluid viscosity (Figure 7-24). The increase in ink film thickness allows more ink to flow away but this can be also affected by rollers velocity, viscosity and tack. Decrease in tack and viscoelasticity decreases dynamics of polymers network as found in chapter 5. Low ink film thickness can produce similar misting image with the rollers speed increase and tack decrease over a misting from higher ink film thickness but with lower velocity and higher tack. The increased misting affects high droplets area variations due to droplets overlapping on the misting trap. As a result, the variation of droplets size increases with the misting rates.

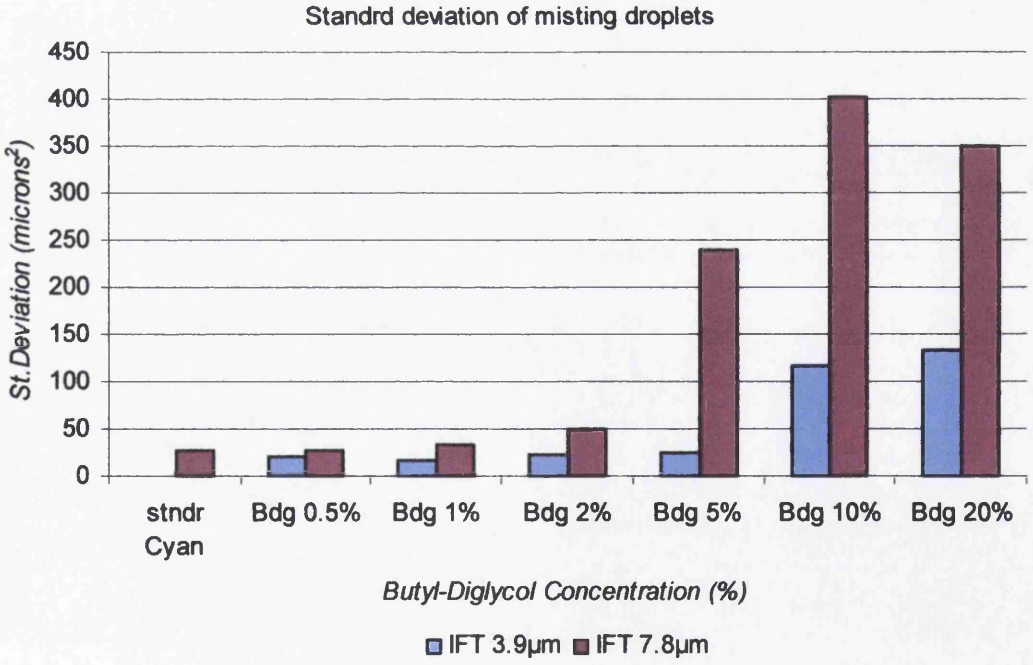

Figure 7-24 Standard deviation of the droplets surface area increases with the ink film thickness. Decrease in viscosity increases instabilities and so variations of droplets area.

7.3.2.3 Surface coverage

Misting droplets are expelled from the ink train and stick on the trap surface. The coverage area reflects the amount of misting generated. Misting gradually increases with decrease in viscosity. Increase Butyl-Diglycol concentration decreases viscosity but also increase transparency and as a result decreases optical density due to absorption and contrast with the substrate colour. Misting coverage area varies due to ink film thickness instabilities along the rollers length as Section 7.3.1.6 described. The measured densities in Figure 7-25 shows misting trap topography across the width compared to the nip profile. The coverage area calculation depends on selective measuring area of the misting trap. The misting increases significantly at the back side of the misting trap where motor roller was located. Coverage area is carried out by the droplets density along the width and the length (full profile) of the misting trap.

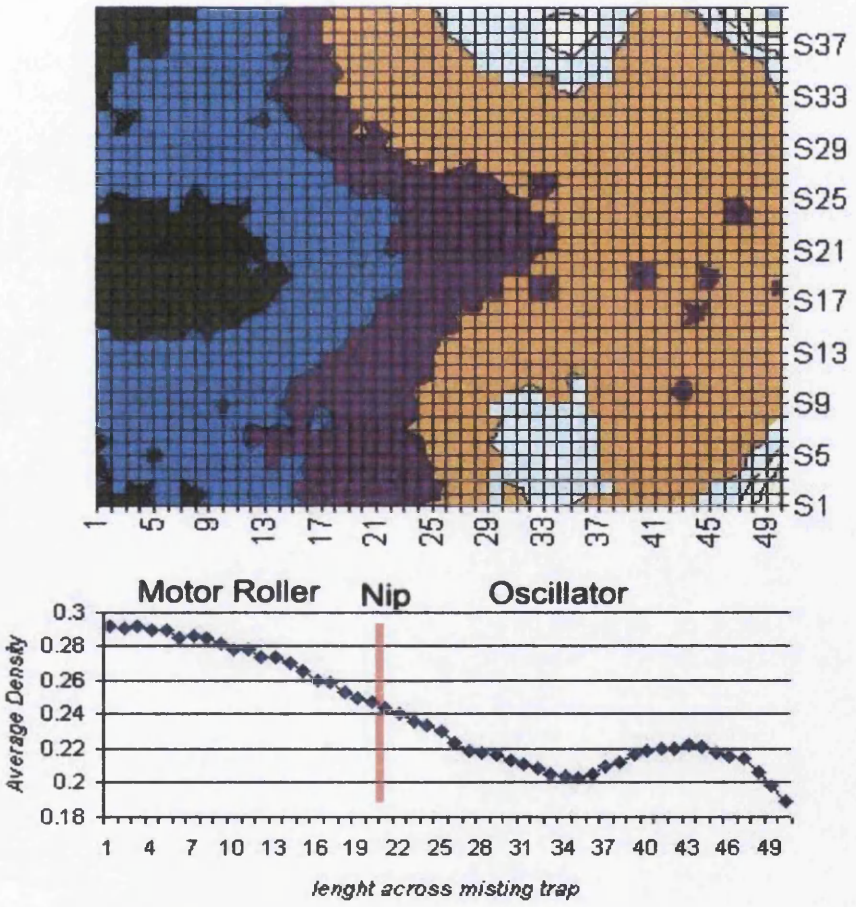

Figure 7-25 Misting coverage area varies across the rollers length and width of the nip. Siignificant increase is illustrated under the metallic roller. The top picture illustrates the areas that misting is increased at the left side which also is the back side of the under the mettalic roller. The bottom graph also indicates the areas on cross direction graph which highlights the misting between the motor side roller (metallic), the nip and the oscillator side.

The flat misting trap was located in front of the nip exit between motor roller and oscillator at the surface of the tack tester. This is also the most accurate capturing configuration for the system where the misting effects increases. Surface coverage increases with decrease in viscosity and tack which as a result increases misting effects (Figure 7-26). More misting droplets generate higher coverage area depends on number and volume of droplets which is described below.

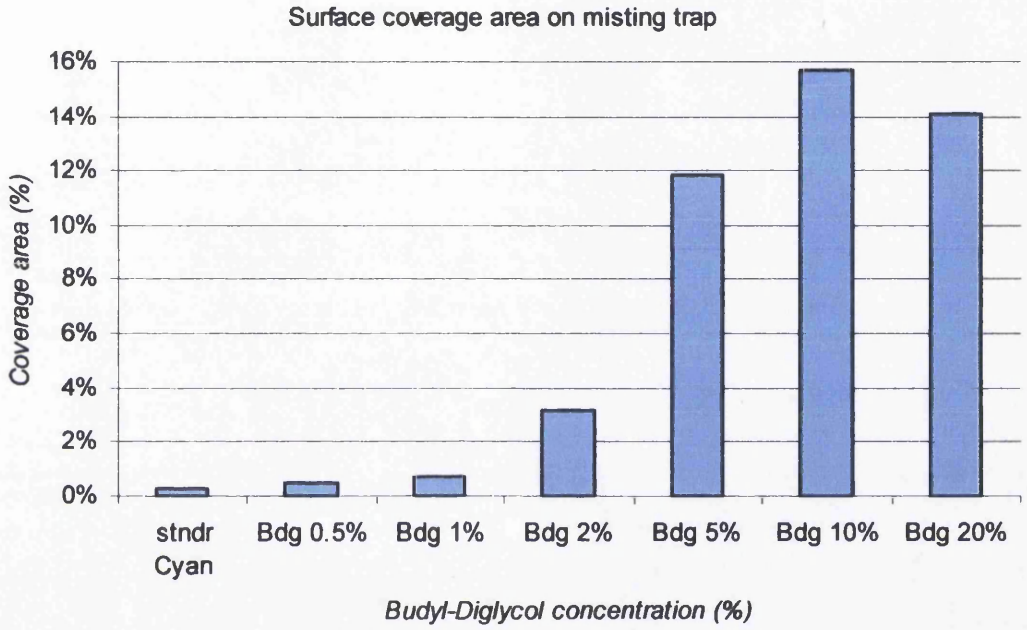

Figure 7-26 The misting coverage area on the trap surface increases with decrease in viscosity.

7.3.2.4 Spreading (droplets quantity)

The misting droplets' spreading describes the number of droplets that spread along the directions of the misting trap. It increases with decrease in viscosity and tack (Figure 7-27). The effect gradually increases as the viscosity decreases. Concentration of 2% Butyl-Diglycol produces the largest difference compared with lower concentrations. This effect continuously increases and 5% generates the double amount of droplets with the same ink film thickness of 7.8mμ as shown in section 7.3.1.2. The concentration of 20% Butyl-Diglycol decreases droplets number in compare with 10% dilution due to significant decrease in viscosity. This increases absorption by the porous surface of the misting trap. The decrease of viscosity also

increases transparency and decreases image contrast of the misting trap. As a result, the analysis shows a lower number of droplets while the misting effect is significantly higher as an image on the misting trap (figure 7-5).

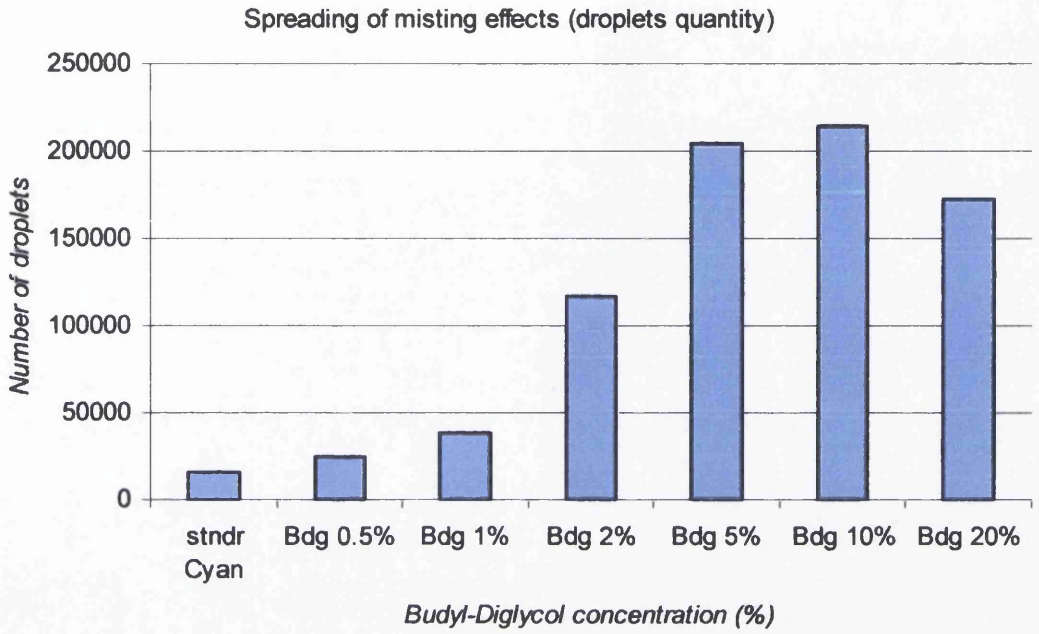

Figure 7-27 Number of droplets increases with misting effects and decrease of viscosity.

7.3.2.5 Misting effect

The misting effect was calculated as a function of the misting characteristics. The misting occurrence was the number of droplets versus the average droplets area. Finally, the misting effect was calculated as the ratio of occurrence to the characteristic viscosity of the ink dilution.

Misting effect = $(Nd/Sv)/\eta^*$ (40)

Figure 7-28 illustrates the misting effect in comparison with the average size of droplets. The calculation of the misting effect demonstrates higher accuracy than the individual characteristics such the droplets area and the number of droplets.

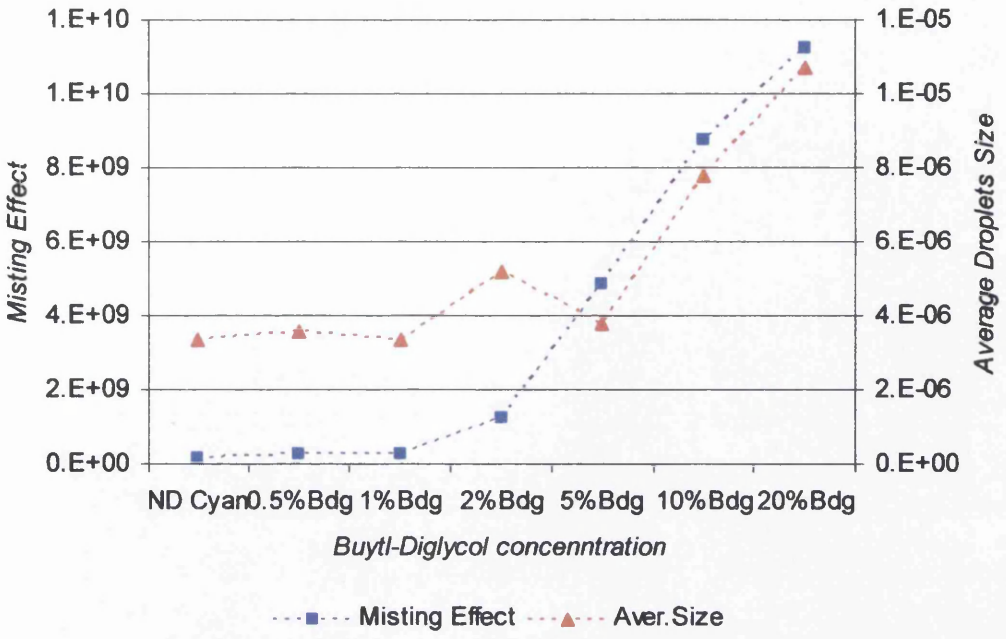

Figure 7-28 The calculation of the misting effect illustrates higher accuracy than the indivudual misting characteristics such as the average droplets size.

7.4 Discussion

Misting was examined as the dynamic fingerprint of the ink profile and ink film thickness variations along the distribution rollers. Misting is strongly related with ink film thickness. Misting increases with distribution speed and tensile forces which generates instabilities leading to filaments failure and formation of satellite droplets. Higher volume droplets are also formed by the filaments viscoelastic deformation during filaments rupture where ink ligaments fly away due to tangential forces.

The misting increases with increased ink film thickness and decreased viscosity. The number of misting droplets also increases with the viscosity decrease and surface tension. This indicates an effect of capillary number which decreases with Butyl-Diglycol concentration (Figure 7-29). The capillary number was suggested by Owens (2005) to affect misting. The results of the current work reported in this chapter indicate that the misting becomes critical as the Capillary number is reduced. The ink filaments split unequally (or the one side split first) and aggregated ink parts are forced to extend and finally to flow away due to centrifugal forces. Decrease in surface tension and viscoelasticity decreases capillary number and the adhesive dynamics with tack. Capillary number determines an inverse relationship with

misting rates. As a result, misting increase with the rollers velocity and the decrease of the dynamics in polymers network. The instability of misting is affected by extreme changes of the ink transfer mechanisms parameters such as distribution speed, temperature, ink volume, rollers surface qualities and rollers ratio (separation angle).

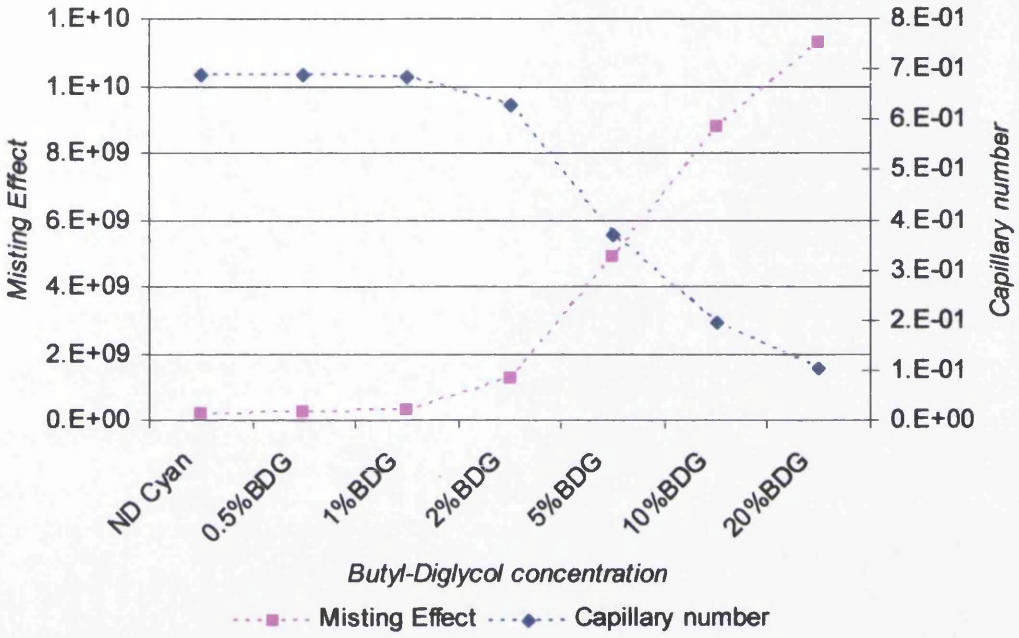

Figure 7-29 Butyl-Diglycol concentration decreases capillary number. The misting effect increases with the decrease of capillary number. This indicates an inverse relationship between misting and capillary number.

The decrease in viscosity leads the lower speed to generate similar misting rates to the higher viscosity fluid at higher speed. Misting is a ratio of the speed versus viscosity or tack and ink film thickness. The distribution speed increase affects filaments uniformity. The filaments generate aggregate parts through the filaments length and split is not symmetric. The ink filaments are deformed by the elongation mechanisms at the nip exit and undergo viscoelastic deformation. The deformed filaments are forced to follow tangential forces and generate higher droplets size away from the nip exit. The reduction in viscosity decreases tack as described in chapter 4 and forces a higher volume of ink to flow away and so larger droplets are formed on the substrate due to increased ink thickness that show higher colour densities. There are possibilities for overlapping effects but was not possible for real

time measurements at the current work. Although, some overlapping was confirmed by ellipsoidal droplets however they were not calculated.

The rollers ratio affects misting due to changes of the separation angle at the nip exit. Carvalho (1996) stated that the film thickness ratio is proportional to the roll speed ratio. The results of the current experimental work indicate independent split ratio with the rollers ratio which is close to 0.5 in line with the findings of MacPhee 1998). Owens (2005) developed the misting number which increases with extensional rate as a function of roll size, rollers ratio, speed ratio and position along the roller surface with a constant value for ribbing. However, the misting number gives an average prediction and does not refer to specific areas of roller or any variation of adhesive dynamics according to ink film thickness. As a result, the misting number becomes a different expression of the capillary number which is static and not dynamic. The ribbing patterns are responsible for filaments formation as seen in the Chapter 6. The misting effect increases with inversed relationship with the capillary number.

The oscillator randomises these patterns but the frequency forms ink volume variation across the roller length in high amplitude wave-like profile (Figure 7-30). The misting wave patterns are affected by oscillation mechanisms which forces the ink volume to be transferred along the surface of the roller during distribution process. This mechanism forms this wave-like ink film thickness profile which increases ink volume at the middle and sides of the roller. As a result, misting increase or decrease is affected by this pattern which increase or decrease by oscillation frequency mechanism. The wave like profile causes the ink split to vary across the length and rotational direction of the roller. The droplets increase at the areas where the ink film thickness temporarily increases similarly to the ribbing patterns. The oscillator forces the ink to a lateral flow due to centrifugal forces. The oscillation mechanisms not only increase this flow but also trap an increased amount of ink at the roller's centre area.

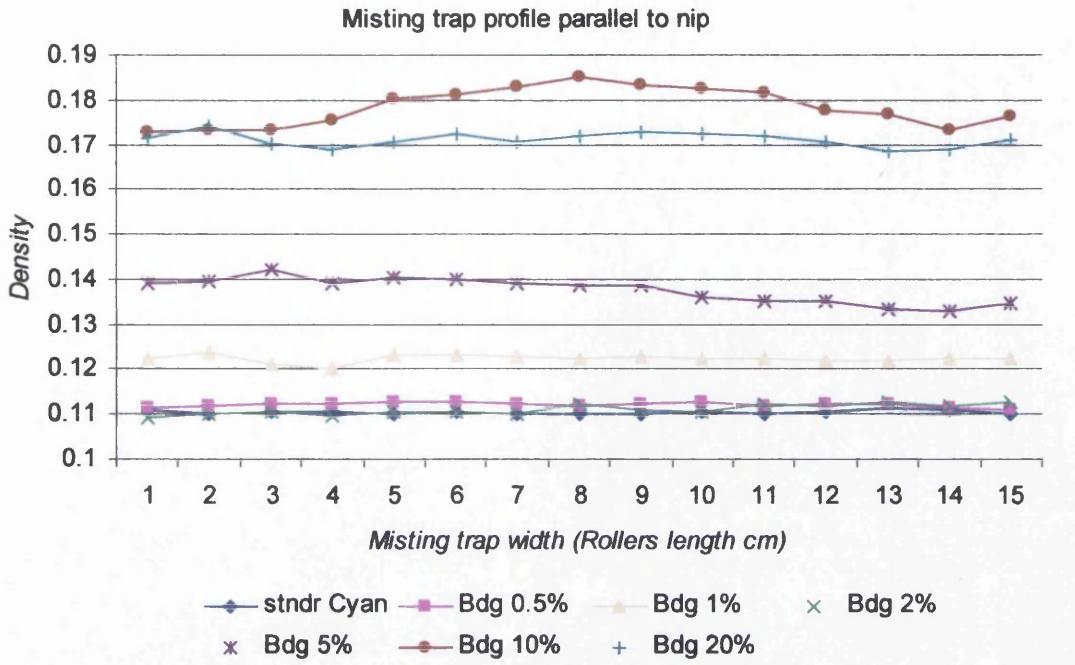

Figure 7-30 Misting profile does indicate significant variations parallel to nip exit. A slight wave shape increase dominates with increase in dilution.

Chou (1997) reported that the period of the variation along the nip increases with the frequency of the oscillation with increase effect of lateral flow. However, the results of the present study show the opposite effect in that ink film thickness period decreases with increase of oscillation frequency although show the same tendency for the ink to flow laterally. The disagreement can be attributed to the configuration of the distribution systems between the closed distribution system of the current work and the printing distribution system of Chou (1997). In his work ghosting had a major influence that does not occur in the current work. The ghosting is the ink transfer instability due to the printing image of the printing press. The ink that transfers to the paper generates a negative image on the rollers with lower ink film thickness due to outgoing ink. The incoming ink generates areas with lower or higher ink film thickness that does not register or overlap with the image on the printing plate. As a result the plate carries ink with different ink film thickness across the width and the length of the image. This generation of these negatives areas on the rollers named "ghosting" because of the ghost image on the rollers.

Changes in oscillation frequency do not significantly change misting spreading tends with the rotation direction although results indicate an influence on ink film

thickness uniformity. Figure 7-31 illustrates the topographic analysis of misting trap with changes in oscillation frequency. The symmetric misting occurs with high frequencies while low frequencies result in asymmetric misting along the rollers length. This is due to the non uniform ink distribution on the rollers. The misting variations occur due to the variation of ink volume on the rollers. Ink distribution is affected by transient effects. The total ink volume on the rollers decreases as ink is lost due to misting. As a result the system never reaches equilibrium and misting varies with the variations of ink film thickness at certain areas on the rollers. This was confirmed by long runs of 30 minutes. This was also significant for most of the trials especially at the highly diluted samples named 5%, 10% and 20% concentration of Butyl-Diglycol.

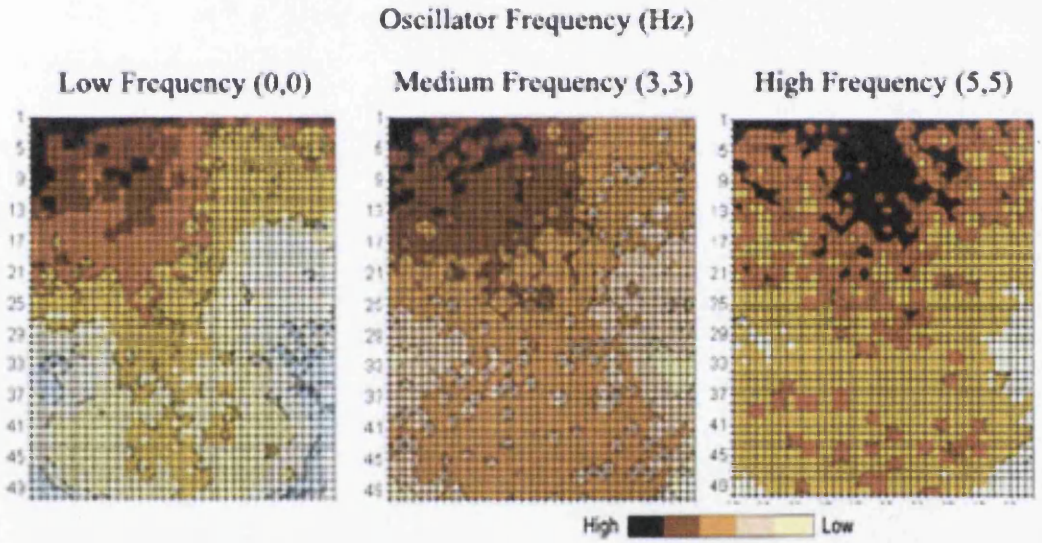

Figure 7-31 Misting effects over changes in oscillation frequency. The effect focuses more to ink distribution and not to spreading trends.

The ink film thickness instability is more visible with the increase of the ink film thickness. The increase dilution (lower viscosity) increases misting effects and a wave shape profile appears with an increase at the middle area as shown (Figure 7-30 and Figure 7-31). The decrease in viscosity increase misting and as a result certain areas with same wave ink profile generate more misting when ink viscosity decreases. Misting profile on the trap is affected by misting rates where higher densities are carried out that respond to increased ink volume across the roller length. This is verified when oscillation mechanism stops and ribbing patterns appear on the rollers (Figure 7-32). The onset of ribbing patterns is faster at the areas with lower

ink film thickness as found through the experiments on ribbing mechanisms. The ribbing image indicates high and low ink film thickness as it was discussed in details in Chapter 6.

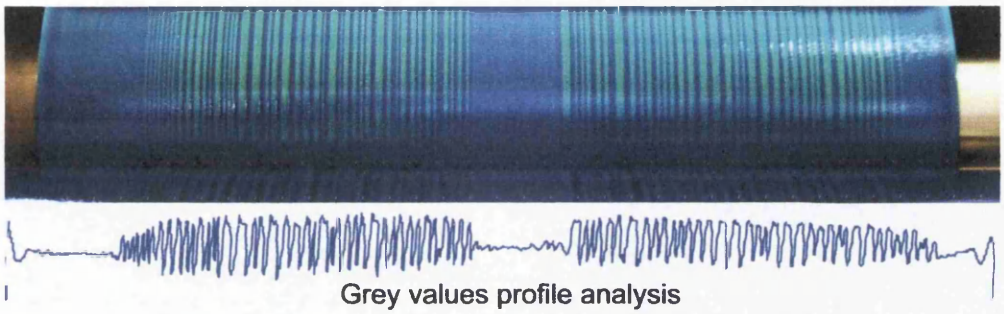

Figure 7-32 Ribbing formation on rollers and calculating ink profile according to grey values on the surface. It indicates the increased ink areas at the middle and sides of the rollers due to oscillation.

The high speed capturing showed that misting occurs due to the filaments multiple break-up (Figure 7-33) and inertial effects as reported also by others (Macphee 1998, Blayo 1998 and Owens 2005). High viscoelasticity and adhesive dynamics allow ink to extend in extremely thin filaments that break-up in multiple points across the length due to increased tensile forces as carried out by high speed video analysis and elongation tests on extension rheometer in chapter 5. The experiments in extensional rheometer showed that filaments thinning time decreases with the elongation speed. The elongation speed is proportional to the tensile forces and as a result filament thinning time decreases with tensile forces.

In additional tests it was found that the filaments split in multiple areas or unequally and form plastic deformable strings. Such results described in Chapter 5 based on extension rheometer tests. The aggregation occurs due to increased adhesive dynamics and surface tension of the polymers network as a function of the ink film thickness or filaments width and extension rate. Those aggregate parts generate instability at the ink filaments with increased volume at the filament's neck. The filaments split unequally at the thinner area of the filament and high volume ink remains on the free surface at the nip exit. It does not fly away at the nip exit because of the increased weight. The centrifugal forces increase at the aggregate parts and filaments once more formed and the break-up generates droplets of higher volume that fly away (Figure 7-34). Their direction is dependent on their volume and the

tangential velocity at the split point of the roller and the effect of gravity. The decrease in viscosity decreases the adhesive dynamics and filaments elongation rates but increase inertial effects of the fluid. As a result fewer droplets with higher volume are formed that interfere with the previous mechanism due to tangential forces.

Verification of those mechanisms was carried out by video capturing techniques on the distribution system and extensional rheometer. Figure 7-35 illustrates instability on filaments formation through high elongation speed of 0.6m/sec (3.6m/min) by using extensional rheometer. During elongation some thick filaments present a temporary plastic deformation and recovery is slow. The distribution systems use much higher rotational speeds and as a result separation speed increases splitting instability of filaments. The deformable ink filaments act like whips after the break-up and instantly generate forces that increase with tangential forces due to the rollers velocity and the deformed part is forced to flow away. Misting also increases by moving the rollers nip to the lower level which allows gravity to interfere with roller velocity at the nip exit. The rollers ratio affects ribbing patterns which affects filaments formation (this was discussed through chapter 6). The relationship between misting and ribbing is examined by using an orthogonal array experiments through the Chapter 8.

Increase in thickness increases tangential forces due to decrease of adhesive dynamics. It increases with decrease in viscosity. Butyl-Diglycol is transparent so concentration affects opacity of ink and 20% causes a significant decrease in pigments concentration and colour density. This affects density measurements that determined lower misting effect than 10% diluted ink. However, a dramatic increase of the 20% diluted ink was carried out by the droplets number and the coverage area of the misting trap.

There is a rheological and parametric threshold that generates significant misting phenomena that can be characterised by low viscoelasticity and tack on high speed distribution system. The results also agree with other studies which characterise the rise of misting by decrease of the Capillary number. In the current study the decrease

of the Capillary number was characterised by decrease in the viscosity and the surface tension.

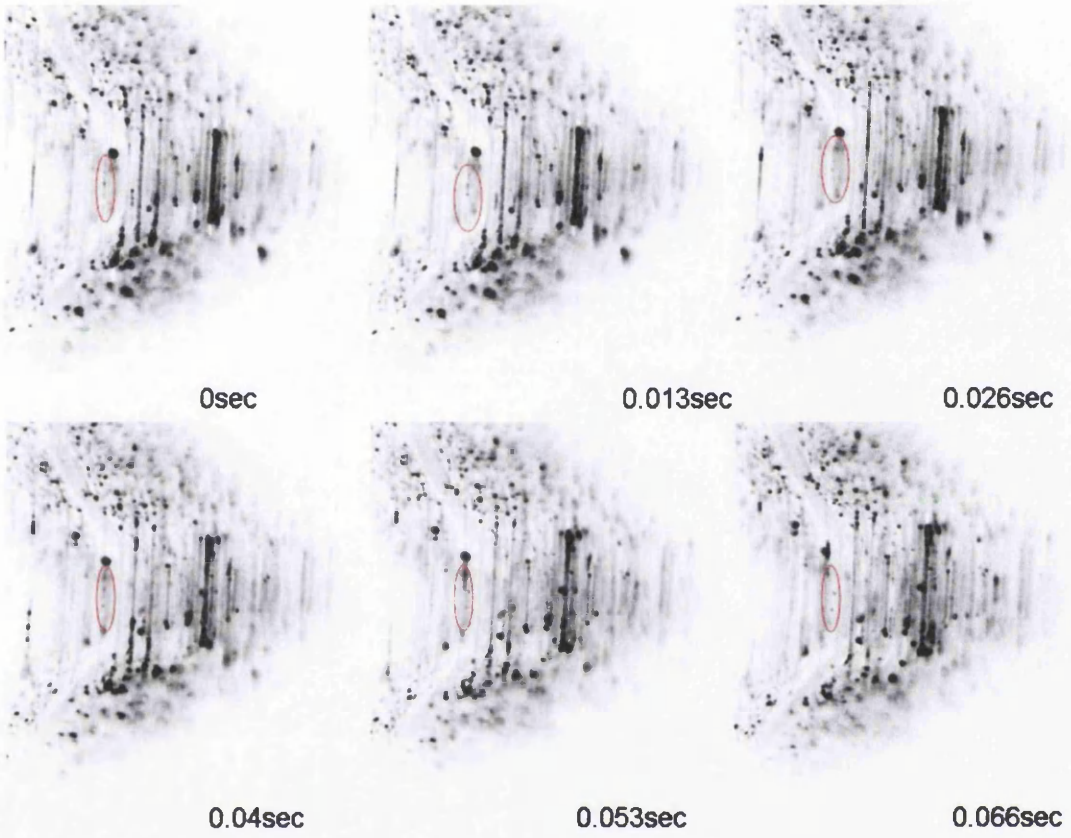

Figure 7-33 The tensile forces at the nip exit generate multiple break-up at the filaments that form satellite droplets. The negative images highlight the droplets due to light scattering during the recording (App. VCD V13).

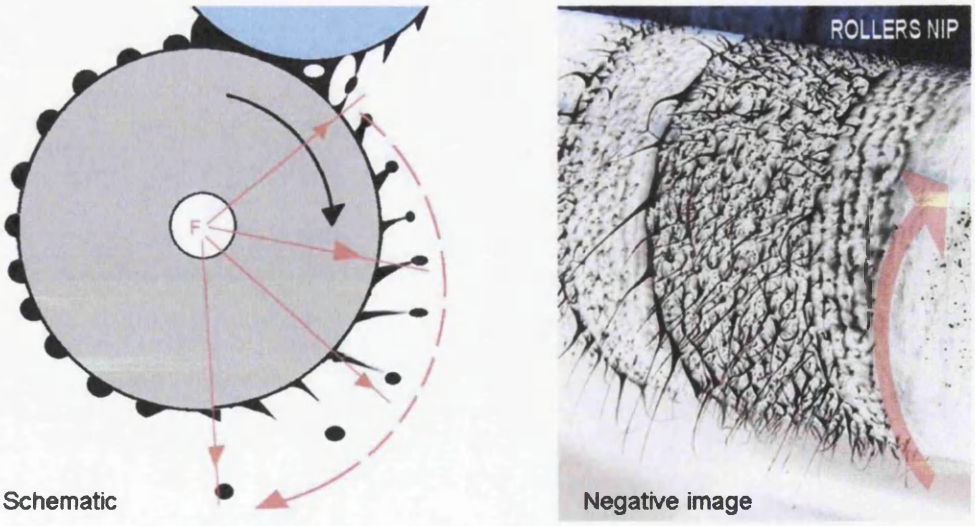

Figure 7-34 The aggregate part force the filament to split unequally and ink part with high volume remain at the free surface of the nip exit. The tangential velocity forces the ink part to fly away and filaments split once more away of the nip exit. The effect increases more with lateral flow of the rollers sides.

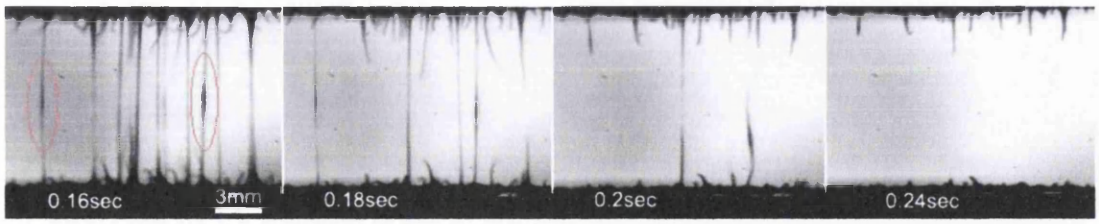

Figure 7-35 Elongation speed (0.6m/sec) generates instability to filaments formation. The ink is deformed not uniform and temporary generates plastic deformation to long filaments. The elasticity makes shorter filaments to act like whips during splitting (App. VCD V11).

The misting also fluctuates with roller surface quality and geometry that are responsible for misting directions (Figure 7-36). The roller surface effect was found out by additional tests on the IGT high speed inking unit. The configuration of the IGT High speed unit looks like the tack tester but with two metallic rollers and one elastic on top as illustrated in chapter 3. The test focused to estimate the effect of roller's configuration and the effect of the surface qualities. The misting analysis verified that the system configuration can affect the misting rates.

The results showed that the higher volume misting droplets were located at the tangential directions of the metallic rollers (rider and oscillator). The inking unit uses significantly lower diameter of metallic rollers with polished surface. The misting trap appeared also high misting effects at the bottom of the system. The surface quality of the roller affects the adhesive dynamics in respect to the capillary number which decreases as the surface tension and the shear viscosity decreases. The elastic roller's surface provides higher surface energy due to roughness of the surface instead of the chromium polish surface of the motor roller. The ink filament splits at the nip exit and continues to elongate due to tangential velocity. Finally, ink parts are forced to flow away and split once more and aboard the roller surface while follow tangential forces of the roller (Figure 7-37).

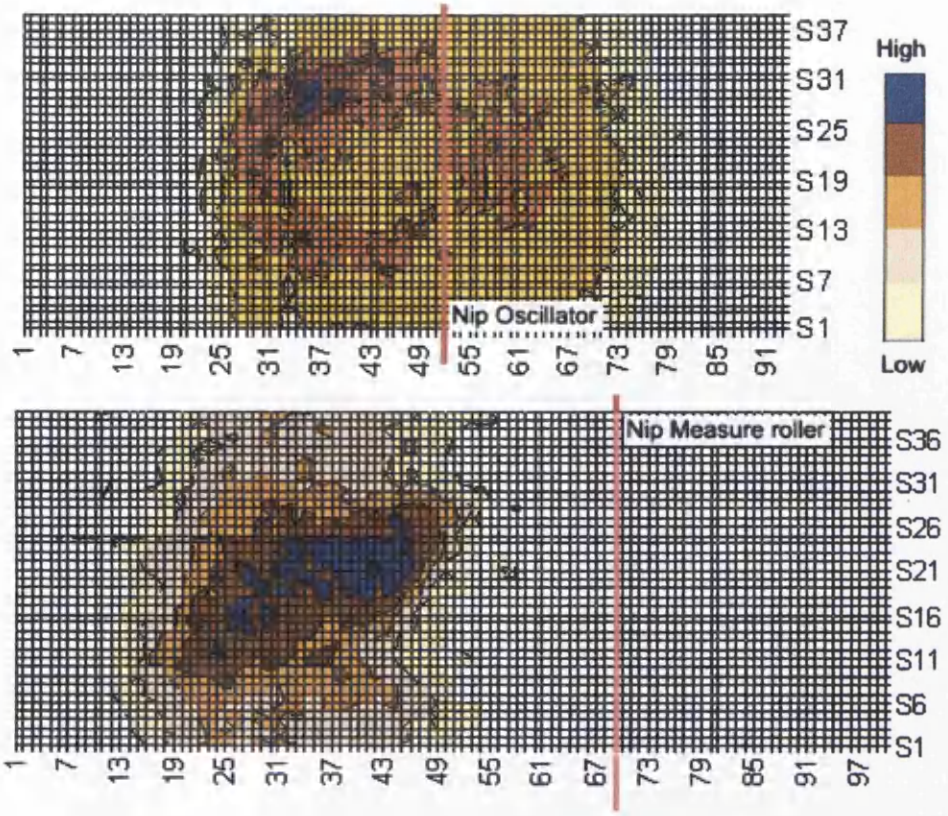

Figure 7-36 Misting droplets tend to follow gravitational directions. The decrease in roller diameter increases misting effects which also affected by rollers surface quality.

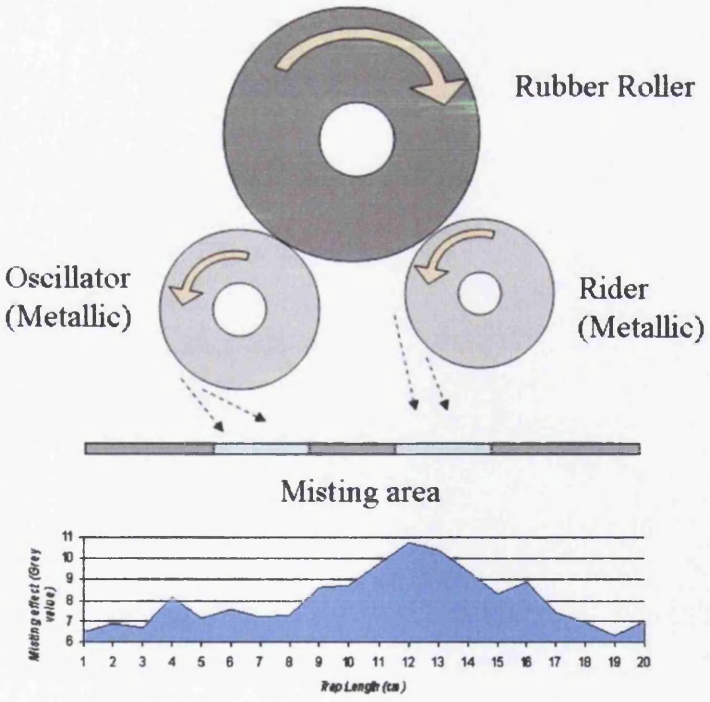

Figure 7-37 Misting is increased at the metallic rollers area away of the nip exit with gravitational trends. The results show similar misting figures from misting tests at the IGT inking unit.

7.5 Conclusions

This Chapter developed methodologies for analysis of the misting. Misting was examined with respect to the film thickness, the rheological profile of the inks and other printing parameters such as rollers velocity, system temperature, tack and rollers geometries. Misting is strictly related with the ink volume on the rollers. Tensile deformation of ink volume generates long and thin filaments that break-up at multiple areas points across the elongation length as demonstrated in Chapters 5 and 6. This affects misting droplets size, spreading rates and variations.

The current results determine two types of droplets that generate the misting phenomenon. The fine droplets are formed at the nip exit and fly around the system in turbulent direction. The droplets with higher ink volume are formed by viscoelastic deformable ink filaments due to tangential forces that increase with gravitational dynamics and form droplets that abort roller surface away of nip exit. The results of this chapter are summarised as follows:

- Misting increases with decreases in viscosity and as a result any parameter that decreases viscosity such as temperature increase. This affects capillary number which decreases as a function of viscosity and surface tension.
- Misting increases with increase of distribution speed.
- Misting also decreases through distribution time as a function of distribution time, ink film thickness and viscosity with respect to ink unit configuration. This increases ink loss and decreases ink film thickness or volume of ink on the rollers.
- Oscillation generates a wave profile of ink through rollers length and as a result misting increases in those areas across the roller length as a function of the periodic increasing ink film thickness.
- Misting increases with gravitational effects which also increase with ink volume or decrease in viscosity. It also increases with decrease of the angle between tangential and gravitational axes due to nip configuration.

- Misting rates depend on roller surface quality and diameter. Metallic rollers tend to generate more misting than elastic rollers. The effect increases also with decrease in roller diameter.
- In order to obtain a detailed profile of misting it is required to measure the number of droplets, the volume, the variations and the coverage area on the misting trap surface.
- Misting characteristics indicate similar trends on variations but only one of them is not possible to provide accurate description. The misting effect is carried out as function of the occurrence by the ratio of average droplets size versus the number of droplets by the influence of the characteristic viscosity at 147/sec^{-1} shear rate.

8. Orthogonal array L18: Effects and interactions of the ink transfer parameters on ribbing and misting mechanisms

8.1 Introduction

The aim of this study is to establish the parameters that affect the ink transfer mechanism instabilities. The ribbing and misting phenomena of viscoelastic fluids, including lithographic inks are directly related to the ink transfer mechanism at the nip exit of the forward roll systems. The understanding of this mechanism on those phenomena and the effects at the process parameters can determine the effects of ink transfer on distribution roll system. The objectives of this study attempt also to establish the relationship between ribbing and misting.

An orthogonal array experiment was used to study ribbing and misting phenomena. While ribbing illustrates the behaviour of the splitting mechanisms under specific environmental conditions, misting is generated by the ink loss from the system. The selection of the appropriate orthogonal array was modified in order to fit with the experimental study on ribbing and misting phenomena. Section 8.3 reports results from the analysis on factors effects. It also deals with the interactions of the orthogonal array through ink film thickness and rollers configuration. Section 8.4 discusses results and relations between parameters and effects on ink transfer mechanisms. The parameters of tack are also analysed in relation to the misting effects and the onset of ribbing and the variations with the factors levels.

8.2 Methodology

The L_{18} orthogonal array allows the study of 7 parameters with 3 levels and one parameter in 2 levels. The trial was carried out on the tack tester. The L_{18} array also allows study of the interaction of two level parameters with one of the three level parameters. If there are any interactions between the other parameters, these are confused across analysis of other factors and cannot be isolated.

The established methodology through this trial is divided into the following steps:

a. Identification of parameters and L18 modification

b. Experimental methodology and samples collection

c. Defining data from samples

d. Analysing data and calculating dominant effects

Each of these steps is combined by processes that are analysed in the following paragraphs.

The IGT tack tester parameters of roller ratio, temperature, distribution time and speed were included in the array. The rheology has also been shown to be critical. Therefore, the neat cyan ink and dilution of 5% Butyl-Diglycol concentration were used to set viscosity factor at two levels. The 5% dilution was selected as it had been found to be a median interaction of Butyl-Diglycol into ink structure and rheological properties. Viscoelasticity and tack were significantly lower than the neat cyan ink and the lower dilutions with Butyl-Diglycol. These two ink samples have viscosities significant different from each other as was determined in chapter 4. The temperature increase produce in both ink samples similar viscosity decrease as was also discussed in chapter 4. This allows the study of two inks without the risk to present a conflict of similar viscosity with each other in different tests. The 5% dilution characterised with significant lower viscosity than the Cyan ink. Higher diluted samples showed a Newtonian behaviour on high shear rates and significant increased misting phenomena through the whole range of process parameters.

The L_{18} orthogonal array was modified to fit with the study parameters of the trial. The array allowed one factor with two levels and up to seven factors with 3 levels. The array was modified by two factors in two levels and four parameters in three levels.

Table 8-1 shows the parameters for each level that were chosen for the trial. The modification of the L_{18} orthogonal array is showed in Table 8-2.

Table 8-1 Study parameters and the levels

Factors	Level 1	Level 2	Level 3	
	Low	Mid	High	
Rollers Ratio	1.85	1.54	-	Per1/Per2
Film Thickness	3.9	7.8	15.6	microns
Distr. Time	180	360	720	seconds
Distr. Speed	100	200	400	m/min
Temperature	15	20	30	Celsius
Viscosity	Litho Ink	Litho Ink	5% Bdg	Dilution

Table 8-2 Modification of L18 Orthogonal array

Factors	2 Roller	3 film thick	3 Time	3 Speed	3 Temp	Viscosity	Error analysis	
Run	a	b	c	d	e	f	XX	VV
1	1.85	3.9	180	100	15	Ink	1	1
2	1.85	3.9	360	200	20	Ink	2	2
3	1.85	3.9	720	400	30	5%bdg	3	3
4	1.85	7.8	180	100	20	Ink	3	3
5	1.85	7.8	360	200	30	5%bdg	1	1
6	1.85	7.8	720	400	15	Ink	2	2
7	1.85	15.6	180	200	15	5%bdg	2	3
8	1.85	15.6	360	400	20	Ink	3	1
9	1.85	15.6	720	100	30	Ink	1	2
10	1.54	3.9	180	400	30	Ink	2	1
11	1.54	3.9	360	100	15	5%bdg	3	2
12	1.54	3.9	720	200	20	Ink	1	3
13	1.54	7.8	180	200	30	Ink	3	2
14	1.54	7.8	360	400	15	Ink	1	3
15	1.54	7.8	720	100	20	5%bdg	2	1
16	1.54	15.6	180	400	20	5%bdg	1	2
17	1.54	15.6	360	100	30	Ink	2	3
18	1.54	15.6	720	200	15	Ink	3	1

The L18 array allows the study of the interactions between the first and the second column. This was chosen in order to study interactions between ink film thickness and the rollers ratio on ribbing and misting phenomena. Roller ratio factor was set at two levels in the first column that allowed interactions with the ink film thickness at three levels in the second column. The rest of the parameters were considered to be independent. An L_{18} array allowed up to eight factors for analysis. Six parameters were considered, leaving two columns empty which were used for estimating experimental error.

A second L_{18} orthogonal array has been also carried out by inverting the levels of rollers ratio. In this L_{18} array the level 1 becomes level 2 and opposite. This was necessary in order to calculate tack values for the whole 18 runs (Figure 8-1). The measure roller of the IGT tack tester was the only one that measures the tack. The oscillator was used as a rider but did not allow tack measurements. The inverted L_{18}* was compared to estimate the repeatability and the accuracy of the experiments. As a result inversion of the results was expected especially for rollers effect. The roller ratio kept constant by the two further arrays XX and VV

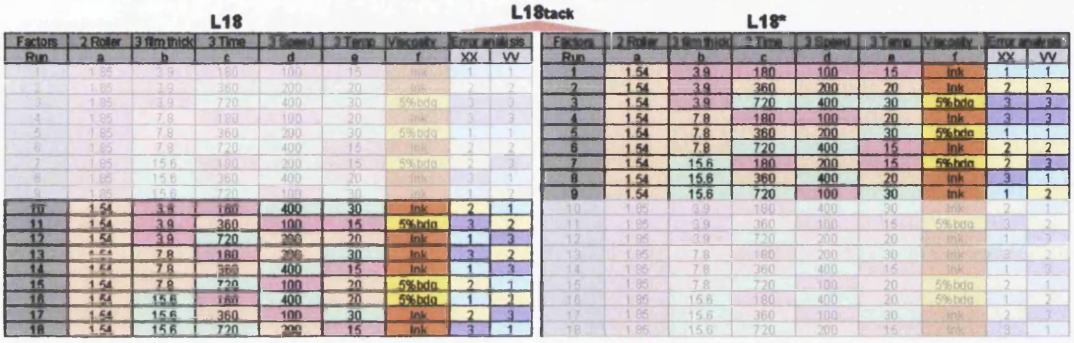

Figure 8-1 The two L_{18} are combined in a 3rd L_{18} for tack measurement. The roller ratio parameter remains constant for the 1st array. The roller configuration that used is that with the measure roller

The IGT tack tester was configured in such a way that with one run two individual samples were collected for misting and ribbing. The misting trap samples were generated during the run and the ribbing samples were captured after the run. Each trial was calculated by two runs. As a result, 36 runs were carried out for the first L_{18} array and 36 more for the roller inverted L_{18}* array.

The methodology was based on the standard operation procedures of IGT tack tester, with the addition of the methodology that was developed for misting and ribbing analysis. Therefore the methodology was divided into the following steps:

Adjusting process parameters on tack tester

Placing of the misting trap surface

Applying and pre-distribution of ink

Run process

Removing misting trap

The most important part of the experiment is the accurate transformation of the printed or the captured image into numerical data for analysis. The characterisation of misting levels by the misting trap analysis was described in Chapter 7. Therefore, misting was defined as follows:

Coverage: The amount of misting ink that is spread on a surface at the nip exit

Droplets size: The average size of the droplets that are captured by the misting trap

Droplet number: The number of the mist droplets on the misting trap

Spreading variation: The uniformity of coverage through the misting trap that is defined by the grey values that trap scanning process generates.

Ribbing was also characterised using image analysis as detailed in Chapter 6. While the ribbing image was derived by imprinting of the ink profile on the rollers, the characterisation of this deformation falls into the following parameters according to instabilities that have been established in Chapter 6 and are summarised as follows:

Surface coverage, the amount of the surface that is covered by ink across the roller length

Ribbing width, the average width of lines across the roller length

Ribbing peaks number, the number of lines that are present per centimetre

Ribbing width variation, the width variation of ribbing lines

Grey values variation, the uniformity of grey values through the imprinted image according to the digitised image by scanning.

Whilst grey values are related to the absorbance and reflectance of light, this was strictly related to the ink distribution across the surface due to the ink splitting mechanism. The digitalised images were calibrated using the digitised image of the original substrate surface.

The analysis process was divided into three main stages according to phenomena that were studied through orthogonal experiment:

1. Establishing ribbing effects analysis
2. Establishing misting effects analysis
3. Establishing related effects between ribbing and misting phenomena

8.3 Results and interactions

The analysis of the effects is divided into the ribbing and misting characteristics. It was stated that ribbing and misting phenomena cannot be described accurately by only one characteristic due to complex morphology as discussed in Chapters 6 and 7.

8.3.1 Ribbing factor effects and instabilities

The ink coverage area along the rollers is the most important parameter in terms of ink transfer mechanism. This determines the uniformity of the ink through the roller train. The more uniform the ink along the roller the less the instability to the printed area as determined in Chapter 6. Figure 8-2 illustrates the factor effects on ribbing coverage area. It shows a major effect of ink film thickness with negligible viscosity effect. Results in Chapter 6 determined that the ink film thickness variations increase significantly in the first minutes with low rollers ratio and high speed. The current results do not indicate significant variations by low distribution speeds and long runs (distribution time). The trends of roller and film thickness effects are the same for both of those arrays. The increased viscosity indicates a slight decrease effect which also shows similar trends with decreased temperature that increases viscosity. The distribution time significantly affects the coverage area between 3 to 6 minutes and changes are insignificant through the higher level (Figure 8-2). The ink film thickness and rollers ratio affect ribbing significantly. The ink coverage area decreases with the ink film thickness. This effect determines a different mechanism when the ink film thickness increases on the rollers and ribbing affects lower ink volume. The error level determines that ink coverage is affected by another parameter or an interaction but this occurs to misting that decreases the ink volume from the surface of the distribution rollers during the run.

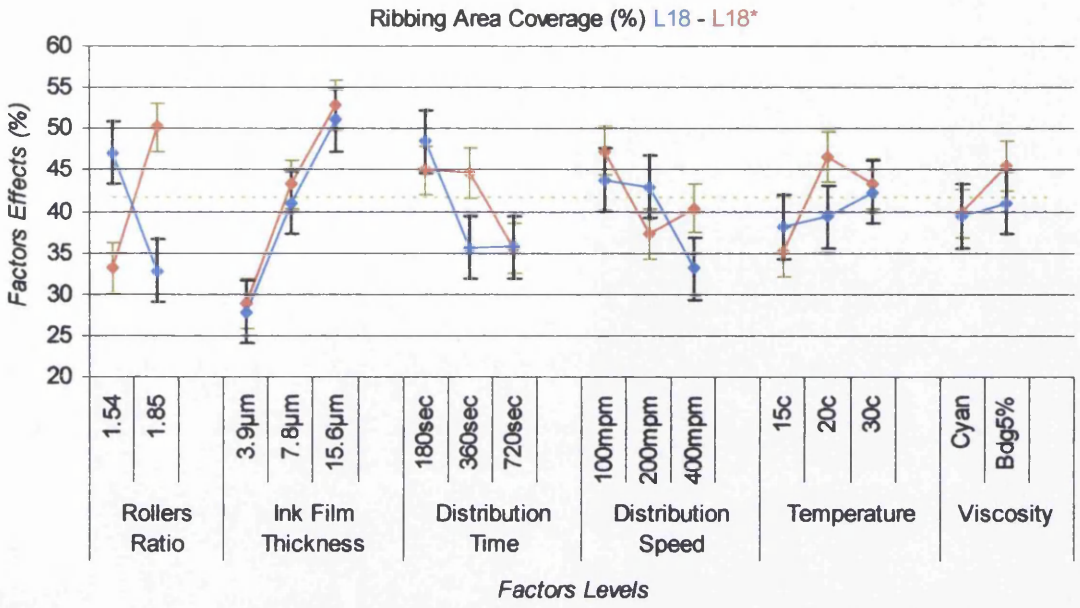

Figure 8-2 Factors effects for ribbing coverage area along the rollers. The ink coverage area decreases significantly during the first minutes with high speed, low rollers ratio as the ink film thickness decreases. Viscosity shows a negligible effect.

The ribbing peak number describes ribbing frequency in terms of how many lines are generated by the splitting mechanism through the nip. Figure 8-3 visualises factor effects for number of ribbing peaks. The major effects are the parameters of roller diameters, ink film thickness, distribution time and temperature. The distribution speed does not show any significant effect on ribbing frequency. Those results indicate the frequency of ribbing peaks increases with the ink film thickness decreases across distribution time and decrease of rollers ratio at high viscosities with the influence of low temperature. Frequency decreases when those levels increase or viscosity decreases. The ribbing number of peaks along the roller does not show any significant effect of misting or any other conflict of the parameters. On the other hand L18* shows some instability that indicates an influence of misting but agrees with the factors effects.

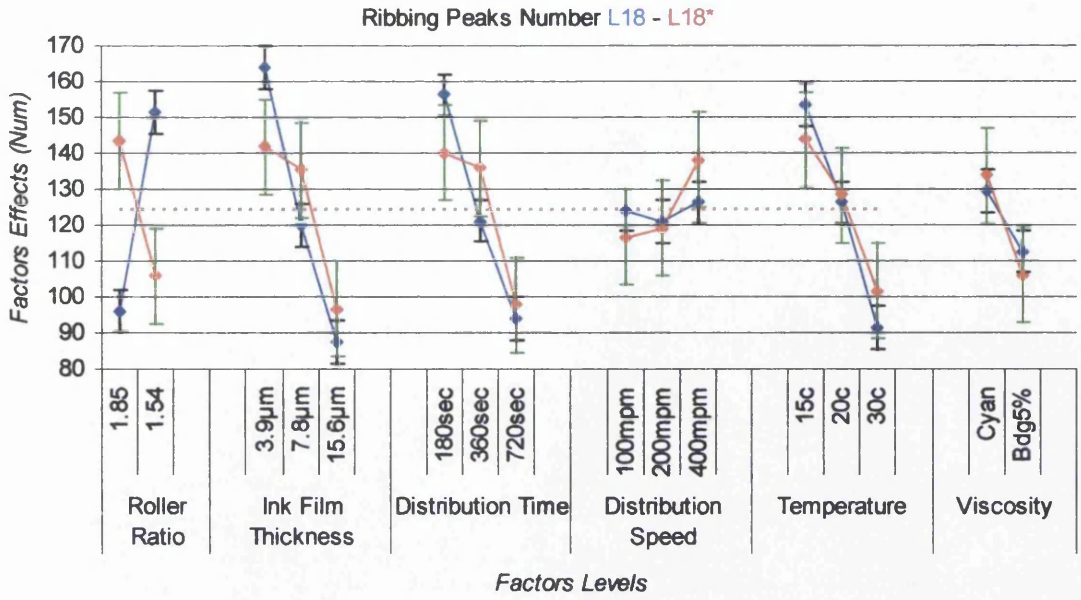

Figure 8-3 The ribbing profile increases in frequency at low rollers ratio and ink film thickness in short distribution time. High viscosity increases frequency also with temperature effect.

Ribbing width describes the average width that is generated for the ribbing patterns. It is one of the most important characteristics for ink transfer uniformity where this indicates the ink film thickness instability along the rollers. The lower the visibility of the effect occurs to the finest ribbing pattern. Ribbing width shows an increase with the ink film thickness with medium influence by the other factors. Viscosity does not have a major effect but an increase in temperature increases ribbing width. Figure 8-4illustrates factors effects from the L_{18} orthogonal array. The L_{18}* plots indicate also an effect of viscosity but decreased effect of distribution speed. The rest of the parameters show similar trends. Rollers ratio also affects ribbing width and decreases with lower level ratio. However, the error level indicates that misting significantly affects ribbing width while it increases with ink film thickness. The ribbing forms longer filaments that are affected by tangential and gravitational forces. As a result, the ink volume decreases and that affects the onset of ribbing and the width that is related to the ink film thickness as discussed also in Chapter 6.

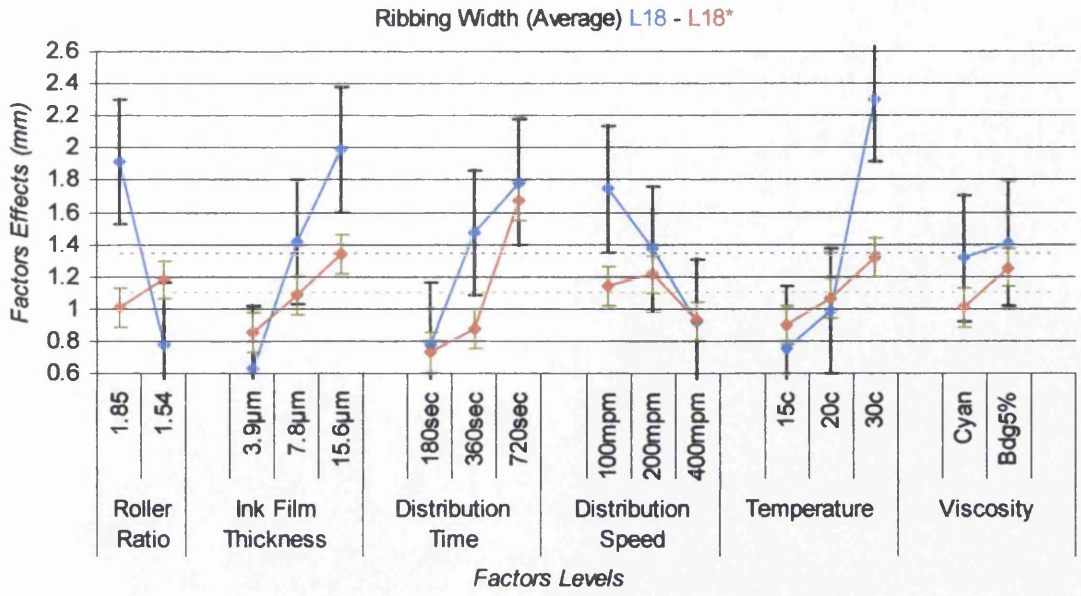

Figure 8-4 The ribbing width decreases with rollers ratio and ink film thickness at low temperature. Distribution time and speed show opposite effect with levels increase.

Ribbing width variation indicates the instability range of the ribbing profile. Figure 8-5 illustrates factor effects according to width variations or instabilities. The effects show linear responses with the factors levels. The decrease in viscosity increases instabilities which also increase with ink film thickness and the distribution time. Decrease of rollers ratio and increased distribution speed reduces ribbing width instabilities. The L18*results (Figure 8-6) highlight major influence by the distribution time and viscosity effects. The decreased viscosity and long distribution run increase dominate high instability on ribbing width. The increase of error range indicates high influence of the misting effects. Error levels determine that ribbing width instabilities are not predictable or linear with the levels of the parameters. Those results agree also with the analysis of the density variations through the profile and not only along the nip.

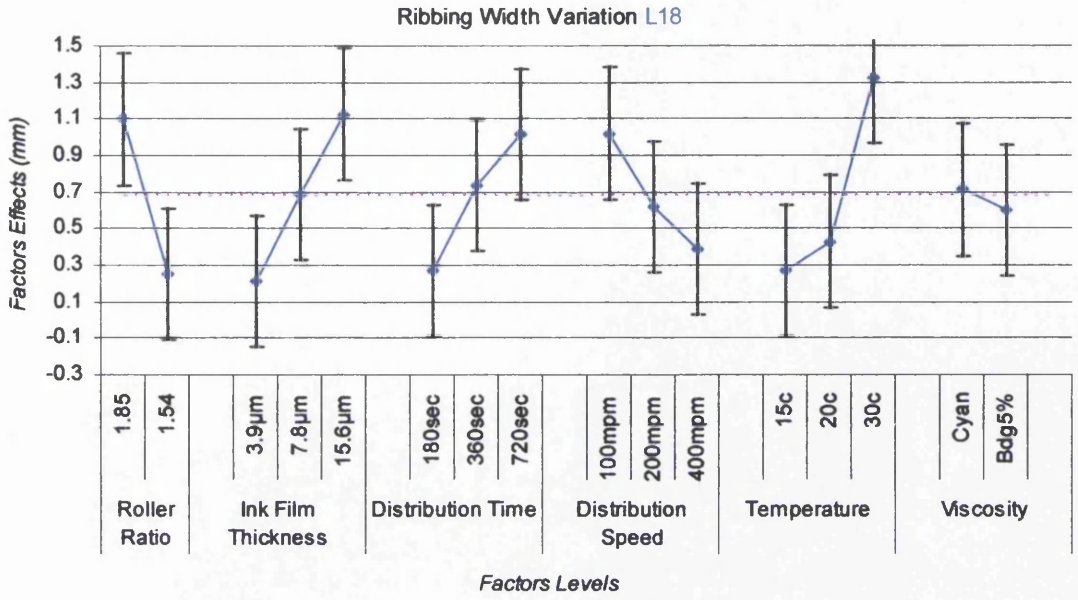

Figure 8-5 Ribbing width variations show high instability with the parameters. The effects trends of the parameters show linear response with the levels. However, the error indicates also that instabilities of the ribbing width exceed the range of the analysis. As a result the error increases with the instabilities.

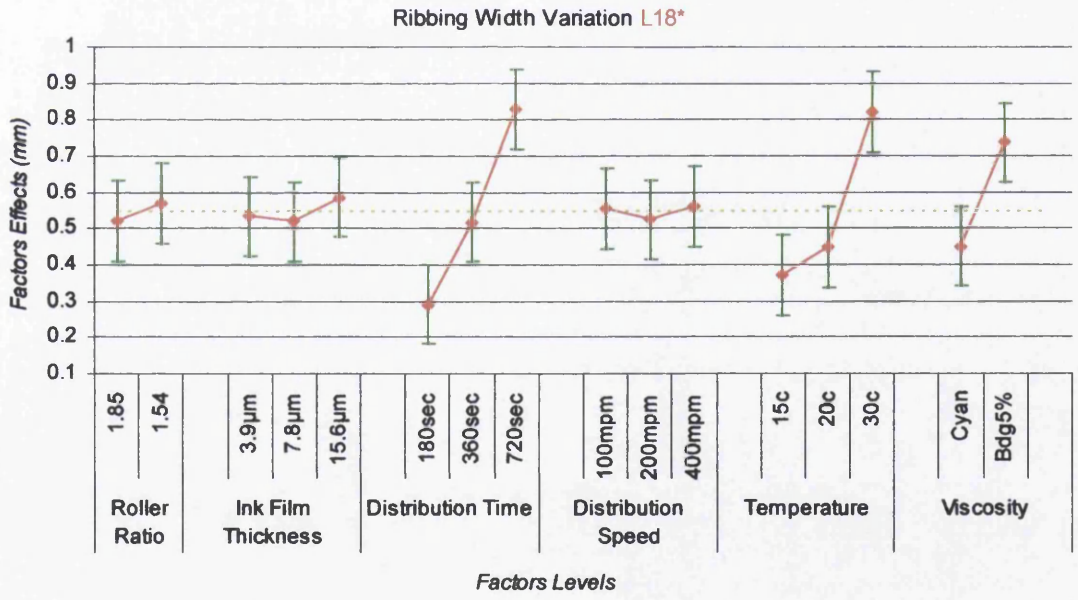

Figure 8-6 Viscosity and distribution time indicate major effect on ribbing width instabilities.

Ribbing density variations do not only involve the peaks but also the area between them and the consistency of the ribbing across the rotating direction. Those characteristics were calculated by density grey values of the capturing ribbing image. The analysis determines dominant effect of ink film thickness levels. Figure 8-7 illustrates factor effects. Ink film thickness indicates high influence to ribbing

instabilities across printing direction. Rollers ratio also affects the instability with an influence of distribution time. This also shows the significant effect of ink film thickness with minimal effects of roller dimensions. The error range determines similar effects with width variation. However, analysis shows that instabilities increase with ink film thickness and depend on rollers ratio and distribution time. The increase in temperature also increases instabilities. This concludes that instabilities occur to misting phenomena that affect ink uniformity across the rotation of the rollers.

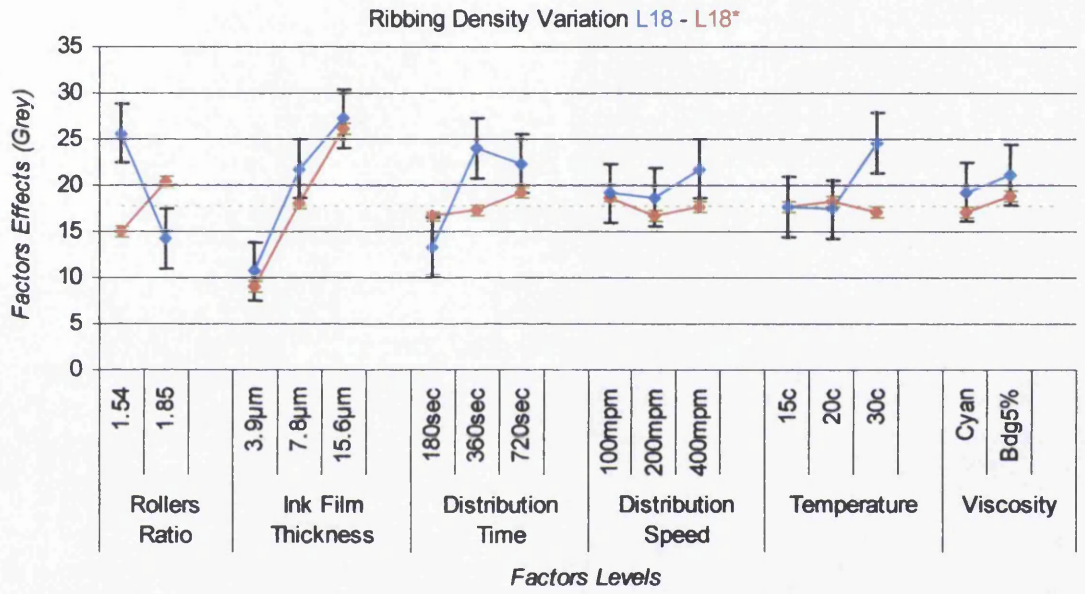

Figure 8-7 Ribbing instabilities increase with the ink film thickness and the rollers ratio. They also increase with time and significant increase of temperature. The error levels indicate also that instabilities are not linear.

Summarising these results, ink film thickness is a major factor that can affect ribbing formation and instabilities. Roller ratio factor indicates medium influence to ribbing formation. Finally, distribution time and temperature are more responsible for ribbing instabilities than for ribbing formation. However, no significant effects are indicated by changes to distribution speed and viscosity levels. However, error range increases or decreases depending on misting effects that decrease ink volume through the ribbing formation on forward distribution rollers. The variation into results between L_{18} and L_{18}* occur to rollers effect that affect misting and ink loss from the system. Those effects are analysed through the following paragraphs.

8.3.2 Misting factor effects

Misting coverage area is the area of the trap that is covered by the mist ink (Figure 8-8). Film thickness represents major effect which is followed by viscosity and rollers ratio. Similar trends are indicated by inversion of roller ratio levels through L_{18}*. Misting increases significantly with ink film thickness and decrease in viscosity. Trends agree with previous discussed results in Chapter 7. Misting increases with ink film thickness, distribution speed and decrease in viscosity caused by the increase in temperature or dilution with Butyl-Diglycol. The amount of lost ink with time decreases the ink film thickness. The ribbing formation increases ink film thickness variation and generates more misting. This highlights a significant interaction by the factors levels were misting and ribbing phenomena are affected by each other.

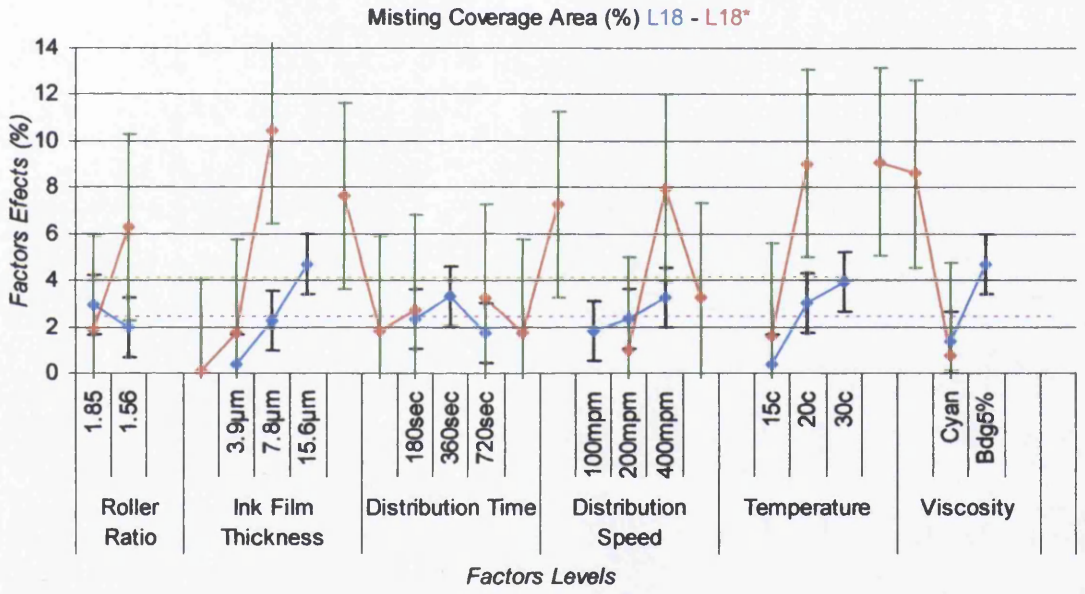

Figure 8-8 Misting coverage effects by factors levels. The error increases with the misting instability due to ribbing effect on the rollers.

Misting droplets distribution is the average droplets area on the misting trap (Figure 8-9). Ink film thickness has a major effect on droplets area generated by misting. All other factors produce effects of the same order as the image of experimental error. Similar results are concluded by L_{18}* with inversion of roller ratio levels and effects increase with the error. Droplets size increases with ink film thickness and can slightly increase with distribution speed. The speed has a non linear effect, disproportionally increasing the misting at the highest speed. The distribution time

shows instability at the middle level. This occurs to distribution time and generation of ribbing on the rollers. The periodic ink film thickness variation along the rollers allows higher tensile deformation of the filaments at the nip exit where ink droplets fly away from the rollers due to formation of longer ink filaments. Temperature and viscosity show similar responses on misting effects.

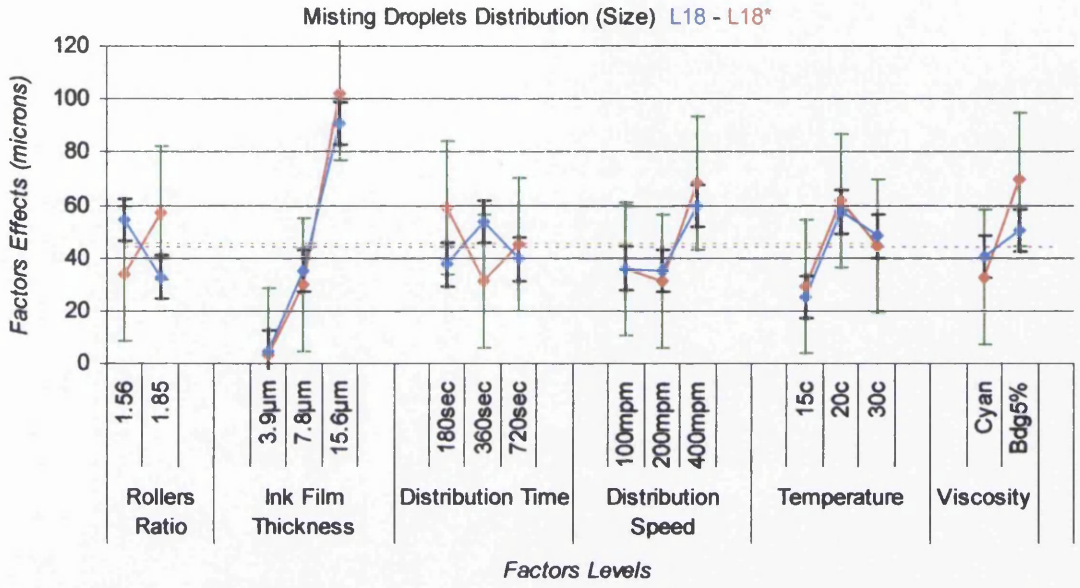

Figure 8-9 Misting droplets size for varying factor levels

Misting droplets dispersion indicates the misting rates according to number of droplets on the misting trap (Figure 8-10). The dominant effects are temperature and dilution, which both affect the viscosity of the ink. The error range occurs to overlapped droplets at the same area. Time and speed generates areas with increased number of droplets even with change in ink film thickness or viscosity. High viscosity ink with high distribution speed and time show similar results to low viscosity at low speed and time as also found in Chapter 7. This may occur to interactions that are not studied by the particular L_{18} array. However, droplet dispersion shows similar trends to the coverage area. The influence of ribbing can be located with the increase to ink film thickness variation that affects the filaments splitting mechanism. The L_{18}* results show a good agreement with these results.

Misting droplets density variation determines the variations in grey density values of the misting ink on the misting trap. This determines the variations of droplets area and uniformity of the distribution (Figure 8-11). Ink film thickness has the highest

effect. Similar results were obtained with the inversion of roller levels as carried out in the L_{18}*. The other factors had little effect. The density variation increases with ink film thickness while increasing the droplets mass range as found in the misting only study (Chapter 7). The range of the finest droplets does not change. The ink film thickness affects higher mass droplets range. Those results verify the presence of two mechanisms, one that forms finest droplets and one that generates droplets according to ink film thickness.

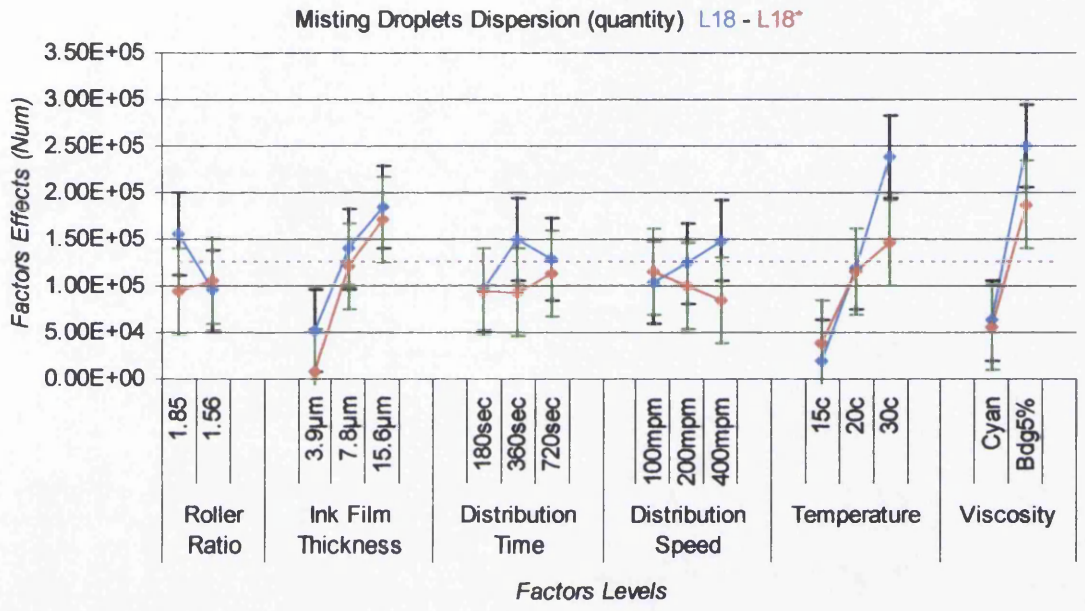

Figure 8-10 Dispersion of droplets effect versus factor levels in L18 experiment

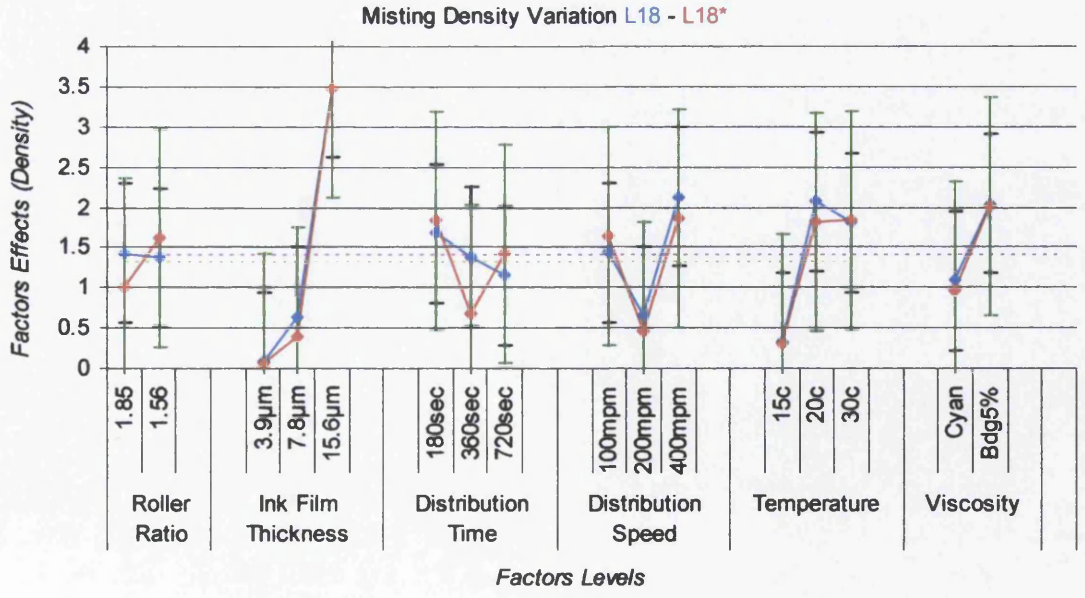

Figure 8-11 Droplets density for the factor levels in the L18 and L18 experiments*

Ink film thickness has a significant influence on the misting profile as was expected from the results in Chapter 7. It was shown also in Chapter 7 which showed that the parameters of roller, distribution time and viscosity affect misting. However, according to the results of the L_{18} experiment they interact with distribution time and produce lower effects. This assumes that the error range increases with the instability of the effect. This probably occurs to distribution time and speed while misting rates decrease ink volume from the system. A long run with medium distribution speed can show similar misting with a short run with high distribution speed. The onset of ribbing increases the local ink film thickness, resulting in long filaments being formed, which were affected by rollers velocity. The absence of oscillator increases the width variation of ribbing. As a result, misting increases at those areas where ink film thickness was increased by oscillator roller mechanism through the distribution process as determined in Chapter 7.

8.3.3 Tack factors effects

Tack results show an excellent agreement with the earlier results in Chapter 4. Distribution time determines consistency and does not affect tack. On the other hand, tack increases with ink film thickness and distribution speed (Figure 8-12). The decreased viscosity reduces the tack values with increase in dilution or system temperature. The error range occurs to the onset of ribbing that decreases coverage area along the rollers and the misting phenomena that decrease ink film thickness. The results verify previous results in Section 4.4.1 and indicate linear effect with factors levels. The consistency of the results determines that there is no interaction between temperature and dilution. The reference viscosity difference was higher than the effect of the temperature to the viscosity. As a result, temperature affects similar the viscosities of the fluids. That also verifies that viscosity of ink does not change through time on distribution roller systems as discussed in Chapter 4 for low shear rates at the nip (147/s).

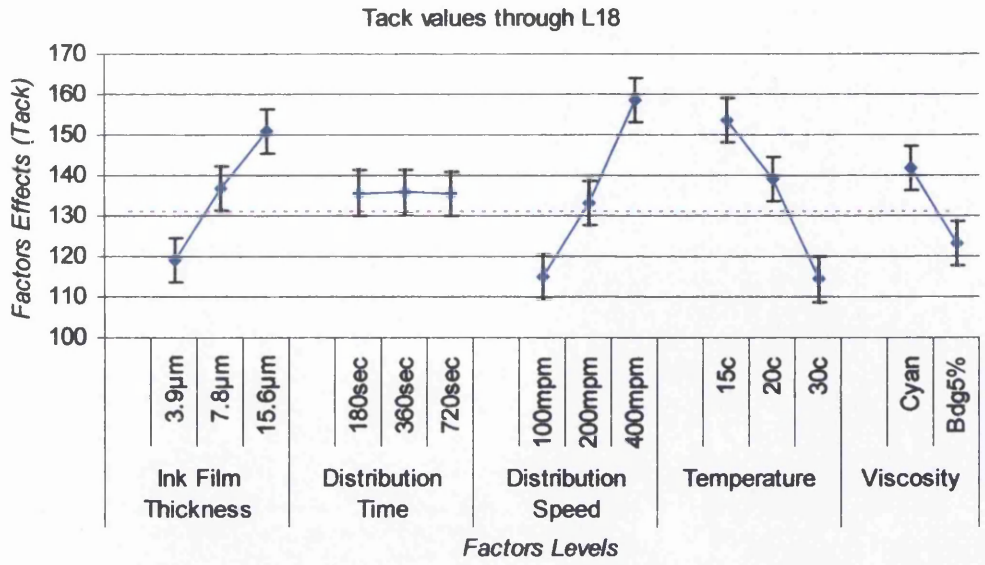

Figure 8-12 Tack increases with viscosity, ink film thickness and distribution speed. Distribution time does not affect tack values of ink.

8.3.3.1 Interactions on ribbing

Ribbing analysis does not indicate significant interactions. The ribbing coverage area does not show any interaction between rollers ratio and ink film thickness (Figure 8-13). The effect increases with the ink film thickness. Similarly, ribbing density variations increase with the ink film thickness and are not affected by rollers ratio. Those effects find very good agreement between L_{18} and L_{18}*. However, some trends for interactions at low ink film thickness are indicated by the number of peaks (Figure 8-14), ribbing width and width variations. This is probably due to distribution time and speed which affect ribbing patterns at low ink film thickness found in Chapter 6, where the ribbing pattern becomes unstable and increases ribbing width variation along the rollers. The interactions show similar responses between the L_{18} an L_{18}* but in cases the interaction is reversed. Ribbing width variations show interaction at low ink film thickness but ribbing width exhibits trends for interaction at high ink film thickness. This agrees with the results in Chapter 6 where variations on ribbing width were observed between rollers with different perimeters. However, the inverse effect of the interactions levels on L_{18}* indicates that other factors and their levels conflict with the roller ratio. It is possible for distribution speed to affect roller ratio with longer filaments and higher elastic deformation. The high distribution speed not only generates misting but also thinner filaments that

affect the onset of ribbing and the average width. However, longer runs increase ribbing width and width variation as discussed in Chapter 6. As a result, the instabilities of ribbing indicate trends of interaction between rollers ratio and ink film thickness.

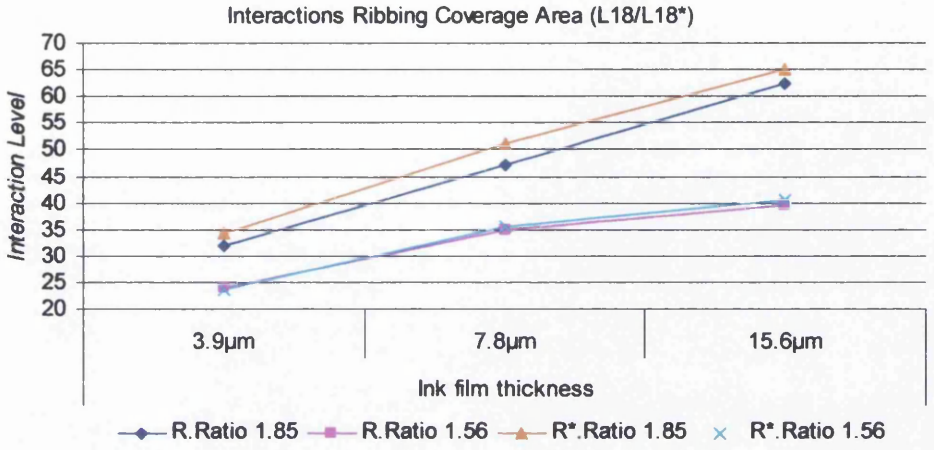

Figure 8-13The ribbing coverage area does not illustrates any interaction of rollers ratio.

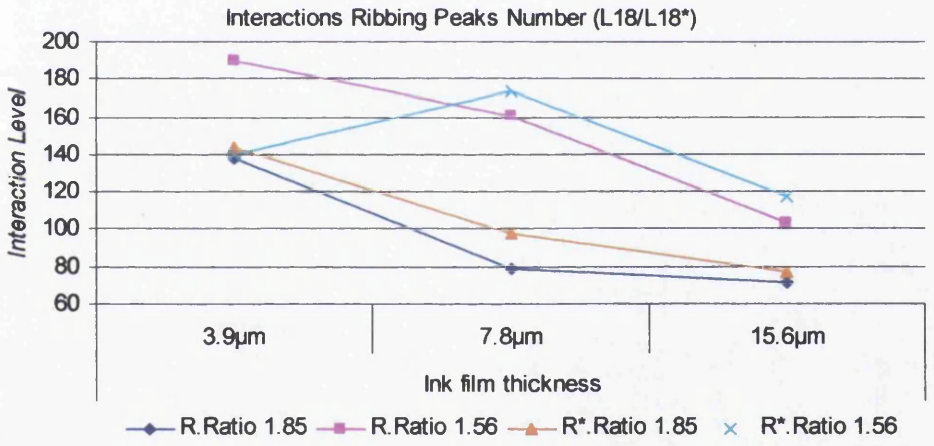

Figure 8-14 The number of ribbing peaks shows trends for some interactions at low ink film thickness. The inconsistent point is affected by the low ink film thickness over distribution time and speed.

8.3.3.2 Interactions on misting

There is little effect on misting caused by the interaction between rollers ratio and ink film thickness. The misting coverage area (Figure 8-15) exhibits interactions trends similar to misting density variations. The L_{18}* illustrates opposite interactions which confirm the effect of rollers on misting. The rollers levels interactions vary with the ink film thickness because misting is affected higher by the other

parameters. The parameters effects showed a significant effect of distribution speed and viscosity but L_{18} does not allow the study of interactions between those parameters. Misting is affected by the motor roller that generates increased volume droplets as discussed in Chapter 6. Misting droplets dispersion determines characteristic interactions at high ink film thickness (Figure 8-16). The influence of rollers ratio is significantly affected by the other parameters of the experiment. The comparisons of these results with those presented previously in Chapter 6 show that at high ink film thickness both rollers ratio generate increased misting. Finally, ribbing also affects the results especially in low and medium levels of ink film thickness.

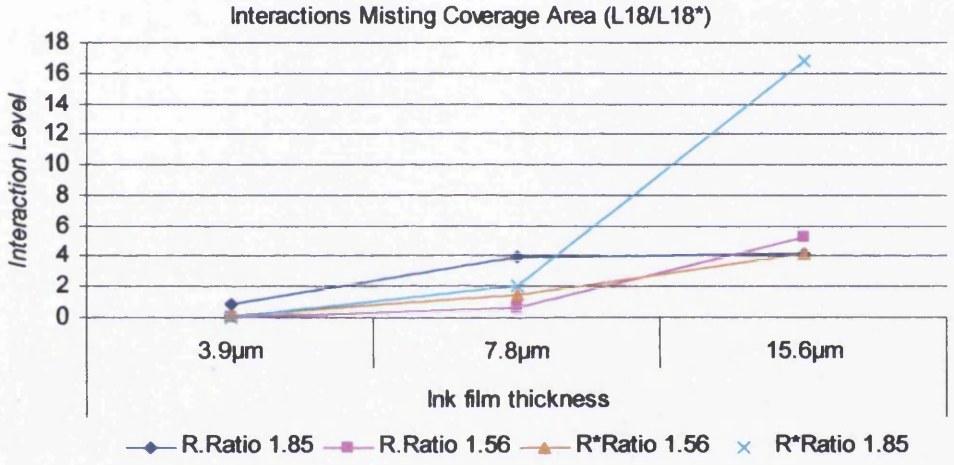

Figure 8-15 The misting coverage area indicates interactions with the increased ink film thickness where both rollers levels generate increased misting.

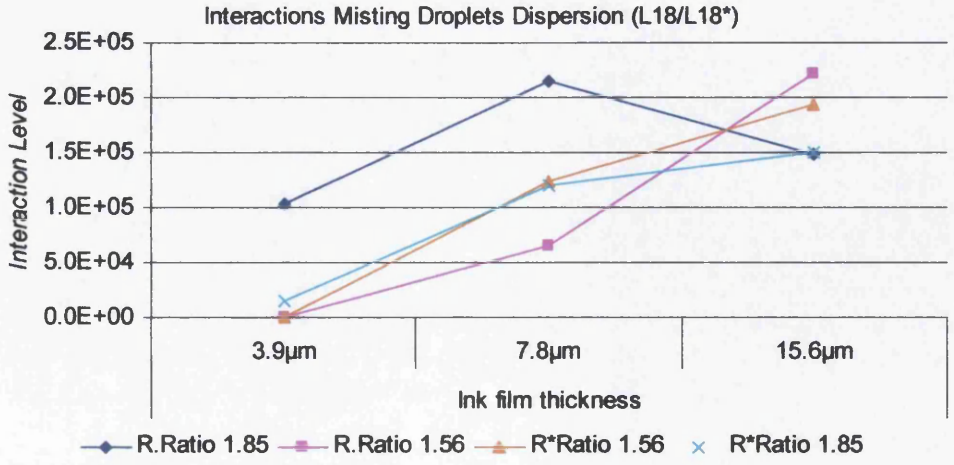

Figure 8-16 Misting droplets dispersion shows significant interactions at high ink film thickness with the rollers ratio levels.

8.4 Discussion

Ink film thickness has significant influence on both ribbing and misting. Roller diameter also affects ribbing patterns but does not show any significant interaction with ink film thickness. Medium effects are obtained by distribution time and system temperature. Misting shows similar influence of the parameters of temperature and viscosity while significant effect are also obtained due to ink film thickness and lower effects by time and roller diameter. Summarising those results, printing quality can be optimised by controlling ink film thickness, viscosity and rollers dimensions with optimum levels the thinner film thickness and system configuration with wider rollers.

The onset of ribbing of viscoelastic fluids is an effect that is related to the tensile deformation of the ink structure. The ribbing profile is not constant but varies with the influence of the process parameters. The misting phenomena are generated by a consequence of the splitting mechanism. Long distribution runs show that increase interaction where eventually misting and ribbing profile change through time. This is also confirmed by tack measurement which is affected by the ink film thickness and its variations along the nip, the viscosity and the distribution speed as shown in Section 8.3.3 and Chapter 6.

Orthogonal array was carried out in order to confirm the results of the process parameters effects on the interaction between the ribbing and misting phenomena as were estimated by the results in previous Chapters. It was expected a factor that decreases ribbing peaks frequency of the profile to increase ribbing width at the same time. These were also the trends that were found through the results of the orthogonal array. The increasing of the ink film thickness increases the coverage area along the rollers by increasing the ribbing width and as a result decreasing the peaks frequency. This increases the ribbing variations along the rollers and the ribbing profile indicates high instabilities. The ribbing with increased ink film thickness highlights wider range of density variations across the profile. Similar results were also confirmed for other parameters such rollers ratio, temperature and distribution speed as found in previous chapters. The decrease rollers perimeter ratio decreases

ink coverage area and ribbing width with increasing frequency and decreased instabilities. Distribution time shows similar responses and further highlights the misting effects. As a result, ink coverage area decreases with distribution time as does the ribbing frequency (peaks number) but increases the variation. Viscosity decreases with increase temperature and dilution as discussed in Chapter 4. As a result, ribbing frequency decreases with viscosity where ribbing width and instabilities increase. Ink coverage along the rollers decreases with frequency where ribbing width and variations increase.

The misting rates increase with the coverage area on the misting trap. The increased misting is characterised by increased droplets distribution range and number of droplets. The increased misting consists of two kinds of droplets. Fine satellite droplets are formed at the rupture of the filaments at the nip exit. Tensile forces generate structure instabilities due to deformation and decreased elasticity. Those agglomerate parts form higher volume droplets that follow the tangential velocity of the rollers and gravitational dynamics. The rates between those two mechanisms depend on viscosity and ink film thickness. Fine satellite droplets are formed with higher viscosities. The decreased viscoelasticity increases the rollers velocity effects and higher volume droplets are formed. However, the misting results conflict with the effect of ink film thickness, rollers ratio and distribution speed which affects misting rates. Those parameters affect the onset of ribbing as described above. As a result, misting rates interact with the onset of ribbing that generates ink film thickness instabilities along the rollers with trends to lateral flow. This also affects droplets dimensions where lateral flow effects increase the volume of droplets at the sides of the rollers. Lateral flow indicates an effect of centrifugal forces on the rollers distribution systems that affect ink distribution as well. Misting phenomena are a sequence of the ribbing mechanism. Misting can not be generated by the absence of ribbing. Both of them are sequenced effects of cavities and filaments formation at the nip exit.

8.4.1 Factor effects and relations

The orthogonal array L_{18} experiment confirmed the effects of process parameters on ribbing and misting. The experiment focused on understanding and establishing

relations between the onset of ribbing and the misting rates. The independent study of the phenomena determined higher effects of the process parameters on ribbing phenomena in Chapter 6 and misting phenomena in Chapter 7. The current results indicate a correlation between ribbing and misting. In order to analyse those mechanisms it is important to understand which levels of the parameters decrease the phenomena and provide uniformity to the ink transfer mechanism. This uniformity is characterised by low ribbing effects and decreased misting. First, it is important to establish which ribbing is low and which is high. The printing process is based on the low abilities of the eye to understand low variations. In Chapter 6 it was discussed that high frequency ribbing and decreased instabilities determine low ribbing. Low instabilities occurred also to low or negligible misting effects as found from the current results.

The prediction of process parameters effects determines the dominant effects between the L_{18} and L_{18}*. This analysis attempts to establish the factors levels that provide uniformity and indicate significant influence. The effects are set in high, medium and low or negligible level. Final analysis L_{18} results and L_{18}* by inversion of rollers ratio levels are transformed into percentage effect to establish the actual effect and also the related effects between misting and ribbing phenomena. The results on the optimum levels and relations are described below.

8.4.1.1 Rating levels for ribbing characteristics

While analysis determines one level for some ribbing quality characteristics, a different level is determined for a different characteristic. Table 8-3 indicates optimum levels for ribbing characteristics and level of factors effects according to L18 orthogonal array. There is a slight difference between the factors and their levels that affect those characteristics. There is a good agreement between L_{18} and the L_{18}* by inversion of roller levels in. Table 8-4.

The increased coverage area shows trends to large roller with low ink film thickness and high time for a long distribution speed. Those levels effect show high or high-medium influence in terms of increased coverage area and so increased ink uniformity. Roller effect presents high effect which followed by the large roller in

optimum level. Ink film thickness presents also high effect with optimum level the 3.8μm which is referred to the lowest level 1. Distribution time concludes high and medium effect which is depended on ribbing characteristics. That gives low time as optimum for ribbing thickness and for thickness and density variations. High time is indicated as optimum for increased ribbing peaks and coverage area. Speed shows medium influence only for increased coverage area with optimum level the longest distribution speed, but no effect for the other characteristics. High temperature can increase in a medium level the ribbing peaks but on the other hand low temperature shows high influence for thin ribbing formation and variations. Viscosity does not significant effect whilst is presented by medium level to the L_{18}* with an influence to ribbing thickness and variations. Free columns present negligible values with a presence of medium level only on thickness variations.

Table 8-3 Rating levels for ribbing profile according to L_{18} orthogonal array

	Optimum Levels for Ribbing Quality Characteristics (L18)									
	Area coverage		Peaks number		Density variation		Thickness variation		Ribbing Thickness	
Factors	Optimum	Effect	Optimum	Effect	Optimum	Effect	Optimum	Effect	Optimum	Effect
Roller	Large	High	Small	High	Large	High	Large	High	Large	High
Film thickness	3.9μm	High	17μm	High	3.9μm	High	3.9μm	High	3.9μm	High
Time	S3	High	S3	High	S1	Meduim	S1	Meduim	S1	Meduim
Speed	T3	Meduim	-	Low	-	Low	-	Low	-	Low
Temperature	-	Low	T3	Medium	-	Low	T1	Meduim	T1	High
Viscosity	-	Low	-	Low	-	Low	-	Low	-	Low
Free (error)	-	Low	-	Low	-	Low	-	Low	-	Low
Free (error)	-	Low	-	Low	-	Low	X3	Meduim	-	Low

Table 8-4 Rating levels for ribbing profile according to L_{18}* by inversion of roller levels

	Optimum Levels for Ribbing Quality Characteristics (L18* invert)									
	Area coverage		Peaks number		Density variation		Thickness variation		Ribbing Thickness	
Factors	Optimum	Effect	Optimum	Effect	Optimum	Effect	Optimum	Effect	Optimum	Effect
Roller	Large	High	Small	Meduim	Small	Meduim	Small	Meduim	Large	Meduim
Film thickness	3.9μm	High	17μm	Meduim	3.9μm	High	-	Low	3.9μm	Meduim
Time	400rpm	Meduim	400rpm	Meduim	-	Low	100rpm	High	100rpm	High
Speed	720sec	Meduim	-	Low	-	Low	-	Low	-	Low
Temperature	15c	Meduim	30c	Low	-	Low	15c	High	15c	Meduim
Viscosity	-	Low	-	Low	-	Low	High R	Meduim	High R	Meduim
Free (error)	-	Low	-	Low	-	Low	-	Low	-	Low
Free (error)	-	Low	-	Low	-	Low	X2	Meduim	-	Low

8.4.1.2 Rating levels for misting characteristics

Misting results show also a small disagreement between two experiments which is significant for roller effect. Table 8-5 indicates optimum factor levels and effects according to L18 orthogonal array.

Table 8-6 is refereed to L_{18} by inversion of roller levels. Ink film thickness presents clear high effect through the complete misting profile with optimum level the low

film thickness this of 3.8μm. Roller effect presents a disagreement between two tables. While it is indicated with medium effect and optimum level the large roller in the first analysis, it is absence or with negligible effect into the second analysis. On the other hand there is a good agreement on temperature and viscosity effect. Both of them determine high viscosity with a medium effect. Viscosity optimum level is the original cyan ink with the highest viscosity. On the other hand temperature optimal effect is defined by low level in the first analysis with this of 15 Celsius for the first analysis while in the second L_{18} presents medium level this of 20 Celsius. Free columns show negligible values with a medium value into misting dots size at the first table that indicate a minimal error to the accuracy of this characteristic.

Table 8-5 Optimum levels for misting quality characteristics according to L_{18} orthogonal array

	Optimum Levels for Misting Quality Characteristics (L18)							
	Area coverage		Dots number		Dots size		Density variations	
Factors	Optimum	Effect	Optimum	Effect	Optimum	Effect	Optimum	Effect
Roller	R2	Medium	R2	Medium	R2	Medium	R2	Medium
Film thickness	F1	High	F1	High	F1	High	F1	High
Time	-	Low	S2	Medium	S2	Medium	-	Low
Speed	-	Low	-	Low	-	Low	-	Low
Temperature	T1	Medium	T1	Medium	T1	Medium	T1	Medium
Viscosity	V1	Medium	V1	Medium	V1	Medium	V1	Medium
Free (error)	-	Low	-	Low	W	Medium	-	Low
Free (error)	-	Low	-	Low	-	Low	-	Low

Table 8-6 Optimum levels for misting quality characteristics according to L18* by inversion of roller levels

	Optimum Levels for Misting Quality Characteristics (L18 invert)							
	Area coverage		Dots number		Dots size		Density variations	
Factors	Optimum	Effect	Optimum	Effect	Optimum	Effect	Optimum	Effect
Roller	-	Low	-	Low	-	Low	-	Low
Film thickness	F1	High	F1	High	F1	High	F1	High
Time	S1	Medium	S1	Medium	S1	Medium	-	Low
Speed	-	Low	-	Low	T1	Medium	-	Low
Temperature	T2	Medium	T2	Medium	T2	Medium	T1	Medium
Viscosity	V1	Medium	V1	Medium	V1	Medium	V1	Medium
Free (error)	-	Low	-	Low	-	Low	-	Low
Free (error)	-	Low	-	Low	-	Low	-	Low

Results can be linked between ribbing and misting phenomena in terms of ink transfer uniformity and decrease ink loss of the system. Dominant effects and optimum levels estimate factors that can affect the ink transfer mechanism. The optimum levels are carried out by the factors levels responses through the L18 and the results are transformed into a percentage range that affects separately and both those phenomena. Figure 8-17 illustrates optimum levels for factor effect according

the results of L18 orthogonal array by calculation of the percentage factor effect. It shows high influence of low ink film thickness. A roller effect is located to the second level as dominant with small difference of the first level. Optimum level of distribution time is characterised by two levels in similar response, those of high and low time. Lowest temperature shows also significant effect for ribbing with insignificant response of high temperature. Finally longest distribution speed and high viscosity also provide a low effect in terms of ribbing uniformity. Summarising those results, ribbing uniformity can be achieved by low ink film thickness and temperature in high or low time using wider rollers when high viscosity and longest distribution speed are followed.

Misting results show also high influence of ink film thickness (Figure 8-18). High viscosity shows also dominant effect which similar to the ink film thickness influence. Low temperature presents also a significant effect on decreased misting with low or medium time as well. The roller dimension can affect and reduce misting while large roller indicates optimum level on misting elimination. Speed does not show a significant effect but indicates some trends to shorter distribution speed. Those results can summarise the complete profile for decreased misting levels on distribution systems. Low ink film thickness with high viscosity can decrease misting when distribution systems with wider rollers run under low time and low temperature as well.

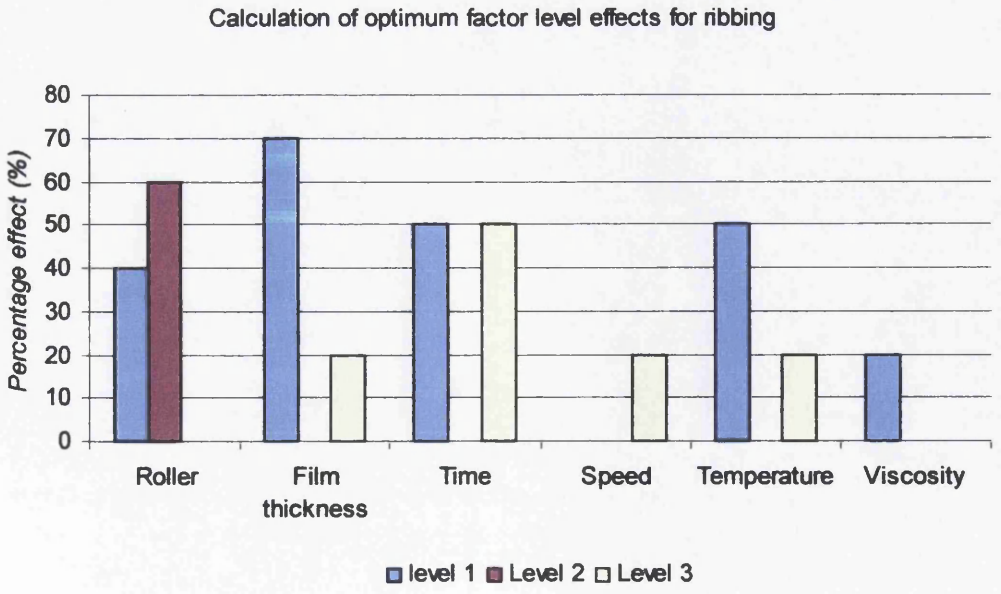

Figure 8-17 Calculation of optimum levels for ribbing according to L18 factor effects.

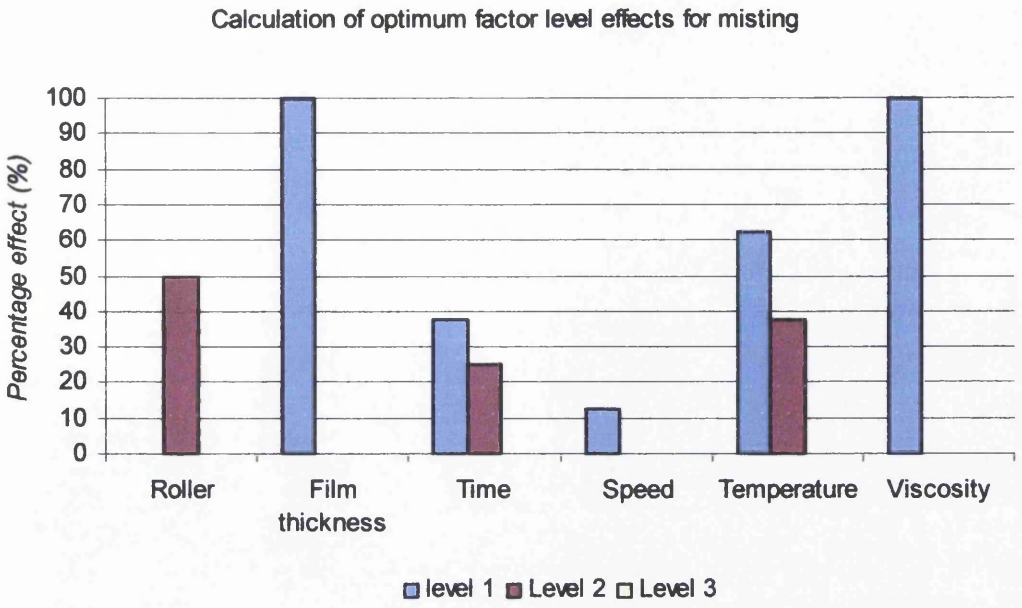

Figure 8-18 Calculation of optimum levels for misting according to L18 factors effects analysis.

These two phenomena can be summarised into one by calculating the concluded optimum levels. The links between a uniform ink film thickness and decreased misting located primary to the low ink film thickness. The levels that indicate low level close to error factors are eliminated and the results are visualised in Figure 8-19. The uniformity range indicates optimum settings for decreased ink transfer instability and ink loss on distribution systems. Low ink film thickness can cooperate satisfactorily with low levels of temperature and distribution time and high roller ratio levels and viscosities for improved quality on distribution systems.

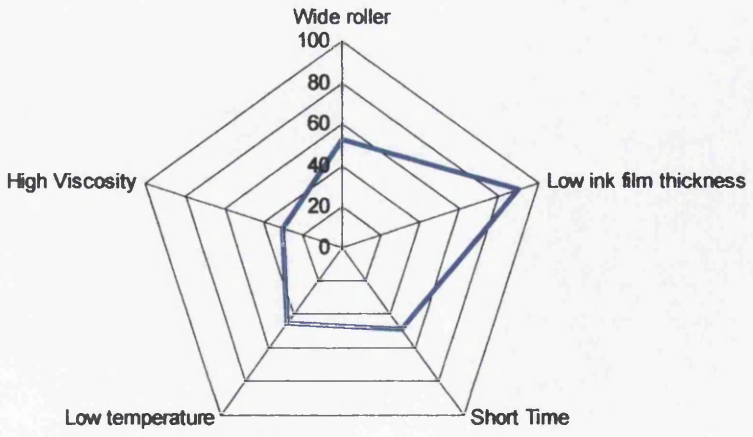

Figure 8-19 Factors levels range that leads to ink transfer uniformity

8.5 Closure

Experiment using L18 orthogonal array was in a good agreement with the expected responses of misting and ribbing phenomena through the ink transfer mechanisms. Interactions were calculated to determine factor effects on ribbing and misting phenomena on roller trains. The current results verified the importance of ink film thickness and system temperature. The rollers ratio showed that also affect misting rates and ribbing patterns. Microstructure deformation of the ink and its intermolecular dynamics during elongation play an important role in these phenomena. Ink transfer uniformity can be achieved by minimising those effects which means minimising instabilities. The misting depended on two different mechanisms that conflict on the misting trap surface but it also occurs to surface qualities. The low ink film thickness indicated an optimum level to minimise instabilities with ribbing and misting effects. The current results can be summarised into the following:

- The ribbing peaks frequency decreases with the increase of ribbing width.
- The increase of the ink film thickness decreases ribbing frequency which tends to decrease with the viscosity.
- The ribbing frequency decreases with increase of rollers perimeter ratio and distribution time. It increases with the distribution speed and the viscosity.
- The tack decreases with the ribbing frequency and ink coverage area along the rollers. It also decreases with distribution time due to ribbing frequency variations and the misting rates that decrease ink film thickness from the distribution rollers. The same ink volume can lead to different ribbing frequencies along the rollers with different tack due to change in coverage area.
- The ribbing frequency and the ribbing width determine the amount of ink film thickness on a known rollers ratio.
- The decrease of frequency tends to increase misting rates due to increase of ink film thickness variation. This produces higher misting (for same ink film thickness with wider range of ink droplets) in the higher speed region.

- The misting rates are constant as long as the ink film thickness is constant. Tack does not change over time when misting is not significant.
- The misting increases with increased ink film thickness, run time (time to collect), decreased viscosity (by temperature or dilution), increase in rollers ratio (different speed of rollers).
- The roller centrifugal forces increase lateral flow of the ink on the rollers. That decreases ribbing frequency and increases misting rate and droplets range.
- Misting indicates the distribution history of the ink film thickness on the rollers. It can vary over time as ink film thickness that forms ribbing. Misting droplets size range increases with ink film thickness and decreases with rollers ratio. Misting appears low, constant and independent from ribbing at low speed

9. Discussion

Lithographic offset printing presses are consisted by ink trains, containing a number of rollers with different circumferences and surface material to repetitively supply ink to the mounted image on the plate cylinder. The inked image is transferred to the blanket cylinder and then to the substrate, which is usually paper, by impression. The inking process of the image is based on the chemical self-repellent interaction between water and oil. The fountain solution, usually water remains on the non image areas and forces ink to stick on the image areas which are water repellent surfaces. The lithographic inks are usually complex formulation and high viscosity fluids with thixotropic behaviour. A number of parameters are involved during the printing production process that affect the inking mechanisms and produce undesirable effects to the printing quality but also to the environment. The Figure 9-1 illustrates some of those parameters that can affect the printing mechanisms in offset lithography and are related to the involving materials on a printing process and press. The parameters can interact between each other based on press configuration or printing system layout, and printing materials such as inks, fountain solution and printing substrates.

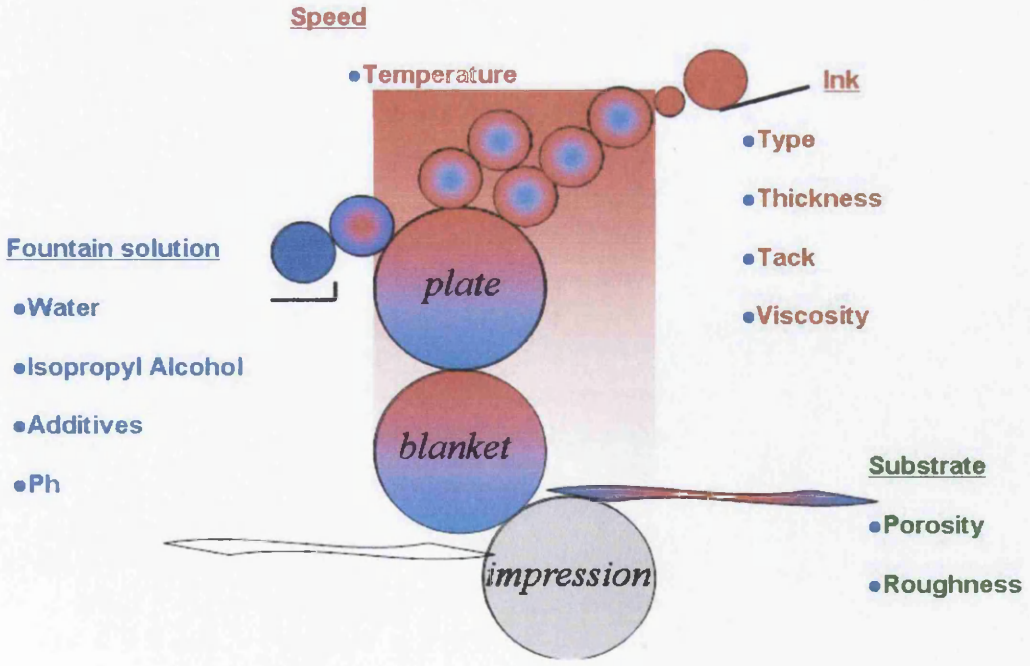

Figure 9-1 The printing parameters on an offset lithographic printing press. The participated materials of the press generate undesirable phenomena which negatively affect printing quality but also working environment. Ribbing and misting are the most important phenomena that are not possible to be solved with the current printing systems and lithographic inks.

The dynamic system of a printing press does not allow experiments or studies on splitting mechanism because it is not possible to monitor the range of the surface or the mechanisms that participate during the printing process. The current study focused on how the ink transfer mechanism generates ribbing and misting phenomena by establishing patterns or instabilities on the roller train distribution systems. It established the influence of the parameters such as ink film thickness, temperature, distribution speed, distribution time and viscosity. It was necessary to explore each mechanism or parameter separately in order to accomplish this study, avoiding the conflict of the phenomena and their effects. As a result, the study was separated in four main stages: the rheological characterisation of the used inks, the capturing and analysis of ribbing profile, the capturing and analysis of misting profile and finally the L18 Orthogonal array experiment (Figure 9-2).

The rheological characterisation consisted three parts: the typical rheology measurements such as shear viscosity, surface tension and thixotropy, the tack measurements and the extensional viscosity. Tack is not a well understood characteristic but usually is related with the stickiness of the ink. However, not much work has been reported about relation with tack and extension viscosity or shear viscosity. Techniques on extension rheometry has been also developed in order to simulate and understanding the ink splitting mechanisms at the printing nip exit. Developed techniques included studies on fluid deformation and flow by using model fluids but also visualisation of a printing nip and the ink splitting mechanisms.

The ribbing and misting are dynamic phenomena that strongly related with the ink film thickness. The capturing of ribbing and misting was never established before by any study in order to understand the effect of the printing parameters. The current work located ribbing and misting phenomena by developing techniques to capture and analyse accurately the influence of the parameters. These techniques set repeatable methodologies that can be used to understand and explain a wide range of other printing processes such flexography and other printing inks.

The development of the methodologies on inks rheology and the established ribbing and misting profile analysis provided a wide range of information and examination that can be used together in order to understand dynamic phenomena on ink

distribution systems. The L18 orthogonal array experiment combined all together in order to understand the influence of the printing parameter. This final experiment showed how misting and ribbing interact between each other and how tack is affected by those phenomena and printing parameters such as temperature, speed, time, viscosity and ink film thickness and possible interactions.

The current study provides the chance to design numerous of applications on testing methods of printing materials on roller coating or printing systems. It shows the importance of the printing parameters and the printing press configuration in order to control related phenomena with the ink transfer mechanism such as ribbing and misting. Similar studies can give the opportunity to improve press designs but also mathematical press models in order to simulate and understand the ink transfer mechanisms.

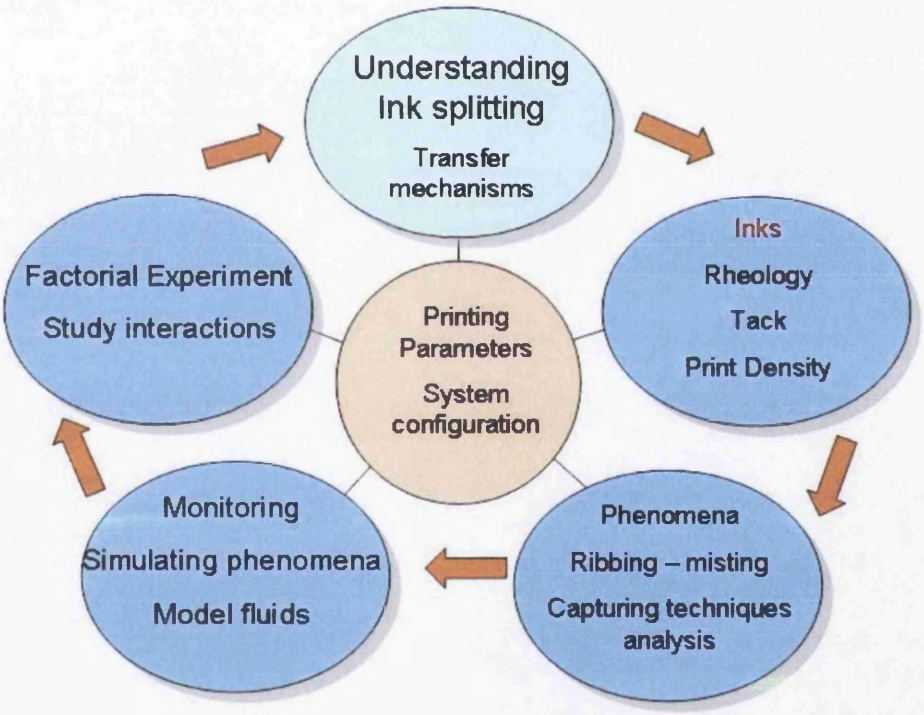

Figure 9-2 The current study was divided by step examination in order to complete the gap of the knowledge between different purposes studies. The established methodologies and developed techniques were used to run a full factorial experiment in order to understand the ink splitting mechanisms by examination of the printing parameters and the related phenomena of misting and ribbing.

9.1 Ribbing instabilities on ink transfer mechanism

The onset of ribbing instabilities depends on a number of parameters such as rollers dimensions, ink film thickness, distribution speed and time with respect to viscosity

according to viscoelastic properties and system temperature. Significant instabilities occur parallel to the nip in which ribbing is formed. Ribbing depends on molecular dynamics and structure of the fluid during extension process through splitting mechanism as concluded by elongation tests in Chapters 5 and 7. Results from the L18 orthogonal array showed that ribbing is affected by ink film thickness and distribution time with respect to speed. Temperature and viscosity do not show a dominant effect on ribbing. The roller dimensions can also affect ribbing formation at low ink film thickness.

Ink intermolecular dynamics decrease with the increase of elongation speed (Figure 9-4). Tensile forces exceed the viscoelastic forces of the ink and the break-up causes cavities which expand into filaments. The higher the speed, the more the filaments are formed with respect to the viscoelasticity, the adhesive dynamics and the ink film thickness along the nip. On forward rolling nip the filaments fold back after splitting and so the ink increases parallel to the rolling direction (Figure 9-5). This is an effect of the separation angle between the two rollers which increase the cavities with distance from the nip outlet. Filaments are deformed and bend into the roller surface due to viscoelastic dynamics of the ink. This depends on the separation angle of the nip which is responsible for the meniscus with respect to the ink film thickness. These two instabilities define how the ribbing is formed.

Banks and Mill (1956) argued that ribbing depends on the capillary number which describes the ratio of the viscous forces to the surface tension. The capillary number of the this experimental work showed a good agreement with misting rates in section 7.1 but not much with the onset of ribbing. Recent work on viscoelastic fluid flow on forward roll coatings found that at any capillary number there is a critical Weissenberg number at which the flow becomes unstable (Zevallos et al 2005). They also suggest the Weissenberg number increases with the stress of the free surface and this leads to ribbing formation. Weissenberg number is the dimensionless number where used to study the viscoelastic fluids which is defined from the shear rate times the relaxation time. The Weissenberg number (We, Wi) of the experiments show that decreases with the decrease in viscosity and the capillary number of the ink dilutions (Figure 9-3). The Weissenberg number of the extension rates (We) indicate slight variation from the shear rates (Wi) which decreases with the viscosity and the

capillary number. Although, the ribbing results showed in chapters 6 and 8 that occur due to a dynamic splitting which involves both tensile stress and elastic stress with respect to intermolecular dynamics and the time scale of observation. Tensile stress generates capillary action at the free area. Both surfaces generate tensile stress due to the adhesion of the ink, so filament is formed. The filament is deformed due to tensile deformation. The filament fails with deformation when it exceeds the elastic limit. Rotation does not allow full recovery speed so the ink is inserted into the next nip inlet with the deformation from the previous splitting. The increased time increases tensile forces and increase cavities. Tensile forces are reduced with the increase of ink film thickness, reducing the number of cavities and filaments. Thus, ribbing depends on ink film thickness which allows dynamics to affect splitting instabilities. This splitting instability mechanism is analysed by examining the captured image of the ribbing patterns. Figure 9-6 shows splitting instabilities into both directions with trends to decrease due to the rotating direction.

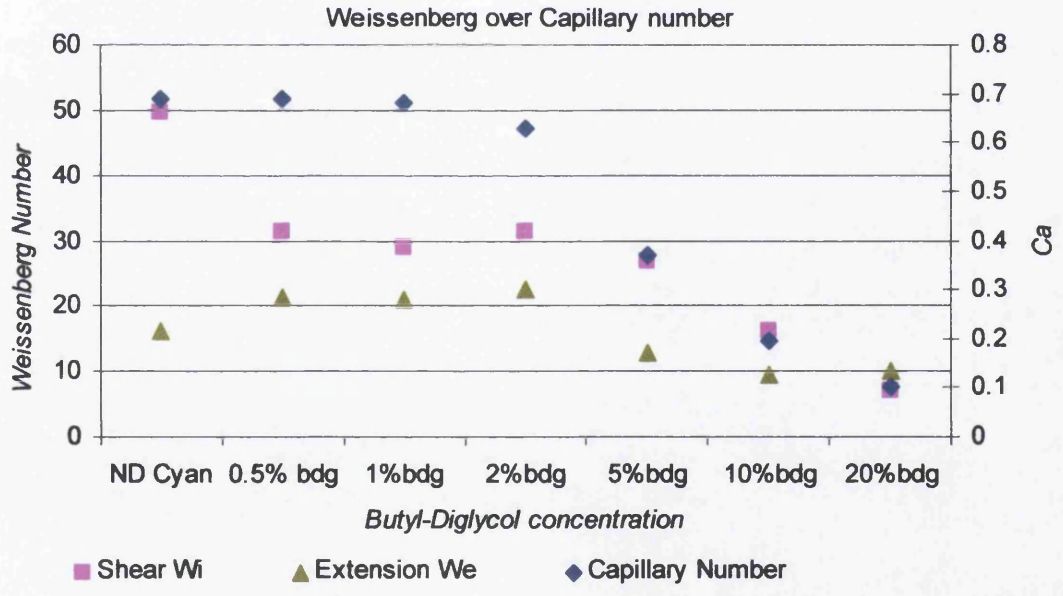

Figure 9-3 Weissenberg number decreases with viscosity of the dilution similar to the capillary number.

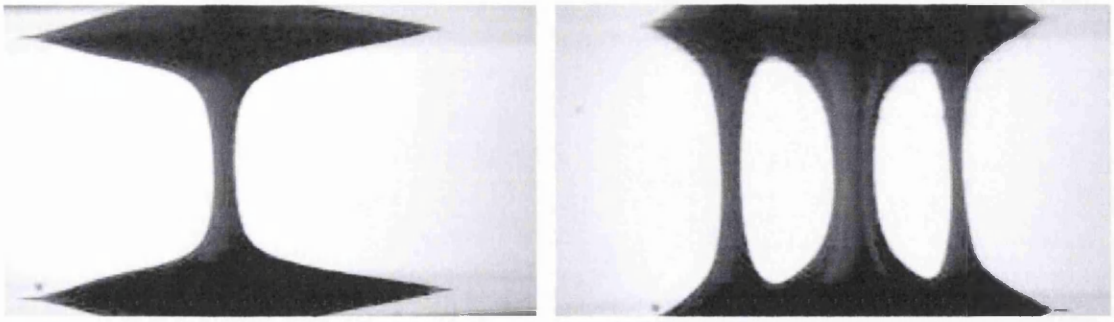

Figure 9-4 Filaments number increases with increased separation speed (right). Low speed allows ink viscoelasticity to forms uniform splitting in a single filament (left).

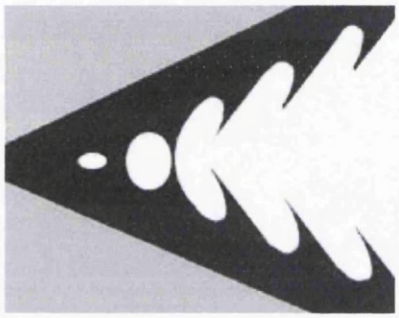

Figure 9-5 High speed video analysis shows that filaments lay down opposite to the rotating direction after splitting and increase ink volume parallel to this direction.

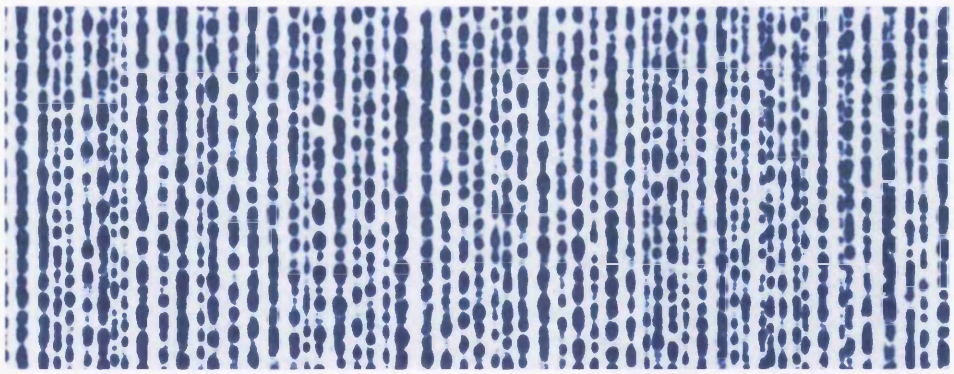

Figure 9-6 Splitting instability is located into both directions of the roller.

The L_{18} orthogonal array indicated a good agreement with the hypothesis on process parameters effect on misting and ribbing phenomena. Ink coverage area decreases with ribbing under the influence of distribution time and roller diameter. Roller diameter varies the splitting angle which also affects variations of the cavities meniscus. When the angle becomes wider, the filaments break-up time decreases with increase of tensile stress due to increase of velocity. The angle decreases with decrease in difference of the rollers perimeters ratio. Distribution time decreases coverage and so it increases ribbing. The ink that forms the ribbing patterns on the

rollers moves laterally with distribution time and this decreases the ribbing frequency along the roller. This occurs due to the rotary speed that forces the ink lines to follow lateral flow along the roller. The lines are combined together and form thicker lines. The lateral flow decreases with the time as the ribbing frequency decreases. As a result, longer distribution time generates ribbing with lower coverage area on the roller, as discussed also in Chapter 6.

The peak number is also affected by the same parameters. Ink film thickness, distribution time and viscosity show a major influence on the formation of ribbing and in terms of peaks or parallel lines. This occurs due to a similar mechanism as described in paragraph above. The increase in distribution time generates fewer lines with higher thickness as function of the distribution speed. Temperature affects the ink viscosity. Viscosity decreases with temperature increase, increasing ink fluidity. Ink also decreases in tack which increases lateral flow rates.

The average ribbing thickness decreases with increased ink film thickness, distribution time and temperature, which decreases viscosity. The parameter of viscosity does not show high effect because temperature affects the viscosity more than the 5% dilution with Butyl-Diglycol (as it was found by tack tests on temperature effects in Chapter 4). The comparison between L_{18} and L_{18}* by inversion of roller levels show that the roller affects the thickness which increases with increase to roller perimeter ratio. This indicates the complexity of the ribbing mechanism. The decrease of splitting angle decreases the tensile stress and so reduces the cavities across the nip as found by extension tests in Section 5.5.1. When the distribution time increases, ribbing average thickness increases due to parallel step moving mechanism of ribbing on rollers. This mechanism is affected more by the increase of temperature than the decrease of viscosity.

Ribbing thickness instability is also affected by distribution time and temperature. Increasing temperature decreases tack and this affects also the lateral flow. Incoming air, which affects the lateral flow, finds free passage due to ribbing at the nip inlet. With increase in time and speed, the incoming air passes the filaments on sides. Individual filaments are met so the intermolecular dynamics combine them into a

wider one with increase in thickness but also increase in the free surface for the incoming air.

Density variations show parallel instabilities in the ribbing direction. Cavities are generated at the nip outlet where expand into filaments which finally split and form a wave-like profile across the width of the roll. This instability decreases when the ink film thickness increases. Dots are formed in row after splitting due to three dimensions perturbation that generates cavities to the orthogonal axis of the nip. This effect is related to thickness variations while dots increase with film thickness. This is an effect of the surface tension or the adhesive character of the ink. The ink extension thickening with extension mechanism as found by extension rheometry in Chapter 5 (section 5.4.2). Dots are formed that increase in volume with the ink film thickness. Due to different roller circumferences, dots do not come in the inlet at the same location so an ellipsoidal dot is formed at the nip outlet.

This phenomenon does not show any influence of other studied parameters. However, ink dots are arriving in the inlet in different volumes and locations and trap air. This air possibly affects the ink structure at the nip exit and generates cavities which expand to filaments. At a steady state, the ink volume ellipsoidal profile is related to the ratio of the two rollers circumferences. As a result ink increases in those areas and generates a different pattern parallel to ribbing with respect to the ink volume at the nip inlet. The increased ink film thickness decreases variation according to density. However, the extremely increased ink volume does not show differences according to grey scale. The variations are decreased because the ink thickness exceeds the saturation density. Variations are more detectable when the ink film thickness decreases.

9.2 Misting and splitting instability

Ink film thickness significantly affects the misting phenomena according to L18 analysis. Misting occurs due to the splitting instability during filaments formation. Increased ink film thickness increases the misting phenomena, with respect to distribution speed and viscosity. Interactions occur between distribution time with speed and temperature with viscosity. Due to onset of ribbing formation, the ink film

thickness increases in certain areas while it is reduced between them. This ink thickness increases with time. While at the beginning of the distribution process ink is low, the thickness increases with the time due to ribbing and forms higher thickness which also forms longer filaments.

Filament stretching generates intermolecular instability. The filament breaks up into two areas between the roller surface. The effect increases with the air that is trapped to the nip inlet. The increased ink allows more air to pass through the nip. Thicker filaments are formed with the dynamic instability due to trapped air bubbles. While rollers stretch the ink at the nip exit, thicker and longer filaments generate aggregated parts along the filaments. Due to separation time, the ink splits into three parts (Figure 9-7). Two ink parts follow the rollers surface due to the adhesive dynamics of ink and one forms the satellite droplet.

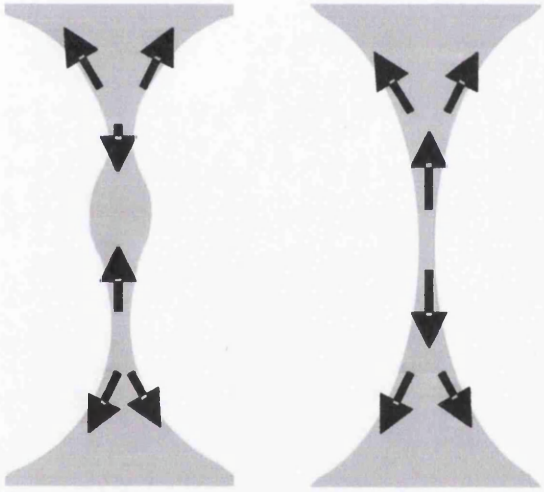

Figure 9-7 Splitting instability due to intermolecular dynamics during filaments stretching. Droplet formation caused on high speed stretching (left). Uniform splitting does not form droplet (right).

The fly away direction of the satellite droplets depends on the break-up of the two thinning points. However, misting is significantly increased by the metallic roller direction as shown in Section 7.3.1.6. This generates two hypotheses. The first hypothesis is that the adhesive forces decrease on the metallic roller surface. The second hypothesis is that droplets are generated by gravitational forces which increase by the metallic roller velocity. Both of them are reliable however, the surface quality effect is more accurate when misting traps from different nips are

compared. Two nips vary at the area of the splitting mechanism on the same roller. The nip with the measurement roller is located on the top of the motor roller and the one with the small roller is located on the front side. However, both of these nips generate similar misting direction, which are located at the bottom area of the metallic roller. Misting is increased on both sides when small elastic roller is present and smaller droplets are formed. Droplets dimensions depend also on the two rollers ratio that are involved in the nip region and decrease in size as the rollers difference increases. Similar results were determined by the metallic rollers of the IGT inking unit. The misting was increased to the gravitational direction of the two metallic rollers as shown in Chapter 7.

Current results and the L_{18} analysis indicate the ink film thickness has a major effect on misting. Each of the misting characteristics increases with the ink film thickness such as coverage area, dots size, variations on size and densities. The increase misting indicates increased coverage area on the trap surface. The misting is carried out by calculation the motor roller side of the trap area because the study focuses on ribbing effects and not on roller effects. There is a significant difference between the two rollers effects. Small roller generates more misting and smaller droplets while large roller generates misting with only a few large droplets when the ink film thickness is significant increased. Misting increases with increased speed and decreased viscosity. Chapter 6 showed that an increase of Butyl-Diglycol dilution with the ink decreases viscoelasticity and tack. Surface tension decreases and smaller droplets are formed that generate misting. Misting droplets are divided into two categories in terms of size. Droplets are divided into those that follow the splitting velocity of the rollers and have certain direction and those that are extremely small and generate a mist around the system.

The increased difference between these two generates a variation in size of droplets. While several droplets fall in the same location a large droplet is carried out due to overlapping effect. Misting size cannot be calculated accurately but it is an average estimation according to the sum of droplets. The ribbing formation shows the uniformity of the ink across the rollers. The uniformity in thickness indicates the ink distribution is uniform. However, misting is generated in uniform levels through the nip. Misting traps illustrates increase effect at roller sides due to lateral flow of the

ink. This shape changes with the dimensions of rollers and it is always under the motor roller. Two characteristic shapes are generated. Figure 9-8 illustrates the characteristic X for the low roller ratio and H for the high low ratio. Two hypotheses are possible for this result. The misting shape is a result of the splitting history and ink distribution is a result of splitting and post-splitting velocity due to centripetal forces of the metallic roller.

Ink shows adhesive dynamics with roller surface due to tack. Rotation generates lateral flow between the nip regions as in ribbing. Misting is uniform at the beginning as the ink film thickness is uniform across the roller. After ribbing is generated, the lines begin to move laterally during rotation. The two rollers are a closed loop system in which the ink rotates under accelerating circular motion which increases ink velocity in the splitting region. Shapes X and H are different by the velocity angle of the sides. The excess ink between the two rollers generates misting because ink is increased on the rollers sides. Rotation generates a characteristic V from the sides to the middle of the roller and opposite so an X-shape is generated. While ribbing is characterised by peaks that generate a W-shape profile, misting is characterised by longer X profile which can vary by ratio of the two rollers at the nip contact.

However, the two mechanisms of misting occur in different splitting locations. The fine misting is generated by the multi rupture of the filaments at the nip exit. Recent studies with high viscous resins (High viscosity IGT oil, measured tack 300) determined high misting at the nip exit which increased with the film thickness (Figure 9-9). This indicates fine misting droplets of inks occur due to the resins or the carrier of the ink. This misting increases with the longer filaments that occur with higher ink film thickness. Elongation speed and adhesive dynamics generate agglomeration of the ink structure that increases surface tension. This effect increases with the influence of trapped air bubbles in the ink. Figure 9-10 illustrates air bubbles that appear on the roller surface after distribution stopped. These ink parts tend to follow the tangential velocity which increases with the gravitational forces (Figure 9-11). The dynamics generate elongation and finally the agglomerate parts split and generate high volume droplets with tangential direction. This second split can form more fine satellite droplets with the filament rupture which interfere

with the agglomerated parts that form high volume droplets. This effect increases at rollers with polish surface qualities with decrease of the cohesive and adhesive dynamics between ink and surface.

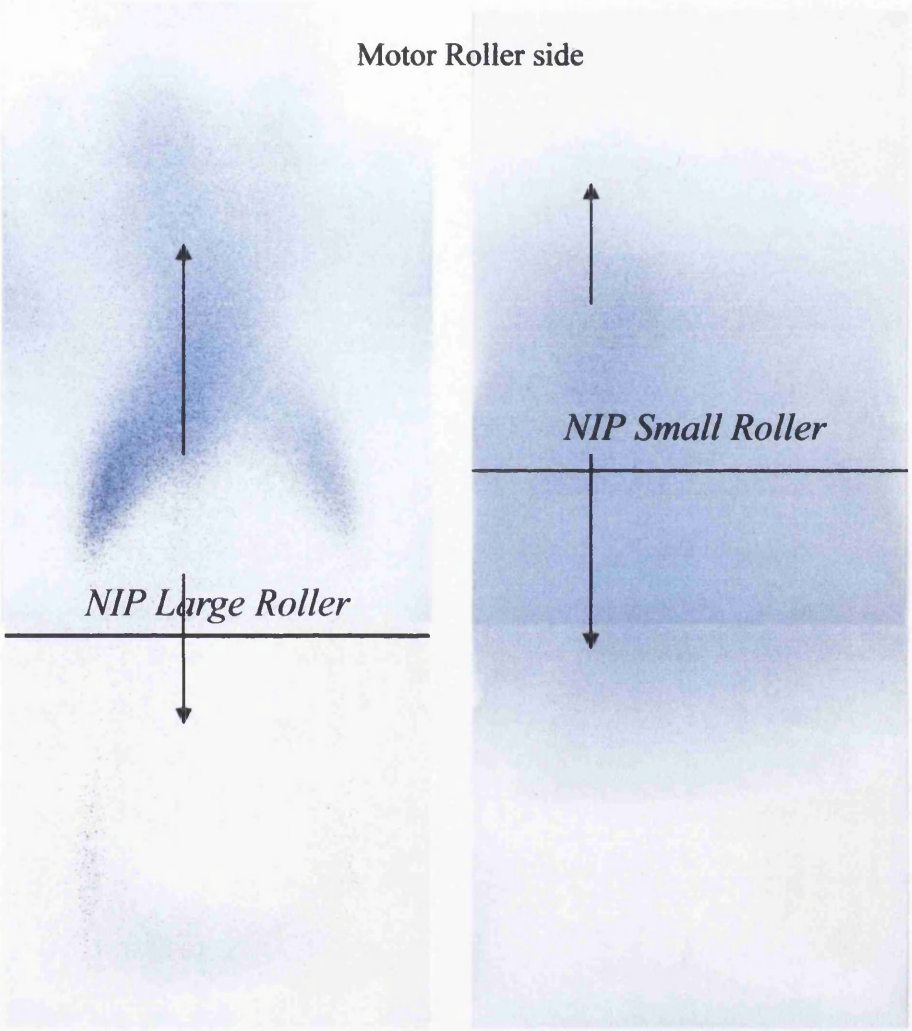

Figure 9-8 Misting increases to the bottom area where gravitational forces are applied to the rotating direction of the motor roller. Small elastic roller with 1.85R. Ratio shows increased misting (right) while misting decreases to the large roller with 1.56R. Ratio (left).

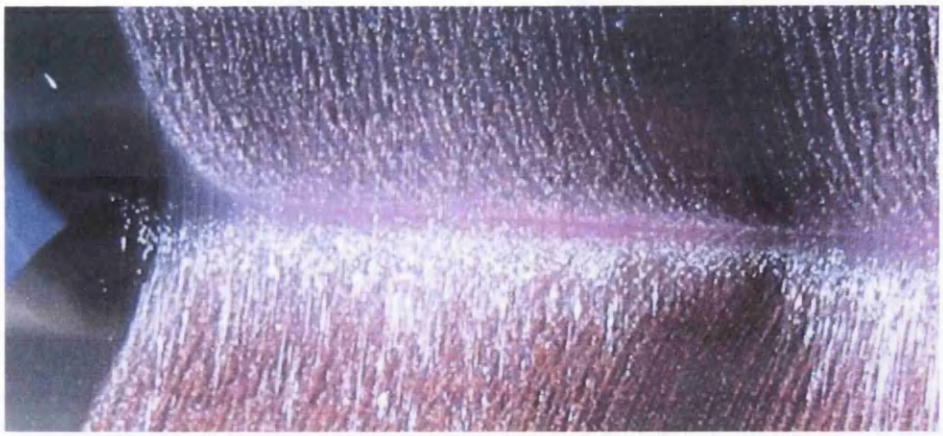

Figure 9-9 The high viscosity IGT oil generates more misting in regards with the studied inks. Measured tack value 300 at 0.8m/s

Figure 9-10 The trapped air comes on the surface of the elastic (left) and the metallic (right) roller after distribution stopped.

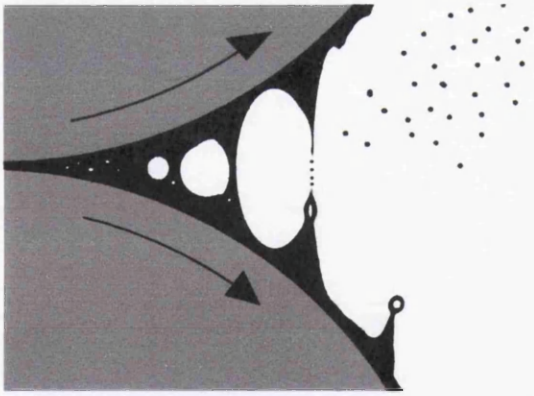

Figure 9-11 Schematic diagram of the established misting mechanisms. The fine misting droplets are formed due to multi rupture of the filaments at the nip exit. On the other hand, trapped air bubbles or ink agglomeration forms higher droplets size that splits again later with the tangential velocity.

9.3 Related phenomena on ink transfer mechanisms

Mathematical models of ink distribution in offset printing calculate the ink volume as an averaged ink volume area per cell on the perimeter of the rollers. As a result there are no cavitation or ribbing effects and no misting. Misting not only occurs at the nip

exit due to fine droplets but also occurs due to the agglomerate parts that split away after the nip that generate both misting but also dropping phenomena of higher ink volume droplets. These phenomena decrease ink film thickness on the system but also randomise ink volume to the following rollers. Ribbing is formed with the cavities at the nip exit where ink filaments are formed and deformed during splitting. The rollers velocity does not allow ink structure recovery and this deformation affects the following splitting at the next nip.

9.3.1 The ribbing effects on ink splitting

Chou (1997) calculated the ink transfer mechanism in lithographic printing process through a mathematical model. Other authors (Guerrette 1985, MacPhee 1998, Paikos 2003) also developed similar models to study ink transfer mechanism. Their results concluded that mathematical models overestimated ink transfer and disagreed with long term ink transfer instabilities of the press (Paikos 2003). Chou (1997) claimed that ribbing had no significant effect on press due to oscillator rollers and as a result he did not calculate ribbing in his model. The results of this thesis show that ribbing is not only long term instability but also affects ink transfer between the nips. The ribbing instability increases with the ink film thickness which also increases with the distribution speed and becomes a three dimensional instability. The oscillator mechanism can randomise the patterns but does not stop the mechanism. As a result, the ribbing instability exists but as a stochastic piled surface on the rollers (Figure 9-12). The ink volume is not constant through the ink transfer and along the rollers surfaces. In order to calculate similar behaviour, any mathematical model of the distribution system will have to take into account the onset of ribbing. This depends on the resolution of the matrix of the mathematical models. The ribbing frequency decreases with the increase of ink film thickness. The cells analysis of the roller model needs to change with the ink film thickness of each of the cells to calculate the deformation of the splitting. The ribbing formation on the rollers can be randomised by the oscillator roller and produce a chess-mat. This is the closest profile that fits ribbing in the mathematical model. Figure 9-13 illustrates a schematic approximation of the ink on the roller surface.

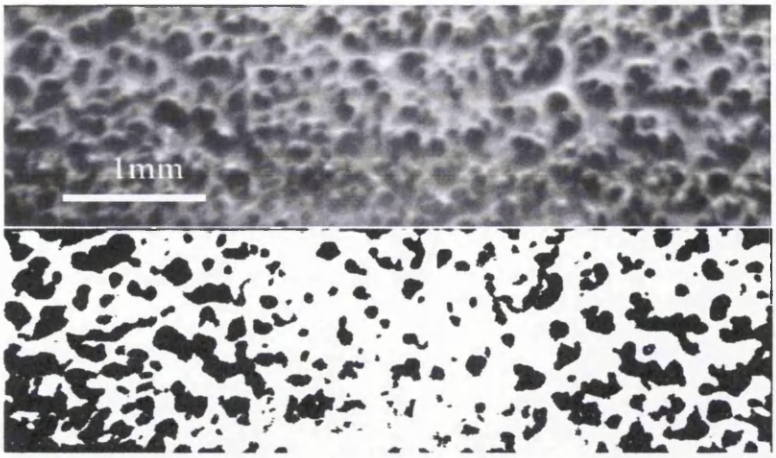

Figure 9-12 The oscillator randomises the ribbing patterns but cavities and filaments deformation generate a stochastic piled ink surface on the rollers. The image illustrates the ink quality on the IGT printing disc.

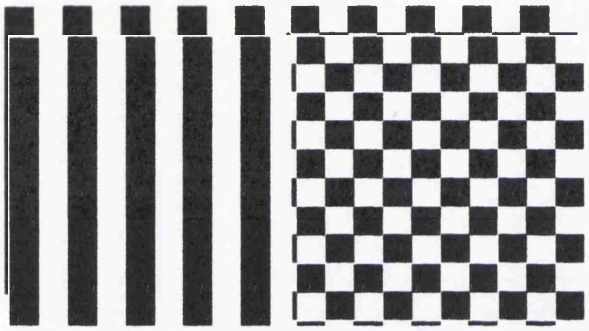

Figure 9-13 The onset of ribbing on the rider roller becomes a chess-mat profile with the oscillator roller. The analysis of the ribbing frequency decreases with the ink film thickness increase on the rollers.

9.3.2 Inking unit configuration and misting

Misting is a complex phenomenon in lithographic printing process. It is not clear where the misting begins or stops and which droplets size belongs to misting. Misting consists of two mechanisms and eventually two different splits. As a result, misting increases at the nip exit with viscosity while increases with velocity and viscosity decrease as also found by Blayo et al (1998). Misting in forward roller distribution systems cannot be solved by modification of inks viscoelasticity. The solution for misting is based on the press unit layout and the distribution system configuration or another mechanistic approach.

Misting increases with the small elastic rollers and the polished surfaces. This leads to the result of wider dimension roller that decreases rollers velocity especially for

the elastic rollers. The reduction depends on speed and viscosity but the results from the current work indicate a reduction from 10% to 50% depend on the parameters. Polished surfaces demand surfaces with higher surface energy with respect to the rubber rollers.

The configuration of the inking unit can affect the misting rates. The rollers size, forward direction and surface qualities are important as much as the location of the next roller and the previous on the ink train. This can be explained by two examples that produce or decrease misting. Figure 9-14 illustrates two examples of rollers configuration for three rollers. The good configuration is based on the concept of the misting ink being trapped by the next rollers. The rotating direction of the first rubber roller-El1 transfers the higher ink film thickness. At the nip exit the misting ink tends to go to the next rubber roller-El3 and follow the nip entrance. The bad configuration allows the ink to escape at the nip exit. The nip exit of rubber roller-El1 and the metallic roller-M2 steers at the free area of the ink train and fine droplets can escape.

The metallic roller surface of the tack tester does not come in contact with any roller at the bottom are where gravity accelerates with roller velocity. The deformable agglomerate ink parts are free to escape due to the dynamics that are applied at this region. These examples focus on the first splitting in order to highlight the importance of the train configuration for the misting. Therefore, the misting phenomena can be controlled by the rollers train configuration in terms of rollers ratio, surface qualities, perimeter and splitting directions. The configuration becomes more important as the ink film thickness increase where increases misting rates. The misting droplets effect on the next roller is negligible instead of cavities and deformation effects that generate ribbing or piled surfaces.

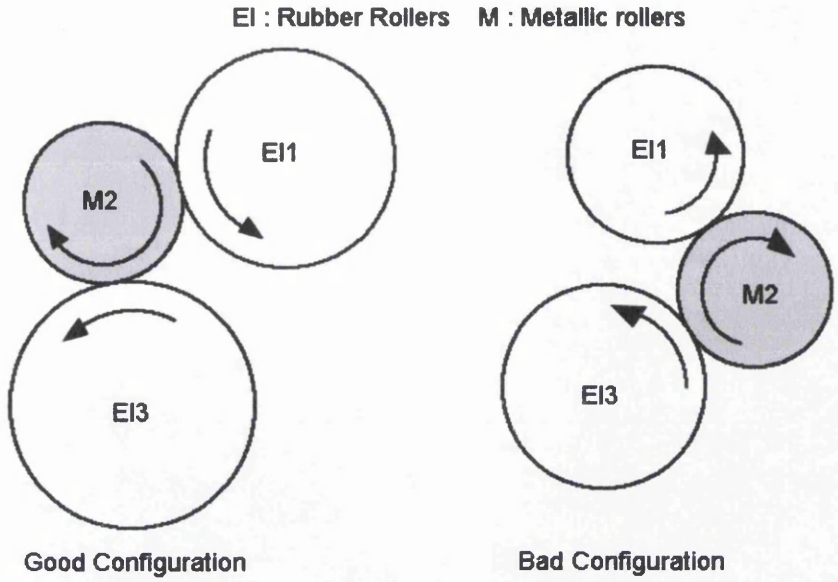

Figure 9-14 The good configuration of the roller train forces the misting ink to the next roller. The bad configuration allows open areas for the misting ink to escape.

9.3.3 Rheology on the lithographic press

The viscosity is fully involved with the ink transfer mechanism and the lithographic printing process. Viscoelasticity rates of the ink affect the ink transfer mechanism. The viscoelasticity decreases when the elastic modulus dominates to the viscous modulus. This difference increases with the shear stress where viscosity and ink flow decreases. However, the current results do not show high shear thinning effect of the ink at the nip rollers region of an elastic and rigid roller. This was determined by relationship of viscosity with tack in Chapter 4 which determined 147/s shear rate according to tack. This was experimentally found by the tack and viscosity responses between the ink dilutions. A high shear region is located at the duct roller where the ink is sheared between the ductor roller and the steady ductor plate. This mechanism may decreases viscosity 50% to 60% depends on the ductor roller speed. This is based on the shear rheometer where the compression of the plate dropped the viscosity 50%. The shear rates of the nip through the ink train do not exceed the shear thinning effects of the ink feeding mechanism. Therefore, viscosity is affected mainly by the system temperature or the fountain solution. The emulsification effects with the fountain solution depend on its additives. Temperature has a large effect on ink viscosity. Modern lithographic presses use water supply through the rollers drums to stabilise the system temperature and the inks viscosity. This probably

eliminates a lot of the shear thinning behaviour of the ink through the distribution system or makes it more unstable. The ink viscosity increases with decrease in temperature. This may affect ribbing patterns that indicate the periodic ink film thickness variation along the rollers.

The tack decreases with viscoelasticity of the ink. The increased tack determines also viscous material and this tends to decrease misting of the splitting mechanism and to increase ribbing patterns as found in Chapters 6 and 7. The viscocapillary thinning rates of the lithographic inks determine similar results relaxation rates with extension thickening trends as found in Chapter 5. High tensile stress is applied by the splitting mechanisms at the nip exit of the rollers. This exceeds significantly the elongation speeds of the rheometer. The high speed elongation tests show significant decrease of extension thickening rates. Elongation rheometry can determine the profile of ribbing that is generated at the splitting mechanism by the contact angle at the break-up time.

9.4 Closure

Current work deals with the ink transfer mechanism and the related phenomena that occur during ink splitting at the nip exit. Rheological characterisation characterised ink performance through a series of test in order to determine the accurate profile. It was found that the process parameters can affect significant the ink performance. Misting and ribbing phenomena are related with the ink splitting mechanism and show a significant influence with the ink film thickness. The effect increased with the presence of air that generates cavitation at the nip exit.

Ribbing occurs in ink deformation under high strain rates. The high tensile stress deforms the generate viscoelastic deformation along filament length and generate instabilities. The filaments expand at the nip exit and break in multiple areas. This mechanism forms micro droplets with negligible weight and turbulence direction. On the other hand deformed filaments are forced to flow away due to tangential velocity which increases with gravitational dynamics.

The lower ribbing frequency forms thicker and longer filament the produce high misting rates. However, high misting rates decrease ink film thickness from the

rollers surface. This leads to progressive increase of ribbing patterns frequency. Both of these phenomena can indicate the amount of the ink on rollers surface by detailed monitoring. Finally a significant effect is determined by the presence of air. Lateral flow on the rollers and filaments rupture may be a related to the effect of the air in the nip inlet.

10. Conclusions and recommendations for future work

The fundamental phenomena related to the ink transfer mechanism in lithographic offset printing have been investigated. The study focused on factors which affect the ribbing and misting phenomena. These phenomena are related to the ink transfer mechanism and instabilities within the ink splitting mechanism at the nip exit. The ribbing and misting phenomena affect the ink film thickness along the rollers. The process parameters influence such phenomena in ink distribution systems. The distribution rollers train configuration significantly affects these mechanisms.

The ribbing profile is characterised by peak frequency and amplitude which is primarily related to the ink film thickness. The oscillator roller decreases the frequency and increases the lateral flow at the roller nip. Ribbing is primary generated due to the elongation mechanism at the nip exit, where ink is deformed in filaments due to cavities and splits. The cavities are generated between areas with lower ink film thickness along the roller length at the nip exit due to decreased intermolecular dynamics and viscoelastic failure of the ink structure. The subsequent splitting through the nips generates ribbing. The ribbing profile indicates the amount of ink film thickness along the roller length. The fine ribbing patterns are characterised by high ribbing frequency and high amplitude. The ribbing width is affected by the rotations due to filaments deformation and can vary by the distribution time and speed or rollers ratio. The onset of ribbing is affected by the separation angle and the rheological profile of the ink. The separation angle is a function of rollers ratio and the ink film thickness. Ribbing formation is affected by viscosity changes and as a result by temperature that affects viscosity. The elongation mechanism affects the elasticity of the structure and generates deformed thin filaments. Ribbing width increases with decrease in ink elasticity and viscosity.

Tack decreases with the ribbing frequency and ink coverage area along the rollers. It also decreases with distribution time due to ribbing frequency variations and the misting rates that decrease the ink film thickness on the distribution rollers. Different ribbing frequencies by the same ink volume along the rollers do not have the same

tack. The increase of the ink film thickness decreases ribbing frequency which tends to decrease with the viscosity.

The misting increases with the decrease in ribbing peak frequency. The decrease of ribbing frequency tends to increase misting rates due to increase of ink film thickness variation. This produces higher misting (for same ink film thickness with wider range of ink droplets) in higher speed region. The misting rates are constant as long as the ink film thickness is constant. Tack does not change when misting is not significant. Misting increases by increase of ink film thickness (more ink), time run (time to collect), decreased viscosity (by temperature or dilution), and increase in roller ratio (different speed of rollers). At low speed misting appears low, constant and independent from ribbing. The roller centrifugal forces increase lateral flow of the ink on the rollers, which decreases the ribbing frequency and increases the misting rate and droplet range. The oscillator roller generates a wave profile of ink through the rollers' length and as a result misting increases in those areas across the roller length where ink is increased.

The tack is related to the shear and the extension viscosity and decreases with them. The lithographic ink profile is characterised by steady tack, shear thinning and extension thickening behaviour. Temperature increase affects this behaviour and decreases viscosity with the elasticity. This decreases tack and viscocapillary thinning times. The relations between tack and shear indicate low shear rates at the nip region but do not provide significant shear thinning effects. The shear thinning behaviour decreases with concentration. This also affects thixotropy and relaxation which also decreases. Hysteresis loop area decreases with increase in volume and decreases significantly with increase in temperature. The shear stress and temperature increase indicate a rapid 40% to 60% decrease in viscosity. The extension viscosity indicates extension thickening effect that occurs to relaxation of ink structure. Extension viscosity decreases with decrease in shear viscosity but the thickening effect decreases with tensile stress or elongation speed. The extension of ink affects the small area of fluid that forms the filament.

The decrease in shear viscosity indicates a decrease in tack, viscoelasticity, surface tension and extension viscosity. A forward roll distribution system does not affect

tack when temperature, speed, ink film thickness, and viscosity are constant. The relations between rheology and tack indicate that low shear rates in the nip region do not significantly affect the viscosity of the ink when all the parameters are constant. When viscoelastic fluids become extremely thin, present viscoelastic deformation which forces the filaments to expand while present slow recovery rates.

The misting trap analysis indicates the ink distribution history on the roller train with respect to the rollers ratio, the distribution speed, and ink film thickness. The misting profile is characterised by the range of droplets size and dispersion along the roller nip. Misting increases with decrease in viscosity. This can be the effect of any parameter that decreases viscosity, such as a temperature increase. It increases with gravitational effects which also increase with ink volume or decrease in viscosity. It also increases with decrease of the angle between tangential and gravitational axes due to nip configuration. Misting occurs due to two splitting mechanisms; primary splitting which occurs at the nip exit, and the rollers' velocity. The proportion of these two mechanisms depends on the viscosity, the ink film thickness and the roller ratio. Misting increases on the polished surfaces due to decreased cohesive dynamics. It shows gravitational direction which increase with the roller velocity effects.

10.1 Recommendations for future work

The transfer instabilities occur to ribbing and misting phenomena. This generates a series of suggestions for future studies in order to understand in detail the ink transfer mechanisms.

Ribbing is related to the ink film thickness and it is important to study how the deformed filaments at the nip exit are affected by the nip entrance. This can explain the importance of the ribbing in a mathematical model. It is also relevant to study the effect of the gap at the nip region.

The ink viscoelasticity and the roller surface qualities affect ribbing and misting. It is necessary to establish the rheological profile of the inks and the roller surface qualities that reduce such phenomena. This is important for printing electronics

applications where any ink film thickness instability affects the printing qualities and printed solid areas.

The ink distribution process indicates an accelerating split ratio. The rollers are not necessarily repellent or receptive to the ink. This is generated by a coating process through the ink distribution and generates ink receptive characteristics. Such studies could establish the amount of ink that participates through the ink transfer mechanism and the amount of ink that is stabilised through the distribution process. Through this study long term instabilities on ink transfer mechanism can also be established.

Misting also occurs due to the splitting instability that generates agglomerate parts. It was found also that the trapped air bubbles increase such effects. Thus, it seems relevant to investigate the dynamics of the bubbles with the viscoelastic profile of the inks. Such studies demand transparent fluids in order to monitor such phenomena. As a result, it is important to establish a range of model fluids that can be used to monitor phenomena such as the viscoelastic deformation through the tensile mechanisms.

Finally, it is important to establish standard methodologies on ink materials that characterise not only the rheological profile but also the distribution and printability profile of the inks. The current studies on tack showed that a shortcut can be provided to the time consuming rheological examinations.

Appendix 1. Table for IGT high speed inking unit

IGT

P.O.box 12668
1100 AR Amsterdam
The Netherlands
Tel. +31.20.4099300

Ink Volume and Layer thickness relation for IGT High Speed Inking Unit 4

Volume (ml)		Ink film thickness in micron												Add
0.10	1.00	0.80	1.60	2.40	3.20	1.00	1.50	2.00	2.50	3.00	3.50	4.00	8.00	%
Film (micron)		Required volume from inkpipette in ml												

Unsegmented toproller

Disc type	width	nr.																
ALU A-type	10 mm	1	0.64	6.42	0.12	0.25	0.37	0.50	0.16	0.23	0.31	0.39	0.47	0.55	0.62	1.25	1
		2	0.63	6.34	0.13	0.25	0.38	0.50	0.16	0.24	0.32	0.39	0.47	0.55	0.63	1.26	3
		3	0.63	6.26	0.13	0.26	0.38	0.51	0.16	0.24	0.32	0.40	0.48	0.56	0.64	1.28	4
		4	0.62	6.18	0.13	0.26	0.39	0.52	0.16	0.24	0.32	0.40	0.49	0.57	0.65	1.29	5
	20 mm	1	0.63	6.34	0.13	0.25	0.38	0.50	0.16	0.24	0.32	0.39	0.47	0.55	0.63	1.26	3
		2	0.62	6.18	0.13	0.26	0.39	0.52	0.16	0.24	0.32	0.40	0.49	0.57	0.65	1.29	5
		3	0.60	6.03	0.13	0.27	0.40	0.53	0.17	0.25	0.33	0.41	0.50	0.58	0.66	1.33	8
		4	0.59	5.88	0.14	0.27	0.41	0.54	0.17	0.26	0.34	0.43	0.51	0.60	0.68	1.36	10
	32 mm	1	0.62	6.24	0.13	0.26	0.38	0.51	0.16	0.24	0.32	0.40	0.48	0.56	0.64	1.28	4
		2	0.60	6.00	0.13	0.27	0.40	0.53	0.17	0.25	0.33	0.42	0.50	0.58	0.67	1.33	8
		3	0.58	5.77	0.14	0.28	0.42	0.55	0.17	0.26	0.35	0.43	0.52	0.61	0.69	1.39	12
		4	0.56	5.56	0.14	0.29	0.43	0.58	0.18	0.27	0.36	0.45	0.54	0.63	0.72	1.44	16
	50 mm	1	0.61	6.10	0.13	0.26	0.39	0.52	0.16	0.25	0.33	0.41	0.49	0.57	0.66	1.31	6
		2	0.57	5.74	0.14	0.28	0.42	0.56	0.17	0.26	0.35	0.44	0.52	0.61	0.70	1.39	12
		3	0.54	5.43	0.15	0.29	0.44	0.59	0.18	0.28	0.37	0.46	0.55	0.65	0.74	1.47	19
		4	0.51	5.14	0.16	0.31	0.47	0.62	0.19	0.29	0.39	0.49	0.58	0.68	0.78	1.56	25
Rubber A-type	20 mm	1	0.63	6.33	0.13	0.25	0.38	0.51	0.16	0.24	0.32	0.39	0.47	0.55	0.63	1.26	3
		2	0.62	6.16	0.13	0.26	0.39	0.52	0.16	0.24	0.32	0.41	0.49	0.57	0.65	1.30	5
		3	0.60	6.01	0.13	0.27	0.40	0.53	0.17	0.25	0.33	0.42	0.50	0.58	0.67	1.33	8
		4	0.59	5.86	0.14	0.27	0.41	0.55	0.17	0.26	0.34	0.43	0.51	0.60	0.68	1.37	11
	32 mm	1	0.62	6.23	0.13	0.26	0.39	0.51	0.16	0.24	0.32	0.40	0.48	0.56	0.64	1.28	4
		2	0.60	5.98	0.13	0.27	0.40	0.54	0.17	0.25	0.33	0.42	0.50	0.59	0.67	1.34	9
		3	0.57	5.74	0.14	0.28	0.42	0.56	0.17	0.26	0.35	0.44	0.52	0.61	0.70	1.39	13
		4	0.55	5.52	0.14	0.29	0.43	0.58	0.18	0.27	0.36	0.45	0.54	0.63	0.72	1.45	17
	50 mm	1	0.61	6.08	0.13	0.26	0.39	0.53	0.16	0.25	0.33	0.41	0.49	0.58	0.66	1.31	6
		2	0.57	5.71	0.14	0.28	0.42	0.56	0.18	0.26	0.35	0.44	0.53	0.61	0.70	1.40	13
		3	0.54	5.38	0.15	0.30	0.45	0.59	0.19	0.28	0.37	0.46	0.56	0.65	0.74	1.49	19
		4	0.51	5.09	0.16	0.31	0.47	0.63	0.20	0.29	0.39	0.49	0.59	0.69	0.79	1.57	26
C-type	15 mm	1	0.64	6.38	0.13	0.25	0.38	0.50	0.16	0.24	0.31	0.39	0.47	0.55	0.63	1.25	2
		2	0.63	6.25	0.13	0.26	0.38	0.51	0.16	0.24	0.32	0.40	0.48	0.56	0.64	1.28	4
		3	0.61	6.13	0.13	0.26	0.39	0.52	0.16	0.24	0.33	0.41	0.49	0.57	0.65	1.30	6
		4	0.60	6.02	0.13	0.27	0.40	0.53	0.17	0.25	0.33	0.42	0.50	0.58	0.66	1.33	8
	20 mm	1	0.63	6.34	0.13	0.25	0.38	0.51	0.16	0.24	0.32	0.39	0.47	0.55	0.63	1.26	3
		2	0.62	6.17	0.13	0.26	0.39	0.52	0.16	0.24	0.32	0.41	0.49	0.57	0.65	1.30	5
		3	0.60	6.02	0.13	0.27	0.40	0.53	0.17	0.25	0.33	0.42	0.50	0.58	0.66	1.33	8
		4	0.59	5.87	0.14	0.27	0.41	0.55	0.17	0.26	0.34	0.43	0.51	0.60	0.68	1.36	11
	35 mm	1	0.62	6.21	0.13	0.26	0.39	0.52	0.16	0.24	0.32	0.40	0.48	0.56	0.64	1.29	5
		2	0.59	5.94	0.13	0.27	0.40	0.54	0.17	0.25	0.34	0.42	0.50	0.59	0.67	1.35	9
		3	0.57	5.69	0.14	0.28	0.42	0.56	0.18	0.26	0.35	0.44	0.53	0.61	0.70	1.40	14
		4	0.55	5.47	0.15	0.29	0.44	0.59	0.18	0.27	0.37	0.46	0.56	0.64	0.73	1.46	18
	50 mm	1	0.61	6.09	0.13	0.26	0.39	0.53	0.16	0.25	0.33	0.41	0.49	0.57	0.66	1.31	6
		2	0.57	5.73	0.14	0.28	0.42	0.56	0.17	0.26	0.35	0.44	0.52	0.61	0.70	1.40	13
		3	0.54	5.41	0.15	0.30	0.44	0.59	0.19	0.28	0.37	0.46	0.56	0.65	0.74	1.48	19
		4	0.51	5.12	0.16	0.31	0.47	0.63	0.20	0.29	0.39	0.49	0.59	0.68	0.78	1.56	25

Two segment toproller

ALU A-type	10 mm	1	1.33	13.34	0.06	0.12	0.18	0.24	0.07	0.11	0.15	0.19	0.22	0.26	0.30	0.60	3
		2	1.30	12.99	0.06	0.12	0.18	0.25	0.06	0.12	0.16	0.19	0.23	0.27	0.31	0.62	5
	20 mm	1	1.30	12.99	0.06	0.12	0.18	0.25	0.06	0.12	0.15	0.19	0.23	0.27	0.31	0.62	5
		2	1.23	12.33	0.06	0.13	0.19	0.26	0.06	0.12	0.16	0.20	0.24	0.28	0.32	0.65	11
	32 mm	1	1.26	12.59	0.06	0.13	0.19	0.25	0.06	0.12	0.16	0.20	0.24	0.28	0.32	0.64	8
		2	1.16	11.63	0.07	0.14	0.21	0.28	0.09	0.13	0.17	0.21	0.26	0.30	0.34	0.69	16
	50 mm	1	1.20	12.03	0.07	0.13	0.20	0.27	0.06	0.12	0.17	0.21	0.25	0.29	0.33	0.66	12
		2	1.07	10.72	0.07	0.15	0.22	0.30	0.09	0.14	0.19	0.23	0.28	0.33	0.37	0.75	25
Rubber A-type	20 mm	1	1.30	12.96	0.06	0.12	0.19	0.25	0.06	0.12	0.15	0.19	0.23	0.27	0.31	0.62	6
		2	1.23	12.28	0.07	0.13	0.20	0.26	0.06	0.12	0.16	0.20	0.24	0.29	0.33	0.65	11
	32 mm	1	1.25	12.54	0.06	0.13	0.19	0.26	0.06	0.12	0.16	0.20	0.24	0.28	0.32	0.64	9
		2	1.16	11.56	0.07	0.14	0.21	0.28	0.09	0.13	0.17	0.22	0.26	0.30	0.35	0.69	17
	50 mm	1	1.20	11.96	0.07	0.13	0.20	0.27	0.06	0.13	0.17	0.21	0.25	0.29	0.33	0.67	13
		2	1.06	10.61	0.08	0.15	0.23	0.30	0.09	0.14	0.19	0.24	0.28	0.33	0.38	0.75	28
C-type	15 mm	1	1.32	13.15	0.06	0.12	0.18	0.24	0.06	0.11	0.15	0.19	0.23	0.27	0.30	0.61	4
		2	1.26	12.63	0.06	0.13	0.19	0.25	0.06	0.12	0.16	0.20	0.24	0.28	0.32	0.63	8
	20 mm	1	1.30	12.97	0.06	0.12	0.18	0.25	0.06	0.12	0.15	0.19	0.23	0.27	0.31	0.62	5
		2	1.23	12.31	0.07	0.13	0.20	0.26	0.06	0.12	0.16	0.20	0.24	0.28	0.33	0.65	11
	35 mm	1	1.25	12.47	0.06	0.13	0.19	0.26	0.06	0.12	0.16	0.20	0.24	0.28	0.32	0.64	9
		2	1.14	11.42	0.07	0.14	0.21	0.28	0.09	0.13	0.18	0.22	0.26	0.31	0.35	0.70	18
	50 mm	1	1.20	12.00	0.07	0.13	0.20	0.27	0.06	0.13	0.17	0.21	0.25	0.29	0.33	0.67	13
		2	1.07	10.66	0.08	0.15	0.23	0.30	0.09	0.14	0.19	0.23	0.28	0.33	0.38	0.75	25

Four segment toproller

ALU A-type	10 mm	1	2.87	28.72	0.03	0.06	0.08	0.11	0.03	0.05	0.07	0.09	0.10	0.12	0.14	0.28	6
	20 mm	1	2.71	27.13	0.03	0.06	0.09	0.12	0.04	0.06	0.07	0.09	0.11	0.13	0.15	0.29	11
	32 mm	1	2.54	25.44	0.03	0.06	0.09	0.13	0.04	0.06	0.08	0.10	0.12	0.14	0.16	0.31	17
	50 mm	1	2.33	23.26	0.03	0.07	0.10	0.14	0.04	0.06	0.09	0.11	0.13	0.15	0.17	0.34	24
Rubber A-type	20 mm	1	2.70	26.99	0.03	0.06	0.09	0.12	0.04	0.06	0.07	0.09	0.11	0.13	0.15	0.30	12
	32 mm	1	2.52	25.25	0.03	0.06	0.10	0.13	0.04	0.06	0.08	0.10	0.12	0.14	0.16	0.32	17
	50 mm	1	2.30	23.01	0.03	0.07	0.10	0.14	0.04	0.07	0.09	0.11	0.13	0.15	0.17	0.35	25
C-type	15 mm	1	2.78	27.85	0.03	0.06	0.09	0.11	0.04	0.05	0.07	0.09	0.11	0.13	0.14	0.29	9
	20 mm	1	2.71	27.08	0.03	0.06	0.09	0.12	0.04	0.06	0.07	0.09	0.11	0.13	0.15	0.30	11
	35 mm	1	2.49	24.95	0.03	0.06	0.10	0.13	0.04	0.06	0.08	0.10	0.12	0.14	0.16	0.32	18
	50 mm	1	2.31	23.14	0.03	0.07	0.10	0.14	0.04	0.06	0.09	0.11	0.13	0.15	0.17	0.35	24

Appendix 2. Frequency sweep test

Viscous modulus dominates to elastic modulus with complex viscosity dependent on frequency for the low diluted ink with Butyl-Diglycol.

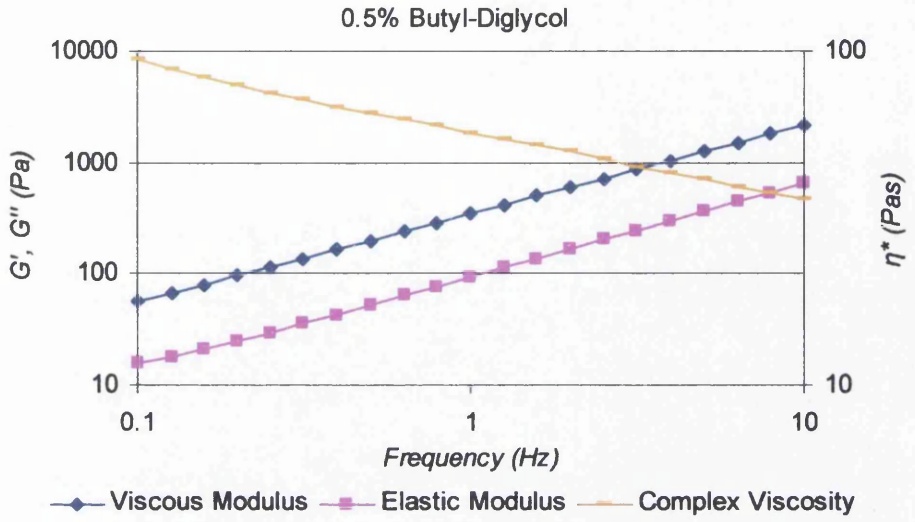

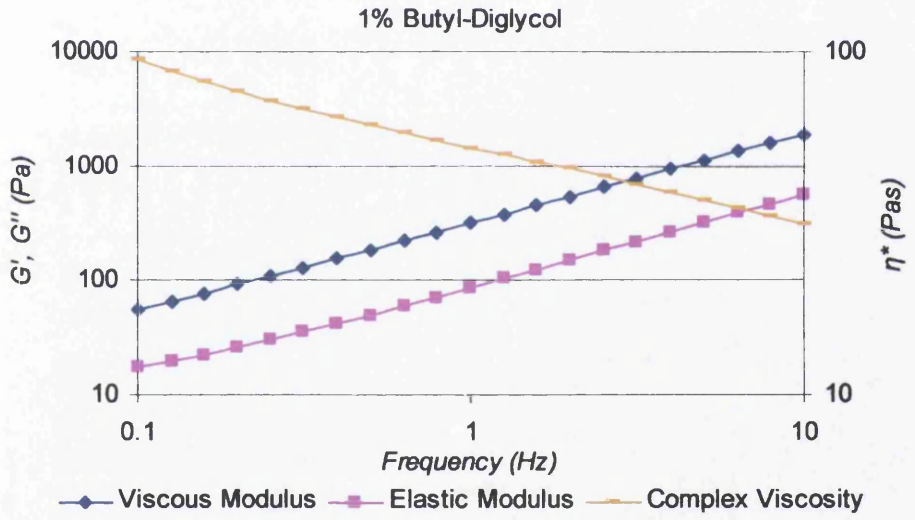

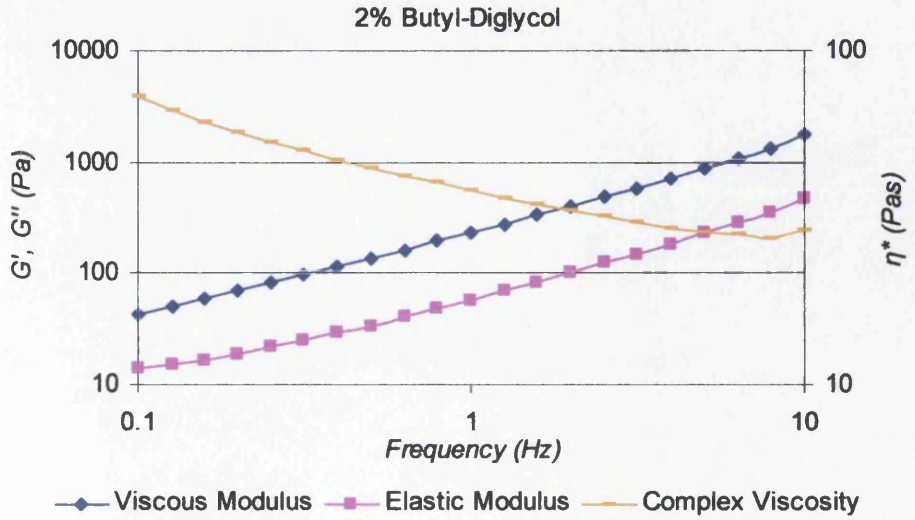

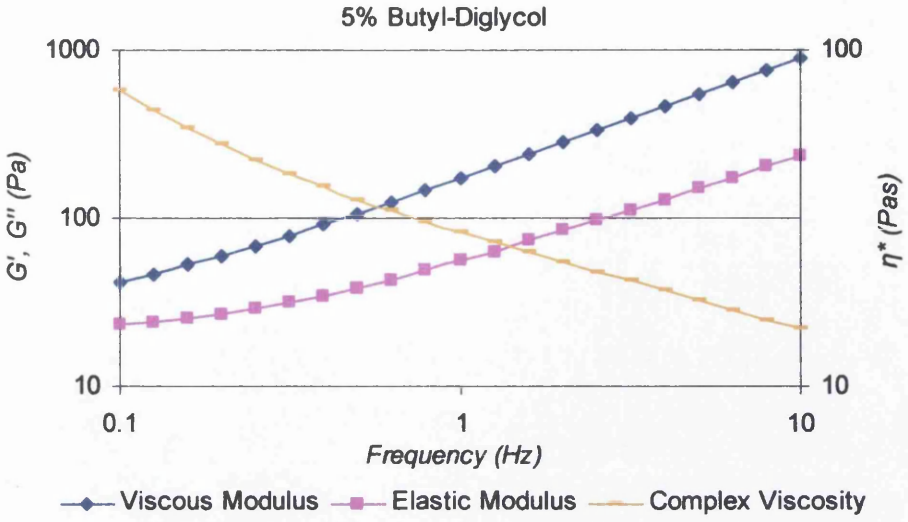
5% Butyl-Diglycol
1000
100
10
100
10
0.1
1
10
G', G'' (Pa)
η* (Pas)
Frequency (Hz)
Viscous Modulus
Elastic Modulus
Complex Viscosity

Appendix 3. Orthogonal Array L18 and L18* Modification

Orthogonal Array was carried out by two tables. The difference occurs to the rollers ratio factor that was set in two levels. In the second L18* the rollers ratio levels are inverted. This allows calculating tack because only one roller operates as measure roller on the IGT tack tester. On the other hand, this allows studying the effect of the parameters settings with the rollers perimeter effect.

Othrogonal Array L18								
Factors	2 Roller	3 film thick	3 Time	3 Speed	3 Temp	Viscosity	Error analysis	
run	a	b	c	d	e	f	XX	VV
1	a1	b1	c1	d1	e1	R	1	1
2	a1	b1	c2	d2	e2	R2	2	2
3	a1	b1	c3	d3	e3	5	3	3
4	a1	b2	c1	d1	e2	R2	3	3
5	a1	b2	c2	d2	e3	5	1	1
6	a1	b2	c3	d3	e1	R	2	2
7	a1	b3	c1	d2	e1	5	2	3
8	a1	b3	c2	d3	e2	R	3	1
9	a1	b3	c3	d1	e3	R2	1	2
10	a2	b1	c1	d3	e3	R2	2	1
11	a2	b1	c2	d1	e1	5	3	2
12	a2	b1	c3	d2	e2	R	1	3
13	a2	b2	c1	d2	e3	R	3	2
14	a2	b2	c2	d3	e1	R2	1	3
15	a2	b2	c3	d1	e2	5	2	1
16	a2	b3	c1	d3	e2	5	1	2
17	a2	b3	c2	d1	e3	R	2	3
18	a2	b3	c3	d2	e1	R2	3	1

Othrogonal Array L18*								
Factors	2 Roller	3 film thick	3 Time	3 Speed	3 Temp	Viscosity	Error analysis	
run	a	b	c	d	e	f	XX	VV
1	a2	b1	c1	d1	e1	R	1	1
2	a2	b1	c2	d2	e2	R2	2	2
3	a2	b1	c3	d3	e3	5	3	3
4	a2	b2	c1	d1	e2	R2	3	3
5	a2	b2	c2	d2	e3	5	1	1
6	a2	b2	c3	d3	e1	R	2	2
7	a2	b3	c1	d2	e1	5	2	3
8	a2	b3	c2	d3	e2	R	3	1
9	a2	b3	c3	d1	e3	R2	1	2
10	a1	b1	c1	d3	e3	R2	2	1
11	a1	b1	c2	d1	e1	5	3	2
12	a1	b1	c3	d2	e2	R	1	3
13	a1	b2	c1	d2	e3	R	3	2
14	a1	b2	c2	d3	e1	R2	1	3
15	a1	b2	c3	d1	e2	5	2	1
16	a1	b3	c1	d3	e2	5	1	2
17	a1	b3	c2	d1	e3	R	2	3
18	a1	b3	c3	d2	e1	R2	3	1

Appendix 4. Ribbing, Rollers Ratio and Ink Film Thickness interactions for L18/L18* Orthogonal Array

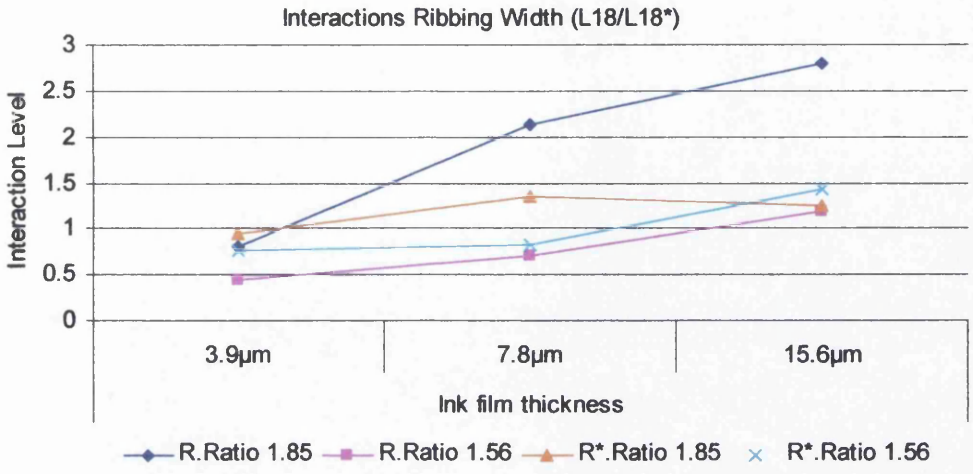

The rollers ratio show some interactions with the inversion of levels. This indicates an effect with the other factors levels of the array.

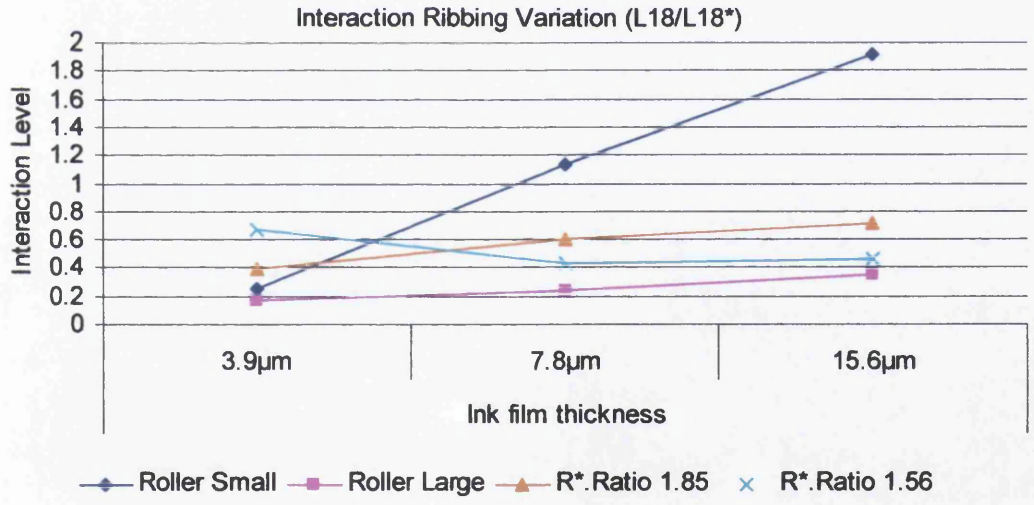

Rollers ratio interacts with the low level of ink film thickness and affects instabilities on ribbing .

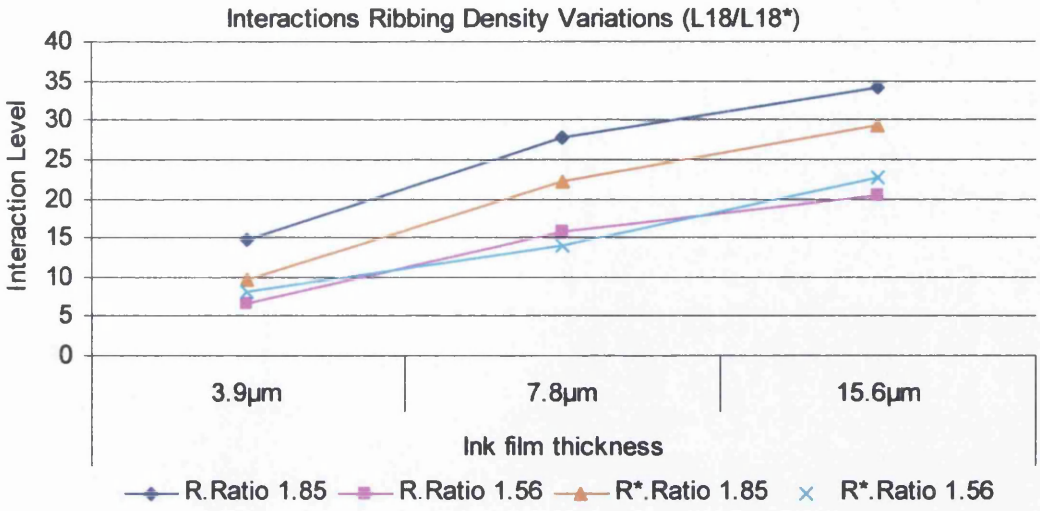

Ribbing variations increase with the ink film thickness and no specific interactions are indicated with rollers ratio levels.

Appendix 5. Misting, Rollers Ratio and Ink Film Thickness interactions for L18/L18* Orthogonal Array

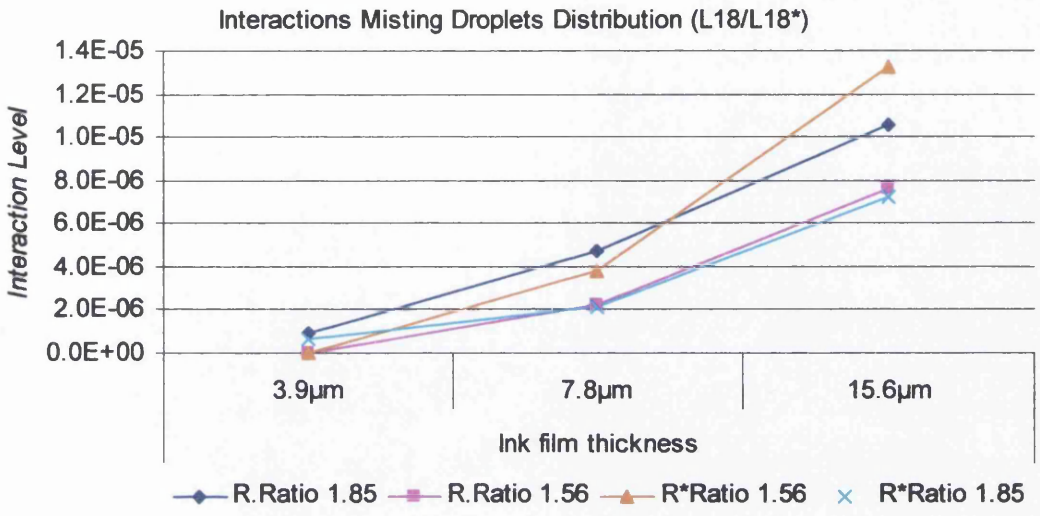

The roller ratio indicate interaction with the low ink film thickness at misting droplets dimensions.

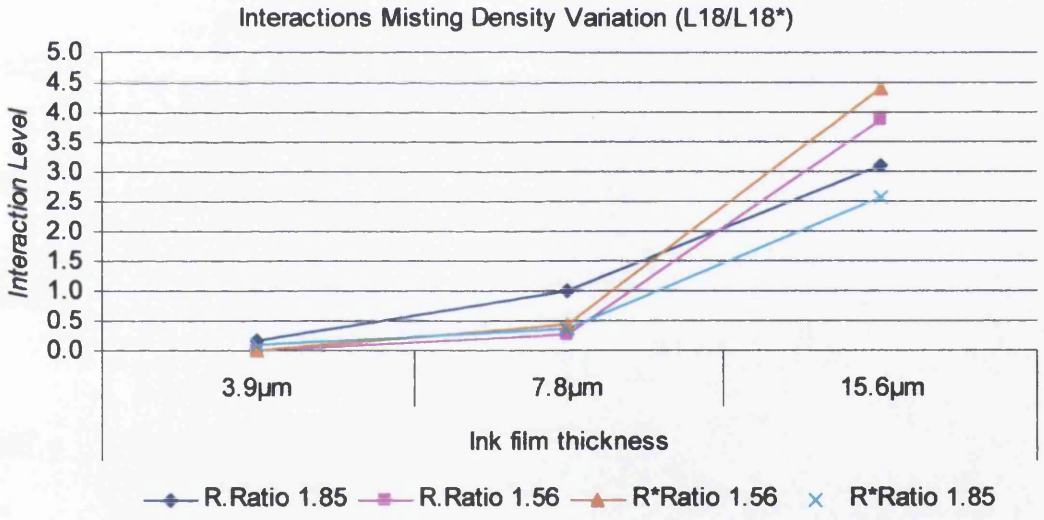

Misting increases in variations between the rollers ratio when ink film thickness increases.

References

Adams R. and Romano F.J, 1996, "Computer to Plate: Automating the printing industry", GATF, Pittsburg, ISBN 0-883-62191-6.

Al-Ganainy G. S. and Mostafa M. M, 2004, "Transient Creep and Creep Recovery Behaviour of Cu-2wt%Sn Alloy Near the Transformation Temperature", Egypt J. Sol. Vol. 27, No. 1, pp. 121-133.

Amari T, Wei X. and Watanabe K., 1992, "Viscoelastic properties of suspensions in parallel superposition of steady flow and oscillation", Theoretical and Applied Rheology, pp. 573-579

Anna L.S, McKinley H.G, Nguyen A.D, Sridhar T, Huang J. and James F.D, (2001), "An interlaboratory comparison of measurements from filaments-stretching rheometers using common test fluids", Journal of Rheology, Vol. 45, No. 1, pp. 83-114.

Aspler J.S, Zang Y.H., and Larondo L. 1997, "Printing tack development and coated paper structure", TAGA proceedings, pp. 1-19.

Atzelt B.P, 1996, "User documentation of the program system INKTEAM V.2", Technical University of Chemnitz

Banks W. and Mill C. 1954 "Some observations on the behaviour of liquids between rotating rollers", Royal Society Proceedings A222, pp. 414-419.

Bazilevsky A.V., Entov V.M, Lerner M.M. and Rozhkov A.N, 1997, "Failure of Polymer Solution Filaments", Polymer Science Ser. 39, pp. 316-324.

Bazilevsky A.V., Entov V.M. and Rozhkov A.N, (1990), "Liquid Filament Microrheometer and Some of its Applications", Third European Rheology Conference, Elsevier, pp. 41-43.

Bird B.R, Curtiss C.F. Armstrong R.C. Hassager O., 1987, "Dynamics of Polymeric Liquids", second ed., John Wiley & Sons, New York. ISBN 0-471-80245-X.

Bisset D.E., Goodacre C., Idle H.A., Leach R.H., Williams C.H., 1979, "The printing ink manual", Third edition, Northwood Books, U.K. ISBN 0-948-90581-6.

Blayo A., Fang Waig Sandrine, Gandini A., Le Nest J.F., 1997, "Study of ink misting phenomena", TAGA Conference Proceedings, pp. 791-806.

Blayo A., Gandini A., Le Nest J.F, 1996, "Rheological properties of heatset inks", TAGA Conference Proceedings, pp. 36-43.

Bradford J.R., 1954, "Lithographic press ink distribution studies by radiotracer techniques", TAGA Conference Proceedings, pp. 1-14

Breede H. M., 2006, "Handbook of graphic arts equations", PIA/GATFpress, Pittsburgh, ISBN 0-883-62246-7

Carvalho M. S., 1996, "Roll coating flows in rigid and deformable gaps", Ph.D. thesis, University of Minnesota, Minneapolis

Carvalho M. S., Anderson T.J. Scriven L.E., 1994 "Ribbing instability in forward deformable roll coating", TAPPI Coating Conference Proceedings, pp. 99-107.

Chou S.M., 1992, "Viscosity measurements of viscoelastic inks at high shear rates", TAGA Proceedings, pp. 388-408

Chou S.M. and Bain L.J., 1996, "Computer simulation of offset printing: I. Effects of image coverage and ink feed-rate", TAGA Proceedings, pp. 523-547.

Chou S.M., 1997, "Computer simulation of offset printing: II. Effects of vibrator oscillator and image layout", TAGA Proceedings, pp.94-118.

Chou S.M., Fadner T.A., Bain L.J., 1990, "Structural recovery of printing inks studied by steady shear rheometry, TAGA Conference Proceedings, pp. 280-312

Christiansen S., 1995, "Resins are Gaining Weight", American Ink Maker 73, No. 101, pp. 14-60.

Coco C.E. and. Cockerline K.B, 1988, "Using the prufbau test to predict web offset piling" TAPPI, pp. 35-39.

Cohu O. and Magnin A., 1995, "Rheometry of paints with regard to roll coating process", Journal of Rheology, Vol. 39, Issue 4, pp. 767-785.

Coyle C.W. Macosko, L.E. Scriven, 1990, "Stability of symmetrical film splitting between counter- rotating cylinders", J. Fluid Mech. 216, pp. 437-458.

Coyle D. J., 1984, "The Fluid Mechanics of Roll Coating: Steady Flows, Stability, and Rheology", PhD Thesis, University of Minnesota.

Coyle D. J., 1992, "Roll Coating Flows II: The Ribbing Instability" Industrial Coating Research, Vol. 2, pp. 33-45.

Coyle D., Macosko C. and Scriven L. 1990 "Stability of Symmetric Film-Splitting Between Counter-Rotating Cylinders", Journal of Fluid Mechanics 216, pp.437-458.

De Grâce J.H., Mangin P.J., 1988, "A mechanistic approach to ink transfer Part II: The splitting behaviour of inks in the printing nips", APST, Vol. 19, Pentech Press, U.K, pp. 146-161.

Deganello D., and Lubansky A.S., 2007, "Measuring extensional characteristics of printing inks", Printing Future Days, Chemnitz, Germany, PFD proceedings, pp. 223-227

Destree M. T., 1994, "The Lithographers Manual", Graphic Arts Technical Foundation, 9th Edition. ISBN 0-88362-169-X

Entov V.M., Hinch E.J, 1997, "Effect of a spectrum of relaxation times on the capillary thinning of a filament of elastic liquid", J. Non-Newtonian Fluid Mech. 72, pp. 31-53.

Evans P.S.A., Harrey P.M., Ramsey B.J. and Harrison D.J., 2001, "Component attachment in Lithographic film circuits", Circuit World, pp. 282-286.

Ferry J. D., 1980, "Viscoelastic properties of polymers", 3rd Edition, John Willey & Sons, New York, ISBN 0-471-04894-1

Fuchs B., Lindqvist U., Wallstrom E., 1991, "Avoiding problems of ink emulsification in keyless offset systems", APST, Vol. 21, Pentech Press, U.K., pp. 296-311

Grove D.M, Davis T.P, 1992, "Engineering quality and experimental design", Longman, ISBN 0-824-78246-1.

Guerrette J. D., 1985, "A steady state inking system model for predicting ink film thickness distribution", TAGA Conference Proceedings, pp. 404-425

Hayashi T., Amari T., 1992, "Dynamics of ink transfer and splitting of emulsified ink", TAPPI, pp. 75-80

Huang J. and Goodman R.M., 1995, "Modeling studies of ink, plate and fountain interactions by contact angle measurements", TAGA Proceedings, pp. 873-882.

Hull H.H. 1968, "The theoretical analysis and practical evaluation of roller ink distribution systems", TAGA Conference Proceedings, pp. 288-315

Juza J. 1997, "The pendant drop method of surface tension measurement: equation interpolating the shape factor tables for several selected planes", Czech Journal of Physics, Issue 47, pp. 351-357.

Kipphan H., 2001, "Handbook of print media", Springer-Verlag, Germany, ISBN 3-540-67326-1.

Lepoutre P., 1978, "Liquid Absorbency and Coating Porosity", TAPPI, Vol. 61, Issue 5, pp. 51-55.

Li J, Miller R. and Mohwald H, (1996), "Characterisation of phospholipid layers at liquid interfaces 2. Comparison of isotherms of insoluble and soluble films of phospholipids at different fluid/water interfaces", Colloids and Surfaces, A: Physicochemical and Engineering Aspects 114, Elsevier, pp. 123-130.

Lopez, L. Pauchard, M. Rosen, M. Rabaud, 2002, "Non-Newtonian effects on ribbing instability threshold", J. Non-Newton. Fluid Mech. 103, pp.123-139.

Lubansky A.S., Boger D.V., Servais C., Burbidge A.S., and Cooper-White J.J., 2007, "An approximate solution to flow through a contraction for high Trouton ratio fluids" J. Non-Newtonian Fluid Mech. 144, pp. 87-97.

Lubansky A.S., Yeow Y.L., Leong Y.K., Wickramasinghe S.R., and Han B., 2006, "A general method of computing the derivative of experimental data", AICHEJ 52, pp. 323-332.

Lubansky S.A, Boger V.D. and Cooper-White J.J, 2005, "Batchelor's theory extended to elongated cylindrical or ellipsoidal particles", Journal of Non-Newtonian Fluid Mechanics, Issue 130, pp. 57-61.

MacPhee J. and Lind J.T., 2002, "Insight into the relationship between print density and ink film thickness", TAGA Proceedings, pp. 479-496.

MacPhee J., 1995, "A reactively simple method for calculating the dynamic behaviour of inking systems", TAGA Conference Proceedings, pp. 168-183

MacPhee J., 1998, "Fundamentals of lithographic printing, Volume 1 – Mechanics of printing", Chapters 2-6, GATF press, U.S.A, ISBN 978-0883-62214-8.

McGlashan A.S, O'Brien T.V, Awati M.K. and Mackay E.M, (1998), "Approximate elongation flow properties utilising the opposed orifice technique and Correction for shear and inertia", Rheological Acta Vol. 37, pp. 214-222.

McKay R., 1994, "Effectiveness of pigments in suppression of misting of lithographic printing inks", In FATIPEC Congress Vol. 22, pp. 137-150.

McKinley G. and Hassager O., 1999, "The Considered Condition and Rapid Stretching of Linear and Branched Polymer Melts", Journal of Rheology 43, No. 5, pp. 1195-1212.

McKinley H.G, Anna L.S, Tripathi A. and Minwu Yao M, (1999), "Extensional rheometry of polymeric fluids and the uniaxial elongation of viscoelastic filaments", IPPS Proceedings, pp. 1-14

Meggs P. B., 1998, "A History of Graphic Design", 3rd Edition, John Wiley & Sons, Canada, ISBN 0471291986.

Melia M.C., 1974, "Studies of ink transfer to paper in offset litho printing" PhD Thesis University of Manchester

Mewis J., Dobbels F., 1981, "Nip flow and tack of printing inks", Ind. Eng. Chem. Prod. Res. Dev., pp. 515-519

Mill C.C, South G.R., 1967, "Formation of ribs on rotating rollers", J. Fluid Mech. 28, pp. 523-529.

Mill C.C., 1961, "The behaviour of printing on rollers", JOCCA, Vol.44, pp. 596-601.

Mill C.C., 1974, "Ink distribution systems", British ink makers Vol.16, No5, pp. 15-17

Miller J. and Meyers R., 1958, "A Photographic Study of Liquid Flow in a Roll Nip", Transactions of the Society of Rheology, Vol.2, pp. 77-93.

Miller J., 1956, "A Kinematic Study of the Splitting of Thin Liquid Films", PhD thesis Lehigh University.

Mouw T., 1995, "Sphere vs. 0°/45° A discussion of instrument geometries and their areas of application", X-Rite Technical Sheet. Doc CA00015a.

Oittinen P., Kainulainen J. and Mickels J., 1992, "Rheological properties, setting and smearing of offset news inks", Graphic Arts in Finland Vol.21, pp. 3-9

Owens M. S., 2005, "Misting in forward roll coating, Structure-Property-Processing Relationships", PhD Thesis, University of Minnesota, U.S.A

Paikos I., 2003, "An investigation into the cause of print variation during start-up transients in web offset inking systems", PhD Thesis, Swansea University, U.K.

Pangalos G., Dealy J.M., Lyne M.B., 1985, "Rheological properties of news inks", Journal of Rheology, 29, pp. 471-491.

Phadke S.M., 1989, "Quality Engineering using Robust Design", Prentice Hall, New Jersey, ISBN 9780137451678.

Podhajny M. R., 2002, "What is the role of tack in printing inks?", PFFC, Penton Media, pp. 24

Robertson A. R., 1977, "The CIE colour difference formulae", Color Research and Application 2, pp. 7-11.

Rosenberg A., 1999, "A closer look to ink splitting", FOGRA Research Report, RN: 52.023

Ross Phillip J., 1996, "Taguchi Techniques for Quality Engineering" McGraw-Hill, second edition, ISBN 0070538662

Savage M. D., 1977, "Cavitation in Lubrication Part I: Boundary conditions and Cavity Fluid Interfaces", Journal of Fluid Mechanics No 80, pp. 743-755.

Savage M., 1984, "Mathematical model for the onset of ribbing", AIChE Journal 30, pp. 999-1002.

Savage M.D. 1992, "Meniscus instability and ribbing", Industrial Coating Research, Vol. 2, pp 47-58.

Sherma Adhay, 2003, "Understanding Color Management", Delmar Publishers, ISBN 1-4018-1447-6

Sjodahl L.H., 1951, "Ink flow on rotating rollers", American Ink Maker Vol.3, pp. 31

Smith D. and Chu S., 1999, "Response of flexible polymers to sudden elongational flow", Science 281, pp. 1335-1340.

Smith D.L, Engle L. S., Howard J. and Jones W, 1956, "Film splitting on rotating rollers", TAPPI, Vol 49, pp. 147-151

Spiegelberg H.S, Ables C.D. and McKinley H.G, (1996), "The role of end-effects on measurements of extensional viscosity in filament stretching rheometers", Journal of Non-Newtonian Fluid Mechanincs, Vol. 64, pp. 229-267.

Szabo P., 1997, "Transient filament stretching rheometer I: Force balance analysis", Rheologica Acta 36, pp. 227-284.

Thompson M.J., 2002, "The microstructure and rheology of emulsions of water in lithographic printing ink." Ph.D, University of Cambridge, UK.

Thomson I.G., Young F.R., 1975, "High-speed photographic studies of ink filamentation", Journal of the Oil and Colour Chemists' Association, Vol. 58, pp. 389-392.

Traber K., Has M. and Dolazelek F., 1992, "Thermal balance of inking systems of high speed presses", FOGRA, Research Report, RN: 32.111

Tropea C, Yarin AL. and Foss J.S, 2007, "Handbook of experimental fluid dynamics", Springer, Heidelberg, ISBN: 978-3-540-25141-5.

Trouton F.T., 1906, "On the coefficient of viscous traction and its relation to that of viscosity", Proceedings of Royal Society 77A, No 519, pp 426-440

Vlachopoulos G., 2003, "Evaluation of drying mechanisms in coldest lithographic printing", MSc Thesis, Swansea University, U.K.

Voet A., 1956, "Ink misting and its prevention", American Ink Maker 34, No. 2, pp 32.

. Walker W.C., Fetsko J.M., 1955, "A concept of ink transfer in printing", American Ink Maker, Vol. 33, No. 12, pp. 38-44, 69-71

Wickman M., Hallstensson K. and Strom G., 2001 "Interactin between printing ink binders, printing ink oil and fountain solutions" TAGA Proceedings, 212-223

Wirz B., 1964, "Studies on inkers for letterpress and lithographic rotary presses", TAGA Proceedings, pp. 102-117

Wood H. A. W., 1918, "Apparatus for inking printing presses", U.S Patent 1275348

Wu N., Auerbach R. and Catena R, 1999, "Effect of hydrophilic and lipophilicity balance on rheological properties of pigment dispersions", TAGA Proceedings, pp. 650-661.

Zevallos G., Carvalho M. and Pasquali M., 2004, "Forward roll coating flows of viscoelastic liquids", Journal of Non-Newtonian Fluid Mech 130, pp. 96-109, USA.